ORNL/Sub/79-24712/3

# ADVANCED ELECTRIC HEAT PUMP
# FINAL REPORT

## DUAL-STROKE COMPRESSOR AND SYSTEM DEVELOPMENT

Prepared by

S. E. Veyo and T. J. Fagan

December 1983

Report Prepared by
Westinghouse Electric Corporation
R&D Center
1310 Beulah Road
Pittsburgh, Pennsylvania 15235

Under
Subcontract 86X-24712C

for

Oak Ridge National Laboratory
Oak Ridge, Tennessee 37830
operated by
UNION CARBIDE CORPORATION
for the
U.S. DEPARTMENT OF ENERGY
Under Contract No. W-7405-eng-26

NOTICE

This report was prepared as an account of work sponsored by an agency of the United States Government. Neither the United States Government nor any agency thereof, nor any of their employees, makes any warranty, expressed or implied, or assumes any legal liability or responsibility for any third party's use or the results of such use of any information, apparatus, product or process disclosed in this report or represents that its use by such third party would not infringe privately owned rights.

ADVANCED ELECTRIC HEAT PUMP

DUAL-STROKE COMPRESSOR AND SYSTEM DEVELOPMENT

S. E. Veyo and T. J. Fagan

## ABSTRACT

This report documents in summary form the development of an advanced electric heat pump by Westinghouse for the United States Department of Energy under contract 86X-24712C with the Oak Ridge National Laboratory. A two-capacity, residential, advanced electric heat pump utilizing a unique dual-stroke compressor has been developed. Two nearly identical preprototype split systems of nominally 3.5 tons maximum cooling capacity have been designed, built and laboratory tested. The estimated annual energy efficiency of this advanced system is 20 percent better than a two-speed electric heat pump available at contract inception in 1979. This superior performance is due to the synergism of a high-efficiency, dual-stroke reciprocating compressor, a dual-strength high-efficiency single-speed single-phase hermetic drive motor, a single-width, single-entry high-efficiency indoor blower with backward curved cambered plate blades, a high-efficiency multivane axial flow outdoor fan, high-efficiency two-speed air mover motors and a microprocessor control system. The relative proportions of heat exchangers, air flows and compressor size as well as the ratio between high and low capacity have been optimized so as to minimize the annual cost of ownership in a northern climate. Constraints placed upon the optimization and design process to ensure comfort provide heating air with a temperature of at least 90°F and provide cooling with a sensible-to-total capacity ratio of not more than 0.7. System performance has been measured in the laboratory in accordance with applicable codes and procedures. Performance data plus hardware details are provided.

TABLE OF CONTENTS


| | Page |
|---|---|
| ABSTRACT | ii |
| LIST OF FIGURES | iv |
| LIST OF TABLES | vi |
| 1.0 INTRODUCTION | 1 |
| 2.0 SUMMARY AND CONCLUSIONS | 3 |
| 2.1 Summary | 3 |
| 2.2 Conclusions | 24 |
| 3.0 SYSTEM PERFORMANCE | 25 |
| 3.1 Measured Steady State Performance - Preprototype Number One | 25 |
| 3.2 Cyclic Degradation | 30 |
| 3.3 Frost Accumulation | 32 |
| 3.4 Measured Steady State Performance - Preprototype Number Two | 33 |
| 3.5 Seasonal Performance | 35 |
| 4.0 COMPONENT DESCRIPTION | 40 |
| 4.1 Compressor | 40 |
| 4.2 Outdoor Fan | 58 |
| 4.3 Indoor Blower | 71 |
| 4.4 Refrigeration System Description | 80 |
| 4.5 Controls | 98 |
| 5.0 INDOOR UNIT PACKAGE | 113 |
| 6.0 OUTDOOR UNIT PACKAGE | 123 |
| 7.0 COMPARISON WITH OPTIMIZED CONFIGURATION | 128 |
| 8.0 REFERENCES | 132 |
| 9.0 ACKNOWLEDGEMENT | 134 |
| APPENDIX A - PROTOTYPE NUMBER ONE - SYSTEM INSTRUMENTATION | 138 |
| APPENDIX B - TEST FACILITY DESCRIPTION | 143 |
| APPENDIX C - SEASONAL PERFORMANCE TABLES | 153 |
| APPENDIX D - REVERSING VALVE STUDY | 174 |

## LIST OF FIGURES


| | | Page |
|---|---|---|
| Fig. 1 | - Two-capacity advanced electric heat pump measured heating performance | 4 |
| Fig. 2 | - Two-capacity advanced electric heat pump measured cooling performance | 5 |
| Fig. 3 | - Preprototype heat pump outdoor unit | 8 |
| Fig. 4 | - Cutaway drawing of preprototype advanced electric heat pump | 9 |
| Fig. 5 | - Preprototype outdoor fan propeller | 10 |
| Fig. 6 | - Preprototype fan and diffuser subassembly | 11 |
| Fig. 7 | - Preprototype heat pump indoor unit | 13 |
| Fig. 8 | - Exposed view of refrigeration machine module | 14 |
| Fig. 9 | - High-efficiency blower wheel | 15 |
| Fig. 10 | - Preprototype indoor unit with access panels removed | 16 |
| Fig. 11 | - Advanced electric heat pump refrigeration circuit | 18 |
| Fig. 12 | - Crankshaft with dual-stroke cam | 19 |
| Fig. 13 | - Control schematic | 21 |
| Fig. 14 | - Comparison of analytically predicted and measured heating performance (Preprototype Number 1) | 26 |
| Fig. 15 | - Comparison of analytically predicted and measured cooling performance (Preprototype Number 1) | 27 |
| Fig. 16 | - Dual-stroke cam | 41 |
| Fig. 17 | - Dual-stroke cam positions | 42 |
| Fig. 18 | - Cross section of oil-cooled compressor with direct suction | 44 |
| Fig. 19 | - Discharge valve cantilevered flapper with end restraint | 46 |
| Fig. 20 | - Compressor motor efficiency vs shaft power (25°C winding temperature) | 48 |
| Fig. 21 | - Prototype dual-stroke compressor performance (R-22) | 49 |
| Fig. 22 | - Preprototype oil cooled dual-stroke compressor - discharge line view | 53 |
| Fig. 23 | - Exploded view of preprototype oil cooled dual-stroke compressor | 54 |
| Fig. 24 | - Breadboard outdoor fan performance (6 inch diffuser, pitch angle $\alpha_{g_R} = 33.8°$) | 60 |

Page


Fig. 25 - Outdoor air mover preprototype 62

Fig. 26 - View of diffuser and motor cover for outdoor air mover preprototype 64

Fig. 27 - Fan motor speed-torque characteristics (analytically estimated) 66

Fig. 28 - Indoor air mover assembly 76

Fig. 29 - Performance characteristics, preprototype blower (dimensions in inches) 77

Fig. 30 - Hi-Re-Li circuit - heating 81

Fig. 31 - Hi-Re-Li circuit - cooling 82

Fig. 32 - Subcool heating/superheat cooling circuit with electric valve, heating 86

Fig. 33 - Subcool heating/superheat cooling circuit with electric valve, cooling 87

Fig. 34 - Indoor coil circuit (heating mode) 89

Fig. 35 - Top refrigerant circuit indoor coil preprototype number two - heating mode 91

Fig. 36 - Outdoor heat exchanger configuration 94

Fig. 37 - One of four outdoor heat exchanger slab circuits 95

Fig. 38 - Side view of indoor unit with plumbing details 99

Fig. 39 - End view of indoor units with plumbing details 100

Fig. 40 - Microprocessor board schematic 102

Fig. 41 - Digital and analog input schematic 103

Fig. 42 - Display schematic 104

Fig. 43 - Input filter and relay driver schematic 105

Fig. 44 - Power supply, deadman and control relay output schematic 106

Fig. 45 - Sketch of indoor package assembly 114

Fig. 46 - Selected indoor package design assembly 115

Fig. 47 - Airflow path and module arrangement options 121

Fig. 48 - Cut-away illustration of the outdoor unit 124

Fig. 49 - Outdoor unit assembly drawing 125

# 1. INTRODUCTION

This report documents in summary form the development of an advanced electric heat pump by Westinghouse for the United States Department of Energy under contract 86X-24712C with the Oak Ridge National Laboratory.

The Advanced Electric Residential Heat Pump Research and Development Program[1] has as its objective the development of a preproduction prototype commercially and economically viable advanced heat pump that can provide satisfying performance with an annual energy efficiency at least twenty percent better than the most efficient units available in the market place in early 1979.

A concomitant objective was that the degree of improvement realized, combined with the projected units sold, should result in a significant national energy savings within 15 years of product introduction.

The residential electric heat pump is an embodiment of the well-known vapor compression refrigeration machine. As such, it represents a mature technology, and, therefore, higher efficiency inevitably is achieved only with higher product cost. The market for residential heat pumps is extremely cost-competitive and has been dominated historically by the new home builder in the southern states, where comfort cooling is in demand. It is not surprising, therefore, that until very recently, heat pump manufacturers have concentrated on large-volume, low-cost, cooling machines of modest efficiency, which can also provide limited heating.

Eleven percent of domestic energy consumption is used for residential space heating and 0.7 percent for residential air conditioning[11]. Because of a higher population density and a more severe winter climate, 90 percent of the energy consumed for residential space heating is consumed in the North, where the annual heating requirement exceeds 5000 degree F days. This makes the development of an economically viable heat pump for the northern climate an obvious goal if a significant national energy savings is to be realized. Previous work has shown that the key to an effective northern-climate heat pump is finding a low-cost means to achieve capacity modulation[2].

In early 1979, a newly introduced two-speed (therefore, with modulatory capacity) heat pump was identified as the unit whose annual performance was to be surpassed by 20 percent. We have achieved this objective as proposed with a vapor compression refrigeration system that uses R-22 as the working fluid. This report documents both the design of the preprototype system and system performance. Previous reports document the analysis of sales potential[3] and the component development effort[4].

## 2. SUMMARY AND CONCLUSIONS

### 2.1 Summary

A two-capacity, residential, advanced electric heat pump utilizing a unique dual-stroke compressor has been developed. Two nearly identical preprototype split systems of nominally 3.5 tons maximum cooling capacity have been designed, built and laboratory tested. The estimated annual energy efficiency of this advanced system is 20 percent better than a two-speed electric heat pump available at contract inception in 1979. This superior performance is due to the synergism of a high-efficiency, dual-stroke reciprocating compressor, a dual-strength high-efficiency single-speed single-phase hermetic drive motor, a single-width, single-entry high-efficiency indoor blower with backward curved cambered plate blades, a high-efficiency multivane axial flow outdoor fan, high-efficiency two-speed air mover motors and a microprocessor control system. The relative proportions of heat exchangers, air flows and compressor size as well as the ratio between high and low capacity have been optimized* so as to minimize the annual cost of ownership in a northern climate. See Section 7.0 and Reference 5. Constraints placed upon the optimization and design process to ensure comfort provide heating air with a temperature of at least 90°F and provide cooling with a sensible-to-total capacity ratio of not more than 0.7. System performance has been measured in the laboratory in accordance with applicable codes and procedures.[6] Measured heating performance is shown in Figure 1 and measured cooling performance in Figure 2. The estimated seasonal performance of this system, based upon the data of Figures 1 and 2 is compared in Table 1 with the estimated performance of high-efficiency systems available in 1979-81 (based upon published manufacturers data) as installed in a 1600 $ft^2$ dwelling with level 2 insulation in the various DOE climate regions typifying the

* NOTE: Advanced components such as the dual-stroke compressor, air movers, and microprocessor controller, plus the package design, the refrigerant flow control means, and reversing valve performance characteristics were being developed concurrently with the development and application of the optimization process. Allocated resources were exhausted before the final performance and cost characteristics of the constitutive design elements were available for inclusion in the optimization process. Reapplication of the process would yield a better approximation to the optimum heat pump configuration.

Curve 731186-8

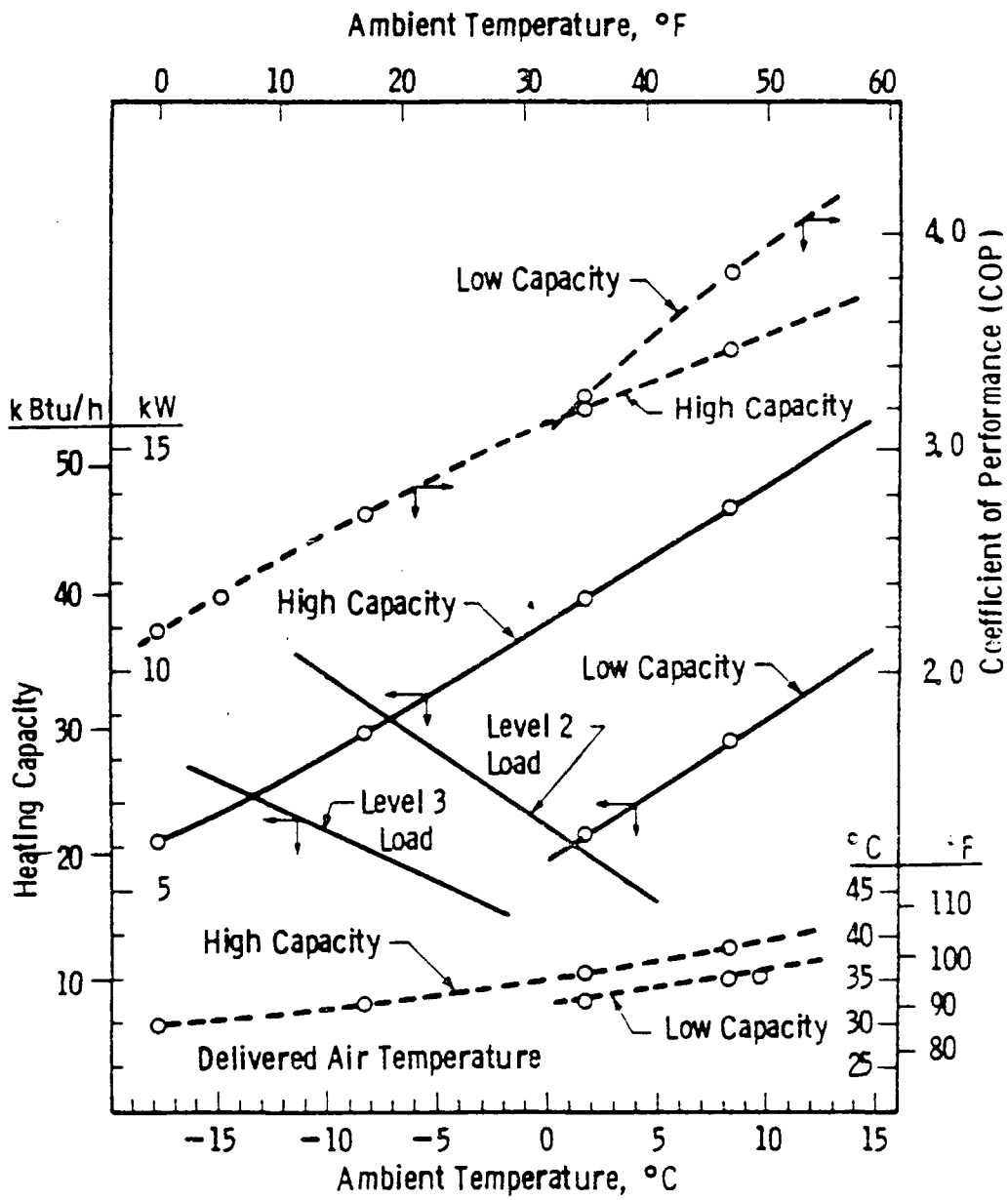


Fig. 1 - Two-capacity advanced electric heat pump measured heating performance

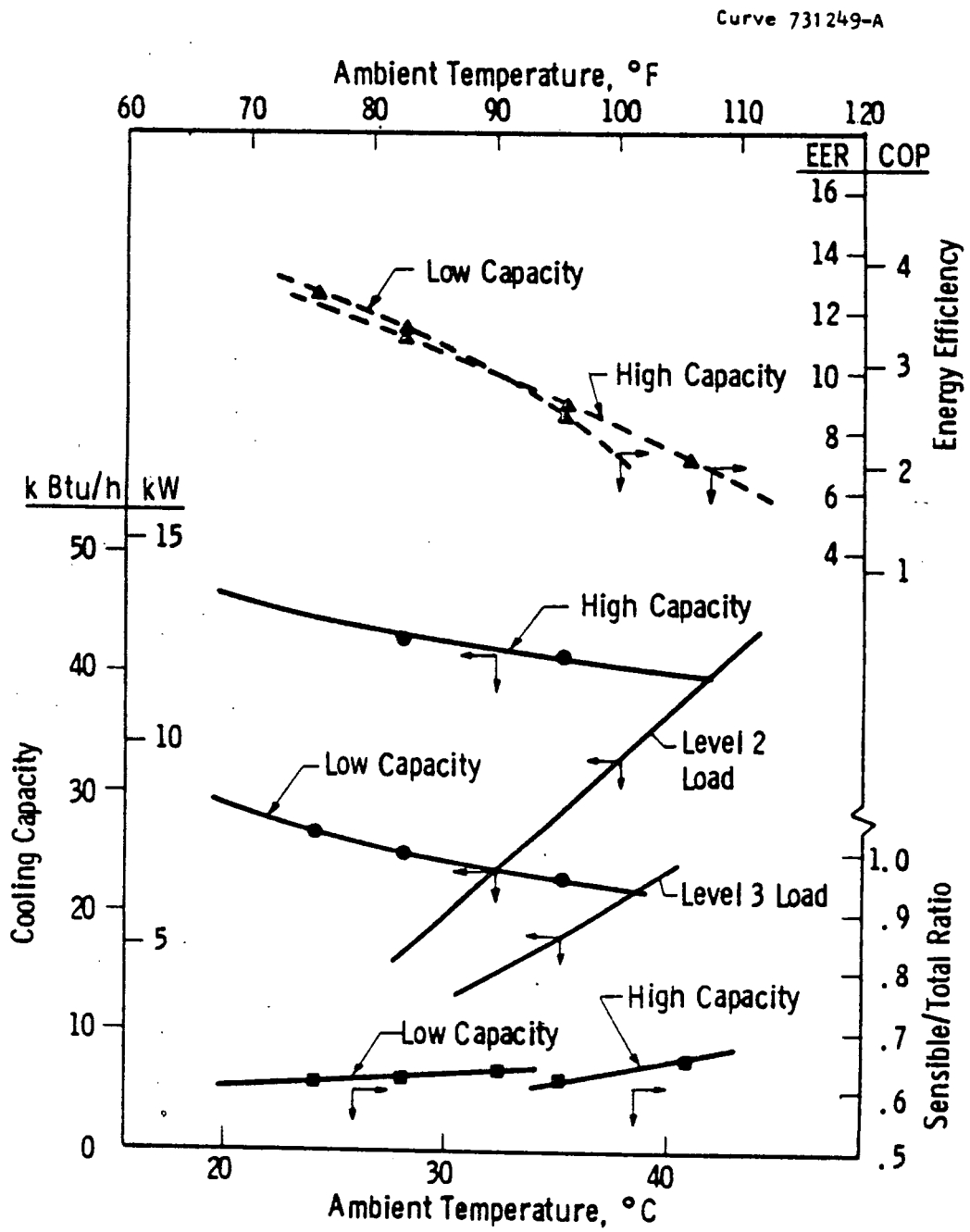


Fig. 2 - Two-capacity advanced electric heat pump measured cooling performance

TABLE 1

Comparison of Seasonal Performance[1]
(1600 sq. ft. Level 2 House)[2]

| Climate Region (DOE) | | II[3] | III[4] | IV[5] | V[6] |
|---|---|---|---|---|---|
| Heating Load (MMBtu) | | 31.56 | 68.77 | 109.78 | 128.60 |
| Cooling Load (MMBtu) | | 83.92 | 39.87 | 16.61 | 20.87 |
| Dual-Stroke | Installed Cost[7] | 1.54 | 1.54 | 1.49 | 1.50 |
| Heat Pump | Ownership Cost[9] | 1.07 | .97 | .88 | .86 |
| (3.5 ton) | Energy Cost | .89 | .78 | .73 | .73 |
| | HSPF (Btu/Whr) | 10.55 | 9.41 | 8.81 | 7.92 |
| | SEER (Btu/Whr) | 9.10 | 10.08 | 10.28 | 10.30 |
| High-Efficiency | Installed Cost[8] | 1.00 | 1.00 | 1.00 | 1.00 |
| Single-Speed | Ownership Cost[9] | 1.00 | 1.00 | 1.00 | 1.00 |
| Heat Pump[10] | Energy Cost | 1.00 | 1.00 | 1.00 | 1.00 |
| (2.5 ton) | HSPF (Btu/Whr) | 8.43 | 7.10 | 6.35 | 5.50 |
| | SEER (Btu/Whr) | 8.04 | 8.40 | 8.41 | 8.45 |
| High-Efficiency | Installed Cost[8] | 1.55 | 1.55 | 1.53 | 1.51 |
| Two-Speed | Ownership Cost[9] | 1.14 | 1.09 | 1.02 | .99 |
| Heat Pump[11] | Energy Cost | 1.01 | .94 | .90 | .89 |
| (4 ton) | HSPF (Btu/Whr) | 8.72 | 7.69 | 7.17 | 6.26 |
| | SEER (Btu/Whr) | 8.22 | 8.65 | 8.54 | 8.67 |
| High-Efficiency | Installed Cost[8] | 1.26 | 1.26 | 1.25 | [illegible] |
| Single-Speed | Ownership Cost[9] | 1.20 | 1.10 | 1.02 | .99 |
| Heat Pump[12] | Energy Cost | 1.16 | 1.04 | .96 | .94 |
| (4 ton) | HSPF (Btu/Whr) | 7.75 | 7.10 | 6.72 | 5.95 |
| | SEER (Btu/Whr) | 7.08 | 7.50 | 7.54 | 7.56 |

NOTE: Installed cost, ownership cost and energy cost are multiples of those for a high-efficiency single-speed heat pump in each region.

1. Westinghouse modified DOE Procedure (based on Ref. 6)
2. Ref. 2
3. Phoenix, AZ
4. Nashville, TN
5. Pittsburgh, PA (Cleveland weather)
6. Minneapolis, MN (Madison weather)
7. Estimated
8. Estimated via market study
9. Energy (@ 4.97c/kWh) + amortized Installed cost (15-year life and 3% true interest) + maintenance (2.5% of installed cost per year)
10. Mfg. A, single-speed
11. Mfg. B, two-speed
12. Mfg. A, single-speed

continental United States. Table 1 indicates that the advanced dual-stroke heat pump will exceed the energy efficiency of the targeted two-speed high-efficiency heat pump during the heating season by 20 percent or more in the northern climatic regions of the U.S. (DOE regions IV and V). Annually, the two-speed heat pump consumes more than 20 percent more electricity than the advanced dual-stroke unit in DOE climatic regions IV and V and 20 percent more in DOE region III.

The heat pump outdoor unit shown in Figure 3 is 44 inches long with trapezoidal-shaped end plates 34 inches wide at the base, 31 inches wide at the top and 31-1/2 inches high. The self-contained individually telescoping legs permit the unit to be elevated as much as two feet above the mounting surface and provide for easy installation on uneven terrain. In northern climates, an installation height of at least 15 inches is recommended in order to forestall snow blockage. A cut-away installation drawing is shown in Figure 4.

Air is ingested into the outdoor unit from all four sides and exhausted vertically upward. The heat exchanger within the outdoor unit is of the plate fin on tube design, three rows deep and has 13 rippled fins per inch. This heat exchanger is composed of four horizontal tube slab coils arranged in a "W" pattern. The face of the slab coils is oriented at an angle of 68$^{o}$ to the horizontal in order to facilitate water runoff. The bottom of each coil hangs completely free, thereby preventing the accumulation of ice between the coil and the unit structure. See Section 6.0 and Reference 4 for additional package information. The two-speed outdoor air mover is a high-efficiency axial flow design and is constructed as a subassembly for insertion into the unit wrapper. The propeller is shown in Figure 5 and the air mover subassembly in Figure 6. The fan motor is designed for high reliability as well as high efficiency. See Section 4.2 and Reference 7 for additional information. It is worth noting that all coil surfaces are well protected from damage. During shipping, the telescopic legs retract completely into the unit, permitting a compact shipping carton.

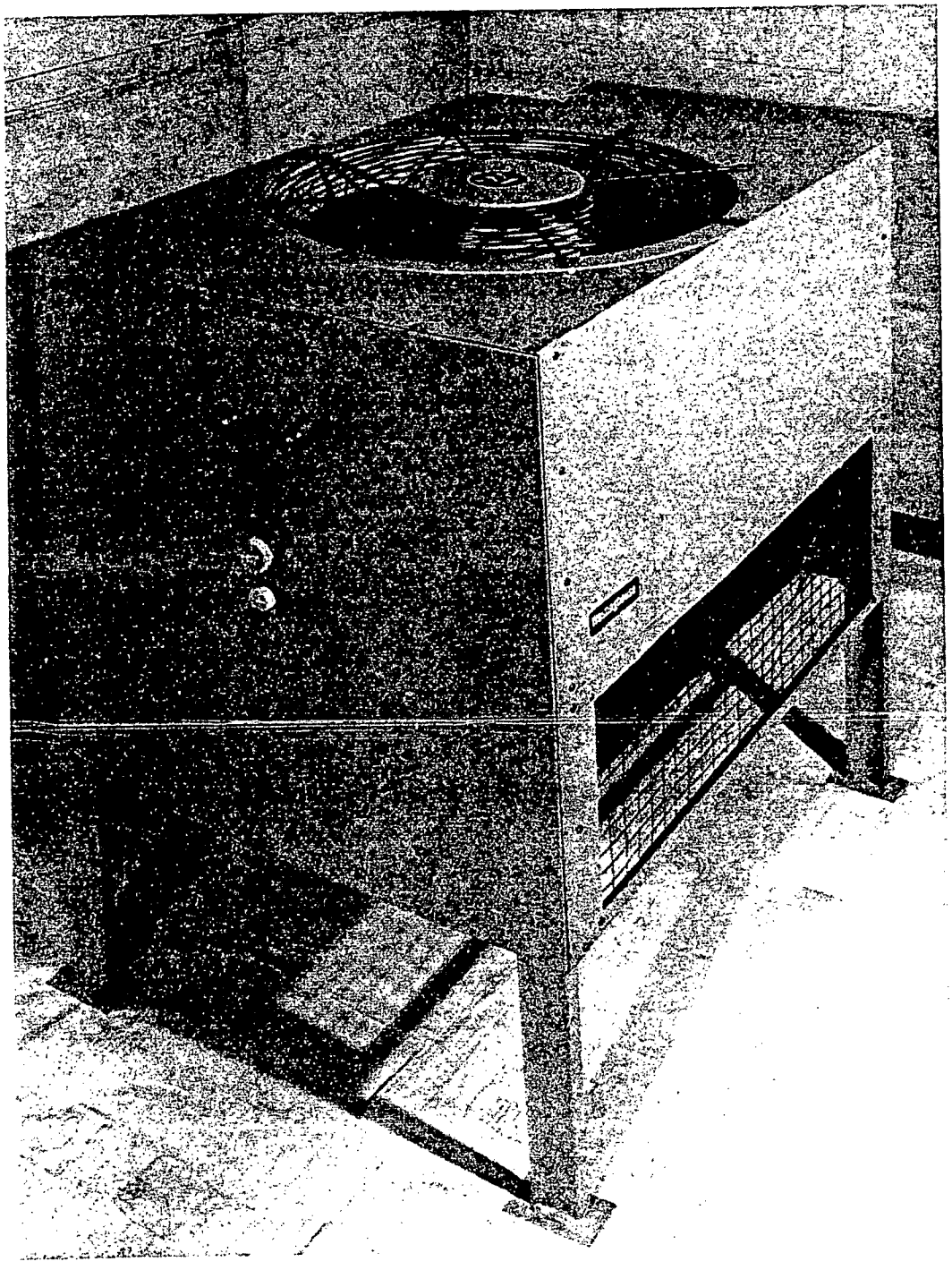

Fig. 3 - Preprototype heat pump outdoor unit

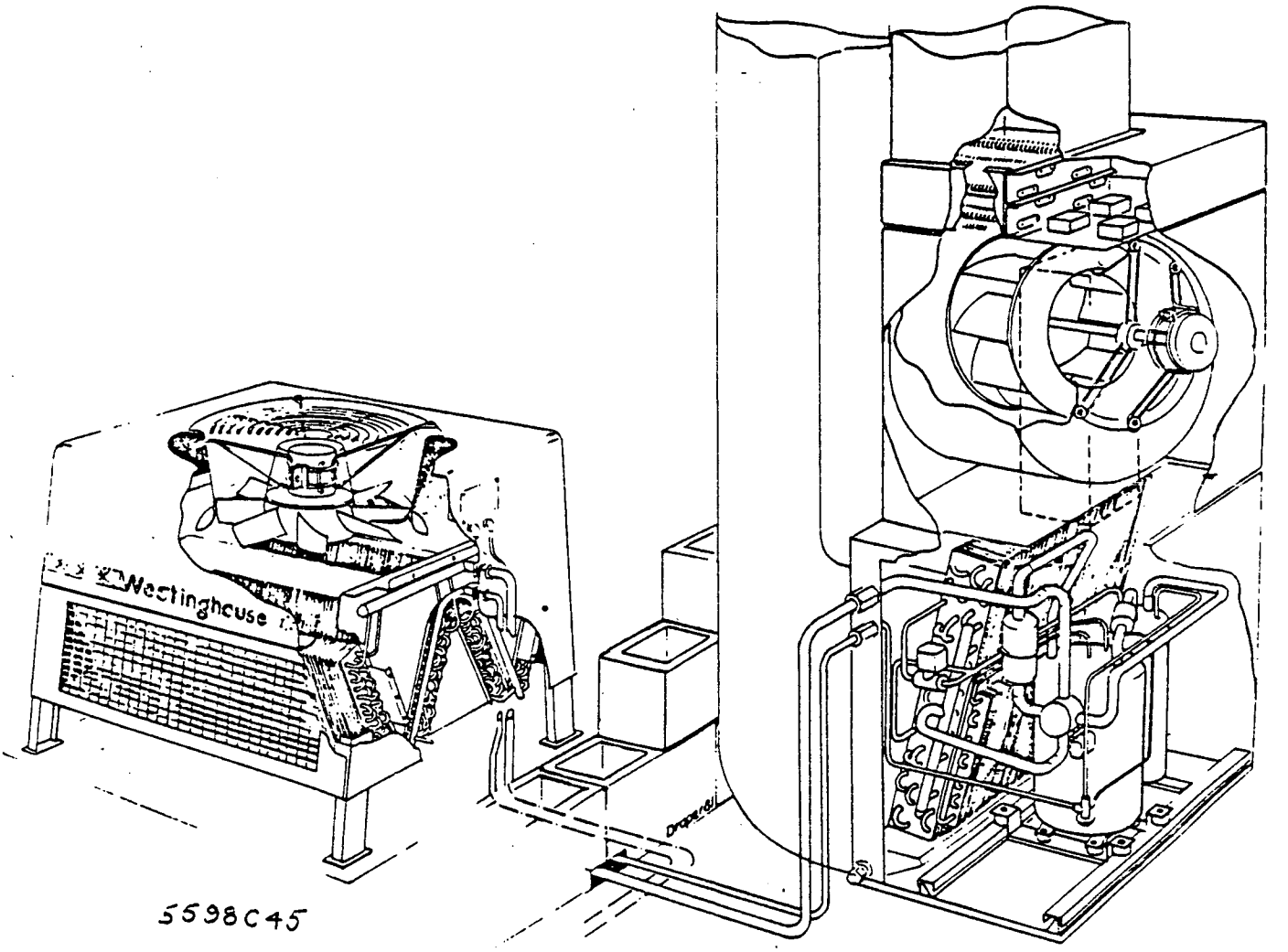


Fig. 4 - Cutaway drawing of preprototype advanced electric heat pump

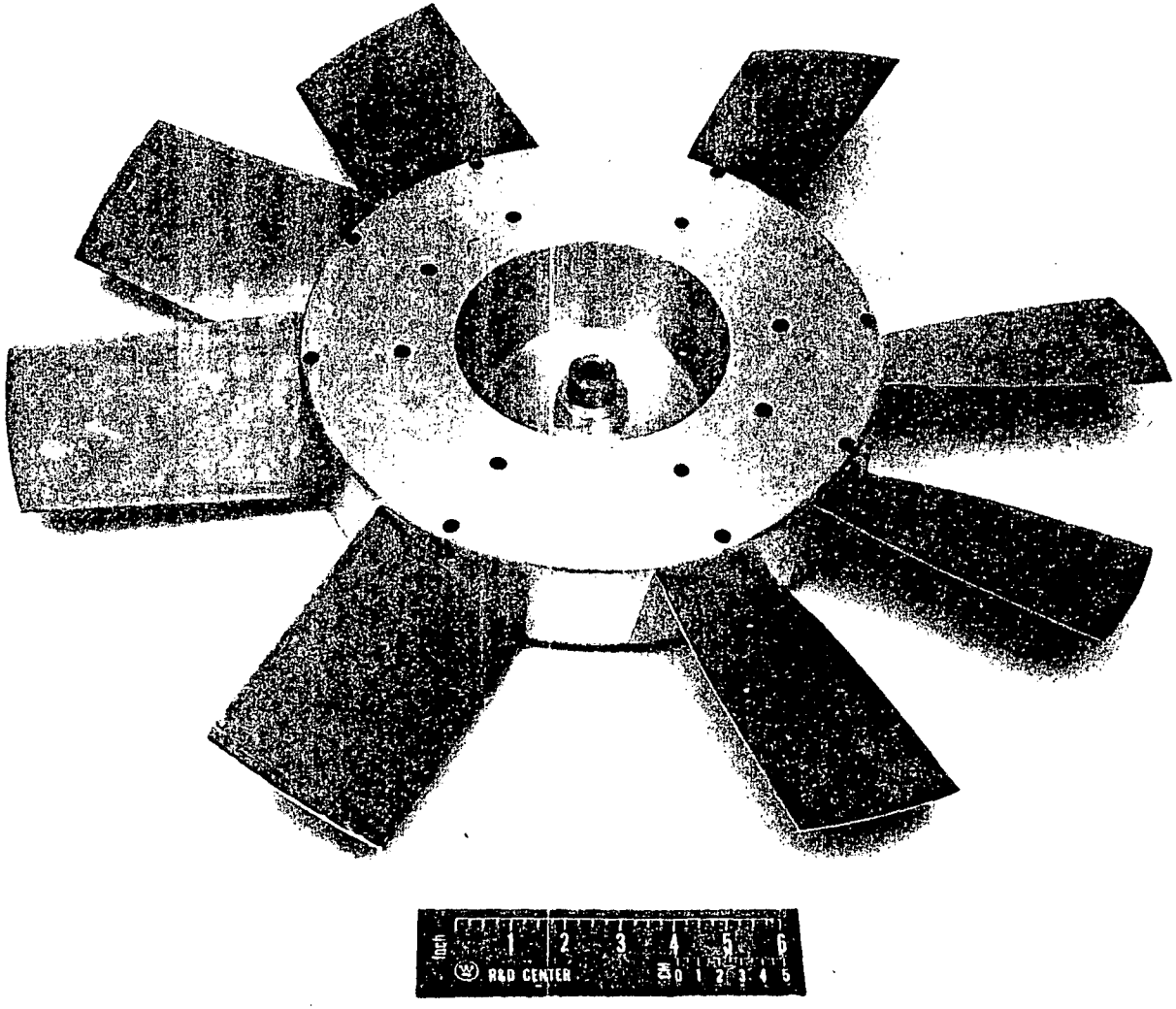


Fig. 5 - Preprototype outdoor fan propeller

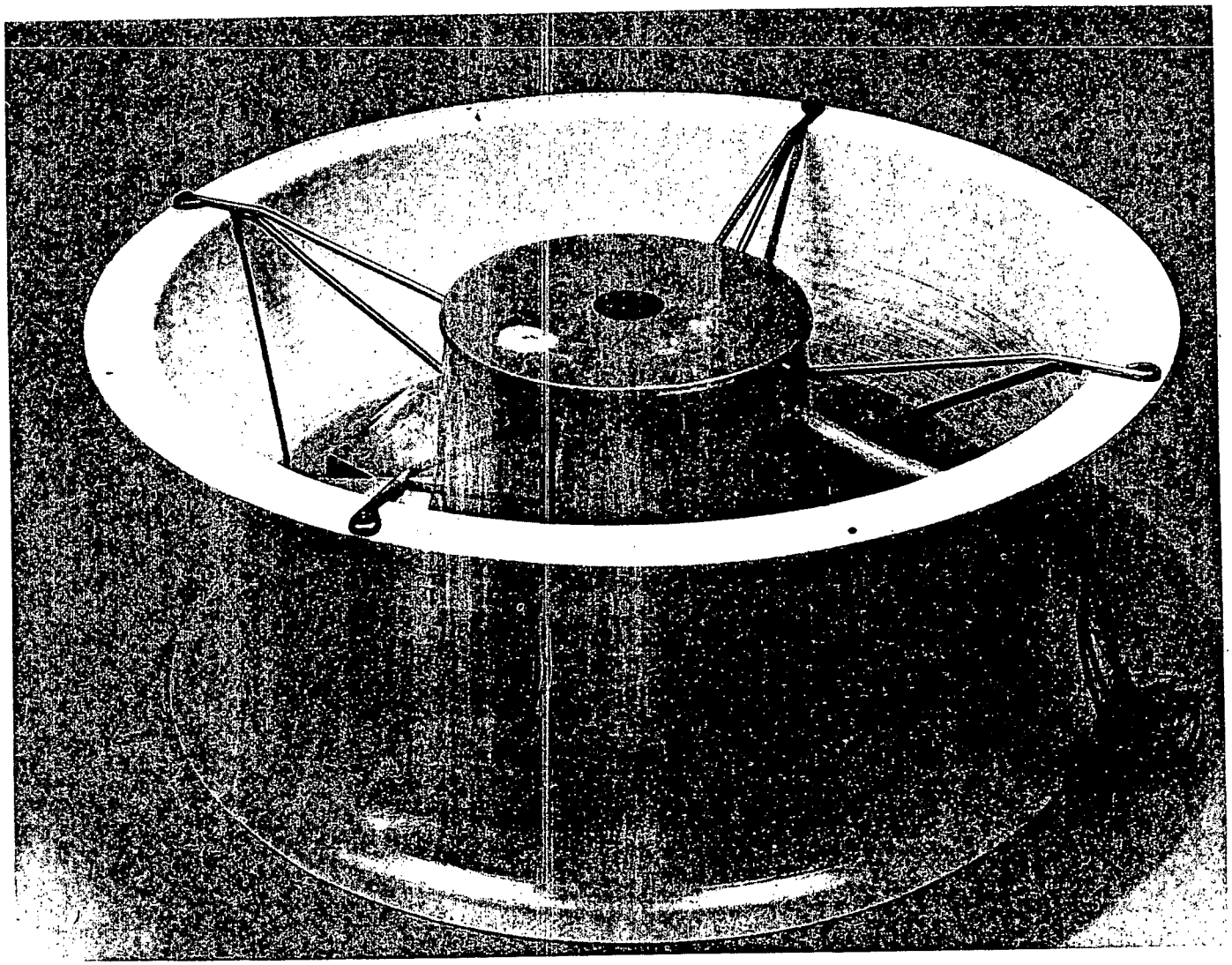

Fig. 6 - Preprototype fan and diffuser subassembly

The indoor unit shown in Figure 7 is modular in four sections. The bottom module shown cut away in Figure 4 and in Figure 8 contains the indoor refrigeration machine consisting of an advanced high-efficiency dual-stroke compressor, a Hi-Re-Li® type suction line accumulator, a four-row, single slab, plate fin on tube refrigerant to air heat exchanger, a one row oil to air heat exchanger, an electrically controlled bidirectional expansion device, a four-way refrigerant flow reversing valve, a suction line filter dryer, a muffler in the compressor discharge line and an electrically operated solenoid valve to partition the indoor coil for low capacity operation. At installation, precharged refrigeration lines are connected between the indoor and outdoor unit to complete the refrigerant circuit. An access panel permits easy servicing of components. The compressor is mounted via four vibration isolators to two lateral support beams. Each of these beams is mounted to a subframe with acoustic isolator bushings. The subframe is interfaced with the module structure, using a pair of longitudinal slide rails. If the compressor ever requires service, parting four refrigeration lines and loosening two clamps permits the compressor subframe to be pulled out on the integral slides.

The air mover and controls module is shown stacked upon the refrigeration machine module. The air mover module contains the high-efficiency two-speed blower with backward curved blades shown in Figure 9 mounted in a volute scroll, plus a control box which contains all contactors and capacitors. See Section 4.3 and Reference 8 for additional blower details. An access panel provides for servicing of blower motor and control elements, as shown in Figure 10.

The microprocessor chassis box is shown mounted on the front of the air mover module in Figure 7. See Section 4.5 for additional information.

The uppermost module contains the resistance heat elements, main fuses, and the terminals for single-point power connection.

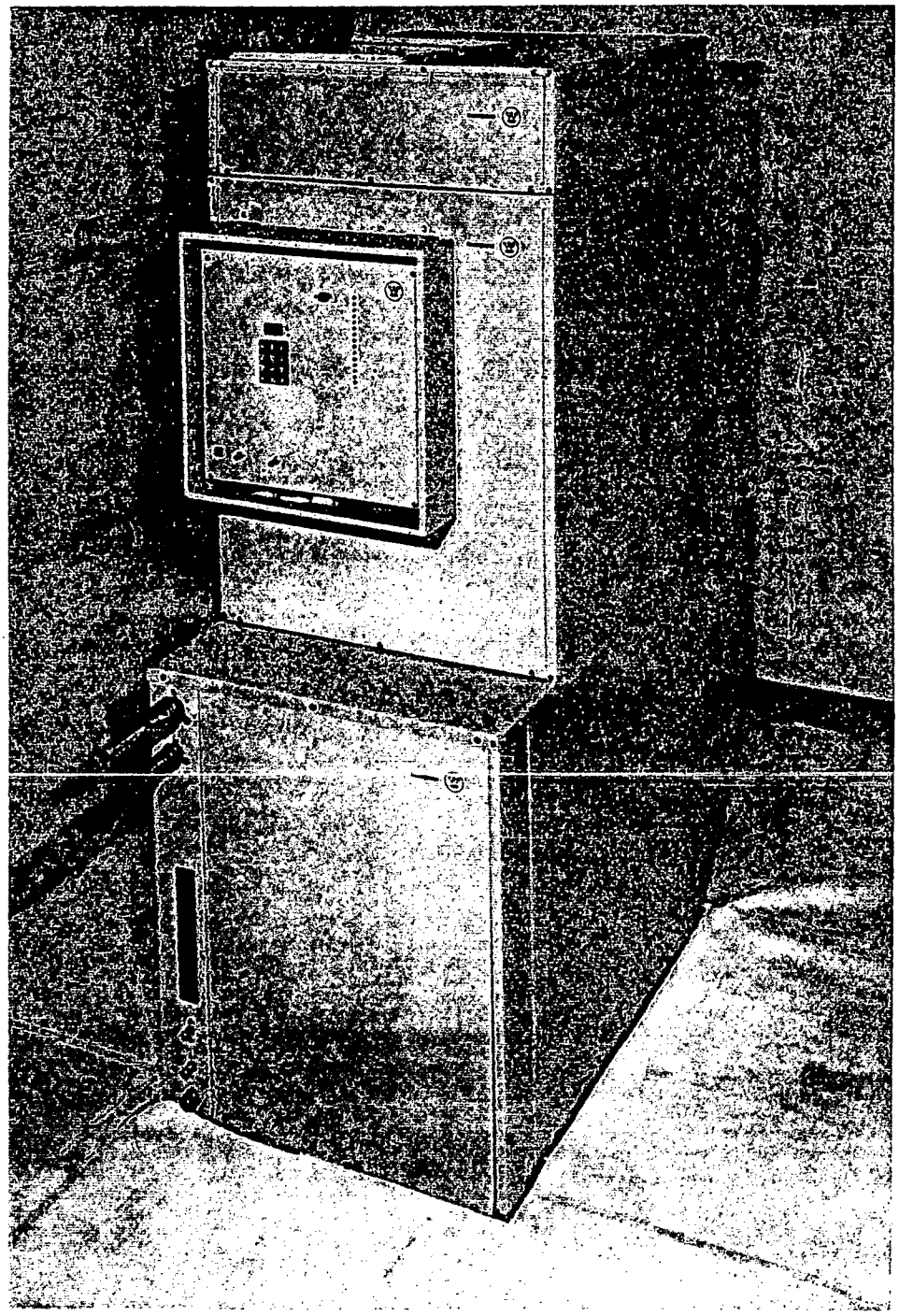

Fig. 7 - Preprototype heat pump indoor unit

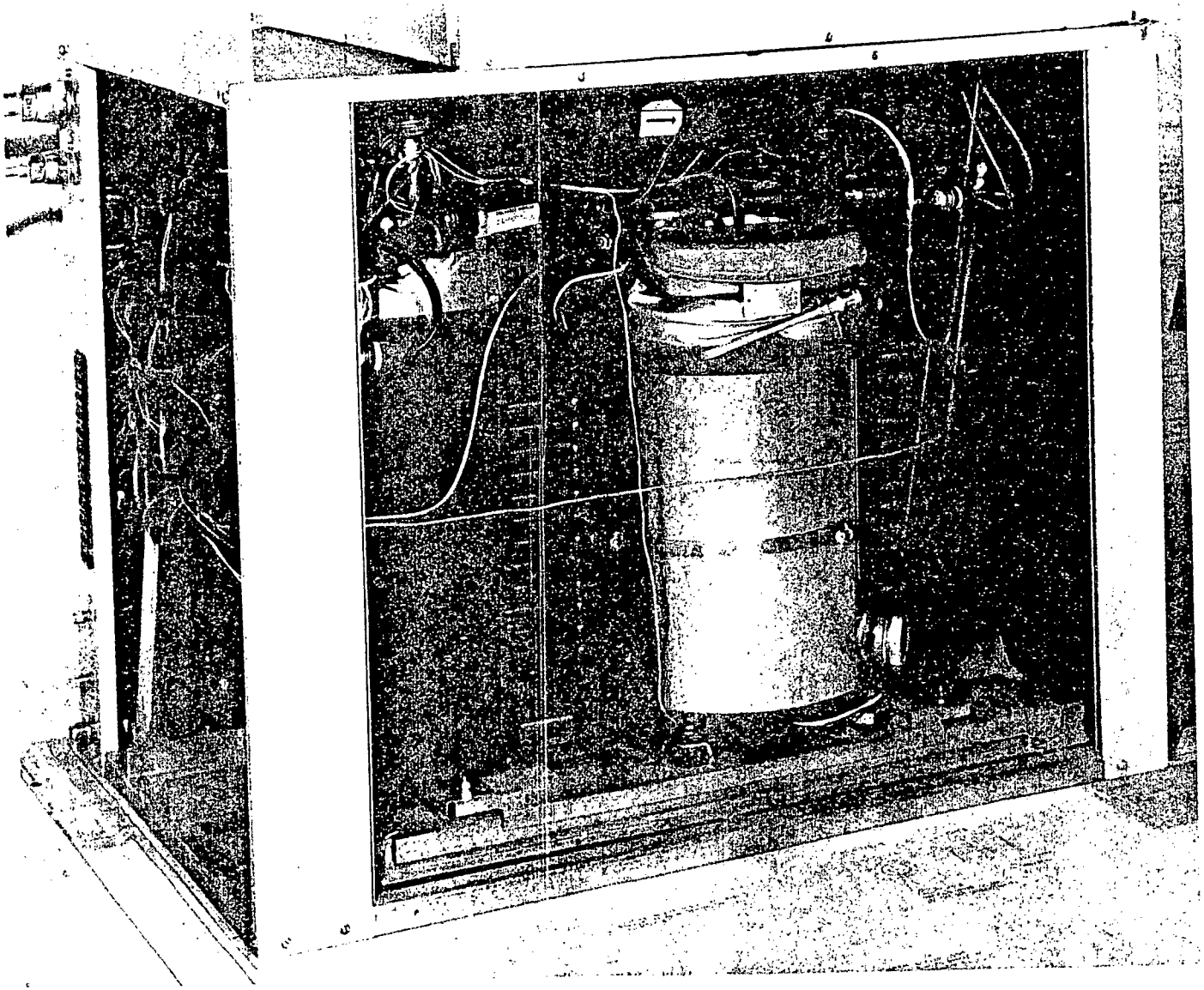

Fig. 8 - Exposed view of refrigeration machine module

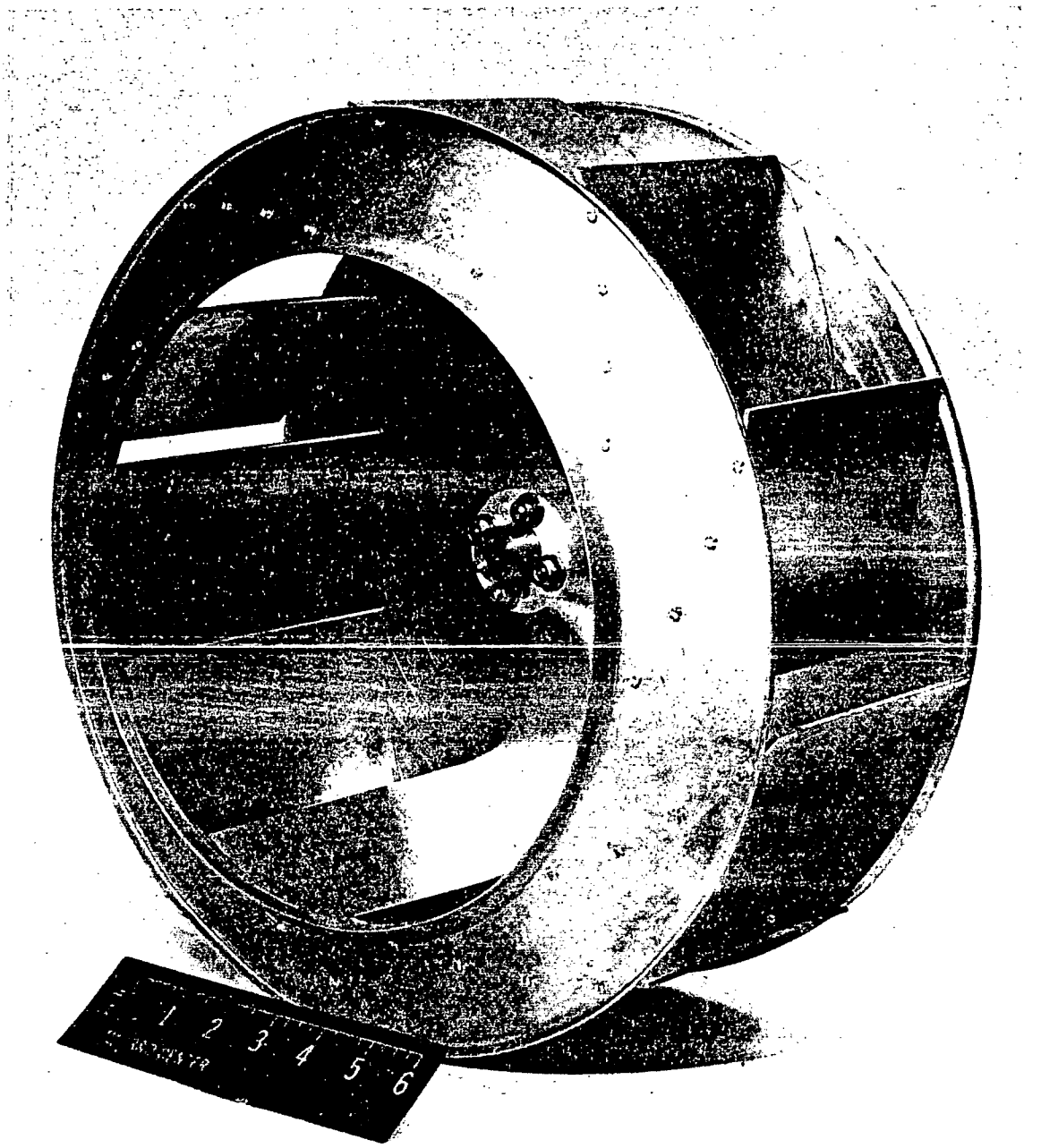


Fig. 9 - High-efficiency blower wheel

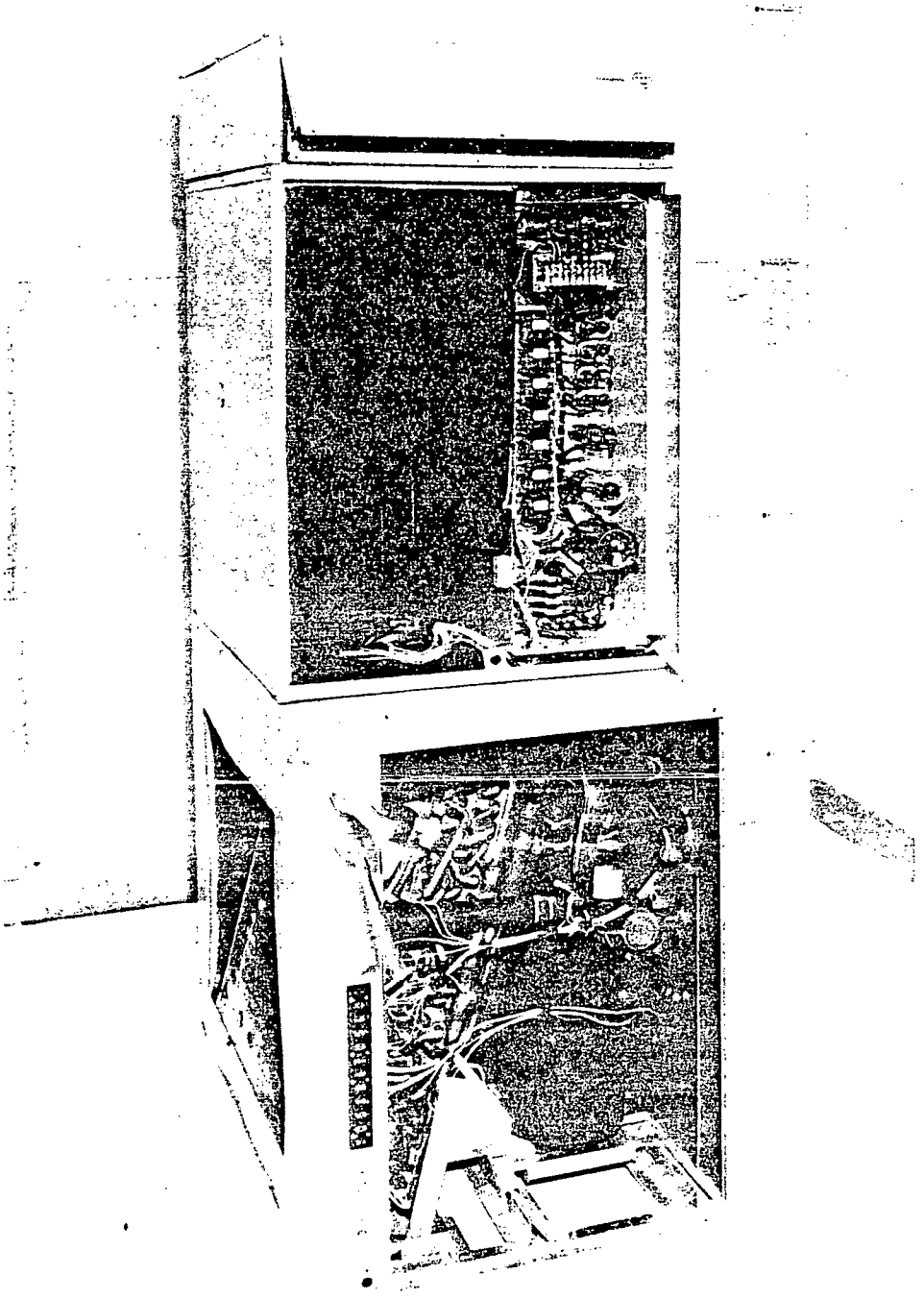

Fig. 10 - Preprototype indoor unit with access panels removed

The indoor unit is 22.5 inches wide, 36 inches deep and 63 inches high. These dimensions permit closet mounting, with either side or bottom air entry. Air entry in the upflow mode can be accommodated from either side or from the bottom with minor manipulation of the blower subassembly and the air mover module housing. Horizontal air flow installation is easily accommodated by stacking the air mover module alongside the refrigeration machine module. The resistance heat module is field modified to either a left- or right-handed configuration, as required. See Reference 4 and Section 5.0 for additional packaging information.

The design of both indoor and outdoor units permits flexible installation in any climatic region with high performance, reliability and ease of service.

A schematic of the refrigerant circuit for the system is shown in Figure 11. Note that the excitation of the electric expansion valve is a preprogrammed function of the outdoor ambient temperature in order to effect the desired level of condenser subcooling during heating and evaporator superheat during cooling. See Section 4.4 for additional refrigerant circuit information.

The high-efficiency hermetic compressor utilizes a unique, patented, low-cost means to achieve two-step capacity modulation via stroke change. The concept employs a circular, eccentrically bored cam between crankpin and connecting rod. The cam is shown mounted on the crankshaft in Figure 12. The action of the cam is such that it is driven against one of two rotational stops attached to the crankpin, depending upon the direction of rotation of the crankshaft.

In one cam position, the connecting rod reciprocates at its maximum stroke, displacing the piston to its minimum clearance volume position at top dead center. At the other cam position, corresponding to crankshaft rotation in the opposite sense, the connecting rod reciprocates with a much shorter stroke, and thus, with a much greater clearance volume at top dead-center position. The ratio of minimum to maximum compressor stroke is determined by the cam eccentricity. In the

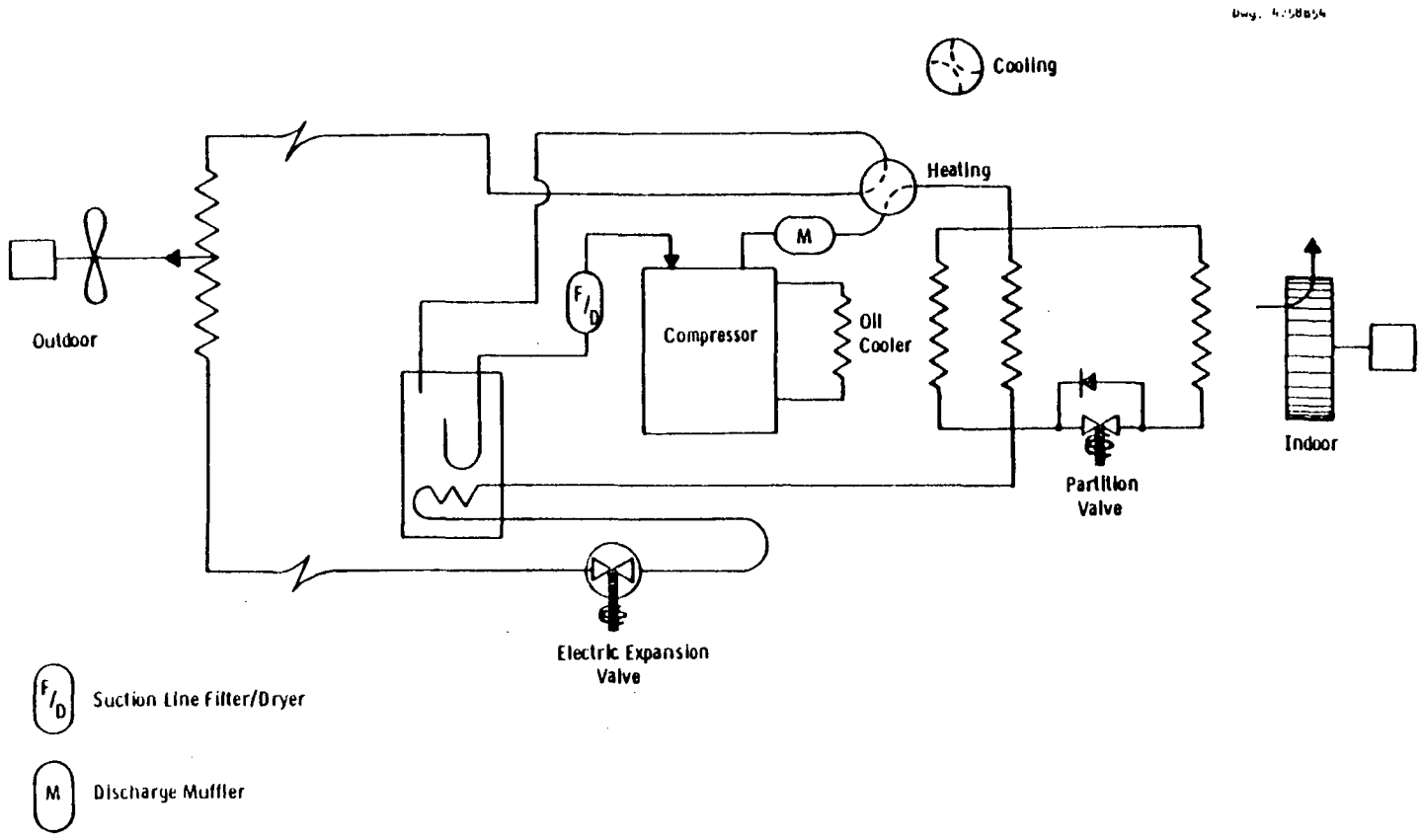


Fig. 1 - Advanced electric heat pump refrigeration circuit

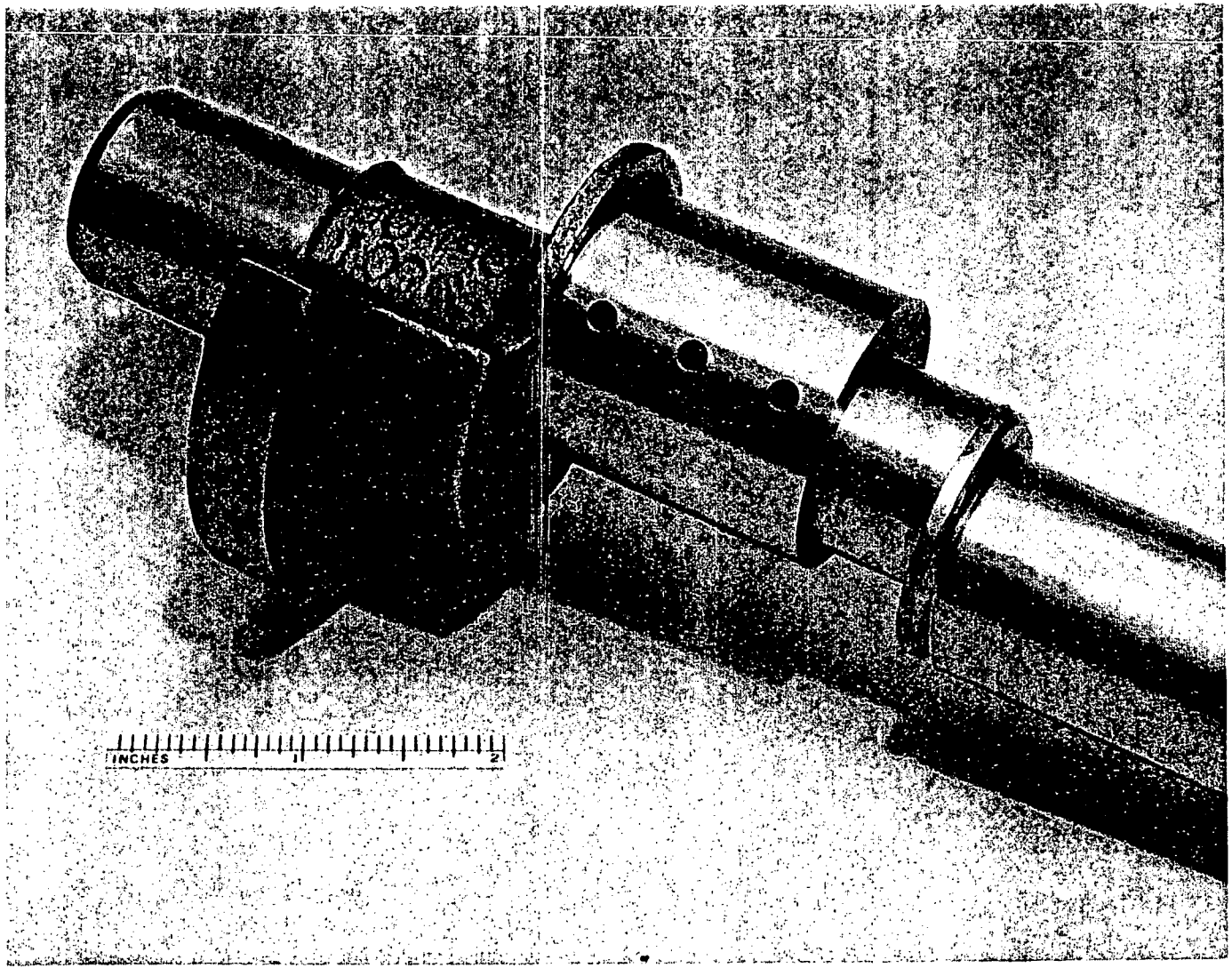


Fig. 12 - Crankshaft with dual-stroke cam

shorter stroke position, compressor flow rate, hence capacity, is decreased by both the reduction of piston displacement and the reduction of compressor volumetric efficiency because of increased clearance volume. In addition to the dual-stroke mechanism, the preprototype compressor embodies complimentary efficiency improving design features. These include (1) the use of an oil circulation pump and an external air cooled oil cooler to remove drive motor heat, compressor thermal losses and frictional dissipation so that the suction gas may be ducted directly to a liquid separator and then to the compressor cylinders; (2) a cantilevered flapper discharge valve, an open center suction valve and a crowned piston to decrease clearance volume and improve compressor breathing thereby improving volumetric efficiency; (3) a low pressure drop discharge manifolding system with an external muffler, and (4) a matched dual-strength, high-efficiency drive motor. Additional compressor details can be found in Section 4.1 and Reference 4 and 9.

A schematic drawing of the control system is shown in Figure 13. An autotransformer (150 VA) is used to supply 24 VAC from the secondary winding to the control relays and from the multitapped primary winding appropriate voltages are available to permit independent energization of main and auxiliary windings of both the blower and fan motors through the appropriate capacitor network. See Section 4.5 for details. This permits deep speed reduction for the air mover motors with high efficiency. Both air mover motors have integral thermal protection and separate line fuse protection for each winding. Autotransformer taps for ±10 percent of nominal voltage (230 VAC) are provided so that the air movers can be set to operate at proper speed(s) over a range of supply line voltages. The outdoor fan motor is heated during off-cycle cold weather ambient conditions by passing a trickle current through the auxiliary winding in order to keep the motor dry and free turning.

The compressor is switched between high and low capacity by reversing the direction of rotation of the single-speed drive motor.

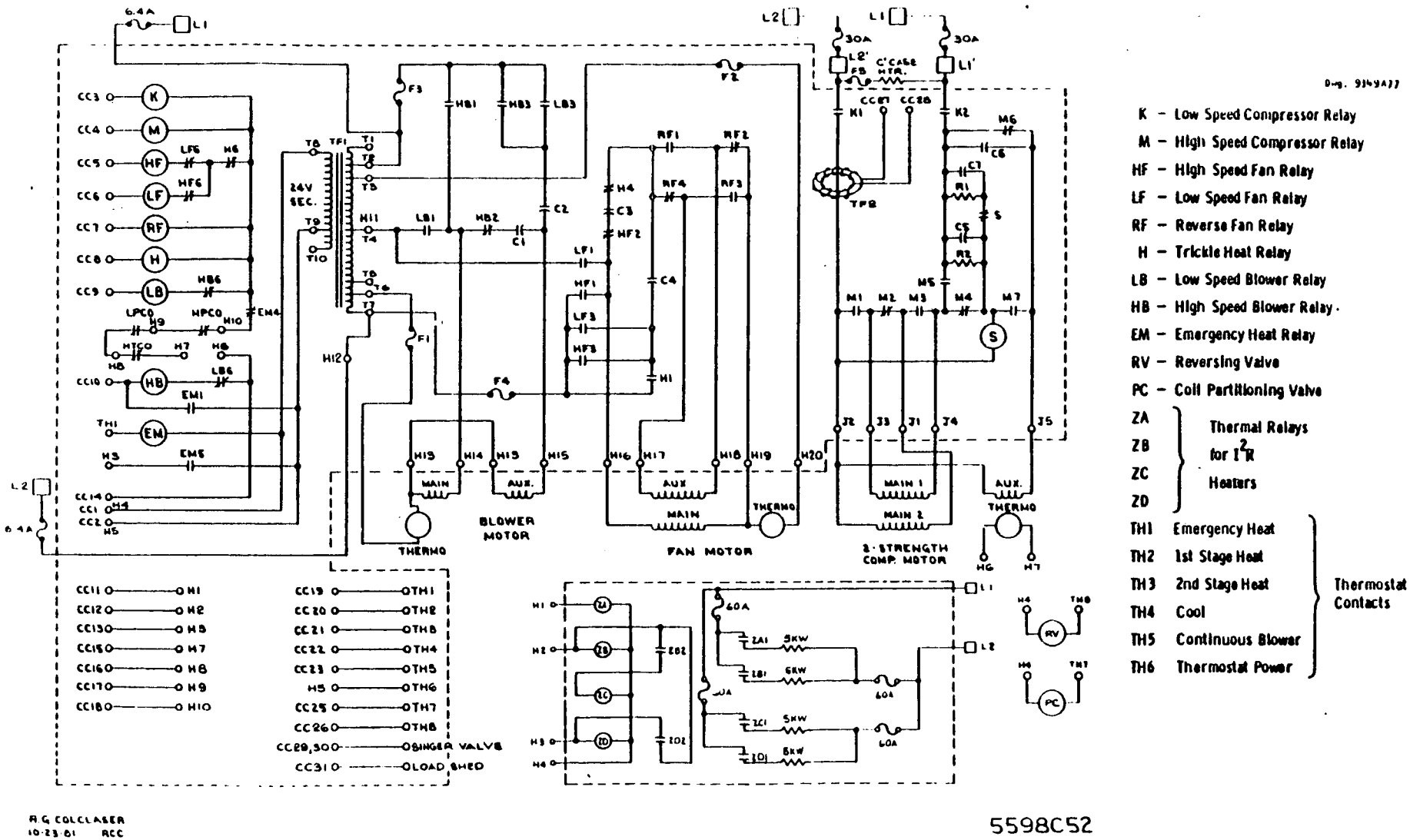


Fig. 13 - Control schematic

The compressor drive motor is a high-efficiency dual-strength design. Dual-strength operation is accomplished through an interchange of the roles of main and auxiliary winding, a reconnection of the two halves of the main winding from parallel to series connection, plus a switching in the arrangement of capacitors. Capacity switchover is accomplished automatically upon demand by first switching off the compressor motor, then rearranging the motor and capacitor connections to enable motor rotation reversal, and then restarting after a suitable time delay. Note that a current transformer is provided to sense that the compressor is indeed off before attempting capacity switch-over. Compressor motor thermal protection is provided by sensing the temperature of the auxiliary winding and providing external means for shut off.

The belly band crankcase heater is the self-regulating temperature type. The compressor is protected from extreme operating conditions by (1) a high pressure cut-out, and (2) a high discharge temperature cut-out in the compressor discharge line, (3) a low pressure cut-out in the suction line, and (4) two line fuses. Additional system protection features are part of the microprocessor software. See Section 4.5 for additional control information.

In cooling mode the indoor air mover operates at high speed for both compressor capacity modes. The outdoor fan will run at high speed during cooling until the outdoor ambient temperature drops below a set value, typically 75°F. During low-capacity cooling one-third of the evaporator coil is valved out of circuit in order to maintain adequate moisture removal.

In heating mode the outdoor fan runs at high speed and the indoor blower speed varies between high and low corresponding to the compressor capacity mode. After the compressor cycles off, the blower runs until the delivered air temperature drops to a preset value.

Defrost control is of the demand type. Whenever the temperature difference between the evaporator inlet and the outdoor ambient exceeds a critical value (typically 20°F) a defrost is initiated. A back up

timer will initiate a defrost after accumulating 4.27 hours (256 minutes) of compressor run time without a defrost at ambient temperatures below 40°F. Note that 256 represents the maximum number of minutes that can be counted and accumulated in an 8 bit memory register. During the defrost cycle the electric expansion valve is driven to the fully open position so as to maximize defrosting refrigerant flow. Defrost termination is initiated whenever the temperature of the refrigerant leaving the outdoor coil exceeds a specific value or when a defrost cycle has lasted longer than ten minutes.

Before returning to normal heating mode, the outdoor fan starts, runs for a period of time in the reverse direction to blow frost-melt water off the coil and then stops. Additional control system details are provided in Section 4.5

The control system is designed to provide user comfort with high system efficiency through system management. In addition it is designed to protect the system in the event that a system component fails or some anomalous operating condition arises. Should the microprocessor fail, the system will revert to the emergency heat mode. The state of the various relays and protective cut outs are continuously monitored and stored in memory so that in the event of a fault or system failure, the microprocessor memory can be interrogated to determine conditions just prior to the fault.

The dry weight of the preprototype advanced heat pump is 445 pounds for the indoor unit and 258 pounds for the outdoor unit. The unit including 20 feet of connecting lines is charged with 16.5 pounds of Refrigerant 22 and 2.25 pounds of DuPont Zephron$^R$ lubricating oil. The vapor line (heating) is 1.125 inch I.D. tubing and the liquid line 0.50 inch outside diameter. The estimated suggested retail price for this heat pump is $3100, approximately 25 percent more than a conventional heat pump of comparable maximum capacity. See Sections 5.0 and 6.0 for additional details.

## 2.2 Conclusions

(1) The advanced electric heat pump with dual-stroke compressor meets its performance objective by providing an estimated annual energy efficiency 20 percent better than the most efficient heat pump available at contract inception while maintaining traditionally accepted levels of comfort in both heating and cooling.

(2) The dual-stroke compressor, indoor blower, and outdoor fan can save sufficient energy relative to their commonly used alternatives so as to permit recovery of their premium first cost in less than four years of operation.

(3) The dual-stroke mechanism for capacity modulation is low in cost and is, in all likelihood, the lowest cost alternative available.

(4) A procedure for optimizing heat pump system proportions based upon estimated annual performance and life-cycle cost has been developed and applied.

(5) Additional testing, especially under field conditions, is necessary before commercialization can be expected.

(6) Reapplication of the optimization process would yield a better approximation to the optimum heat pump system since the process was halted prior to the availability of final performance and cost characteristics of constitutive design elements.

## 3. SYSTEM PERFORMANCE

### 3.1 Measured Steady State Performance - Preprototype Number One*

Several test runs were completed at each of the DOE test conditions[6]. The test results for the heating runs with the lowest energy balance errors are tabulated in Table 2 and plotted in Figure 14 along with the analytically predicted heating performance.**

In the high-capacity mode, the maximum difference between measured and predicted capacity is less than four percent, and the measured coefficient of performance is within five percent of the predicted value. The measured delivered air temperature is within 1°F of the predicted value over the entire operating range.

In the low-capacity mode the maximum difference between predicted and measured capacity is five percent. The coefficient of performance is higher than predicted at 35°F and 47°F and four percent less than predicted at 62°F. The measured delivered air temperature is within 2°F of the predicted value at all ambient temperatures.

The test results for cooling operation are summarized in Table 3 and plotted in Figure 15 along with the analytically predicted cooling performance.** In the high-capacity mode the capacity is four to ten percent less than predicted. This is primarily due to a higher than predicted refrigerant pressure drop in the evaporator. This results in a lower than expected compressor suction pressure and refrigerant flow. The lower than anticipated average evaporator temperature results in a higher latent capacity than predicted and a sensible/total capacity

---

* System instrumentation is given in Appendix A. Test facilities are described in Appendix B. Test procedure is in accordance with Reference 6.

** The system performance model used supersedes that used in the optimization analysis since it includes models for the components used in the preprototype whereas the optimization procedure utilized preliminary information.

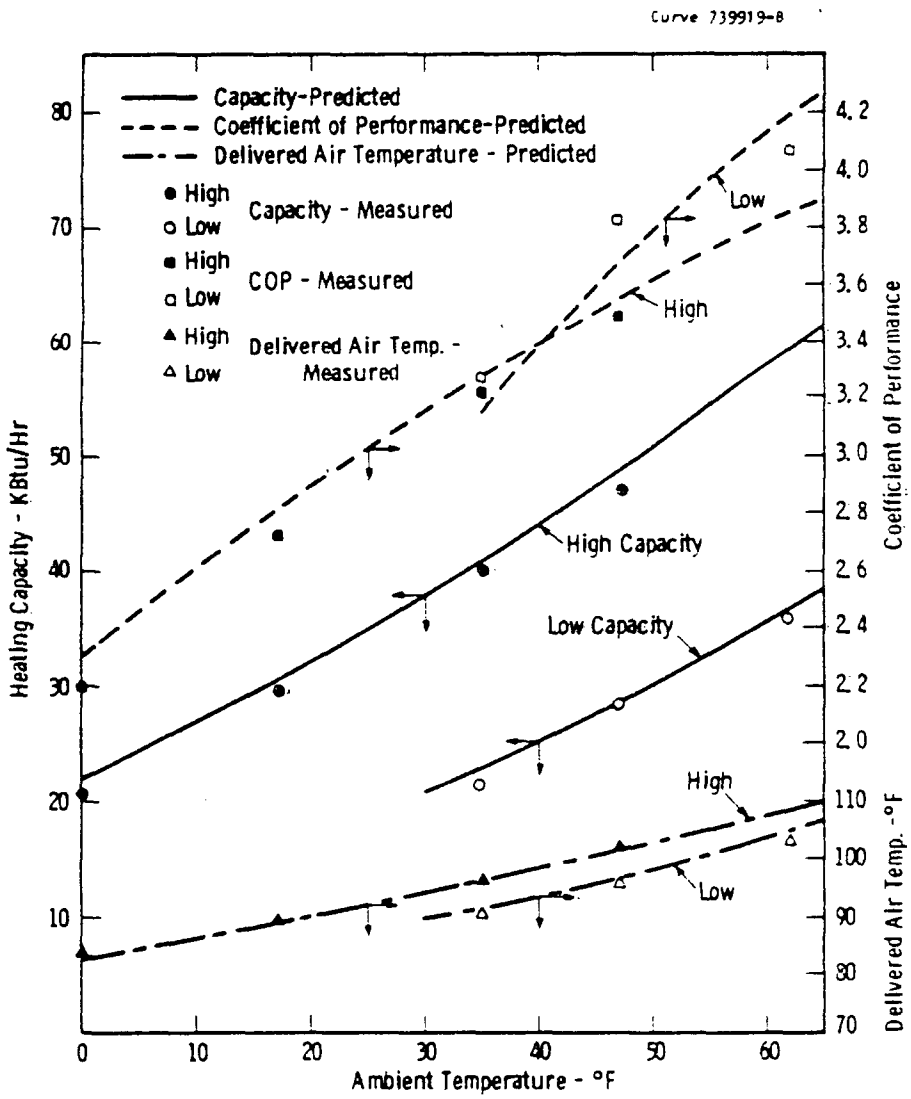


Fig. 14 - Comparison of analytically predicted and measured heating performance (Preprototype Number 1)

Curve 739920-B

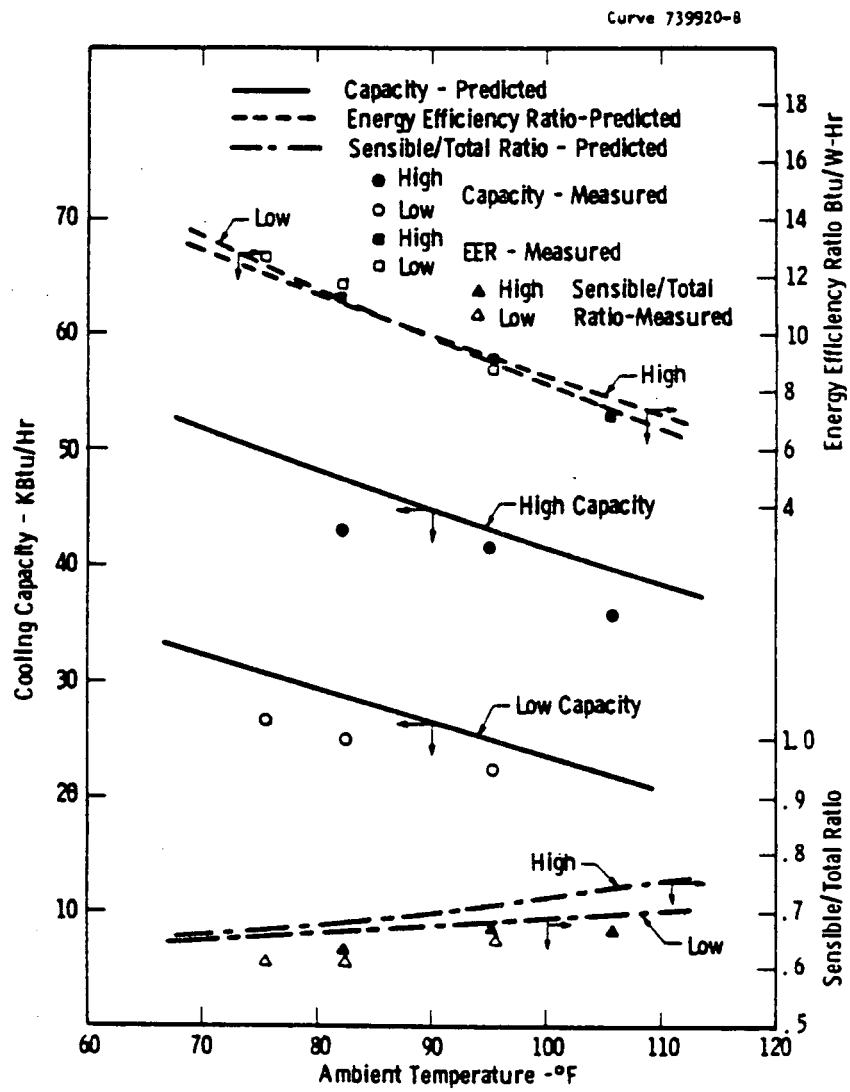


Fig. 15 - Comparison of analytically predicted and measured cooling performance (Preprototype Number 1)

TABLE 2

Preprototype Number One Measured Heating Performance

| Ambient Temp. °F | Heating Capacity Btu/hr | Power Input Watts+ | Coefficient of Performance+ | Delivered Air Temp. °F |
|---|---|---|---|---|
| | | High Capacity | | |
| 47 | 46829 | 3948 | 3.48 | 102* |
| 37 | 39809 | 3649 | 3.20 | 96 |
| 17 | 29392 | 3181 | 2.71 | 89*** |
| 0 | 20864 | 2787 | 2.19 | 84*** |
| | | Low Capacity | | |
| 62 | 37384 | 2713 | 4.04 | 103 |
| 47 | 28693 | 2195 | 3.83 | 95** |
| 35 | 21484 | 1930 | 3.26 | 91 |

* indoor air flow = 1300 scfm @ 1080 rpm
outdoor air flow = 3100 scfm @ 856 rpm

** indoor air flow = 923 scfm @ 772 rpm

***resistance heaters (normally enabled below 18°F) not used in this test

+a) Does not include crankcase heater power which averages approximately 40 W, but is a function of crankcase temperature

b) Does not include control relay power which ranges between 7 and 30 W, depending upon control state

c) Does not include microprocessor power of approximately 60 W

TABLE 3

Preprototype Number One Measured Cooling Performance

| Ambient Temp. °F | Cooling Capacity Btu/hr | Power Input Watts+ | Energy Efficiency Ratio Btu/W-hr+ | Sensible/ Total Ratio |
|---|---|---|---|---|
| | | High Capacity | | |
| 82 | 42734 | 3817 | 11.2 | 0.63 |
| 95 | 41466 | 4571 | 9.1 | 0.67* |
| 106 | 35586 | 5043 | 7.1 | 0.67 |
| | | Low Capacity | | |
| 76 | 26611 | 2110 | 12.6 | 0.61 |
| 82 | 24991 | 2192 | 11.4 | 0.61 |
| 95 | 22551 | 2630 | 8.6 | 0.65 |

*indoor air flow = 1335 scfm at 1089 rpm (wet coil)

outdoor air flow = 2600 scfm at 851 rpm

+a) Does not include crankcase heater power which averages approximately 40 W, but is a function of crankcase temperature

b) Does not include control relay power which ranges between 7 and 30 W, depending upon control state

c) Does not include microprocessor power of approximately 60 W

ratio lower than expected. The measured energy efficiency ratios are in good agreement with the predicted values. At 106°F the lower than predicted capacity is partly due to the fact that the desired suction pressure could not be obtained due to inadequate capacity in the expansion valve. This problem was eliminated in the second preprototype by using an expansion valve with a larger orifice.

In the low-capacity mode the measured capacity was 9 to 12 percent less than predicted, primarily due to a higher than predicted refrigerant pressure drop in the evaporator. The measured latent capacity was higher than predicted giving sensible/total ratios less than anticipated and well below the desired maximum value of 0.7 over the normal operating range.

### 3.2 Cyclic Degradation

The DOE cyclic degradation tests[6] were performed in heating and cooling modes at both capacity levels. The results are summarized in Table 4.

In the heating mode in high capacity a $C_D$ of 0.18 was obtained by starting and stopping the indoor blower at the same time as the compressor. By allowing the indoor blower to operate for 60 seconds after compressor shutdown a $C_D$ of 0.04 was obtained. In the low-capacity mode, in heating, a $C_D$ of 0.28 was obtained by starting and stopping the indoor blower simultaneously with the compressor. Allowing the blower to operate for either 30 or 60 seconds after compressor shutdown reduced the $C_D$ to 0.20. Delaying by 20 seconds the start of the indoor blower after compressor start in combination with a 30 second delay in blower shutdown after compressor shutdown lowered the $C_D$ to 0.18.

The values of $C_D$ obtained during cooling tests were unexpectedly high. In the high-capacity cooling mode a $C_D$ of 0.29 was obtained with a 30 second delay in blower startup and shutdown. The minimum value of $C_D$ obtained in low-capacity cooling was 0.34 with a 90 second delay in blower startup and shutdown plus decreasing the expansion valve

Table 4

Measured Cyclic Degradation Coefficients - Preprototype Number One

| | Blower On Delay-seconds | Blower Off Delay-Seconds | $C_D$ |
|---|---|---|---|
| High-Capacity Heat | 0 | 0 | .18 |
| | 0 | 60 | .04 |
| Low-Capacity Heat | 0 | 0 | .28 |
| | 0 | 30 | .20 |
| | 0 | 60 | .20 |
| | 20 | 30 | .18 |
| High-Capacity Cool | 30 | 30 | .29 |
| Low-Capacity Cool | 0 | 0 | .52 |
| | 0 | 30 | .54 |
| | 20 | 30 | .42 |
| | 40 | 30 | .39 |
| | 90 | 90 | .36 |
| | 90 | 90 | .34* |

*Expansion valve voltage reduced 50 percent for 120 seconds following compressor start

opening at compressor shutdown and maintaining the reduced opening for 120 seconds after compressor startup. This procedure permits some realization of the cooling effect available from the evaporator liquid inventory on shutdown and permits more rapid attainment of steady state conditions upon startup. The high values of $C_D$ in cooling are felt to be the result of the heating effect of the indoor compressor plus the oil cooler during the off cycle.

Test results emphasized the necessity of completing several cycles to obtain accurate results. There is a marked "ratcheting" effect and the first two or three cycles gave significantly lower values of $C_D$ than subsequent runs in both heating and cooling. For example, the results for low-capacity cooling mode with 90 second fan delays on both startup and shutdown are shown in Table 5. Inspection of the data shows that true steady state operation is not achieved during the six minute on time. This appears to be the result of the thermal inertia of the heavily insulated code test boxes rather than the heat pump itself.

TABLE 5

Measured Cyclic Degradation Coefficient as a Function of Cycle Number (Low-capacity cooling mode, 90 second fan delays start and shutdown)

| Cycle | $C_D$ |
|---|---|
| 1 | 0.21 |
| 2 | 0.31 |
| 3 | 0.36 |
| 4 | 0.36 |

### 3.3 Frost Accumulation

The large outdoor coil surface results in a lower than normal temperature difference between the coil surface and ambient air. This reduces the driving potential for mass transport resulting in an unusually low rate of frost accumulation. In the low-capacity mode the unit was operated for more than six hours at the DOE frost accumulation test conditions[6] with no significant frost buildup. In the high-capacity mode the unit was defrosted and operated for 4 hours 52 minutes before a second defrost was needed. The integrated capacity between the termination of the first defrost and the termination of the second

defrost was 4.4 percent less than the clear coil value. The integrated energy efficiency ratio was 3.7 percent less than the clear coil value.

### 3.4 Measured Steady State Performance - Preprototype Number Two

Preprototype number two is identical to the first preprototype in most respects. The differences include:

- The positions of the compressor and accumulator have been interchanged to simplify the piping.
- All thermocouple penetrations into the refrigerant circuit have been eliminated to minimize the potential for refrigerant leaks. (Note that preprototype two is intended for field evaluation).
- One hairpin tube in the indoor air-to-refrigerant heat exchanger has been bypassed to repair a refrigerant leak.
- An electric expansion valve with a larger orifice has been used to obtain higher evaporator pressures in the cooling mode.
- The blower discharge area has been increased by reducing the length of the cut off portion of the scroll.

Interchanging the accumulator and compressor and eliminating the thermocouple penetrations have no significant influence on system capacity or efficiency. The loss of one hairpin tube in the indoor coil reduces the effective heat transfer area by less than 2 percent. Circuitry details are discussed in Section 4.4.

Heating test results are summarized in Table 6. Performance is very similar to that exhibited by the first preprototype.

Due to the fact that temperature measurements in the refrigerant circuit were obtained with thermocouples attached to the surface of the piping rather than inserted into the refrigerant stream, these measurements are less accurate than those obtained for preprototype number one. This was reflected in generally less accurate energy balances during the testing.

Table 6

Preprototype Number Two Measured Heating Performance

| Ambient Temp. °F | Heating Capacity Btu/hr | Power Input Watts* | Coefficient of Performance* | Delivered Air Temp. °F |
|---|---|---|---|---|
| | | High Capacity | | |
| 47 | 47771 | 4007 | 3.49 | 101 |
| 35 | 41154 | 3665 | 3.29 | 95 |
| 17 | 29643 | 3187 | 2.72 | 89** |
| 0 | 19029 | 2783 | 2.00 | 83** |
| | | Low Capacity | | |
| 62 | 35955 | 2640 | 3.99 | 102 |
| 47 | 30076 | 2329 | 3.78 | 95 |
| 35 | 22558 | 2085 | 3.17 | 90 |

* a) Does not include crankcase heater power which averages approximately 40 W, but is a function of crankcase temperature

b) Does not include control relay power which ranges between 7 and 30 W, depending upon control state

c) Does not include microprocessor power of approximately 60 W

** resistance heaters (normally enabled below 18°F) not used in this test

Test results for the cooling mode are summarized in Table 7. The energy efficiency ratio for unit two is generally slightly lower than for unit one. This may be the result of the altered refrigerant circuit in the indoor coil. Since one of the six refrigerant circuits has fewer tubes than the remaining five, the refrigerant flow will tend to be higher in this circuit due to reduced pressure drop. However this circuit has less heat transfer surface and its capacity will be lower than the other circuits. The remaining five circuits will have reduced capacity due to reduced refrigerant flow. An unbalanced flow condition is detrimental to heat exchanger performance, particularly in evaporator service.

The increased orifice size in the expansion valve has eliminated the choked refrigerant flow condition in the high-capacity mode at high ambient temperature. Preprototype number two did not exhibit the sharp decline in capacity and efficiency at high ambient temperatures in the high-capacity mode observed in unit one.

### 3.5 Seasonal Performance

Seasonal performance of dual-capacity heat pumps is estimated using the Westinghouse/DOE method, an improved version of the DOE method[6] for calculating heat pump seasonal and annual performance. Comparing to the DOE method, the Westinghouse/DOE method possesses the following features:

1. Site specific seasonal heating and cooling hours, instead of fictitious heating load hours and cooling load hours, are used to calculate the seasonal loads.

2. The heating load is unambiguously defined in terms of the low temperature heat pump balance point.

3. The sensible cooling load line is defined as having the same slope as the heating load line with solar and latent cooling loads considered through use of a parametrically defined multiplicative factor for the load line slope.

Table 7

Preprototype Number Two Measured Cooling Performance

| Ambient Temp. °F | Cooling Capacity Btu/hr | Power Input Watts * | Energy Efficiency Ratio Btu/W-hr * | Sensible Total Ratio |
|---|---|---|---|---|
| | | High Capacity | | |
| 83 | 42222 | 4004 | 10.5 | .70 |
| 96 | 39373 | 4402 | 8.9 | .67 |
| 102 | 37677 | 4587 | 8.2 | .67 |
| | | Low Capacity | | |
| 76 | 28481 | 2425 | 11.7 | .64 |
| 83 | 27373 | 2510 | 10.9 | .63 |
| 91 | 26292 | 2579 | 10.2 | .68 |

* a) Does not include crankcase heater power which averages approximately 40 W, but is a function of crankcase temperature

b) Does not include control relay power which ranges between 7 and 30 W, depending upon control state

c) Does not include microprocessor power of approximately 60 W

4. The optimum host housing size for a given heat pump can be determined.

5. The optimum heat pump capacity for a given host house can be determined.

6. The annual cost (energy cost + capital cost + maintenance cost) of the heat pump is calculated in the computer program.

7. The energy consumed by the crankcase heater and the control equipment can be separately accumulated and included in the energy cost calculation while being excluded from the cyclic degradation estimate.

8. Site specific, instead of regionally averaged, bin temperature data can be used in the performance computation.

9. The cyclic performance degradation associated with switching between high and low-capacity operation for a dual-capacity heat pump is taken into account in the performance computation in addition to an on/off cyclic degradation.

See Reference 5 for additional information. Tables 8 and 9 give the estimated seasonal performance of the advanced heat pump in Minneapolis. Performance details for other cities may be found in Appendix C.

Table 8 - Seasonal Heating Performance in Minneapolis

*** COMPUTATIONAL RESULTS FOR HEATING SEASON ***

| BIN J | T(J) DEG.F | BIN HRS | QDOT1 BTU/H | QDOT2 BTU/H | EDOT1 W | EDOT2 W | BLH BTU/H | CASE | DELTA | BLH/M | E/M BTU/H | RH/M W | BLH W | CASE | DELTA BTU/H | BLH/M | E/M | RH/M BTU/H W |
|---|---|---|---|---|---|---|---|---|---|---|---|---|---|---|---|---|---|---|
| 1 | 62. | 0.119 | 38225. | 55548. | 2575.0 | 4331.5 | 2000. | 1 | 1.0 | 238.0 | 17.7 | 0.0 | 2000. | 1 | 1.0 | 238.0 | 17.7 | 0.0 |
| 2 | 57. | 0.094 | 35048. | 52641. | 2448.3 | 4203.7 | 5333. | 1 | 1.0 | 501.3 | 38.3 | 0.0 | 5333. | 1 | 1.0 | 501.3 | 38.3 | 0.0 |
| 3 | 52. | 0.051 | 31870. | 49735. | 2321.7 | 4075.8 | 8667. | 1 | 1.0 | 442.0 | 34.7 | 0.0 | 8667. | 1 | 1.0 | 442.0 | 34.7 | 0.0 |
| 4 | 47. | 0.058 | 28693. | 46829. | 2195.0 | 3948.0 | 12000. | 1 | 1.0 | 696.0 | 56.5 | 0.0 | 12000. | 1 | 1.0 | 696.0 | 56.5 | 0.0 |
| 5 | 42. | 0.073 | 25516. | 41814. | 2068.3 | 3831.0 | 15333. | 1 | 1.0 | 1119.3 | 94.5 | 0.0 | 15333. | 1 | 1.0 | 1119.3 | 94.5 | 0.0 |
| 6 | 37. | 0.138 | 21774. | 39330. | 1971.9 | 3701.0 | 18667. | 1 | 1.0 | 2576.0 | 236.7 | 0.0 | 18667. | 1 | 1.0 | 2576.0 | 236.7 | 0.0 |
| 7 | 32. | 0.119 | 0. | 36845. | 0.0 | 3571.0 | 22000. | 3 | 1.0 | 2618.0 | 264.4 | 0.0 | 22000. | 3 | 1.0 | 2618.0 | 264.4 | 0.0 |
| 8 | 27. | 0.075 | 0. | 34361. | 0.0 | 3441.0 | 25333. | 3 | 1.0 | 1900.0 | 195.4 | 0.0 | 25333. | 3 | 1.0 | 1900.0 | 195.4 | 0.0 |
| 9 | 22. | 0.084 | 0. | 31876. | 0.0 | 3311.0 | 28667. | 3 | 1.0 | 2408.0 | 252.7 | 0.0 | 28667. | 3 | 1.0 | 2408.0 | 252.7 | 0.0 |
| 10 | 17. | 0.065 | 0. | 29392. | 0.0 | 3181.0 | 32000. | 4 | 1.0 | 2080.0 | 206.8 | 49.7 | 32000. | 4 | 1.0 | 2080.0 | 206.8 | 49.7 |
| 11 | 12. | 0.040 | 0. | 26486. | 0.0 | 3053.2 | 35334. | 4 | 1.0 | 1413.3 | 122.1 | 103.7 | 35334. | 4 | 1.0 | 1413.3 | 122.1 | 103.7 |
| 12 | 7. | 0.031 | 0. | 23580. | 0.0 | 2925.3 | 38667. | 4 | 1.0 | 1198.7 | 90.7 | 137.0 | 38667. | 4 | 1.0 | 1198.7 | 90.7 | 137.0 |
| 13 | 2. | 0.017 | 0. | 20674. | 0.0 | 2797.5 | 42000. | 4 | 1.0 | 714.0 | 47.6 | 106.2 | 42000. | 4 | 1.0 | 714.0 | 47.6 | 106.2 |
| 14 | -3. | 0.019 | 0. | 17767. | 0.0 | 2669.7 | 45334. | 4 | 1.0 | 861.3 | 50.7 | 153.5 | 45334. | 4 | 1.0 | 861.3 | 50.7 | 153.5 |
| 15 | -8. | 0.013 | 0. | 14861. | 0.0 | 2541.8 | 48667. | 4 | 1.0 | 632.7 | 33.0 | 128.8 | 48667. | 4 | 1.0 | 632.7 | 33.0 | 128.8 |
| 16 | -13. | 0.004 | 0. | 11955. | 0.0 | 2414.0 | 52000. | 4 | 1.0 | 208.0 | 9.7 | 46.9 | 52000. | 4 | 1.0 | 208.0 | 9.7 | 46.9 |
| 17 | -18. | 0.001 | 0. | 9049. | 0.0 | 2286.2 | 55334. | 4 | 1.0 | 55.3 | 2.3 | 13.6 | 55334. | 4 | 1.0 | 55.3 | 2.3 | 13.6 |
| 18 | -23. | 0.001 | 0. | 6143. | 0.0 | 2158.3 | 58667. | 4 | 0.0 | 58.7 | 0.0 | 17.2 | 58667. | 4 | 0.0 | 58.7 | 0.0 | 17.2 |
| | | | | | | | | | | 19720.8 | 1753.7 | 756.5 | | | | 19720.8 | 1753.7 | 756.5 TOTAL |

| J | HEAT INPUT** | E. PUMP* | E. REST* | E. CHE* | E. CTL* | E. SUM* | COP |
|---|---|---|---|---|---|---|---|
| 1 | 1552005.75 | 115494.98 | 0.00 | 55154.79 | 38799.95 | 209449.72 | 2.17 |
| 2 | 3269210.75 | 249534.19 | 0.00 | 38977.12 | 30648.70 | 319160.00 | 3.00 |
| 3 | 2882296.25 | 226454.78 | 0.00 | 18159.96 | 16628.55 | 261243.28 | 3.23 |
| 4 | 4538638.50 | 368650.81 | 0.00 | 16502.90 | 18910.90 | 404064.63 | 3.29 |
| 5 | 7299209.00 | 616276.56 | 0.00 | 14247.39 | 23801.65 | 654325.56 | 3.27 |
| 6 | 16798178.00 | 1543272.87 | 0.00 | 9632.30 | 44994.90 | 1597900.00 | 3.08 |
| 7 | 17072064.00 | 1724061.25 | 0.00 | 23449.21 | 38799.95 | 1786310.50 | 2.80 |
| 8 | 12389962.00 | 1274242.37 | 0.00 | 9636.93 | 24453.75 | 1308333.00 | 2.77 |
| 9 | 15702646.00 | 1647619.25 | 0.00 | 4136.61 | 27388.20 | 1679144.12 | 2.74 |
| 10 | 13563747.00 | 1348314.50 | 323910.88 | 0.00 | 21193.25 | 1693418.62 | 2.35 |
| 11 | 9216392.00 | 796388.00 | 676187.31 | 0.00 | 13042.00 | 1485617.37 | 1.82 |
| 12 | 7816544.00 | 591359.00 | 893610.06 | 0.00 | 10107.55 | 1495076.62 | 1.53 |
| 13 | 4656017.00 | 310122.47 | 692708.75 | 0.00 | 5542.85 | 1008374.12 | 1.35 |
| 14 | 5616782.50 | 330769.03 | 1000711.19 | 0.00 | 6194.95 | 1337675.25 | 1.23 |
| 15 | 4125640.25 | 215478.84 | 839676.06 | 0.00 | 4238.65 | 1059393.50 | 1.14 |
| 16 | 1356374.75 | 62966.78 | 306047.63 | 0.00 | 1304.20 | 370318.59 | 1.07 |
| 17 | 360830.47 | 14908.09 | 88433.35 | 0.00 | 326.05 | 103667.49 | 1.02 |
| 18 | 382567.22 | 0.00 | 112091.20 | 489.08 | 326.05 | 112906.32 | 0.99 |

HSPF 7.62 SEASONAL LOAD 128599112.0**

ELECTRICITY INPUT TO HEAT PUMP 11435914.0* ELECTRICITY INPUT TO RESISTANCE HEATER 4933377.0*

ELECTRICITY INPUT TO CRANKCASE HEATER 190386.3* ELECTRICITY INPUT TO CONTROL EQUIPMENTS 326050.0*

TOTAL ELECTRICITY INPUT 16885728.0*

SEASONAL HEATING HOURS 6521.0 HEAT DELIVERED BY HEAT PUMP 111761512.0**

HEAT DELIVERED BY RESISTANCE HEATER 16837616.0** HEAT DEFICIENCY 16837600.0**

RUNNING HOURS HIGH CAPACITY 2589.7 LOW CAPACITY 1492.9

NOTE

(1) * units are watt-hours (Wh)
(2) ** units are Btu
(3) See nomenclature

Table 9 - Seasonal Cooling Performance in Minneapolis

*** COMPUTATIONAL RESULTS FOR COOLING SEASON ***

| BIN J | T(J) DEG.F | BIN HRS | BLC BTU/H | QSS1 BTU/H | QSS2 BTU/H | ESS1 W | ESS2 W | CASE | X1 | X2 | Q/N BTU/H | E/N W |
|---|---|---|---|---|---|---|---|---|---|---|---|---|
| 1 | 67. | 0.268 | 1867. | 27806. | 44220. | 1686.6 | 2947.0 | 1 | 0.067 | 0.000 | 500.3 | 33.5 |
| 2 | 72. | 0.226 | 6533. | 26868. | 43725. | 1855.1 | 3237.0 | 1 | 0.243 | 0.000 | 1476.5 | 110.3 |
| 3 | 77. | 0.234 | 11200. | 25929. | 43229. | 2023.5 | 3527.0 | 1 | 0.432 | 0.000 | 2620.8 | 216.8 |
| 4 | 82. | 0.188 | 15867. | 24991. | 42734. | 2192.0 | 3817.0 | 1 | 0.635 | 0.000 | 2982.9 | 271.6 |
| 5 | 87. | 0.075 | 20533. | 24053. | 42239. | 2360.5 | 4107.0 | 1 | 0.854 | 0.000 | 1540.0 | 153.4 |
| 6 | 92. | 0.008 | 25200. | 23114. | 41743. | 2528.9 | 4397.0 | 3 | 0.000 | 0.604 | 201.6 | 22.1 |
| | | | | | | | | | | | 9322.2 | 807.6 TOTAL |

| J | BLDG LOAD * | HP CAP * | E. PUMP * | E. CHE * | E. CTL * | E. SUM * | COP |
|---|---|---|---|---|---|---|---|
| 1 | 1120102.62 | 1120102.62 | 74930.64 | 41982.73 | 30002.60 | 146915.98 | 2.23 |
| 2 | 3305974.50 | 3305974.50 | 246948.61 | 28722.64 | 25300.70 | 300971.94 | 3.22 |
| 3 | 5868000.50 | 5868000.50 | 485519.78 | 22321.48 | 26196.30 | 534037.56 | 3.22 |
| 4 | 6678820.50 | 6678820.50 | 608008.44 | 11526.22 | 21046.60 | 640581.31 | 3.05 |
| 5 | 3448077.25 | 3448077.25 | 343410.88 | 1842.67 | 8396.25 | 353649.78 | 2.86 |
| 6 | 451384.66 | 451384.69 | 49508.41 | 532.40 | 895.60 | 50936.41 | 2.60 |

SEER 10.30 COOLING DELIVERED 20872360.0** ELECTRICITY INPUT TO HEAT PUMP 1808326.8*

ELECTRICITY INPUT TO CRANKCASE HEATER 106928.1* ELECTRICITY INPUT TO CONTROL EQUIPMENT 111950.0*

TOTAL ELECTRICITY INPUT 2027204.9* SEASONAL LOAD 20872360.0**

COOLING DEFICIENCY 0.0** COOLING COST 100.8 SEASONAL COOLING HOURS 2239.0

RUNNING HOURS HIGH CAPACITY 11.3 LOW CAPACITY 840.3

*** SUMMARY OF THE CALCULATION ***

HEAT PUMP OFF-TIME= 3825.82 ELECTRICITY INPUT DURING OFF-TIME= 191291.14*

HEATING COST= 839.22 COOLING COST= 100.75

FIXED CHARGE= 0.00 SUM OF HEATING AND COOLING COSTS= 939.97

ENERGY COST OF CRANKCASE HEATER AND CONTROL EQUIPMENTS DURING OFF-TIME= 9.51

TOTAL COST= 949.48

HEAT DELIVERED= 128599112.00** COOLING DELIVERED= 20872360.00**

TOTAL BTU DELIVERED= 149471472.00** COST PER MBTU DELIVERED= 6.35

NOTE

(1) * units are watt-hours (Wh)
(2) ** units are Btu
(3) Cost in $US
(4) See nomenclature

# 4. COMPONENT DESCRIPTION

## 4.1 Compressor

The key to a commercially viable high annual performance advanced electric heat pump is a high-efficiency hermetic compressor with low cost capacity modulation means. The performance advantage due to capacity modulation depends upon the range over which the compressor capacity can be modulated (i.e., the ratio of minimum to maximum capacity at a fixed set of conditions) and upon the number of capacity steps available in that range. Although continuous modulation would appear to be most advantageous in terms of performance, capacity modulation by means of two steps can yield performance nearly as good, provided the capacity ratio is judiciously chosen. The known means to provide stepwise variable compressor capacity include two-speed drive motors, cylinder suction cutoff, valve unloaders and parallel compressors. To complement these, Westinghouse has reduced to practice, during this development program, a dual-stroke mechanism that provides a step-wise capacity control of almost any desired capacity ratio at a lower cost than any other system currently available.

Our stroke changing mechanism is described in U.S. Patents 4,236,874 and 4,248,053 and consists of the circular, eccentrically bored cam shown in Figure 16 that mounts on the crankpin of the compressor as shown in Figure 12 and changes radial position relative to the crankshaft as a function of crankshaft rotation. The action of the cam is such that it is driven against one of two rotational stops depending on the direction of rotation of the crankshaft. A sketch of the eccentric cam in its two positions is shown in Figure 17.

In one cam position, the connecting rod reciprocates at its maximum stroke, displacing the piston to its minimum clearance volume

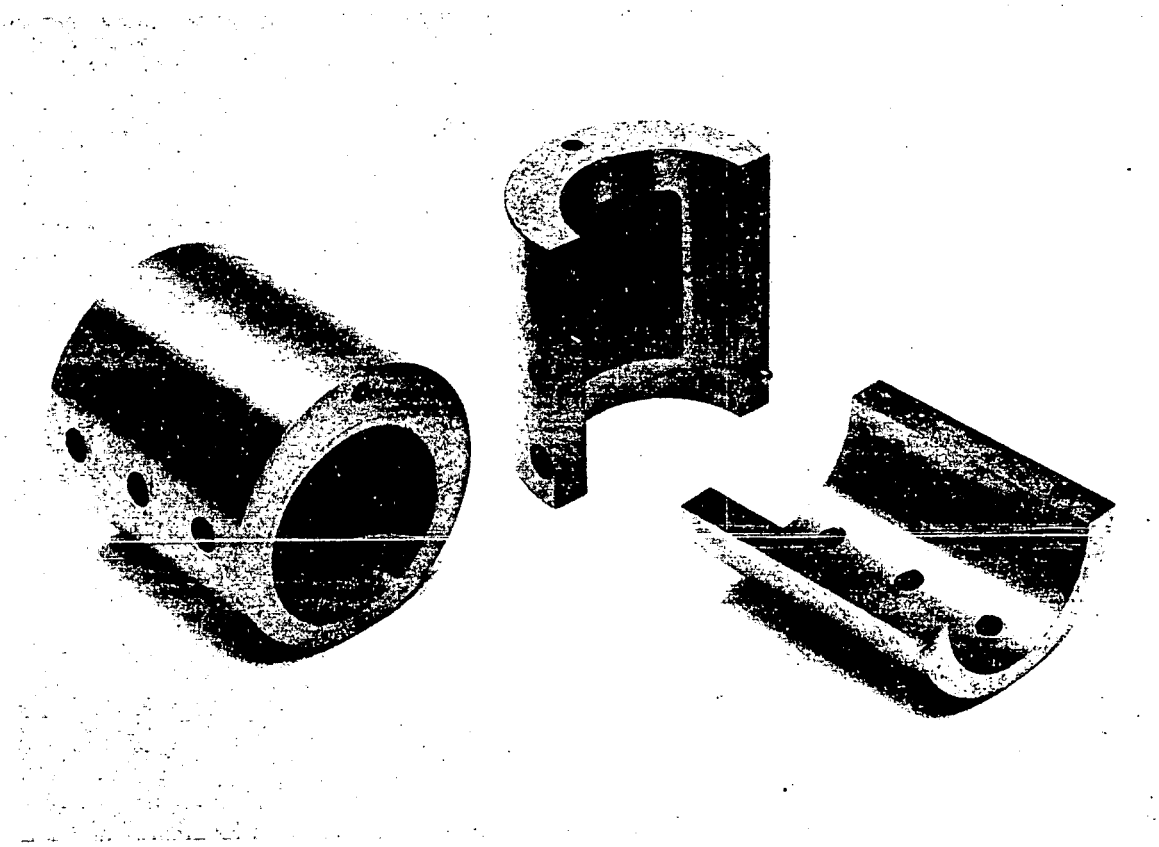

Fig. 16 - Dual-stroke cam

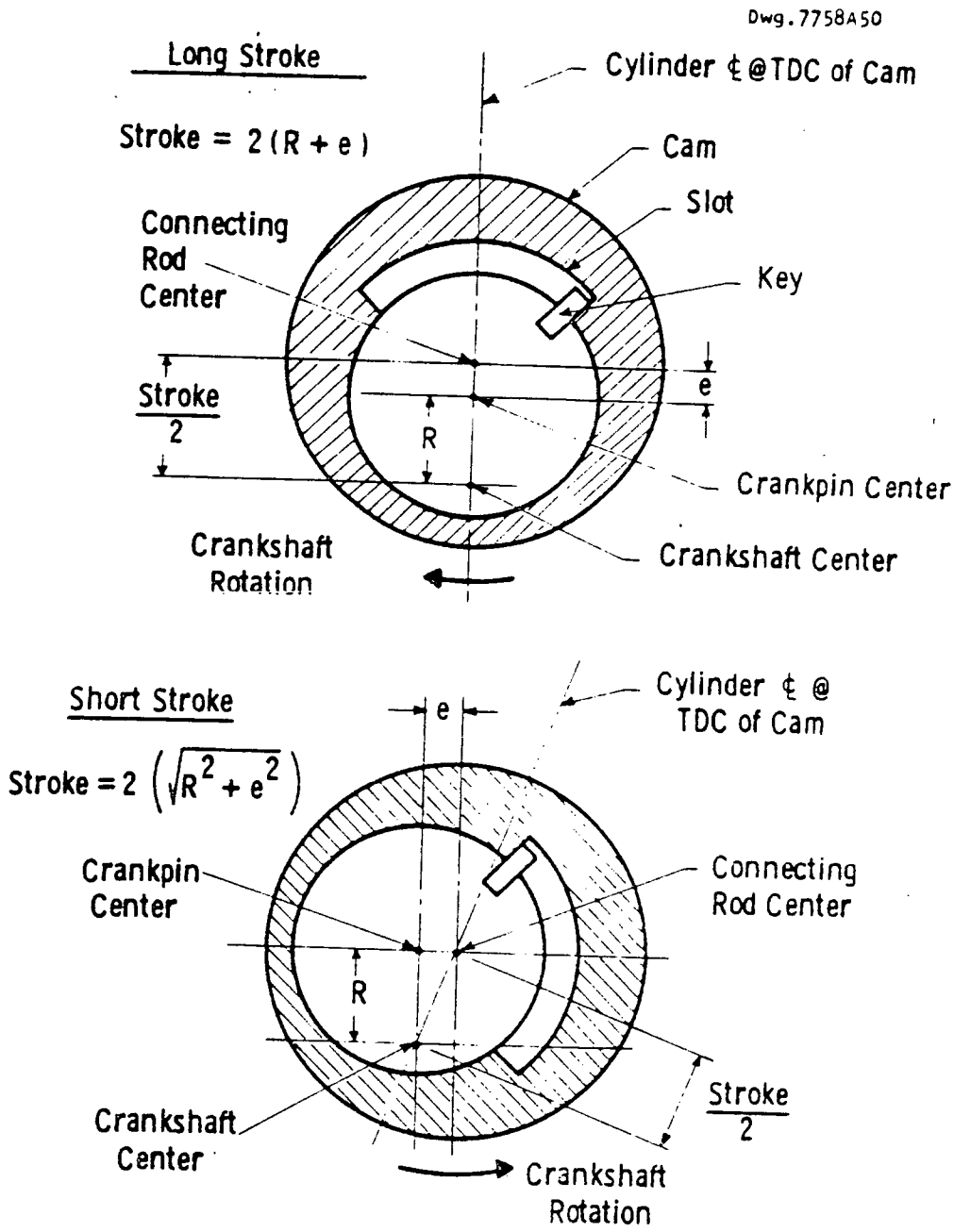


Fig. 17 - Dual-stroke cam positions

position at top dead center. At the other cam position, corresponding to crankshaft rotation in the opposite sense, the connecting rod reciprocates with a much shorter stroke and thus with a much greater clearance volume at top dead center position. In the shorter stroke position, compressor flow rate (i.e., capacity) is decreased by both the reduction of piston displacement and the reduction of compressor volumetric efficiency because of the increased clearance volume. As a consequence, compressor flow rate is reduced more at high pressure ratios than at low pressure ratios. However, since the low-capacity mode of the machine is generally required only during low pressure ratios conditions on the system (i.e., cooling mode and heating mode above 30°F ambient), it is possible to select low stroke cam eccentricities that provide the optimum capacity reduction without appreciably affecting system performance.

The fixed ratio of minimum to maximum compressor capacity is determined by the cam eccentricity. The magnitude of the minimum stroke is bounded between zero and the maximum stroke; its precise value is a subject for system optimization.

The efficiency, capacity and durability of currently available hermetic compressors are limited because the drive motor is cooled by the incoming suction gas. Heat pump compressor mass flow decreases significantly as the suction pressure declines due to cold ambients. Therefore, the means for cooling the drive motor is reduced also. This results in high motor temperature and high suction gas superheat temperature if the entering suction gas is "dry". Further, the potential exists for expansion valve control problems and the danger of liquid "slugging" if the entering gas must be "wet" for adequate motor cooling during cold ambient operation. The system developed for cooling the drive motor with oil and providing a direct passage for the suction gas to enter the cylinders is shown on Figure 18. This system was found to be very effective in maintaining acceptable motor temperature regardless of suction pressure conditions and in maintaining much lower suction gas

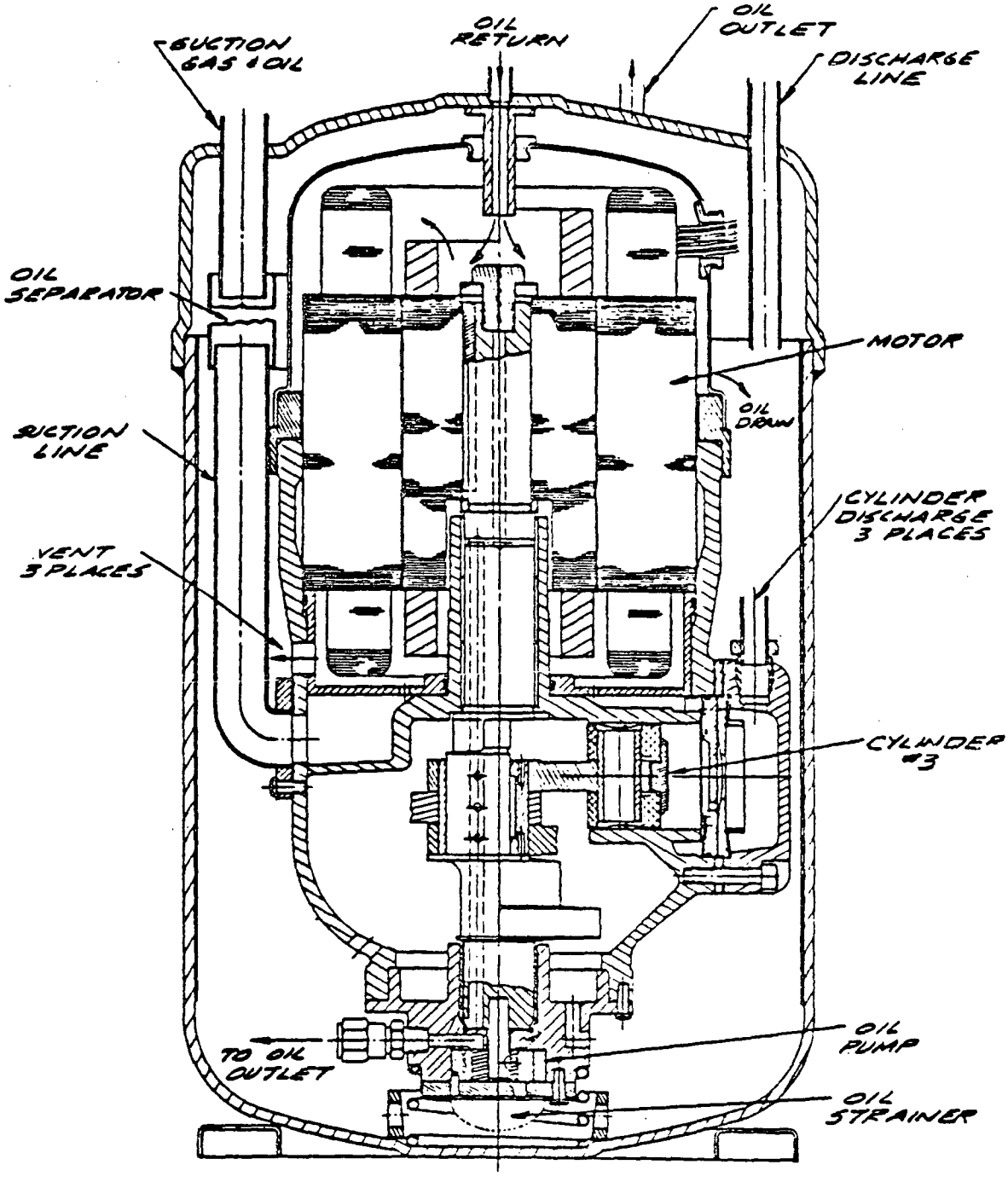


Fig. 18 - Cross section of oil-cooled compressor with direct suction

superheat than is possible with suction gas cooled machines. The resultant improvement in compressor capacity and compressor EER at standard conditions (120°F condensing, 20°F evaporator superheat, 15°F condenser subcooling) is as follows:

Improvement Due to Oil Cooling*

| | 10°F Evap. Temp. | 40°F Evap. Temp. |
|---|---|---|
| Capacity [%] | 12.5 | 3.0 |
| EER [%] | 11.3 | 6.1 |

This system requires an external heat exchanger, and the use of a reversible positive displacement oil pump in the compressor assembly as well as some modifications to the crankcase and piping. The manufacturing cost of the oil system internal to the hermetic shell adds $13.10 to the basic compressor cost.

Although the development program did not include a rigorous analytical approach to valve design, numerous tests of valve types and valve plate configurations were conducted in order to identify potential improvements. The selected configuration consists of an open center ring suction valve, a slightly crowned piston and a unique cantilevered flapper type discharge valve with end restraint as shown on Figure 19. This valve configuration improved both the capacity and EER of a conventional ring valve compressor at standard conditions (120°F condensing, 20°F evaporator superheat, 15°F condenser subcooling) as follows:

Improvement due to Valve Development** (with concomitant clearance volume reduction)

| | 10°F Evap. Temp. | 40°F Evap. Temp. |
|---|---|---|
| Capacity [%] | 14.4 | 7.1 |
| EER [%] | 8.5 | 9.0 |

*Note that the oil cooling subsystem has not been optimized so that still better performance may be achievable.

**Note that further development and optimization may yield still better performance.

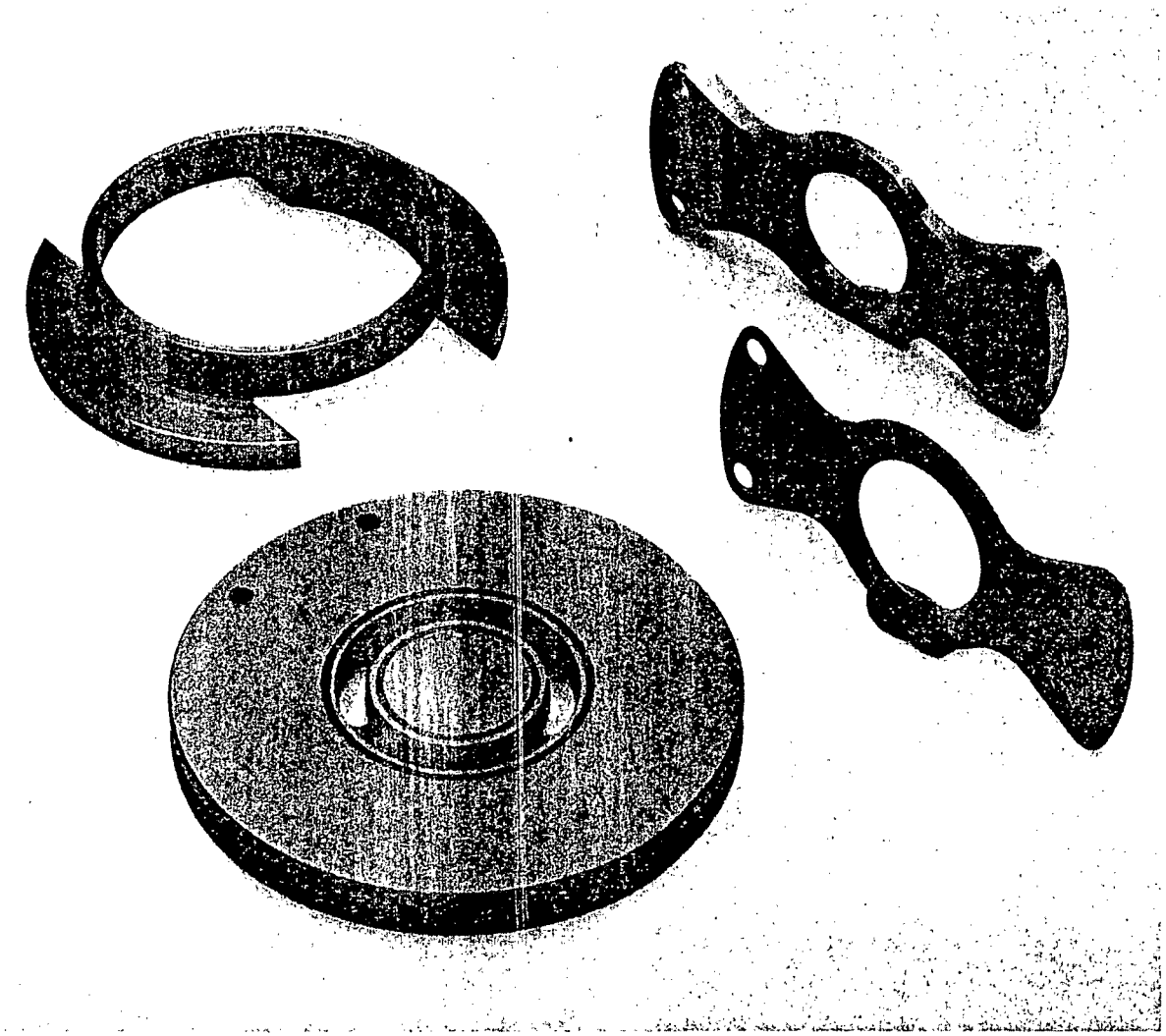

Fig 19 - Discharge valve cantilevered flapper with end restraint

Figure 20 shows efficiency curves for the motors used in the compressor development effort. Curve 1 is the efficiency curve for a new motor designed specifically to match the requirements of the dual-stroke compressor when operating in the high-capacity mode. Curve 3 shows the efficiency of the standard production motor. As can be seen, the efficiency of both motors suffers greatly when used to drive the compressor in its low-capacity mode. Curve 2 shows the efficiency of the new motor designed so as to maintain high efficiency when lightly loaded. At 2.0 hp, the efficiency of the new motor is 87.8 percent, compared to 77.7 percent for the standard motor. At 4.0 hp, a typical operating point in high-capacity mode, the efficiencies of the new and old motors are 89.0 and 85.7 percent, respectively.

The performance of a preprototype compressor is shown in Fig. 21. In the high-capacity mode at 40°F evaporating and 120°F condensing, with 20°F suction superheat and 15°F condenser subcooling, the compressor capacity is 46,000 Btu/h with a COP of 3.28 (EER of 11.2 Btu/Wh). This performance data in tabular form is given in Tables 10 and 11.

The efficiency of this compressor at these conditions exceeds that of presently available compressors by at least ten percent. More significant is the performance at low evaporator temperatures. At an evaporator temperature of 0°F and a condensing temperature of 100°F, the measured compressor capacity is 18,300 Btu/h and the COP is 2.1 (EER is 7.2 Btu/Wh). At 32°F evaporating temperature and 100°F condensing temperature in low capacity and 110°F condensing temperature in high capacity, the capacity ratio is approximately 2:1 with the mean COP between high and low capacity approximately 3.3. When installed in a system, the compressor will not be operated in low-capacity heating mode when the ambient temperature is less than approximately 32°F. Similarly, it will not be operated in the low-capacity cooling mode when the pressure ratio exceeds 3.5.

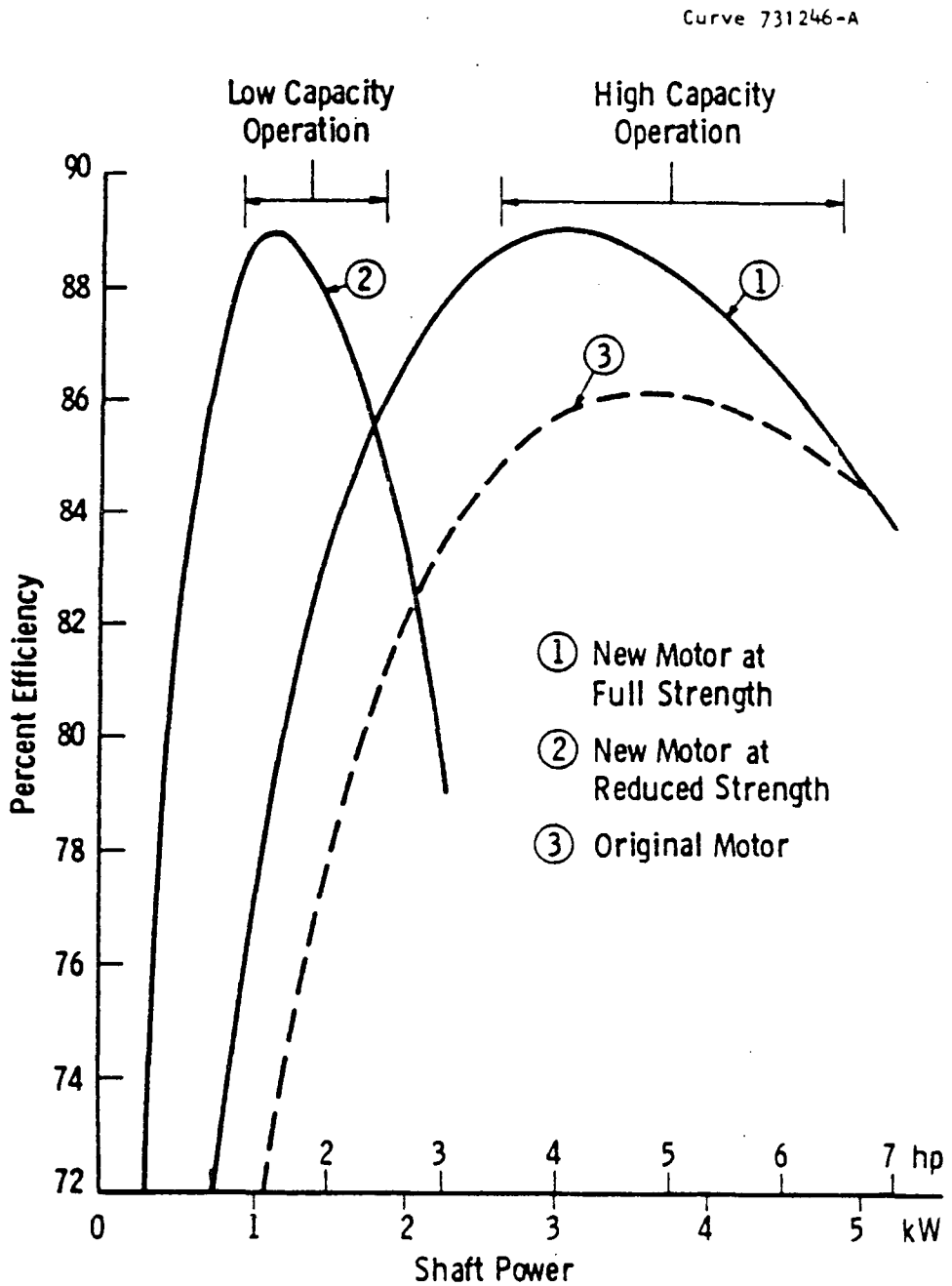


Fig. 20 - Compressor motor efficiency vs shaft power (25°C winding temperature)

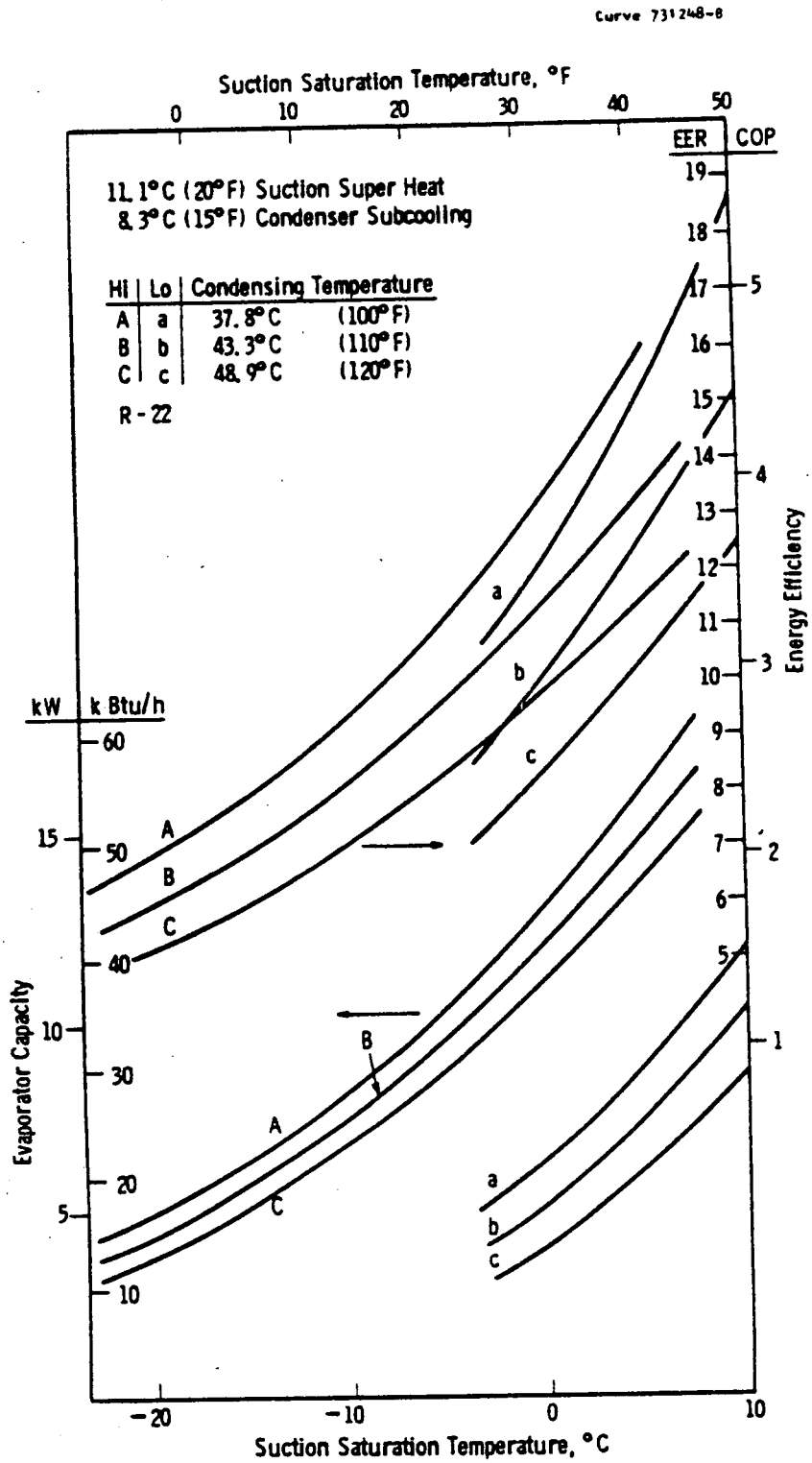


Fig. 21 - Preprototype dual-stroke compressor performance (R-22)

Table 10

Preprototype Dual-Stroke Compressor Performance - High Capacity
(R-22, 20°F superheat, 15°F subcooling, 230 V, 1 phase, 60 Hz)

CAPACITY - BTU/HR

| EVAP TEMP DEG F | CONDENSING TEMPERATURE DEG F 90.0 | 95.0 | 100.0 | 105.0 | 110.0 | 115.0 | 120.0 |
|---|---|---|---|---|---|---|---|
| 0.0 | 21336.4 | 19603.8 | 18257.5 | 17203.0 | 16345.9 | 15591.5 | 14845.5 |
| 10.0 | 28326.2 | 26798.1 | 25394.8 | 24099.7 | 22896.4 | 21768.4 | 20699.4 |
| 20.0 | 35633.4 | 34432.6 | 33153.4 | 31807.6 | 30407.1 | 28963.5 | 27488.7 |
| 30.0 | 44649.1 | 43612.1 | 42376.6 | 40958.6 | 39374.1 | 37639.1 | 35769.5 |
| 40.0 | 56764.8 | 55441.5 | 53907.4 | 52184.2 | 50293.7 | 48257.7 | 46097.7 |
| 50.0 | 73371.6 | 71025.9 | 68589.2 | 66116.3 | 63662.2 | 61281.6 | 59029.5 |

POWER INPUT - WATTS

| EVAP TEMP DEG F | CONDENSING TEMPERATURE DEG F 90.0 | 95.0 | 100.0 | 105.0 | 110.0 | 115.0 | 120.0 |
|---|---|---|---|---|---|---|---|
| 0.0 | 2572.8 | 2530.8 | 2541.1 | 2586.7 | 2650.9 | 2716.8 | 2767.7 |
| 10.0 | 2828.9 | 2860.7 | 2905.5 | 2961.3 | 3026.2 | 3098.1 | 3175.1 |
| 20.0 | 2942.6 | 3055.1 | 3158.5 | 3253.8 | 3342.2 | 3424.8 | 3502.7 |
| 30.0 | 2989.8 | 3171.0 | 3336.4 | 3484.1 | 3611.9 | 3717.7 | 3799.5 |
| 40.0 | 3046.2 | 3265.2 | 3475.7 | 3671.9 | 3847.8 | 3997.5 | 4114.8 |
| 50.0 | 3187.6 | 3394.5 | 3612.7 | 3837.2 | 4062.9 | 4284.9 | 4497.9 |

ENERGY EFFICIENCY RATIO - BTU/W-HR

| EVAP TEMP DEG F | CONDENSING TEMPERATURE DEG F 90.0 | 95.0 | 100.0 | 105.0 | 110.0 | 115.0 | 120.0 |
|---|---|---|---|---|---|---|---|
| 0.0 | 8.29 | 7.75 | 7.18 | 6.65 | 6.17 | 5.74 | 5.36 |
| 10.0 | 10.01 | 9.37 | 8.74 | 8.14 | 7.57 | 7.03 | 6.52 |
| 20.0 | 12.11 | 11.27 | 10.50 | 9.78 | 9.10 | 8.46 | 7.85 |
| 30.0 | 14.93 | 13.75 | 12.70 | 11.76 | 10.90 | 10.12 | 9.41 |
| 40.0 | 18.63 | 16.98 | 15.51 | 14.21 | 13.07 | 12.07 | 11.20 |
| 50.0 | 23.02 | 20.92 | 18.99 | 17.23 | 15.67 | 14.30 | 13.12 |

Table 11

Preprototype Dual-Stroke Compressor Performance - Low Capacity
(R-22, 20°F superheat, 15°F subcooling, 230 V, 1 phase, 60 Hz)

CAPACITY - BTU/HR

| EVAP TEMP DEG F | CONDENSING TEMPERATURE DEG F 90.0 | 95.0 | 100.0 | 105.0 | 110.0 | 115.0 | 120.0 |
|---|---|---|---|---|---|---|---|
| 30.0 | 24418.8 | 22410.1 | 20337.1 | 18253.9 | 16215.1 | 14275.0 | 12488.1 |
| 35.0 | 28454.1 | 26466.2 | 24414.8 | 22322.6 | 20212.2 | 18106.2 | 16027.1 |
| 40.0 | 33591.9 | 31481.4 | 29311.3 | 27085.2 | 24806.8 | 22479.5 | 20106.9 |
| 45.0 | 39510.3 | 37234.5 | 34862.1 | 32405.9 | 29878.7 | 27293.2 | 24662.1 |
| 50.0 | 45887.3 | 43504.4 | 40903.0 | 38148.9 | 35307.8 | 32445.6 | 29627.8 |

POWER INPUT - WATTS

| EVAP TEMP DEG F | CONDENSING TEMPERATURE DEG F 90.0 | 95.0 | 100.0 | 105.0 | 110.0 | 115.0 | 120.0 |
|---|---|---|---|---|---|---|---|
| 30.0 | 1820.2 | 1792.4 | 1759.2 | 1720.9 | 1677.9 | 1630.2 | 1578.3 |
| 35.0 | 1880.5 | 1884.6 | 1883.3 | 1874.9 | 1857.8 | 1830.4 | 1790.9 |
| 40.0 | 1940.8 | 1976.2 | 2005.5 | 2025.8 | 2033.9 | 2026.9 | 2001.8 |
| 45.0 | 1993.7 | 2056.9 | 2113.6 | 2160.1 | 2192.6 | 2207.2 | 2200.4 |
| 50.0 | 2031.8 | 2116.5 | 2195.3 | 2264.5 | 2320.2 | 2358.7 | 2376.3 |

ENERGY EFFICIENCY RATIO - BTU/W-HR

| EVAP TEMP DEG F | CONDENSING TEMPERATURE DEG F 90.0 | 95.0 | 100.0 | 105.0 | 110.0 | 115.0 | 120.0 |
|---|---|---|---|---|---|---|---|
| 30.0 | 13.42 | 12.50 | 11.56 | 10.61 | 9.66 | 8.76 | 7.91 |
| 35.0 | 15.13 | 14.04 | 12.96 | 11.91 | 10.88 | 9.89 | 8.95 |
| 40.0 | 17.31 | 15.93 | 14.62 | 13.37 | 12.20 | 11.09 | 10.04 |
| 45.0 | 19.82 | 18.10 | 16.49 | 15.00 | 13.63 | 12.37 | 11.21 |
| 50.0 | 22.58 | 20.55 | 18.63 | 16.85 | 15.22 | 13.76 | 12.47 |

Figure 22 is a photograph of the high-efficiency, dual-capacity, three cylinder, hermetic refrigeration compressor (without hermetic shell) produced for this advanced electric heat pump program. Figure 23 is an exploded view of the compressor. Superior performance, durability, and heat pump system compatibility have been demonstrated by test.

In order to achieve this level of performance a base line three cylinder radial Westinghouse CD048 hermetic refrigeration compressor of nominally four tons capacity was modified so as to embody the following advanced features:

1. A unique mechanism that changes the stroke of the compressor upon a change in the direction of rotation of the crankshaft.

2. A circulating oil system that cools the drive motor and compressor and rejects the heat external to the compressor hermetic shell.

3. A suction piping system that routes suction gas to a liquid separator and then directly into the cylinders thereby impeding heat transfer and suction gas superheat.

4. A discharge piping system that both impedes heat transfer and reduces discharge pipe losses.

5. An improved valve and valve plate system that reduces both flow impedance and clearance volume thereby improving both capacity and efficiency.

6. A single speed but reversible direction, dual-strength motor that delivers high efficiency at two widely spaced delivered horsepower levels.

The main additions to the compressor that would affect the basic durability of the machine are the dual-stroke mechanism and the reversible oil pump.

The dual-stroke device has demonstrated durable operation during the development period where over 20,000 hours of endurance testing have been accumulated on six compressors. While this experience does not totally qualify the mechanism for immediate incorporation into production compressors, it does indicate good potential for high reliability.

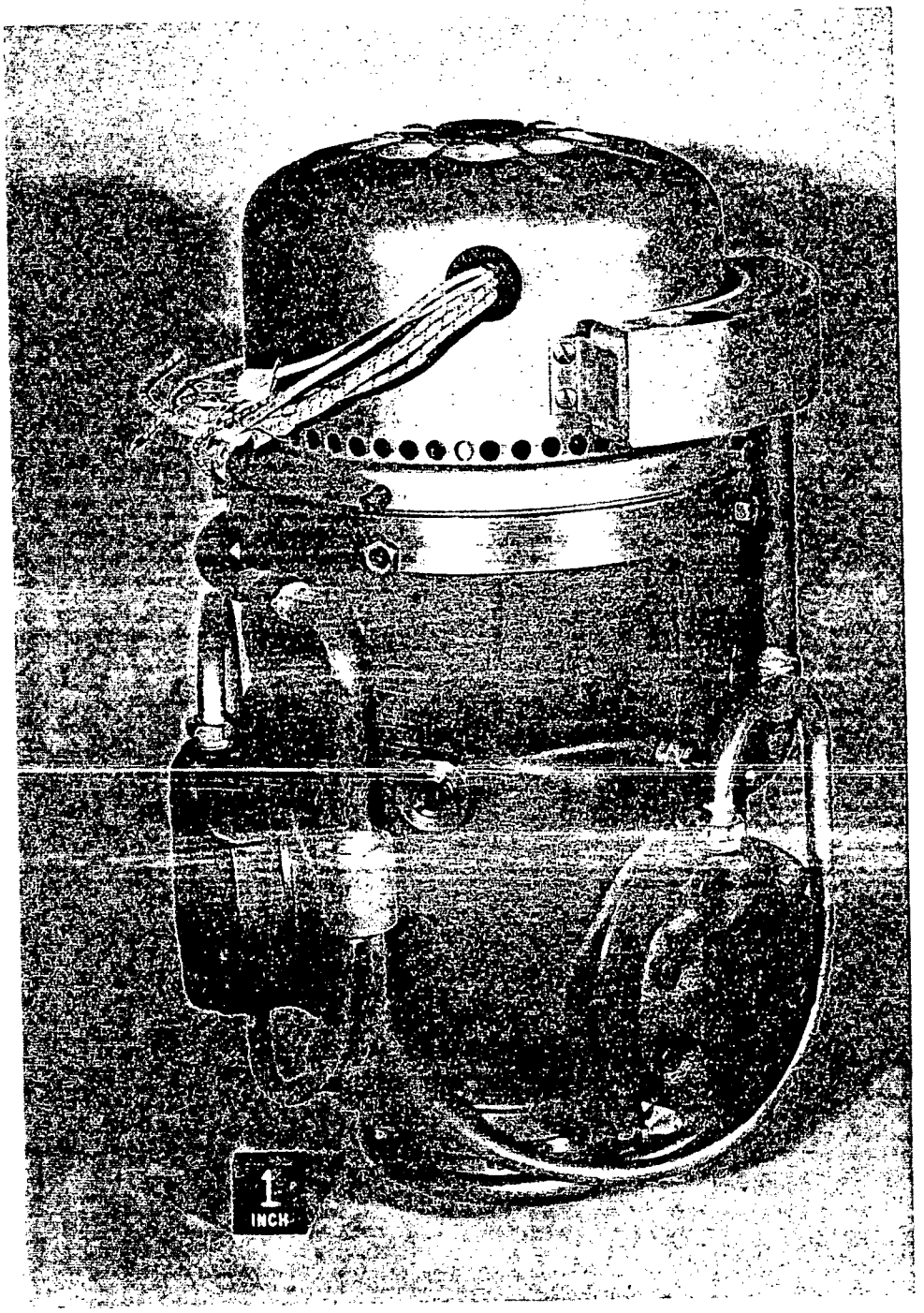


Fig. 22 - Preprototype oil cooled dual-stroke compressor - discharge line view

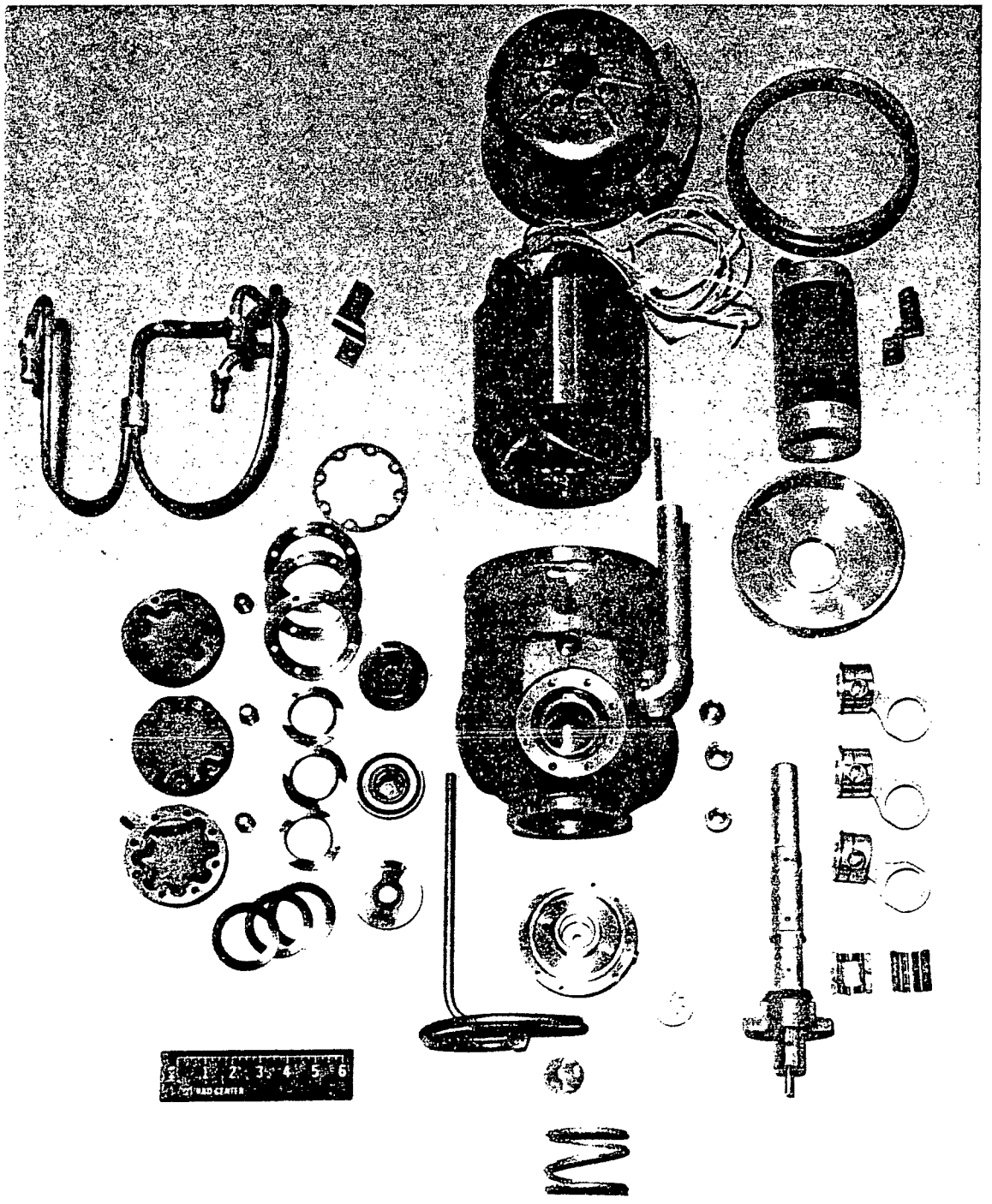

Fig. 23 - Exploded view of preprototype oil cooled dual-stroke compressor

The reversible "Gerotor" oil pump has gained a reputation for high reliability on many other machine products, and the application of the pumping elements to a hermetic compressor assembly should certainly be acceptable. Similar oil pumps are in use for both 3500 and 1750 rpm refrigeration compressors.

The basic durability of the preprototype compressor, based upon the Westinghouse CD048 compressor, with aluminum connecting rods and steel backed babbitt main bearings should be assured since these materials of construction are common practice. In addition, the CD048 compressor has demonstrated good reliability through 15 years of production life.

Table 12 presents an estimate of the cost adders associated with each new or modified component in the dual-stroke compressor. An estimated additional manufacturing cost of $43.87 is incurred when the indicated advanced features are incorporated into the baseline compressor. This incremental compressor cost as seen by the manufacturer will be reflected in the market place as a system cost premium of approximately $110.

Additional information concerning the compressor development effort can be found in References 4 and 9.

Conclusions Relative to the Compressor

1. The Westinghouse/DOE dual-stroke compressor is a low cost, high efficiency, flexible capacity ratio machine.

2. The Westinghouse/DOE dual-stroke compressor has significantly better performance than any other compressor available in the market today.

3. The Westinghouse/DOE dual-stroke compressor concept is generally applicable to any residential advanced electric heat pump or air conditioning system.

Table 12

Analysis of Incremental Costs for the Dual-Stroke Compressor

(Estimated Costs in 1981 dollars)

| | $ |
|---|---|
| Crankcase modifications | 0.80 |
| Crankshaft modifications | 0.25 |
| Cam (labor and material) | 4.00 |
| Lower shell modifications | 1.19 |
| Upper shell modifications | 0.83 |
| High-efficiency motor | 6.71 |
| Capacitor change | (0.80) |
| Reversing contactor | 16.70 |
| Miscellaneous hardware | 1.90 |
| Suction gas-cooled compressor | 30.77 |
| Oil cooler | 5.15 |
| Reversible oil pump | 4.00 |
| Oil pump housing | 3.10 |
| Suction piping | 0.69 |
| Discharge piping modifications | 0.16 |
| Oil Cooling adder | 13.10 |
| Oil-cooled dual-stroke compressor | 43.87 |

4. The incremental cost associated with upgrading the baseline compressor to an advanced dual-stroke unit can be justified through energy savings in any suitably designed system.

5. In quantity manufacture (100,000 units annually) the dual-stroke capacity modulation means is less expensive than presently known alternatives such as two-pole/four-pole two-speed motors, electronic variable frequency drives, geared two-speed drives, parallel compressors, and probably even cylinder suction cut-off schemes.

6. The ratio of low capacity to high capacity is not fixed but is a parameter for system optimization.

7. The dual-stroke concept as reduced to practice appears to be applicable only to multicylinder radial compressors.

8. Low capacity (i.e., short stroke with concomitant high clearance volume) operation should be limited so as to impose pressure ratios less than 3.5:1 in order to ensure the load reversal on the wrist pin necessary for adequate lubrication. (Most residential heat pump applications with saturated suction temperatures greater than 30°F meet this requirement.)

## 4.2 Outdoor Fan

A 3.5 ton conventional heat pump outdoor air mover is required to move large volumes of air (typically 3000 scfm) through the low flow resistance (typically 0.15 inches of water) due to the heat exchanger and protective grilles.

The conventional outdoor air mover is typically a two-to-four bladed propeller fan turning at six-pole (1020 rpm) or eight-pole (825 rpm) speed. The propeller blades are of large chord, more or less shovel-shaped, and riveted to a simple steel spider hub driven by the motor. The blades are of constant thickness, ribbed for stiffness, and of constant camber and incidence with high solidity. The fan hub is open and air may recirculate. The propeller rotates in a running ring or shroud, often without curved inlet flare, and with a clearance of a quarter-inch or more between blade tip and shroud. A restricted fan inlet and a short or nonexistent diffuser ring are commonplace. Consequently, outdoor air mover static efficiencies as applied are generally 20 to 35 percent, rather than the 45 percent peak efficiency indicated in some vendor literature.

The typical fan motor for residential units is a weatherproof, permanent split capacitor type of 1/6 to 1/3 hp rating yielding about 55 percent efficiency. With 35 percent fan static efficiency and a 55 percent efficient motor, the overall air-moving efficiency is only 19 percent, and power consumption is on the order of 250 W. The goal was to halve the outdoor air-moving power.

The preliminary specification for an outdoor air mover called for an air delivery of 2900 scfm against an upstream flow resistance of 0.20 in. of water with a static efficiency of 60 percent. The dry coil unit pressure drop is anticipated to be about 0.1 inches of water. In order to ensure adequate airflow under heavy frosting conditions the fan pressure rise requirement was specified as double the nominal dry coil pressure drop. The motor was required to be at least 65 percent efficient. Air-mover size was constrained to 24 inches in diameter and

12 inches in height, exclusive of mounting flanges. The fan noise was not to exceed a noise rating (SRN) of 20, and a rating of 18 or less was desired.[10]

Since a quiet fan with good static efficiency was required, a multivane, axial flow design was proposed. A fan of this type has five or more blades of relatively narrow chord and low solidity. A large solid hub is used to prevent recirculation.

A breadboard axial fan was fabricated with an acrylic hub and eight acrylic blades. The blades consisted of hot-formed 1/8 inch-thick sheet material mounted on steel tangs to provide adjustable pitch capacity. A stator vane row with 31 stator vanes was used. The stator vanes were also hot-formed from 1/8 inch-thick sheet material and were glued into an annular section consisting of a 12 inch OD inner cylinder and a 24 inch ID ring, both 4 inches long and of acrylic. The diffuser section was formed with a 24 inch ID sheet metal cylinder and a conical sheet metal inner body mounted to the center section of the vane row. Both a 12 inch and a 6 inch diffuser were tested. A fiberglass inlet flare (3 inch radius) and running ring were used. Final test results for the air mover with 6 inch diffuser are summarized in Figure 24. The configuration for this test included all components of the fan: inlet flare, blade row, vane row and 6 inch diffuser.

The performance curves for the breadboard outdoor fan (Figure 24) show that pressure rise and flow rate intersect the system resistance curve (based on 2900 cfm at 0.2 inches of water) slightly above the design target. Static efficiency for this operating condition is 52 percent with a shaft power requirement of 0.185 hp. The characteristic curve for the fan is smooth with no regions of positive or unstable slope. At 80 percent of design flow (2320 cfm), the fan operates stably and smoothly. At flows of less than 80 percent of design, the fan continues to operate in a stable manner with usable flow-pressure performance, but with significant increases in required power and generated noise.

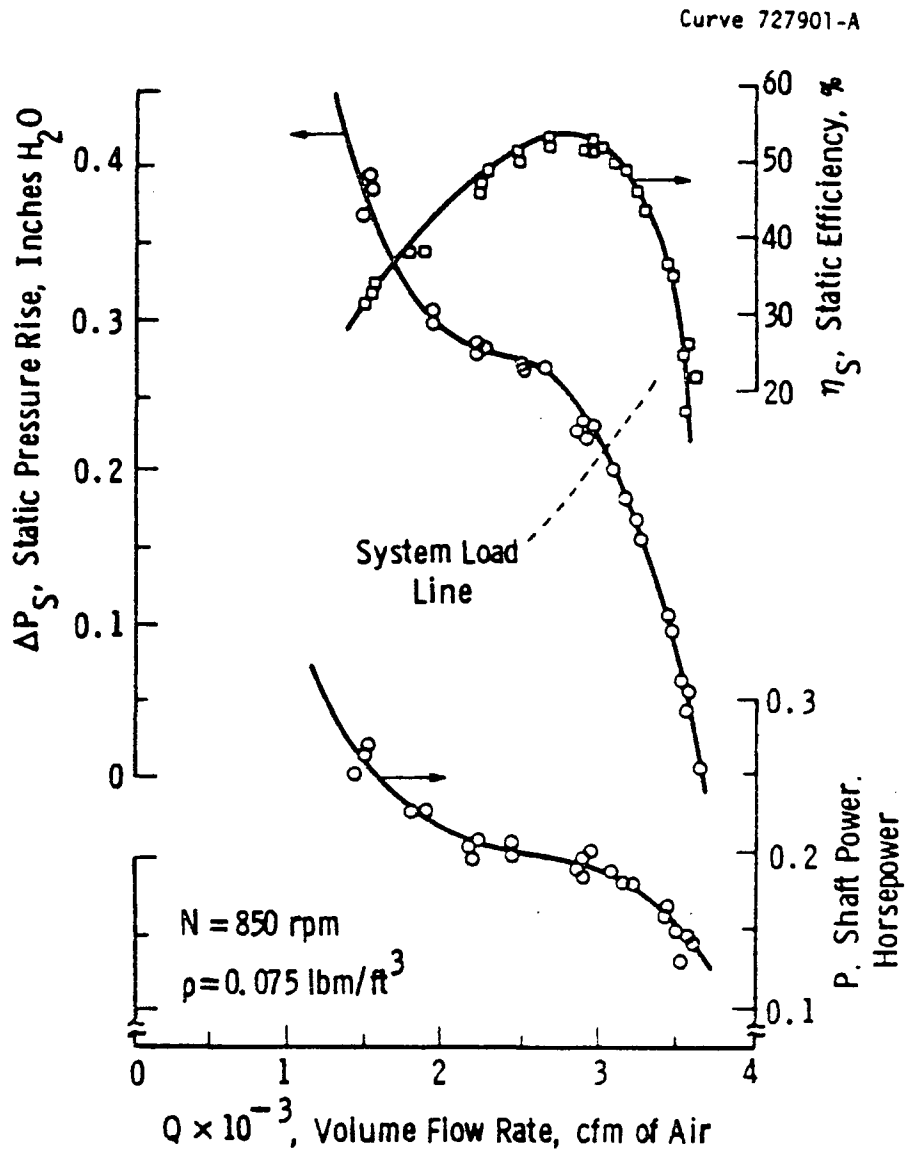


Fig. 24 - Breadboard outdoor fan performance (6 inch diffuser, pitch angle $\alpha_{g_R}$ = 33.8°)

The breadboard fan achieved a static efficiency of 52 percent when delivering 3000 scfm through the specified outdoor unit resistance. The fan required 0.185 shaft horsepower. This performance was acceptable for the preprototype system, but the anticipated cost of an air mover with high solidity stator vane row was judged to be unacceptable.

In order to reduce the cost of the air mover, the stator vane row was removed from consideration. Based upon previous observations this implied that the diffuser stack should either be redesigned or eliminated. It was expected that this would penalize static efficiency by about five percent and thereby raise the shaft power requirement to 0.195 horsepower.

The rather poor performance observed for the annular diffuser with a cylindrical outer wall and inwardly tapered inner wall led us to consider a relaxation in the specification for a 24 inch maximum diameter in order to incorporate an outwardly expanding outer wall for the diffuser. As revised, this specification called for a 27 inch maximum diameter at the exit of the diffuser. In order to achieve adequate diffusion, an inner wall was specified with 7 degree taper.

The propeller blade specifications were also changed so as to increase the pitch angle.

The outdoor air mover as developed for the preprototype advanced electric heat pump is shown in Figure 25. As shown, the conical, outwardly expanding diffuser shroud exit diameter is 27 inches, with the overall diameter of the mounting flange being 31 inches. The overall height of this subassembly is 12 inches and the radius of the ninety degree inlet flange is 2 inches. The propeller, as shown in Figure 5, is 24 inches in diameter with a hub to tip ratio of 0.5. The eight propeller blades of constant chord and nonuniform spacing extend from a clamshell hub. The blade spacing pattern has two planes of symmetry. A propeller molded completely from plastic was considered highly desirable, but project resources would not permit purchase of the

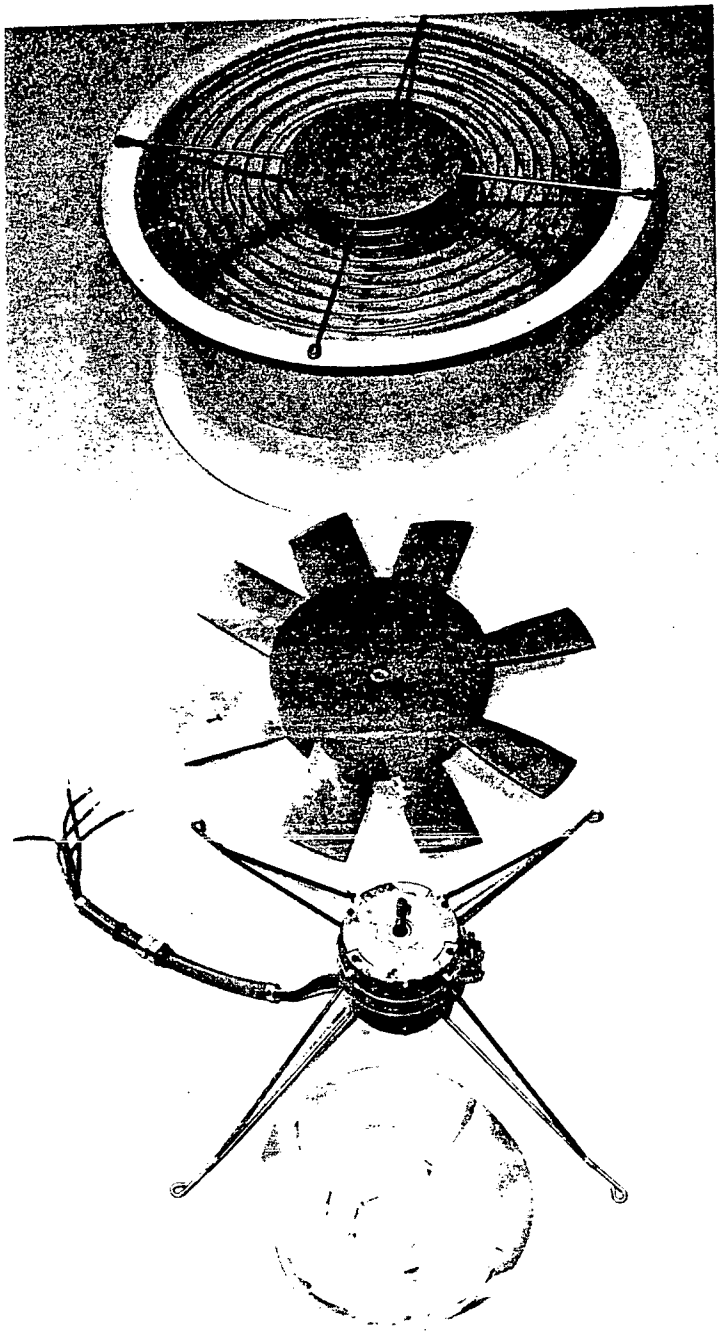

Fig. 25 - Outdoor air mover preprototype

necessary tooling. A fabricated assembly consisting of aluminum sheet blades clamped in a two piece clamshell hub was designed as the best alternative. The fan blades were cut from 2024 aluminum sheet, 0.060 inches thick, annealed, formed in expedient tooling, and then precipitation hardened to T4 temper. Two hubs were machined, one from aluminum and one from Noryl[R] plastic. The production two-piece design is envisioned to use a precision die molded plastic hub and blade clamp.

The fan hub is mounted to the motor shaft via a hub insert and the motor is suspended shaft down in the shroud by a wire form belly band carrier motor support.

In order to cool the motor, airflow through the motor housing, the tapered inner wall of the diffuser, must be ensured. An overhung lid, with an annular gap was tried, but found inadequate. Inasmuch as the wire form protective grille, at the discharge has a center cover disk, a hole was placed in the center of the motor housing end cap. See Figure 26. Since this hole is in a region with higher static pressure than the gap between fan hub and the diffuser center body, the fan will pump air out of the annular gap between hub and diffuser center body, with supply air entering through the hole in the motor center body end cap, the annular gap at the periphery of the center body at discharge, and through the clearance openings for the wire form motor support. The general appearance of this sheet metal diffuser center body/motor cover is not very satisfying but resources did not permit further design refinement. The breadboard fan without stator vane was estimated to require approximately 0.2 hp to deliver 3000 scfm with 0.2 inches of water pressure rise at 850 rpm. The 850 rpm would be consistent with a low resistance rotor for maximum motor efficiency, but since deep speed reduction was considered desirable, a medium resistance rotor would be required and a nominal full speed of 825 rpm would result. At 825 rpm, the airflow would be approximately 2900 scfm as per the initial specification. Although the required shaft power would then be decreased to about 0.18 hp, the motor was specified at 0.2 hp for some design margin.

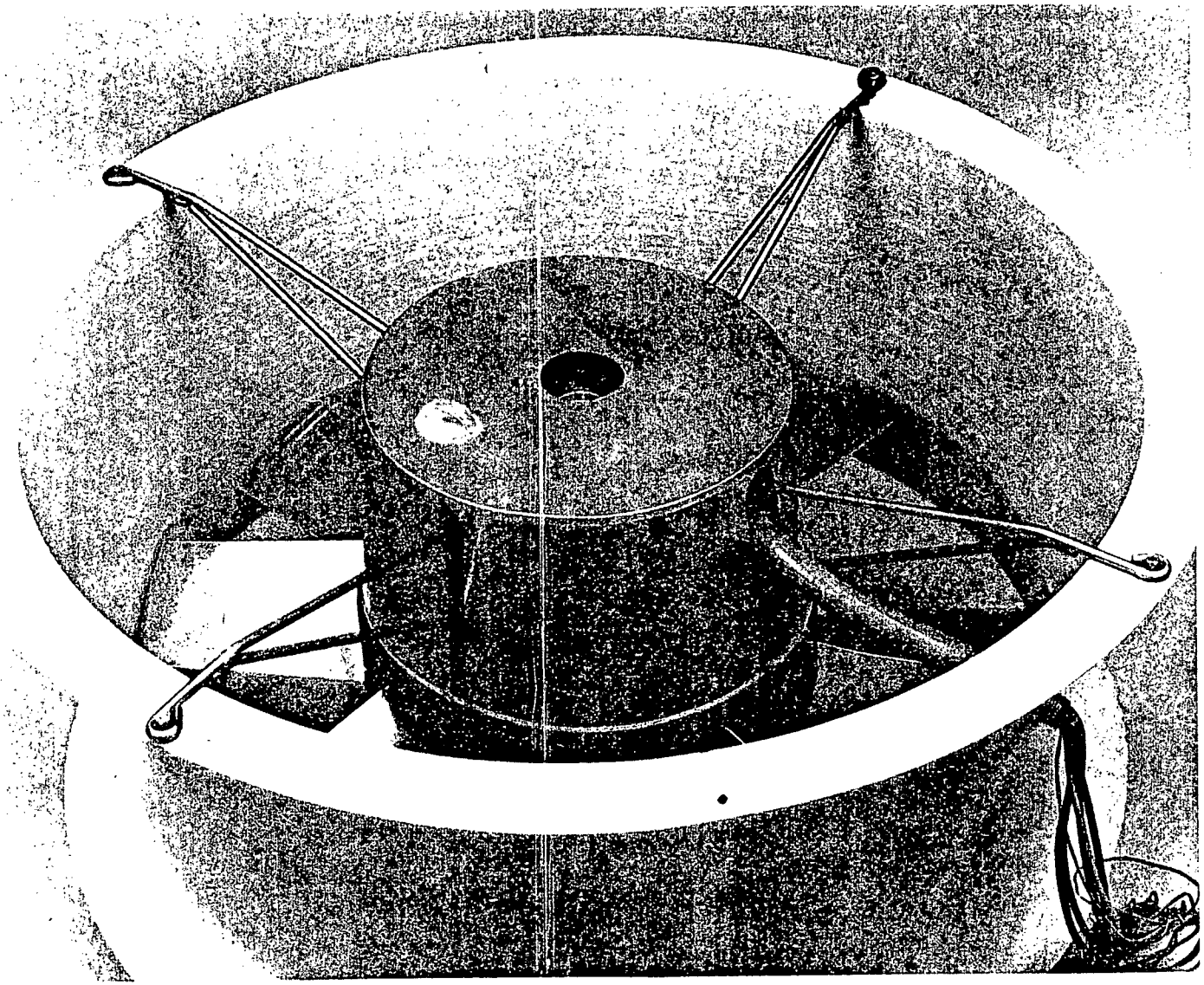

Fig. 26 - View of diffuser and motor cover for outdoor air mover preprototype

The specifications developed for the outdoor fan motor were designed to yield high reliability as well as high efficiency. These specifications are as follows: The heat pump outdoor fan motor is to be a permanent split capacitor type with eight poles, totally enclosed and nonventilated with cooling provided by flowing air over the exterior. Power is to be 230/208 volt, 60 Hz, single phase. Direction is to be reversible by external reconnection. The operational environment is to extend from -20°F to +130°F. The expected life is to be 50,000 hours. The bearing system is to be double sealed ball bearings with synthetic grease (Mobil 28). Auxiliary winding insulation is to be Westinghouse Omega-Klad-EK; main winding insulation is to be Westinghouse Omega-Slip-HA; varnish is to be double dip polyester. Frame length is to be extra long (5.5 inches maximum) and the end bell is to be sealed with silicone rubber, RTV. Independent thermal protection is to be provided with the leads for main and auxiliary windings and the thermal cut-out to be brought out of the frame. Leads are to be 24 inches long and potted in insulation tubes with a sealing grommet. Mounting is to be with shaft vertical and down. Design output is to be 0.20 horsepower at 825 rpm and 65 percent efficiency.

The 0.2 hp, eight-pole fan motor design employs a 2.47 inch stack with an approximate balance between the weight of copper in the main and auxiliary windings. The turns ratio (effective auxiliary turns to effective main turns) is 1.318. The capacitor required for this motor is 4 μfd. The motor has a medium resistance rotor which on a horsepower per unit basis is 0.0654 per unit resistance. One feature of the design effort was an attempt to effect the maximum feasible utilization of the slots, within manufacturing capabilities and to run at design point power close to balanced operation.

Figure 27 shows the computer generated analytically predicted speed vs. torque characteristic for this motor with the medium resistance rotor in place. If a low resistance rotor were to be substituted, the efficiency at full load should improve to 67.5 percent.

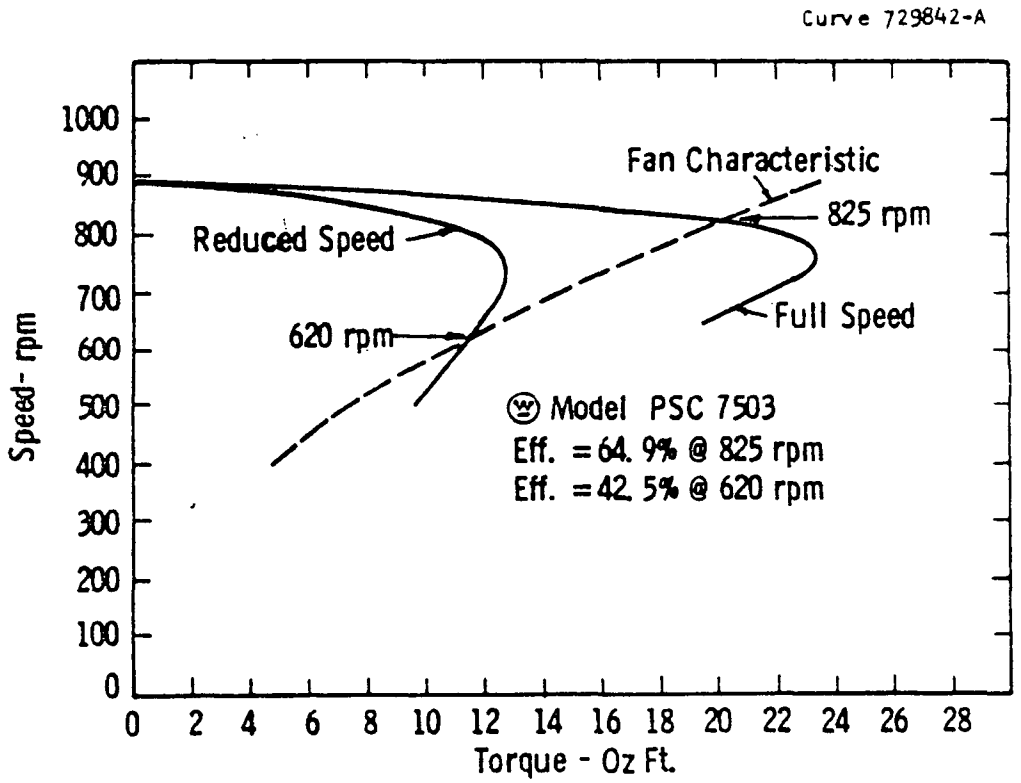


Fig. 27 - Fan motor speed-torque characteristics (analytically estimated)

Table 13

Noise at 860 rpm

| Band No. | Frequency Hz | Sample PWL | Discrete Adjustment | Rating Index |
|---|---|---|---|---|
| 20 | 100 | 79.0 | 0.0 | 1.7 |
| 21 | 125 | 79.9 | -0.5 | 2.0 |
| 22 | 160 | 77.4 | 0.0 | 2.0 |
| 23 | 200 | 77.3 | 0.0 | 2.4 |
| 24 | 250 | 75.2 | 0.0 | 2.3 |
| 25 | 315 | 76.6 | 0.0 | 2.8 |
| 26 | 400 | 76.2 | 0.0 | 3.0 |
| 27 | 500 | 74.9 | 0.0 | 2.8 |
| 28 | 630 | 73.8 | 0.0 | 2.6 |
| 29 | 800 | 73.8 | 2.5 | 3.0 |
| 30 | 1000 | 69.9 | 0.0 | 2.0 |
| 31 | 1250 | 70.1 | 0.0 | 2.3 |
| 32 | 1600 | 68.9 | 0.0 | 2.8 |
| 33 | 2000 | 67.7 | 0.0 | 3.2 |
| 34 | 2500 | 66.0 | 0.0 | 3.2 |
| 35 | 3150 | 64.4 | 0.0 | 3.0 |
| 36 | 4000 | 62.3 | 0.0 | 2.6 |
| 37 | 5000 | 58.7 | 0.0 | 1.9 |
| 38 | 6300 | 55.5 | 0.0 | 1.4 |
| 39 | 8000 | 53.3 | 0.0 | 0.6 |
| 40 | 10000 | 51.3 | 0.0 | 0.2 |

ARI sound rating number: 20. (19.755)

Project resources did not permit the preprototype outdoor air mover to be tested in a test cell. Therefore, it was installed in the preprototype outdoor unit and tested in the heat pump test facility as part of an operating system. As tested, it delivers 3070 scfm through the outdoor unit at 850 rpm with an upstream (suction side) pressure drop of 0.09 inches of water with a dry coil. The fan motor consumes 150 W of electrical power. In low-speed operation the air mover rotates at 609 rpm and consumes 78 W of electrical power, and delivers approximately 2200 scfm.

The second preprototype outdoor unit was tested in the acoustic laboratory reverbatory room for radiated noise. Since the outdoor unit was not coupled to the heat pump control system, noise measurements were obtained for slightly different rpms than prototypical. Noise data are listed in Table 13 for 860 rpm. The SRN[10] (Sound Rating Number) of the preprototype fan is less than 20. Note from Figure 26 that the diffuser walls have not received any acoustic noise treatment. Note also from Figure 25 that the wire form grill is fabricated from rather thin gauge wire. In prototype form a more substantial grill is recommended, since the one used tended to vibrate excessively. The addition of an acoustical noise absorbing material to the diffuser and running ring plus a more substantial grill should lower the SRN.

The factory cost of this air mover subassembly, consisting of shroud, motor cover, motor support, motor, discharge grille, and propeller assembly is estimated at $69.77. This is approximately twice the cost of the conventional outdoor air mover. The electrical energy saving potential of this air mover as applied is approximately 100 watts. The economic value of this energy taken for 4900 hours of operation per year at 5¢/kWh is approximately $24.50 per year. Assuming an effective retail price three times the factory cost yields a payback time of 4.3 years for the premium cost to be associated with this air mover. Note however that if the conventional air mover were coupled to the prototype three row outdoor coil then its energy consumption would be greater than considered.

The radiated noise from this fan does not exceed an SRN of 20. Since no noise abating treatment has been applied to the diffuser shroud and since the grille used is more flexible than desired, a version of this air mover in prototype form should be even quieter.

The static efficiency goal of about 60 percent has been missed, but if a molded fan with airfoil-shaped blades were adopted, then a 55 percent efficient fan is possible at about the same premium cost. In addition, if dual-speed operation of the outdoor fan is abandoned, then the motor efficiency could be improved to about 67.5 percent without any appreciable price increase. Thus, an overall air moving effiency of 37 percent is achievable. This is about twice the efficiency of standard practice.

In addition, it must be noted that the inital flow specification called for 2900 scfm. System optimization studies performed after preprototype hardware specifications were frozen indicate that the optimum air flow is 2600 scfm. Since air horsepower varies as the cube of the flow rate, a fan scaled to this new flow would consume 61 percent of the indicated power or about 91 watts. For a unit of nominally 3.5 tons cooling capacity, this would represent a power reduction of more than half relative to a similar sized heat pump with a conventional fan delivering 2900 scfm. Adoption of airfoil blades and a single-speed fan motor would reduce power consumption still further.

We make the following conclusions regarding this outdoor air mover:

1. The achieved static efficiency of the preprototype outdoor air mover is approximately 50 percent.

2. The preprototype air mover consumes 150 W of electrical power to move 3070 cfm of 47°F air through the preprototype outdoor unit which has a dry coil suction side pressure drop of 0.09 inches of water.

3. The electrical power saved relative to a replacement air mover of conventional construction is approximately 100 watts.

4. The first cost premium of the air mover should be recoverable from energy savings in about four years assuming 4900 hours of operation per year, the cost of electricity at 5¢/kWh, and the effective retail cost at three times the factory cost.

5. The use of airfoil shaped blades (untested) instead of the cambered plate blades as developed would improve static efficiency by about five percentage points.

6. The use of a stator vane row in combination with a diffuser stack (as tested) would improve static efficiency by about five percentage points.

7. Efficiency improvements due to airfoil blading and the incorporation of a stator vane row with diffuser would be cumulative.

8. Airfoil shaped blades appear economically viable only if their incremental cost relative to cambered plate blades is negligible, as might be the case for a molded plastic fan.

9. Implementation of the stator vane row is not economically viable.

Additional information may be found in Reference 7.

## 4.3 Indoor Blower

The duty for a heat pump indoor air handler differs considerably from that of the outdoor fan. The indoor airflow is typically half that of the outdoor unit, while the static pressure rise requirement is much higher. The indoor air handler must provide sufficient static pressure rise to overcome the airflow resistance of the house duct system, the electrical resistance heating elements, the air filter, and the indoor heat exchanger. For a typical (late 1970's) 3.5 ton heat pump, the indoor design airflow is 1575 scfm with an air mover static pressure rise requirement of 0.85 inches of water corresponding to an external pressure drop of 0.35 and internal of 0.5 inches of water. Consideration of specific speed clearly shows that a centrifugal type fan is appropriate for this flow and pressure rise with rpm as available from direct connected four, six and eight-pole motors.

In presently available heat pumps the indoor air mover typically uses a squirrel-cage (forwardly curved vane) blower wheel 9 to 10 inches in diameter and 8 to 12 inches wide with double air entry. The blower wheel is mounted in a simple volute scroll. The motor is of the permanent split capacitor type and of open design, with a rated capacity of 1/3 to 1/2 horsepower. It is typically mounted in the eye of the blower wheel to take advantage of the excellent air cooling available, and it is not uncommon for the delivered power to be 50 percent more than the motor's nameplate rating.

Although the efficiency of a forwardly curved vane centrifugal blower can approach 60 percent, the measured efficiency as typically used is at most 35 percent. This lower achieved static efficiency is due in part to the flow-restricting placement of the direct-drive motor in the eye of the blower wheel. This motor placement prevails because it saves space and reduces cost relative to a belt-drive arrangement. The typical six-pole single-phase ac drive motor, well cooled and operating at high power output, runs with high slip and is between 50 and 60 percent efficient. Overall indoor air-moving efficiency is thus between 17 and 20 percent, with a power consumption between 800 and 900 watts.

Static efficiencies ranging from 60 to 80 percent are achieved commonly in industrial practice using centrifugal blowers with backward curved airfoil-shaped blades and externally mounted drive motors. After accounting for scale or size differences, there is a significantly higher cost to be associated with this higher efficiency due to critical clearance dimensions. As partial cost compensation however, note that if blower efficiency is improved then motor size, and presumably cost are reduced. There exists also the prospect for an increase in motor efficiency. It is well known that because of geometric effects, the achievable efficiency of small fractional horsepower single phase motors is at most 70 percent. The practical horizon for motor efficiency is therefore between 65 and 70 percent, which represents a significant improvement relative to current practice. The prospect is therefore very good for a high-efficiency indoor air mover for residential heat pumps which would roughly halve the required electrical power and have economic and commercial viability.

In order to achieve a doubling in overall air-mover efficiency, a high-efficiency single-entry blower wheel design was proposed, with multiple backward curved airfoil-shaped blades driven by a high-efficiency motor. The design goal was a 65 percent efficient blower driven by a 65 percent efficient motor. The preliminary performance specification for this blower called for a delivered airflow of 1575 scfm with a static pressure rise of 0.85 inches of water. Dimensionally, the air mover was constrained to fit within a cabinet 22.5 inches wide.

The use of backward-curved blade blower technology is necessary to obtain a significant increase in operating efficiency relative to the conventionally applied squirrel-cage blower. Originally, a four-pole blower motor was considered because the motor would be less expensive, and the space occupied by the air mover would be less because the higher-speed blower wheel is smaller. In an additional effort to contain cost and minimize size, a cylindrical blower shroud was used during preliminary testing.

Preliminary testing of the 13.5 inch diameter breadboard blower wheel designed to operate at four-pole speed in a cylindrical shroud revealed a characteristic howling noise that was objectionable. In addition, the performance of an appropriately scaled blower at 12.75 inch diameter yielded 52 percent static efficiency while absorbing 0.4 shaft horsepower. Since six-pole motor speed would yield lower noise and better blower efficiency, our design effort was redirected there. At this reduced rpm, significant efficiency benefits accompanied adoption of a volute shroud.

Prior to the manufacture of our preprototype units, a system design change required a modification in the blower specifications from 1575 cfm to 1400 cfm at 0.85 inches of water static pressure rise, and later to 1400 cfm at 0.95 inches of water pressure rise. Since the backplate and inlet cone for the blower wheel had been procured prior to receipt of the later pressure specification, modification of the design to meet the final design point was constrained slightly. Also, after design of the heat pump indoor unit was completed, the pressure rise requirement at 1400 cfm was revised upward to 1.09 inches of water. These revised specifications on pressure were accommodated by overhanging the blades beyond the back plate diameter. Given the opportunity to redesign the blower again, the blower side plates would be increased slightly in diameter so as to be equal to the blade tip diameter and an increase of approximately 3 to 4 percentage points in efficiency would result.

Two blower wheels were designed, built and tested. The first used airfoil-shaped blades and the second used cambered-plate blades. The blower with airfoil blading was the more efficient by 5 to 8 percent.

The airfoil-bladed blower wheel is most effectively manufactured using a molded plastic design. Certification requirements dictated the use of an expensive plastic. In high-volume production that route is quite viable, and a significant efficiency gain is realizable. However, the tooling required to produce a prototype for this R&D effort was too expensive for the resources available.

Cambered-plate blades are manufactured for a modest tooling investment and common metals can be used to limit cost. Additionally, a prototype model could be fabricated easily for evaluation. The performance penalty suffered upon adopting cambered-plate blades instead of airfoil-shaped blades is modest. Since the use of cambered plate blading allowed us to meet our performance objective while promising lower ultimate cost, cambered plate blading was adopted for the prototype indoor air movers.

The blower motor design for the preprototype heat pump evolved from a 0.4 hp, four-pole motor with "deep" speed reduction capabilities to a 1/3 hp, six-pole design with somewhat less speed reduction potential than in the case of the four-pole motor. The motor finally selected does not represent a precise optimum. This is partially due to the nonstationary targets for the design, necessitated by the overall system optimization study, and by the fact that the effort required to perform a complete suboptimization of the motor did not seem warranted since the contribution of the blower motor to overall system efficiency and system cost is small.

Although the overall length of the blower motor was constrained by the available cabinet width and the size of the blower, the end result of our motor design effort is a blower motor that is considerably more energy efficient than current state-of-the-art motors. The cost premium has a payback period well under four years. It is judged to be close to optimum in design while meeting space constraints.

The 1/3 hp, six-pole blower motor design employs a 1.97 inch stack with an approximate balance between the weight of copper in the main and auxiliary windings. The turns ratio (effective auxiliary turns to effective main turns) is 1.042. The capacitor required is 7.5 μfd. The motor has a medium-resistance rotor which on a horsepower per unit basis is 0.113 per unit resistance. Our goal in the design was to effect the maximum feasible utilization of the slots within manufacturing capabilities, and to run close to balanced operation. The estimated efficiency at full load for this six-pole motor is 67.0 percent.

The indoor air mover as developed for the preprototype advanced electric heat pump is shown in Figure 28. This assembly slips into an air mover cabinet with external dimensions 22.5 inches wide by 30 inches high by 30 inches deep. It is captured in the cabinet using the flanges at the discharge plane of the scroll. A bracket (not shown) secures the end of the scroll opposite the discharge to the cabinet.

The aluminum (3003 H14) blower wheel shown in Figure 9 has an effective blade tip diameter of 16.25 inches and uses ten backward curved, uniformly spaced, cambered plate blades 0.090 inches thick spanning between a conical backplate 0.063 inches thick and an open center conical side plate 0.040 inches thick. The blower shaft is carried within the scroll by two sets of permanently lubricated, sealed, ball bearings, one set mounted to the back plane of the scroll, the other set centered over the inlet opening by a wire form bearing carrier. A rounded conical inlet cone seals the intake side of the scroll to the conical side plate of the blower wheel. The blower motor is axially aligned with the blower shaft and supported by a wire form belly band carrier. The motor shaft and blower shaft are joined by a flexible coupling.

The performance of the preprototypic blower wheel mounted in a mock-up version of the volute scroll and tested in a blower test cell is

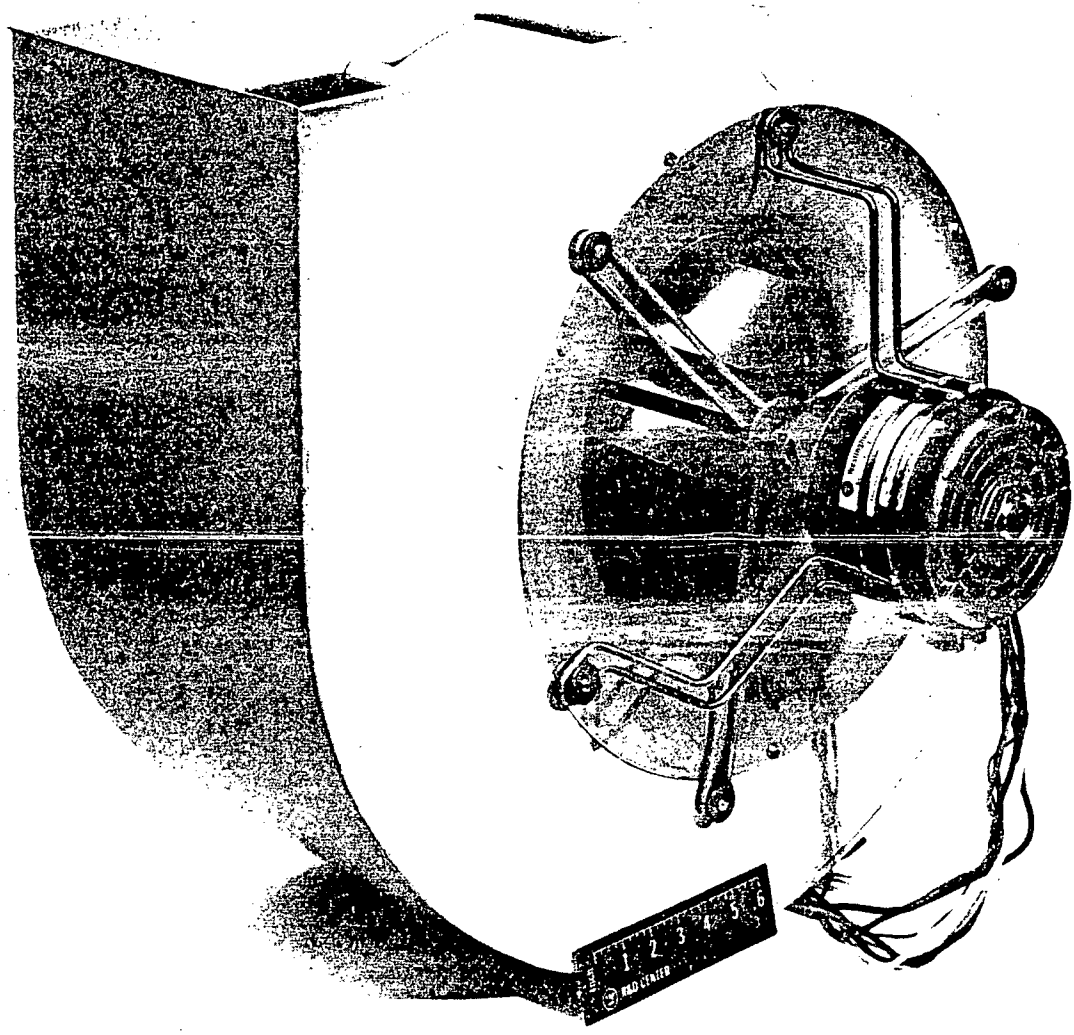


Fig. 28 - Indoor air mover assembly

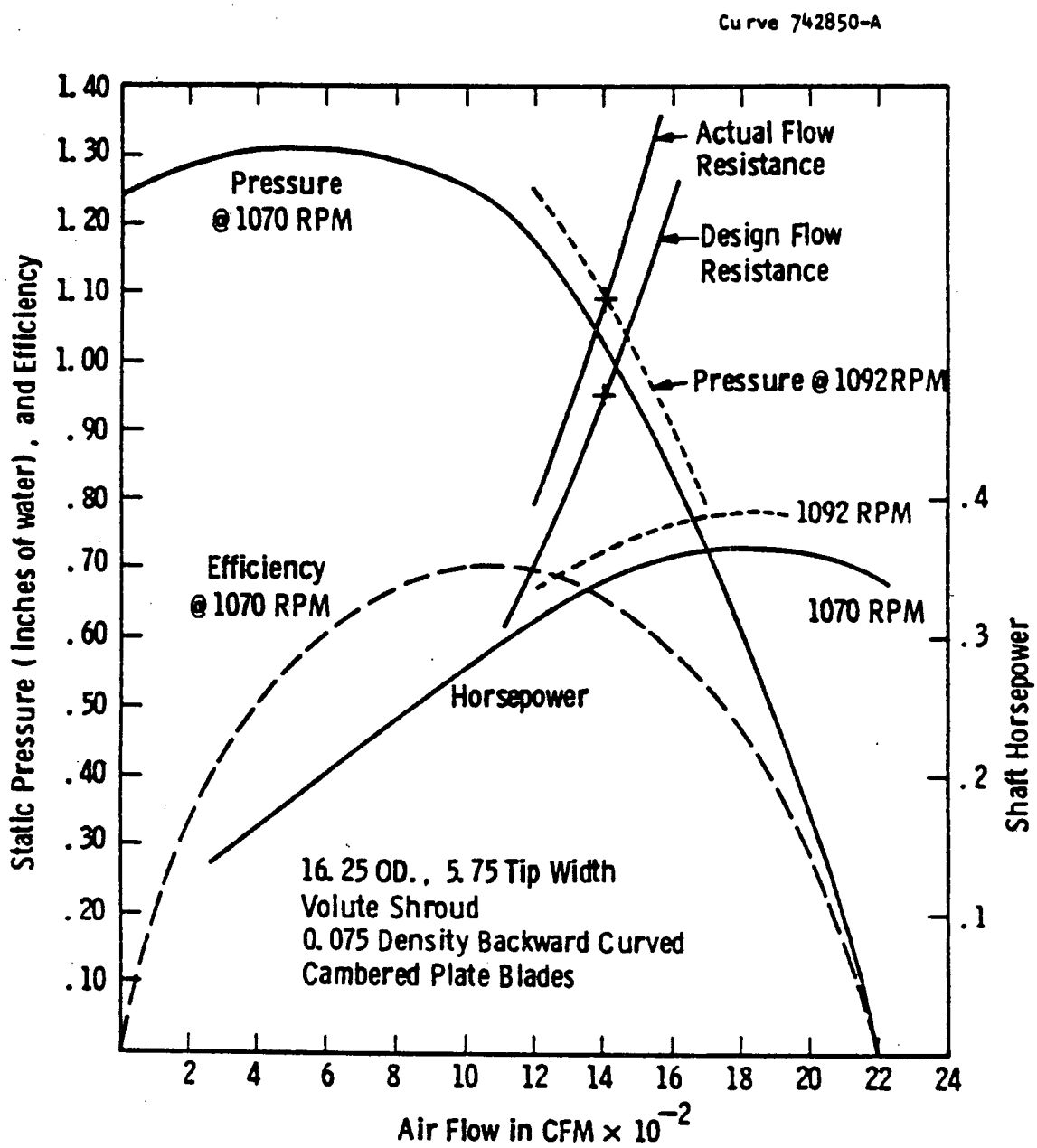


Fig. 29 - Performance characteristics, preprototype blower (dimensions in inches)

shown in Figure 29. Into the design resistance, a parabolic load curve ($P \alpha Q^2$) passing through the origin and the design point (1400 cfm at 0.95 inches of water), the blower requires 0.35 shaft horsepower to deliver 1430 scfm with a pressure rise of 0.98 inches of water at 1070 rpm. The static efficiency is 64 percent. At the peak efficiency of 70 percent, the blower will deliver 1060 scfm with a static pressure rise of 1.23 inches of water and requires 0.29 shaft horsepower. The blower will deliver 1575 scfm with a static pressure rise of 0.87 inches of water at a static efficiency of 58 percent and will require 0.36 shaft horsepower.

As installed in the preprototype heat pump system, the air mover consumes 390 watts when delivering 1405 scfm at 1092 rpm through a dry coil. The homologous fan laws can be used to scale blower performance at 1092 rpm given data at 1070 rpm. The resultant performance is shown in Figure 29. Since the observed flow is 1405 cfm at 1092 rpm the actual resistance curve must pass through this point. The indicated flow resistance is thus 1.09 inches of water. Since the resistance external to the heat pump is fixed at 0.35 inches of water, then the internal unit resistance (with dry coil) must be 0.74 inches of water. The blower shaft power from Figure 29 is 0.365 hp. The static efficiency is then 66 percent, and the motor efficiency 69.8 percent. Overall air moving efficiency is thus 46 percent. The measured electrical power consumption of the preprototype air mover is half that of the air mover in a conventional heat pump of the same nominal capacity (3.5 tons) but higher airflow (1575 scfm) working into the same external flow resistance (0.35 inches of water) but lesser internal pressure drop. Measured electrical consumption at reduced flow is 190 W at 770 rpm.

Our preprototype indoor air mover with cambered plate blades has an air moving static efficiency approximately twice that of current practice with commensurate energy savings.

The estimated factory cost of this air mover (Figure 28) is $55, approximately twice that of the conventional air mover. The annual operating cost for this air mover in Minneapolis is $81 based upon an electricity cost of 5¢/kWh, 1493 hours in low capacity heating with low-speed blower, 2590 hours in high-capacity heating with high-speed blower and 840 hours of cooling with high-speed blower. A conventional air mover and motor applied to the same duty would consume twice the energy in high-speed operation and roughly 2-1/2 times the energy in low-speed operation assuming 770 rpm were available. The prototype air mover would thus save about $88 per year in Minneapolis. We conclude the following concerning the indoor air mover:

1. The preprototype air mover in situ at 1092 rpm consumes 390 W of electrical power to deliver 1405 cfm of 62°F air through the preprototype indoor unit into an external flow resistance with an overall static pressure drop of 1.09 inches of water thus yielding a blower static efficiency of 66 percent and an overall air moving efficiency of 46 percent.

2. The electrical power saved relative to a replacement air mover of conventional construction is approximately 400 watts or 50 percent.

3. The premium first cost of the air mover (blower wheel, scroll, motor, inlet cone, motor support and mounting hardware) should be recoverable from energy savings in less than one year in Minneapolis given that the cost of electricity is 5¢/kWh, and assuming the effective retail cost at three times the factory cost.

4. The use of airfoil-shaped blades instead of cambered plate blades would improve air moving static efficiency by about five percentage points.

5. Replacing the inlet and back plates so as to eliminate the overhung blades would increase air moving static efficiency by about three percentage points.

6. Overall air moving efficiencies in excess of 50 percent in residential heat pumps should be possible using direct drive blowers with backward curved airfoil-shaped blades and high-efficiency motors.

Additional information may be found in Reference 8.

## 4.4 Refrigeration System Description

### Refrigerant Circuit

The Westinghouse/DOE heat pump incorporates a unique refrigerant circuit that is designed to yield a flooded evaporator in the heating mode and evaporator superheat in the cooling mode. Flooded evaporator operation has several advantages over the more conventional superheated evaporator discharge. Since the reciprocating compressor is basically a constant volume flow device, refrigerant mass flow is maximized by maximizing the density of the suction gas. The flooded evaporator system provides nearly saturated vapor at the compressor suction line, thus maximizing density. A flooded evaporator maximizes the utilization of the heat exchanger surface. Since the entire heat exchanger is in two-phase flow, high tube side convection coefficients are maintained and since the refrigerant temperature is nearly uniform and at saturation, the refrigerant-to-air temperature difference is maximized for a given evaporator pressure.

Westinghouse manufactured and marketed a heat pump using a flooded evaporator and subcool control (Hi-Re-Li) in both operating modes for more than a decade. The Hi-Re-Li circuit is shown schematically in Figures 30 and 31. The suction line accumulator protects the compressor from slugging during transients and the heat exchanger in the accumulator provides a heat source for vaporizing stored liquid following such transients. In addition, this heat exchanger is an integral part of the refrigerant control circuit, working in conjunction with the expansion valve to vaporize precisely the amount of evaporator overfeed. The Hi-Re-Li system is relatively insensitive to charge level, provided a minimum charge level is maintained. The system does have disadvantages however. Since the expansion device used could control flow in only one direction a complicated, expensive manifold check valve assembly was required to control the direction of refrigerant flow through the valve. This check valve assembly is a potential source of system failures and the heat leak and refrigerant pressure drop

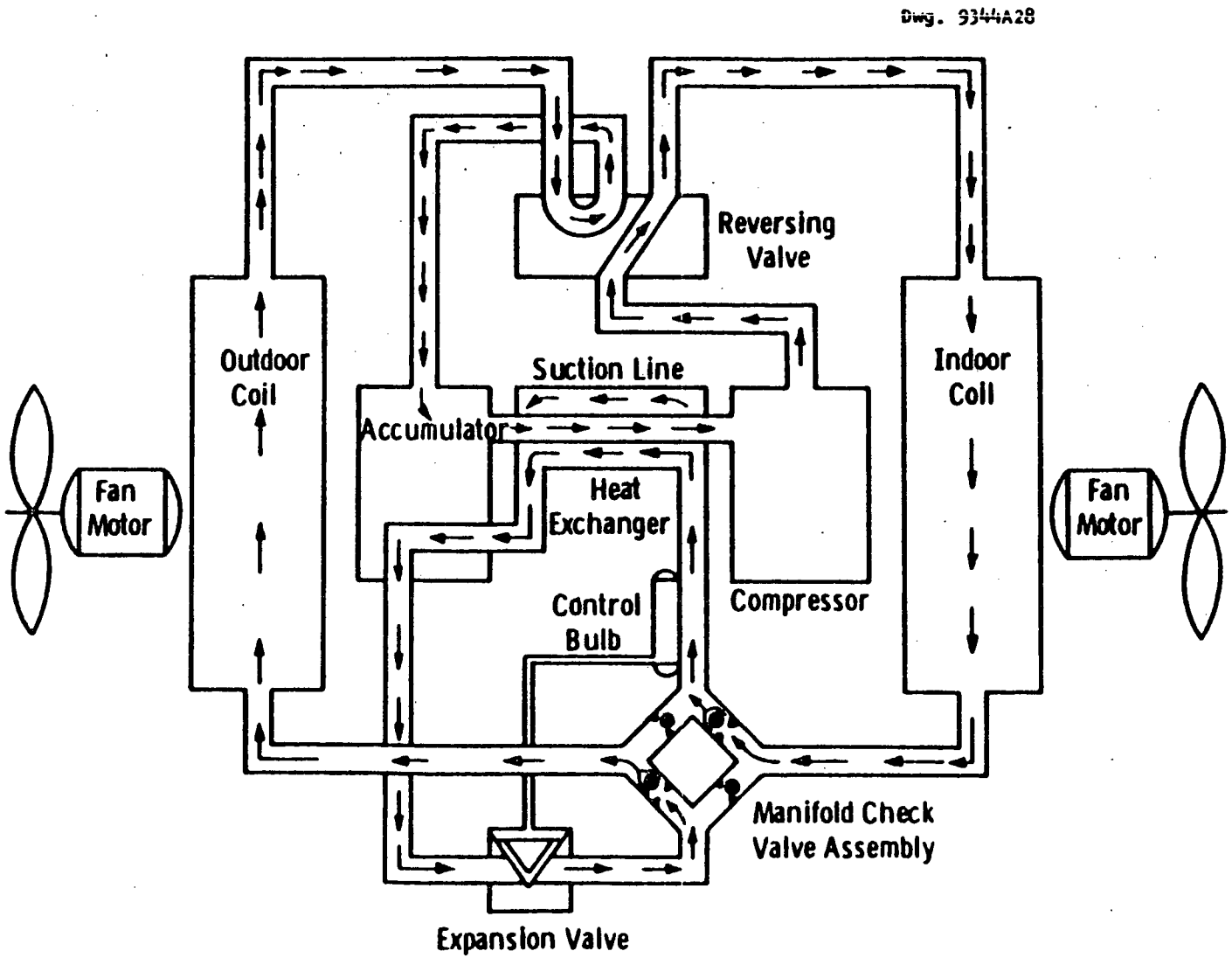


Fig. 30 - Hi-Re-Li circuit - heating

Dwg. 9344A29

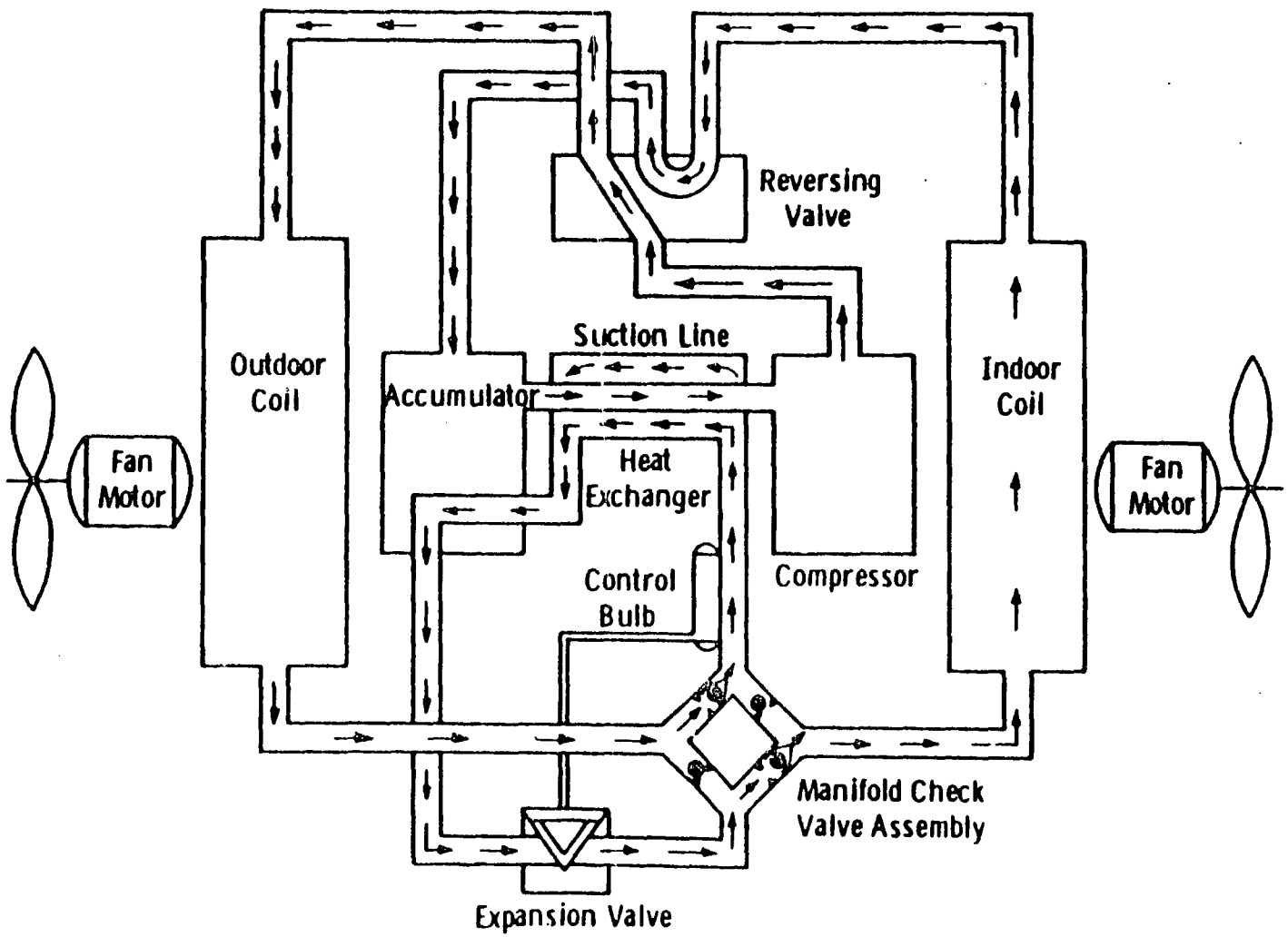


Fig. 31 - Hi-Re-Li circuit - cooling

penalize system performance. While the system is insensitive to charge above a certain level, a charge below the minimum results in a precipitous loss in performance. The method developed to field charge the system is more complex than the method used for conventional systems and some service personnel have had difficulty in learning the method or have been unwilling to learn the method.

The electric expansion valve used in lieu of the bulb controlled expansion valve permits flow in either direction and thereby obviates the check valve assembly. Several possible circuits were evaluated using unit comparison decision making techniques.

The circuit shown in Figures 32 and 33 is the simplest circuit and utilizes a Hi-Re-Li type accumulator. Refrigerant flow control in the cooling mode is designed to be the electrical valve analog of the conventional TXV or evaporator superheat control scheme. The accumulator heat exchanger thermally "short circuits" the evaporator in the cooling mode, but since there is little temperature difference, the heat leak is small. Heat may flow in either direction across this heat exchanger depending upon the evaporator refrigerant pressure drop and the amount of superheat. The system may be field charged in the cooling mode using conventional techniques.

In the heating mode, the circuit is designed to be the electrical valve analog of the Hi-Re-Li condenser subcooling control scheme. Note from Figures 32 and 33 the temperature sensors at midpoint and both terminals of the indoor heat exchanger. Sensing of the midpoint temperature and the appropriate terminus temperature permits evaluation of evaporator superheat or condenser subcooling. The microprocessor is programmed to excite the expansion valve with a voltage which is a prescribed function of ambient temperature. The functional relationship was devised from test data so as to yield the appropriate levels of condenser subcooling or evaporator superheat depending upon operating mode.

Compressor

The dual-stroke compressor incorporates several features which improve seasonal efficiency. See Section 4.1 for details. The compressor capacity and efficiency are significantly improved by using the lubricating oil rather than suction gas to remove electrical, mechanical and windage losses. The lubricating oil is cooled by passing it through a separate one row, single circuit, plate fin on tube heat exchanger located in the discharge air stream of the indoor unit. See Table 14. The heat rejected by the oil to air heat exchanger increases the heating capacity and reduces the cooling capacity by about 2000 Btu/h at rating conditions in high-capacity mode.

The oil to air heat exchanger in the preprototype was located in the discharge air stream so that it could be mounted on the removable skid assembly with the compressor, accumulator, reversing valve and expansion valve to simplify service (See Figures 38 and 39). The oil cooler is approximately half as high as the refrigerant heat exchanger and thus causes some maldistribution in the airflow. Due to location, the inlet air to the oil cooler is hotter than indoor ambient during heating operation and colder than indoor ambient during cooling operation. Consequently, the oil temperatures are significantly higher in the heating mode than the cooling mode, but still within acceptable limits. Locating the oil cooler in the inlet air stream would provide a more uniform compressor operating temperature, reduce the required oil cooler heat exchanger area and increase cooling capacity slightly. Project resources would not permit optimization. A further discussion of the compressor is given in References 4 and 9.

Indoor Heat Exchanger

The indoor air to refrigerant heat exchanger is of conventional construction, but incorporates an unusual refrigerant circuit which maximizes heating performance and provides a comfortable sensible/total capacity split in cooling. Heat exchanger details are given in Table 15. Heat exchanger circuiting is shown schematically in Figure 34.

Table 14

Details of Oil Cooler

| | |
|---|---|
| Type of Coil | Plate Fin Slab |
| Tube Material | Copper |
| Tube Diameter/Wall Thickness | 0.375/0.017 inches (before expansion) |
| Tube Length between End Plates | 26.5 inches |
| Number of Tubes | 12 |
| Number of Tube Rows | One |
| Transverse Pitch | 1.0 inches |
| Coil Height | 12 inches |
| Fin Material | Aluminum |
| Fin Thickness | 0.0075 inches |
| Fin Density | 8.0 fins per inch |
| Fin Width | 0.875 inches |
| Ripples per Pitch/Ripple Height | None |
| Number of Such Slabs Used | One |
| Tilt Angle | 15 degrees |
| Face Area | 2.21 square feet |

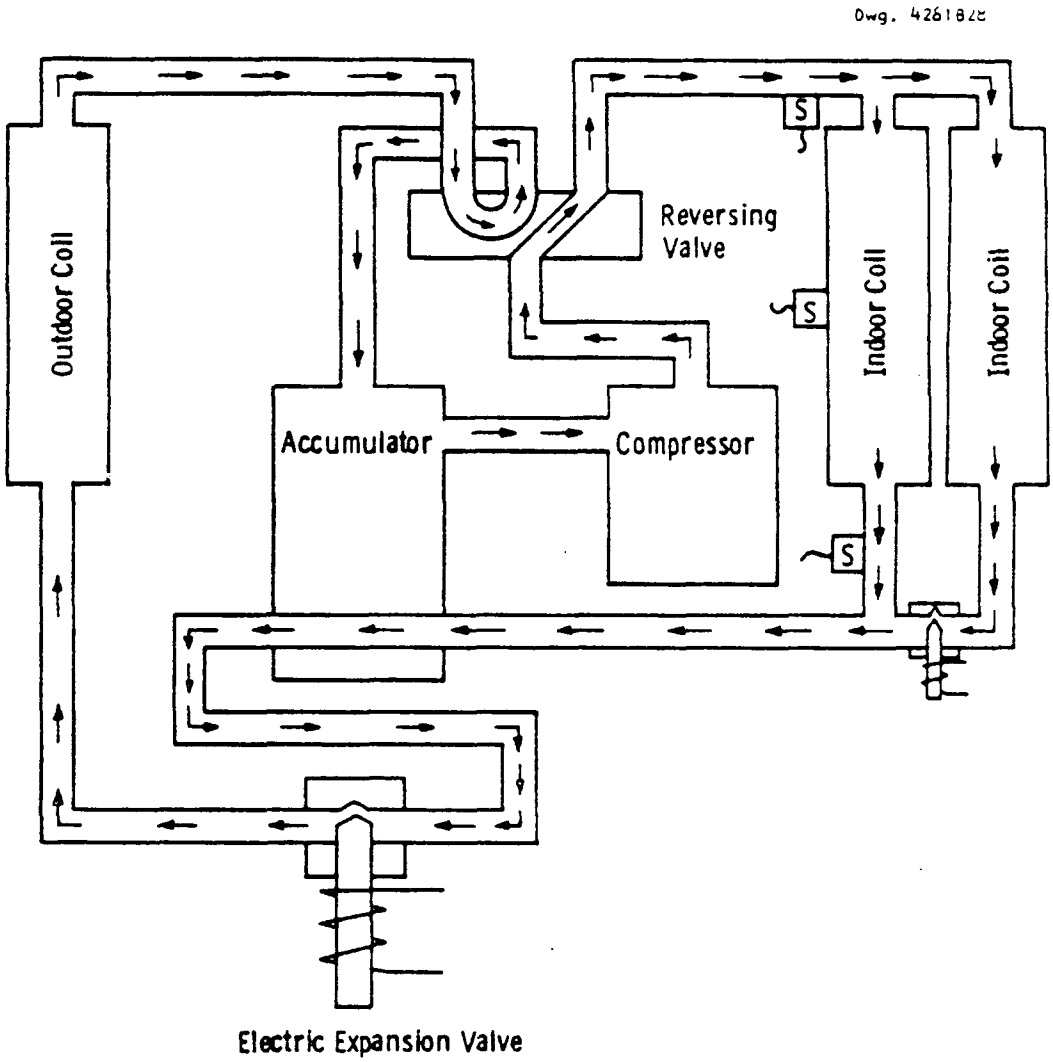


Fig. 32 - Subcool heating/superheat cooling circuit with electric valve - heating (note that indoor coil partitioning solenoid valve is open in heating mode)

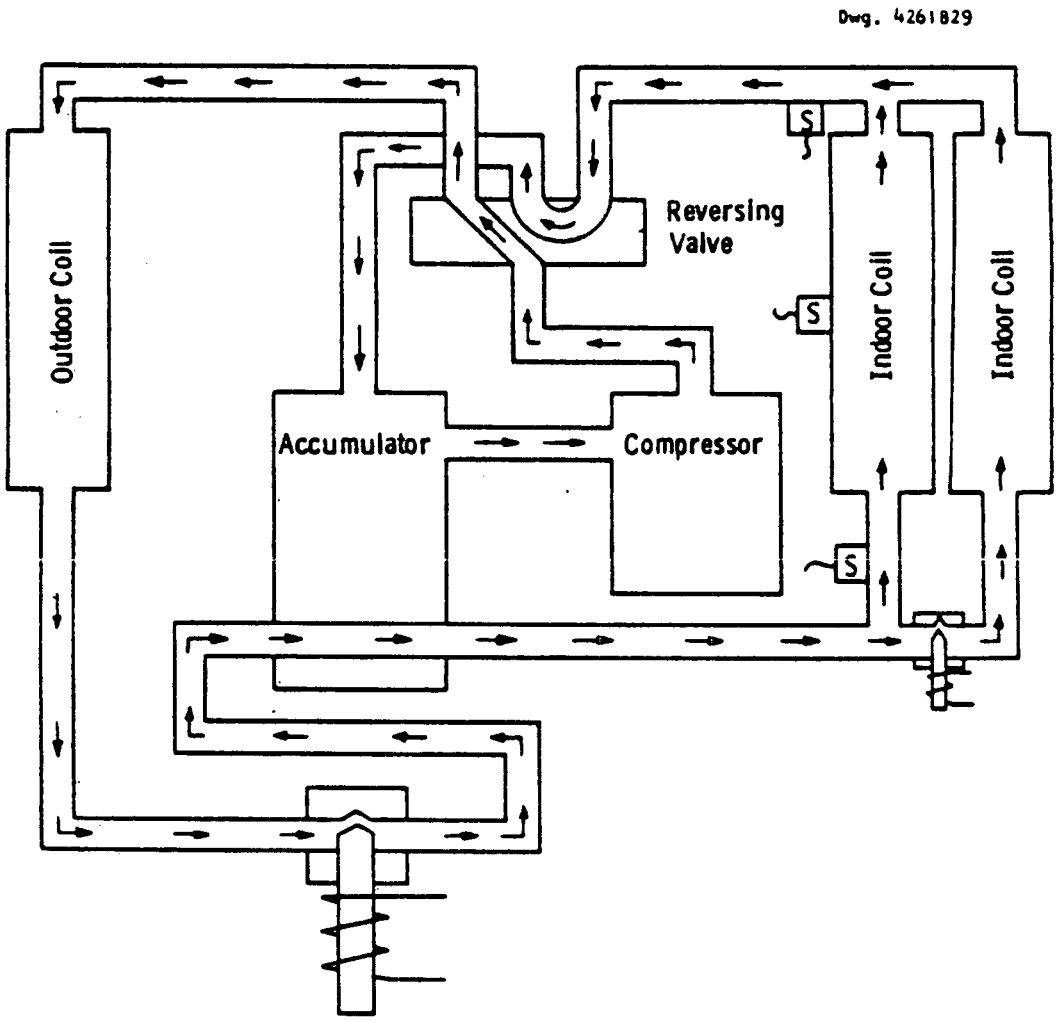


Fig. 33 - Subcool heating/superheat cooling circuit with electric valve - cooling

Table 15

Details of Indoor Refrigerant-to-Air Heat Exchanger

| | |
|---|---|
| Type of Coil | Plate Finned Slab |
| Tube Material | Copper |
| Tube Diameter/Wall Thickness | 0.375/0.017 inches (before expansion) |
| Tube Length between End Plates | 30.5 inches |
| Number of Tubes | 104 |
| Number of Tube Rows | 4 |
| Transverse/Longitudinal Pitch | 1.0/0.867 inch(equilateral) |
| Coil Height | 26.0 inches |
| Fin Material | Aluminum |
| Fin Thickness | 0.0045 inches |
| Fin Density | 13.0 fins/inch |
| Ripples per Pitch/Ripple Height | 2/0.046 inches |
| Number of such Slabs Used | 1 |
| Tilt Angle | 15 degrees |
| Face Area | 5.50 square feet |

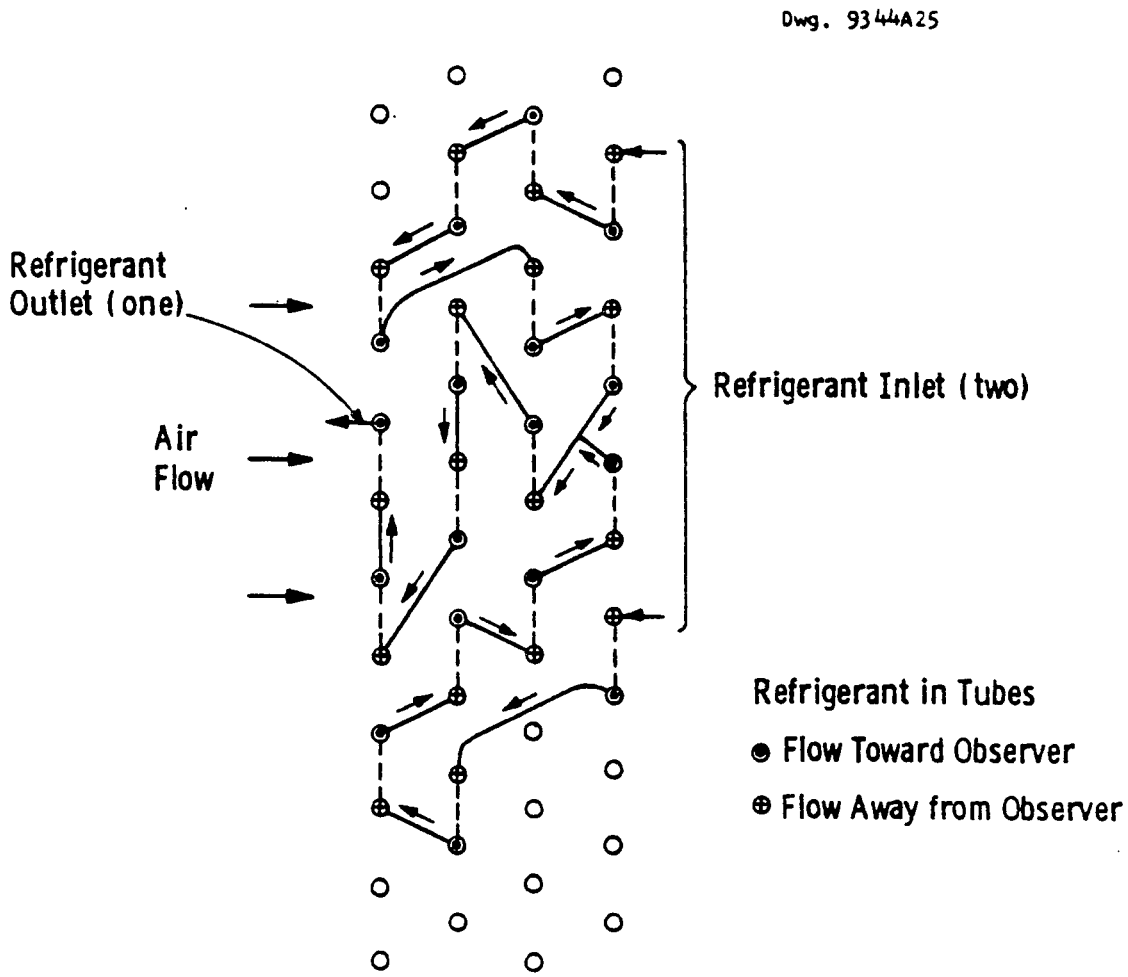


Fig. 34 - One of three indoor coil circuits (heating mode)

In the heating mode, refrigerant enters the coil through six parallel circuits of 12 tubes each. The six circuits are combined into three circuits to maintain high tube side heat transfer coefficients as the refrigerant density increases. The circuit optimization computer program CIRCON (Westinghouse Proprietary) indicates that this circuitry maximizes heating capacity.

Due to an irrepairable leak in one hairpin tube of the indoor heat exchanger for preprototype number two, the upper third of this heat exchanger was modified to the circuit shown in Figure 35. The available heat transfer surface is thereby reduced by about 2 percent.

In the cooling mode, the refrigerant flow is reversed and the refrigerant enters through three parallel circuits which branch into six parallel circuits. This is the proper circuit type for evaporator service. At inlet, the refrigerant density is relatively high and the number of parallel circuits must be kept low to obtain high tube side convection coefficients. As the refrigerant evaporates its density decreases and more parallel circuits are required to avoid excessive refrigerant pressure drop. At the refrigerant flow rates encountered in the high-capacity cooling mode, the refrigerant pressure drop is higher than optimum. For cooling service, a circuit with four parallel paths branching into eight parallel paths would improve performance. However, compromises are necessary to provide good performance in both modes and cooling performance has been sacrificed to improve heating performance. In those regions where a heat pump of this type would have maximum market penetration, far more energy is used in the heating season than in the cooling season.

In the low-capacity cooling mode, the large indoor coil would result in high evaporator temperatures, giving a high EER, but poor moisture removal and comfort under high humidity ambient conditions. Therefore, the coil has been arranged so that one of the three inlet circuits in the cooling mode can be blocked by a solenoid valve. See Figure 11. This lowers the evaporator pressure and temperature and increases the moisture removal rate significantly. The air which passes

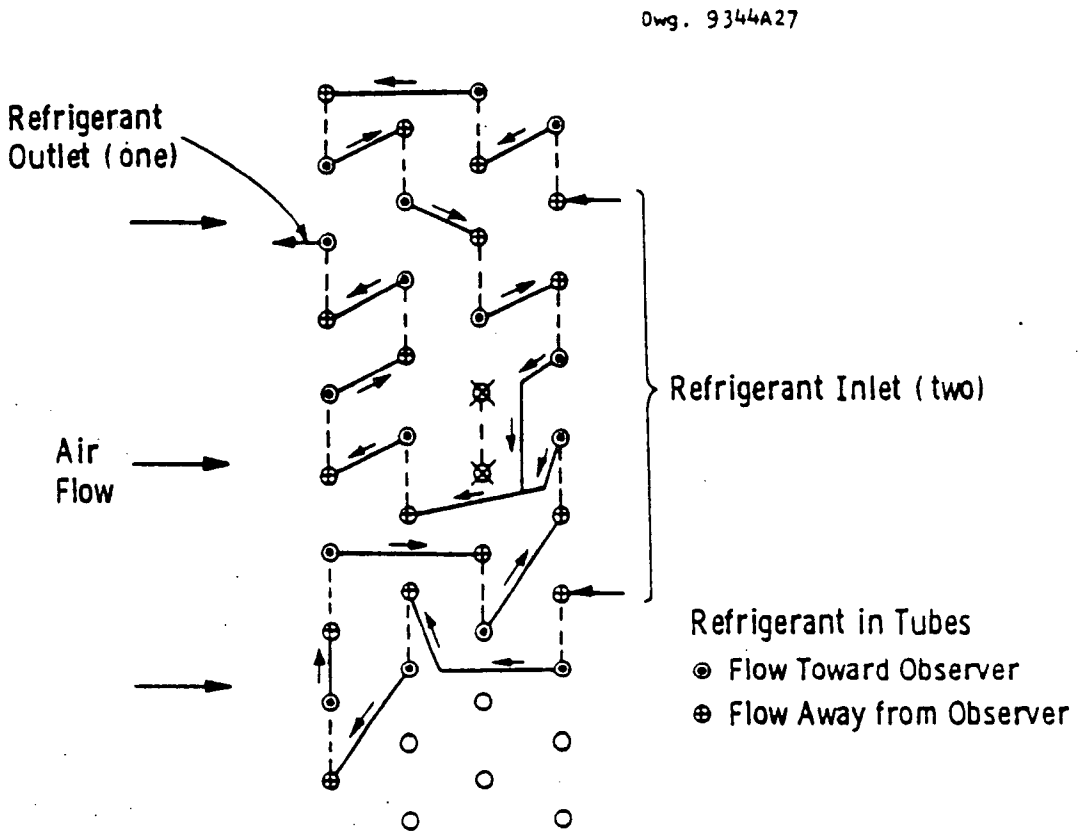


Fig. 35 - Top refrigerant circuit indoor coil preprototype number two - heating mode

through the inoperative portion of the coil mixes with cool dry air discharged from the operative portion of the coil giving a comfortable return air temperature and sensible/total capacity ratio.

Since a conventional solenoid valve may fail to open under an adverse pressure gradient, a bypass and check valve have been installed in parallel with the solenoid valve to ensure that all circuits will operate in the heating mode. Recent conversations with a solenoid valve manufacturer indicated that valves of the direct acting type are available that open reliably with an adverse pressure difference. This would allow elimination of the bypass and check valve, simplifying the circuit.

Outdoor Heat Exchanger

The outdoor heat exchanger is of conventional construction and is circuited to optimize performance in the heating mode. Four separate three row coils arranged in a "W" shape are used. See Figure 36 and Table 16 for details. The refrigerant circuitry is shown schematically in Figure 37. In the heating mode each coil has a single refrigerant circuit of 14 tubes each at inlet, branching into two parallel 14 tube circuits. Thus there are four parallel circuits at the inlet and eight at the outlet, giving a refrigerant pressure drop of 2 to 4 psi, which has been shown to be near optimum for evaporator service.

In the cooling mode, there are eight parallel circuits at inlet and four parallel circuits at outlet. This results in a refrigerant pressure drop in the 0.5 to 1.5 psi range, which is less than optimum for condenser service. The four parallel circuits at outlet make it difficult to retain enough liquid refrigerant in the coil to provide an optimum amount of subcooling.

Since the four slab coils used in the prototype do not have adjacent manifolding a separate subcooler was not provided in order to simplify the refrigerant piping and reduce cost. A modest improvement in cooling performance could be obtained by adding a separate subcooler.

Table 16

Details for Outdoor Refrigerant-to-Air Heat Exchanger

| | |
|---|---|
| Tube Material | Copper |
| Tube Diameter/Wall Thickness | 0.375/0.017 inches (before expansion) |
| Tube Length between End Plates | 38 inches |
| Number of Tubes per slab | 42 |
| Number of Tube Rows | 3 |
| Transverse/Longitudinal Pitch | 1/0.867 inches (equilateral) |
| Coil Height (one slab) | 14 inches |
| Fin Material | Aluminum |
| Fin Thickness | 0.0045 |
| Fin Density | 13.0 fins/inch |
| Ripples per Pitch/Ripple Height | 2/0.046 inch |
| Number of slabs | 4 |
| Face Area (total - 4 slabs) | 14.78 square feet |

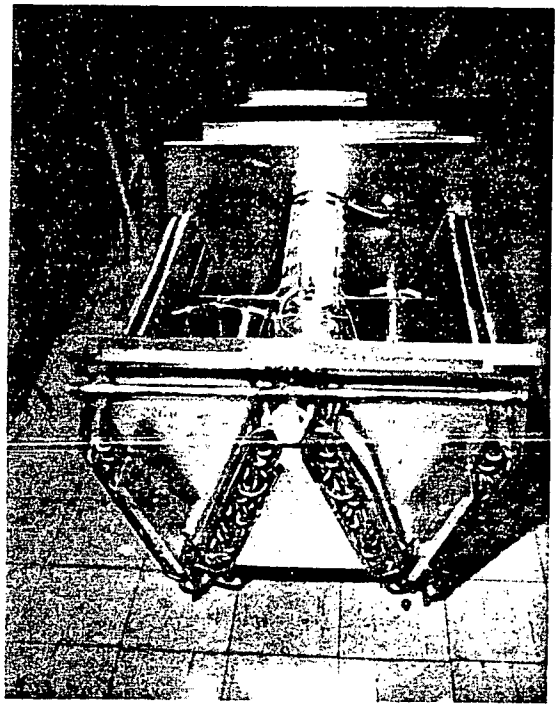

Fig. 36 - Outdoor heat exchanger configuration

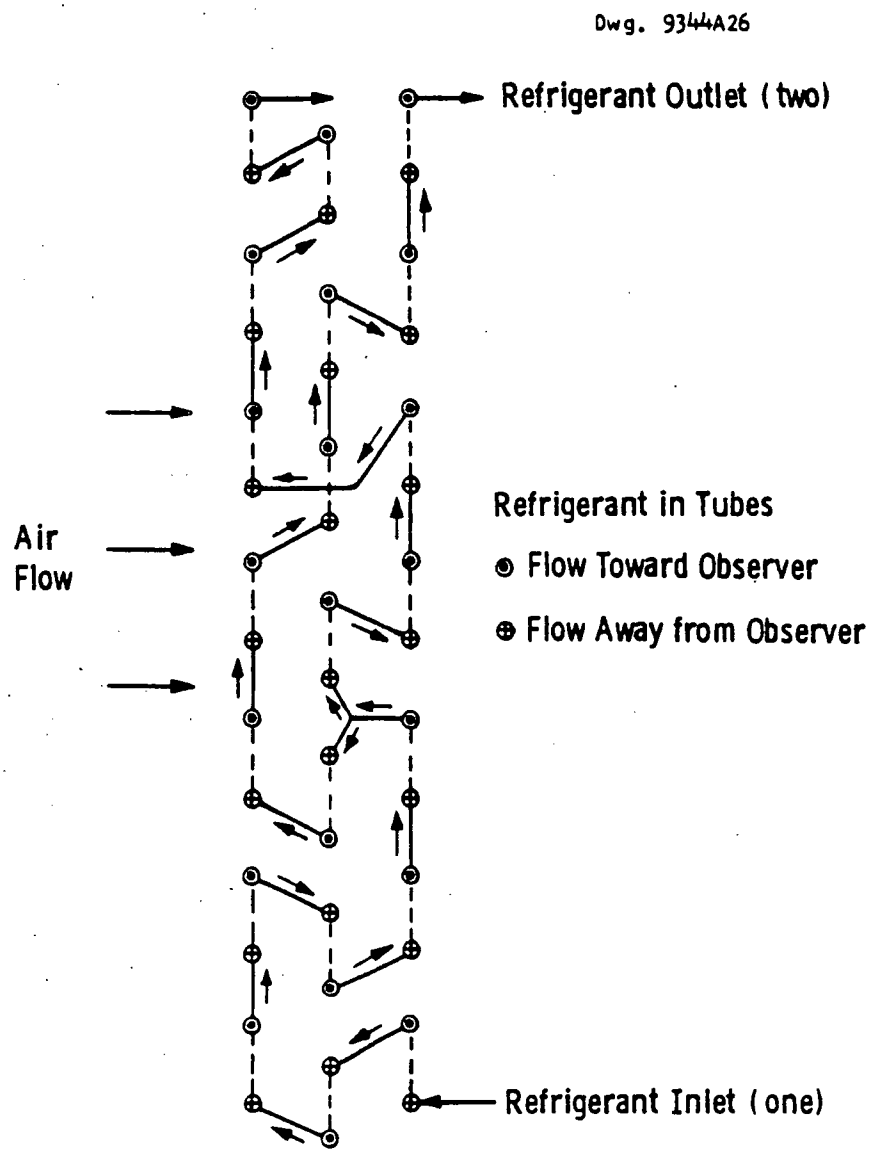


Fig. 37 - One of four outdoor heat exchanger slab circuits (evaporator refrigerant flow pattern shown, condenser is reverse)

## Suction Line Accumulator

The accumulator is a standard four ton Westinghouse Hi-Re-Li unit manfactured by Refrigeration Research Inc. (#7403). The design is conventional with the exception of a coil of 0.375 inch od tubing located at the bottom of the accumulator to provide a heat source for operating in the flooded evaporator mode. An orifice and screen at the bottom of the "J" tube provides oil return.

## Expansion Valve

Singer Model 625 electric expansion valves with equalization ports are used in both prototypes. Prototype one uses a 625-035 valve with a 0.093 inch orifice. Prototype two uses a 625-036 valve with a 0.109 inch orifice. The valve construction is similar to a thermostatic expansion valve, but the diaphragm which moves the valve stem is deflected by an electrically heated bimetallic element rather than the pressure on a trapped refrigerant charge. Refrigerant flow may be in either direction when an equalization port is used. The equalization port is connected to the compressor suction line so that refrigerant which leaks past the valve stem seal is returned to the system rather than condensing in the diaphragm chamber and preventing valve closure. The capacity of the valve is higher in the preferred flow direction and the valve is arranged so that the flow is in the preferred direction during heating mode operation.

## Reversing Valve

Several reversing valves were tested and the Product Engineering Model 103-1 valve was selected for use in the prototype. See Appendix D. This valve, with a nominal 4 ton capacity, gives low refrigerant pressure drop and flow leakage and has proven highly reliable in endurance testing. The internal heat leak is somewhat higher than competing valves due to the large internal surface areas, but heat leak is less damaging to system performance than refrigerant pressure drop or flow leakage.

Suction Line Filter Drier

An ALCO ASD 45 S 7 V filter drier is used. This unit is recommended by the manufacturer for much larger capacity units, and was adopted for the advanced heat pump in order to provide sufficiently low suction line pressure drop.

Muffler

A Refrigeration Research FR-M5 1762 muffler is used in the compressor discharge line.

Solenoid Valve

An Alco #200RA-4S-4T valve is used to partition the indoor heat exchanger.

Indoor Blower

The design and performance of the high-efficiency indoor blower and dual-speed blower motor are described in section 4.3 and in Reference 8.

Outdoor Fan

The design and performance of the high efficiency outdoor fan are described in section 4.2 and in Reference 7. The outdoor fan operates in high speed in the heating mode at both capacity levels. In the low-capacity cooling mode at ambient temperatures below 82°F the low speed can be used to reduce noise.

Controls

The microprocessor based control circuitry is described in section 4.5 and in Reference 4. Microprocessor control maximizes performance by providing optimum subcooling in the heating mode and optimum superheat in the cooling mode. In addition to the control function it provides anomaly detection, component protection and diagnostic information.

Plumbing Details

Figures 38 and 39 in conjunction with Table 17 give the plumbing details of preprototype #2.

## 4.5 Controls

The advanced electric heat pump uses a microprocessor to oversee and manage the system. The microprocessor initiates action by activating microcontrol relays which in turn activate the 24 V/240 V control relays shown in the schematic diagram, Figure 13. Schematic drawings of the microprocessor control system are given in Figures 40 through 44. Note that the microprocessor system documented here is a breadboard, not a preprototype. As such it is constructed for maximum flexibility rather than minimum cost.

The microprocessor based control system performs several functions:

- Selection of system capacity
- Sequential closure of operating relays
- Modulation of the expansion valve voltage
- Defrost
- Fault detection and system protection.

The operating mode (heat vs cool) is selected manually by a switch on the thermostat. The compressor capacity, indoor blower speed, outdoor fan speed and number of stages of resistance heat are selected by the microprocessor according to the outdoor ambient temperature and the thermostat stage according to the logic shown in Tables 18 and 19.

The sequence of operations in the heating mode is shown in Table 20. When the outdoor ambient temperature exceeds a preset value, typically 40°F, no trickle heat is used and step 1 is omitted. When resistance heat is required the number of stages used is selected by the microprocessor based on preset temperature setpoints, current outdoor ambient temperature and thermostat stage as noted previously. The required number of stages are enabled simultaneously, but thermal relays

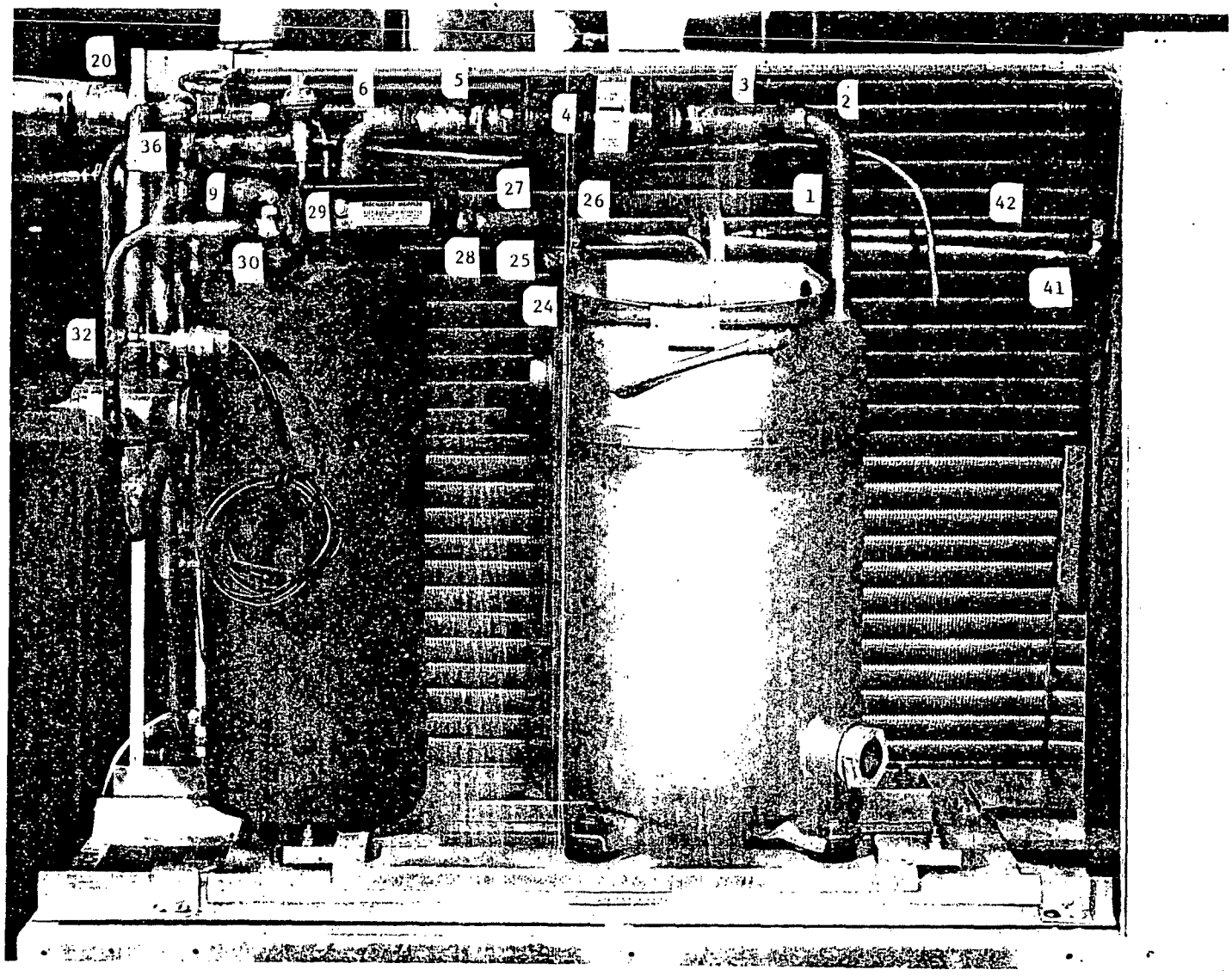


Fig. 38 - Side view of indoor unit with plumbing details

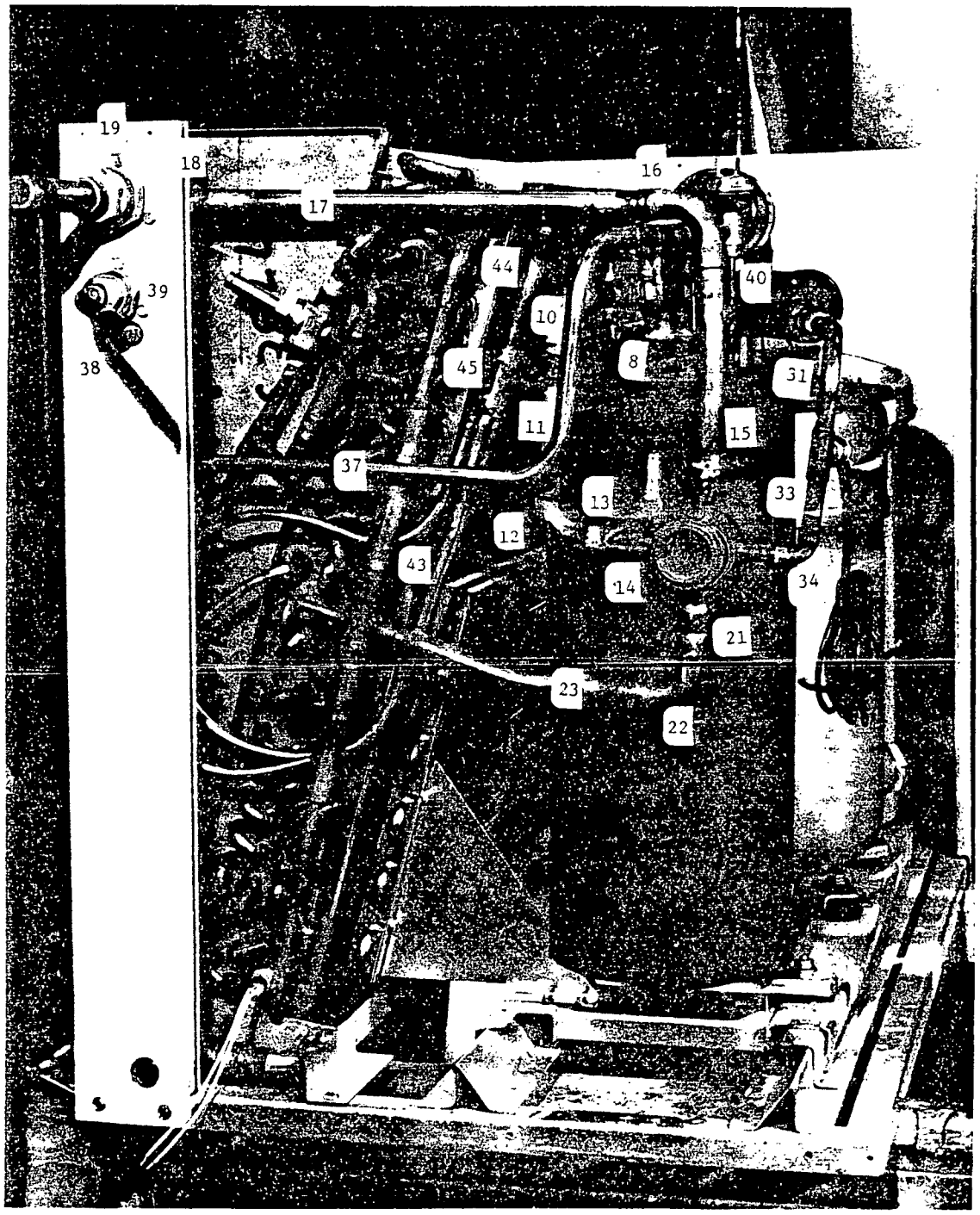


Fig. 39 - End view of indoor unit with plumbing details

Table 17 - Prototype No. 2 Plumbing

1. Suction line projecting 5 inches from compressor top
2. 7/8 inch dia. long radius elbow
3. 7/8 inch OD, 2-1/4 inch long tube
4. ALCO ASD 45 S 7 V filter drier
5. 7/8 inch OD, 3-1/2 inch long tube
6. Long radius elbow (same as 2 above)
7. 7/8 inch OD tube, 3 inches long (vertical to accumulator outlet)
8. 7/8 inch OD long radius street ell into "in" of accumulator bushing reducer to 3/4 inch dia.
9. 3/4 inch dia., 2-1/2 inches long tube
10. 3/4 inch dia. long radius elbow
11. 3/4 inch OD tube, 4 inches long (vertical)
12. Long rad. elbow (same as 10)
13. 3/4 inch OD tube, 1-1/2 inches long into
14. 3/4 inch dia. port (horizontal) of rev. valve, Product Engrg. No. 103-1
15. 3/4 inch dia. tube vertical, 6-3/8 inches long
16. 3/4 inch dia. long radius elbow
17. 3/4 inch dia. 13-1/2 inches long tube
18. Reducer 3/4 inch to 7/8 inch dia.
19. 7/8 inch dia. short radius street ell for 7/8 tube into
20. Aeroquip 5750, S2-14-12B
21. 1 inch long, 3/4 inch dia. cu. tube
22. Short radius 3/4 inch dia. elbow
23. 7-1/2 inch long, 3/4 inch dia. tube
24. 1-1/2 inch long by 1/2 inch dia. steel S tube on can
25. 1/2 inch dia. Cu Tee
26. 1/2 inch dia. street ell short radius
27. 3-1/2 inch long, 1/2 inch OD Cu tubing
28. 1/2 inch reducer to muffler inlet, 5/8 inch
29. Muffler PR-M5 1762
30. 1/2 inch reducer
31. 7-3/4 inch long, 1/2 inch dia.
32. 1/2 inch reducing "Tee" to 1/4 inch dia. (HP cutout)
33. 2-1/2 inch L, 1/2 inch D
34. 1/2 inch dia. short radius elbow
35. 4 inches long, 1/2 inch OD Cu (horizontal) (TXV to Aeroquip)
36. Tee 1/2 inch dia. (Schraeder tap)
37. 23-3/4 inches long, 1/2 inch dia.
38. 1/2 inch dia. street ell into
39. Aeroquip 5750 S2-8010B
40. 3 inches L, 3/8 inch tubing (accumulator to TXV)
41. 38 inches L, 3/8 inch dia. tubing to oil cooler
42. 21 inches L, 3/8 inch dia. tubing to oil cooler
43. 1/4 inch OD tubes 23 inches long (each of 3) distributor to coil
44. 3.8 inch OD, 14 inches long accumulator to distributor
45. Distributor Sporlan 1613-3-1/4 - none

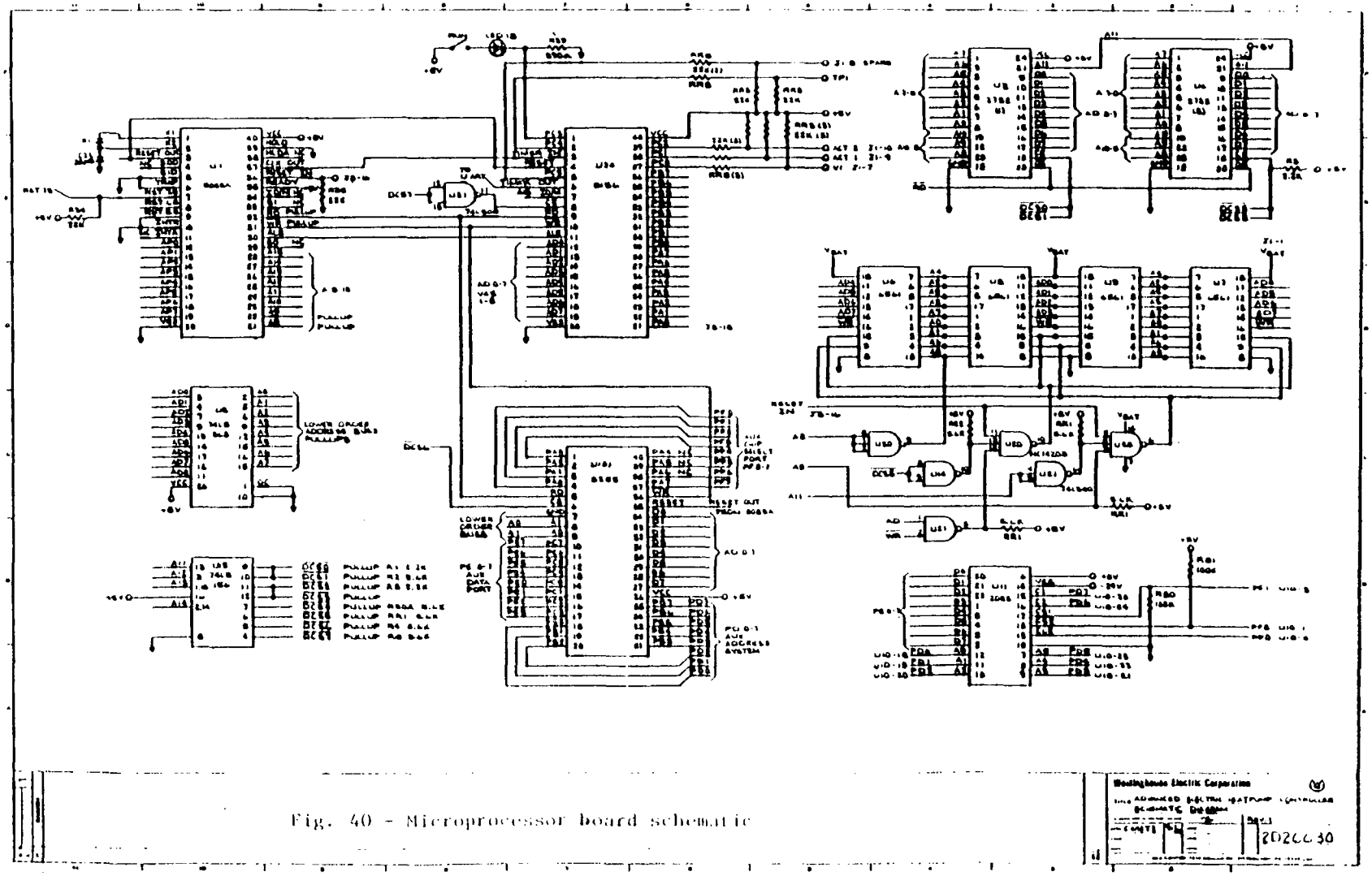

Fig. 40 - Microprocessor board schematic

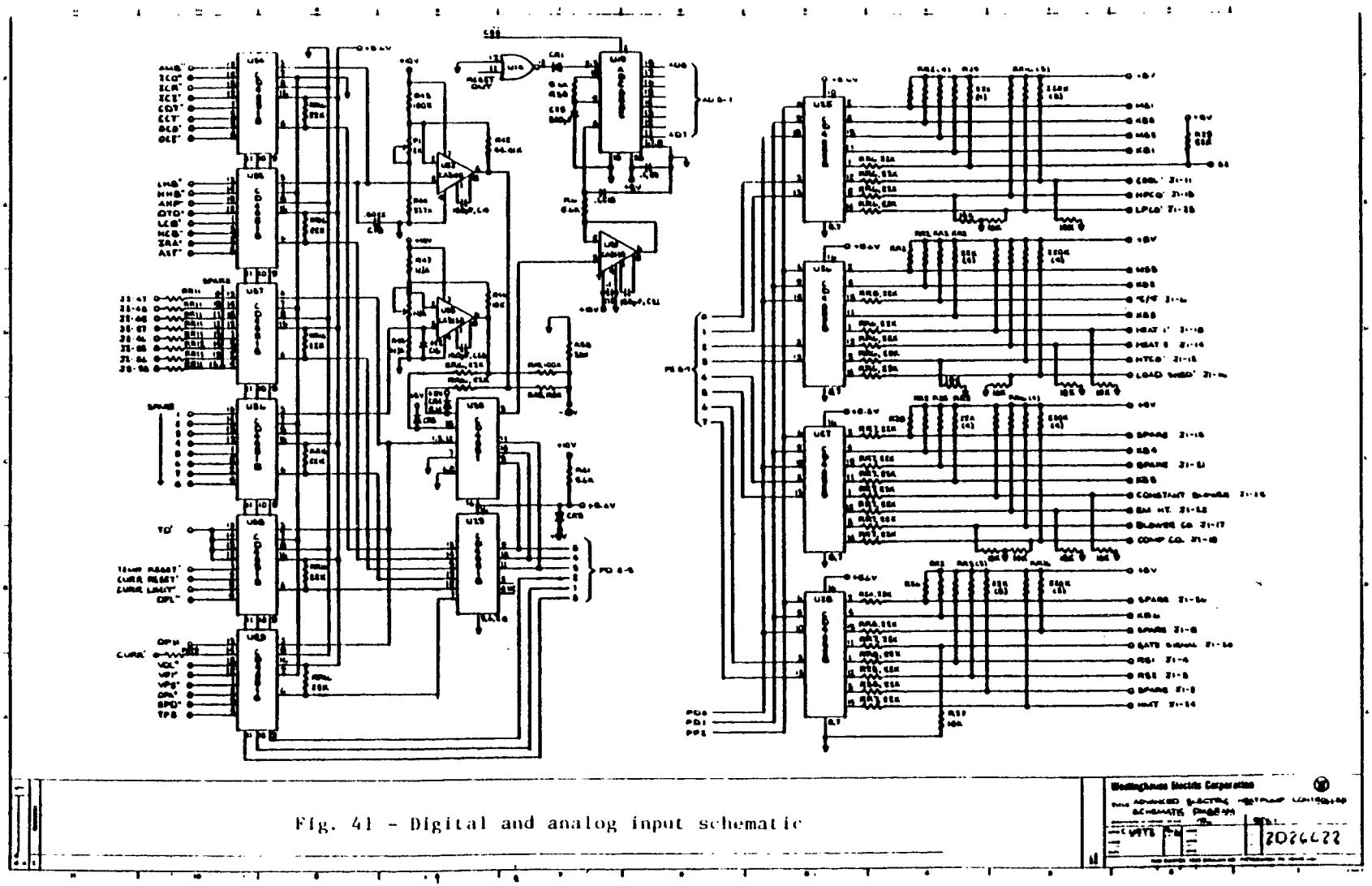

Fig. 41 - Digital and analog input schematic

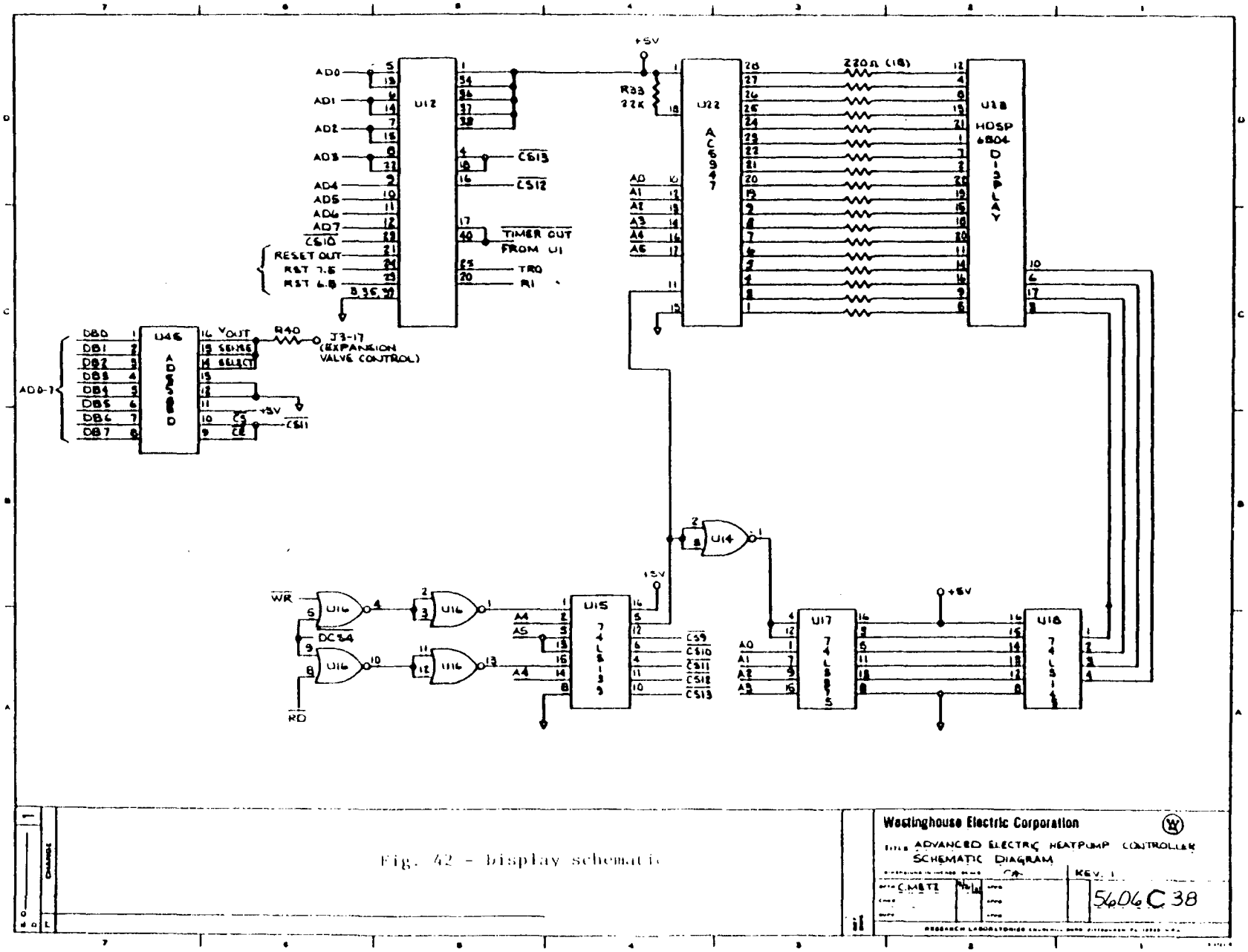


Fig. 42 - Display schematic

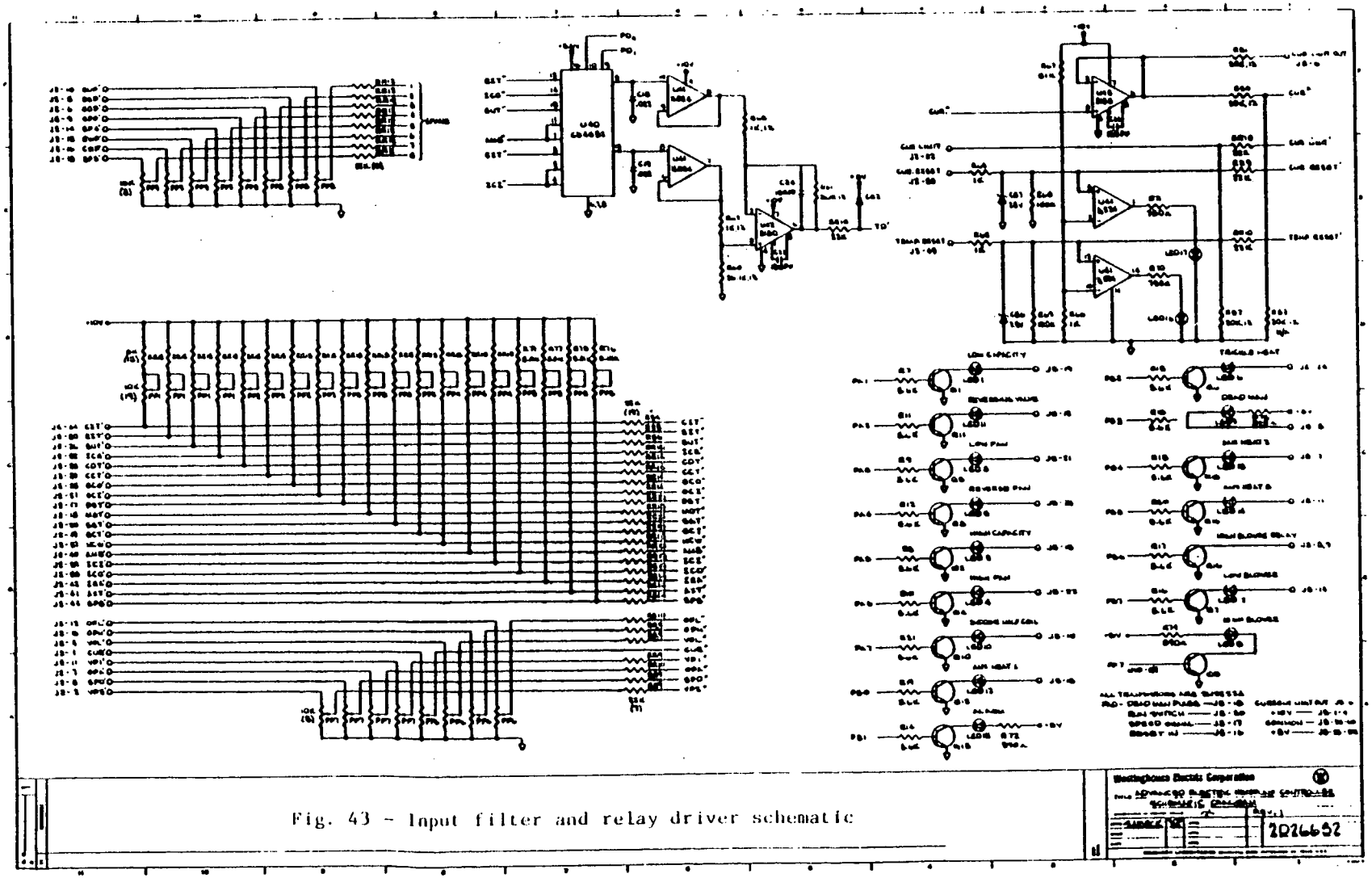

Fig. 43 - Input filter and relay driver schematic

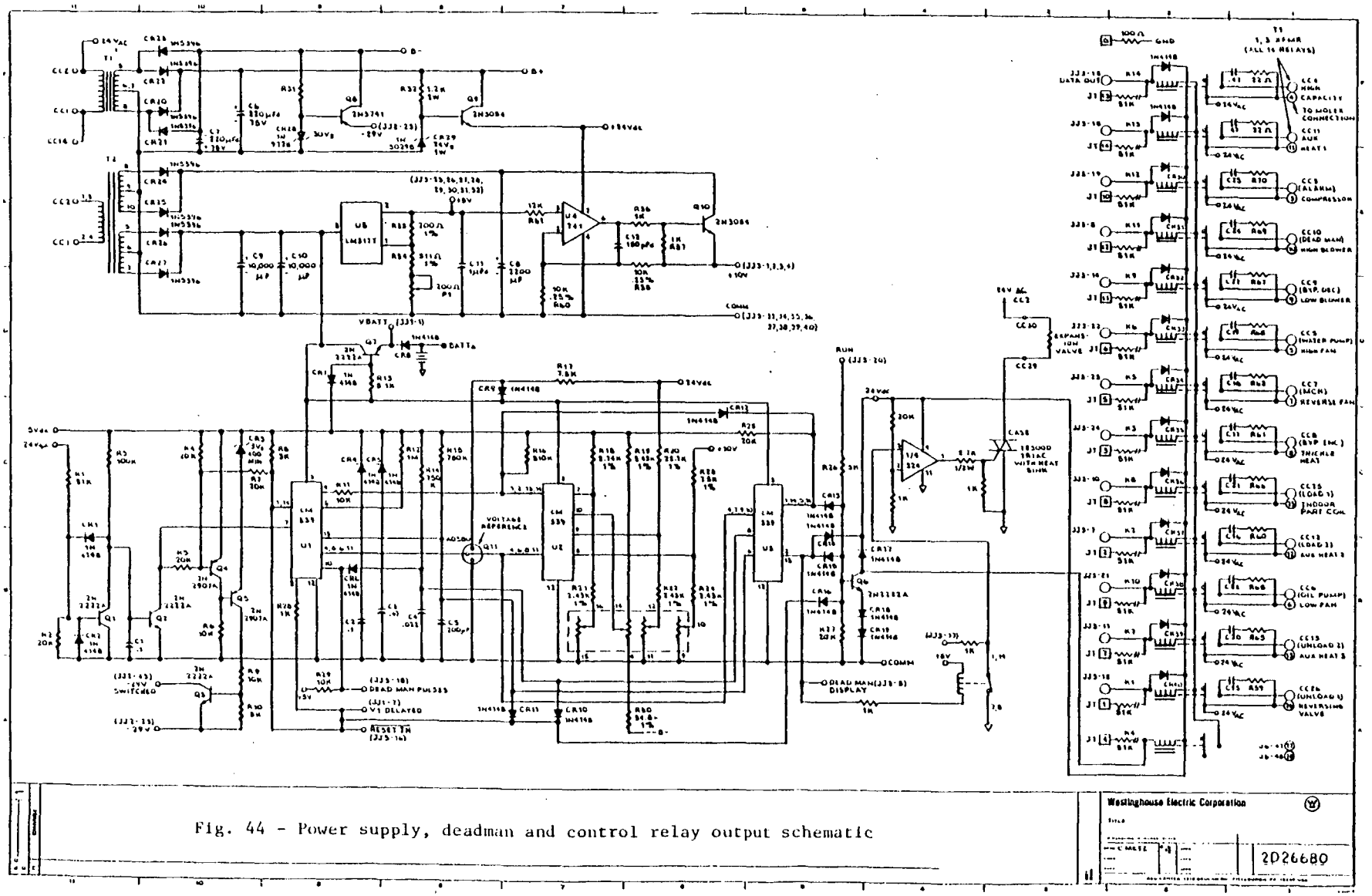


Fig. 44 - Power supply, deadman and control relay output schematic

Table 18

Relay State Matrix for Heating Mode
(Four stages of resistance heat)

| Outdoor Temp., T | Thermostat Ht 1 | Thermostat Ht 2 + Δ Time | Low Comp. | High Comp. | Aux Ht 1 | Aux Ht 2 | Aux Ht 3 | Low Fan | Hi Fan | Low Blower | High Blower |
|---|---|---|---|---|---|---|---|---|---|---|---|
| T ≥ HHBP | 1 | 0 | 1 | 0 | 0 | 0 | 0 | 0 | 1 | 1 | 0 |
| | 1 | 1 | 0 | 1 | 0 | 0 | 0 | 0 | 1 | 0 | 1 |
| HHBP > T ≥ LHBP | 1 | 0 | 0 | 1 | 0 | 0 | 0 | 0 | 1 | 0 | 1 |
| | 1 | 1 | 0 | 1 | 0 | 0 | 0 | 0 | 1 | 0 | 1 |
| LHBP > T ≥ H1BP | 1 | 0 | 0 | 1 | 0 | 0 | 0 | 0 | 1 | 0 | 1 |
| | 1 | 1 | 0 | 1 | 1 | 0 | 0 | 0 | 1 | 0 | 1 |
| H1BP > T ≥ H2BP | 1 | 0 | 0 | 1 | 1 | 0 | 0 | 0 | 1 | 0 | 1 |
| | 1 | 1 | 0 | 1 | 0 | 1 | 0 | 0 | 1 | 0 | 1 |
| H2BP > T ≥ H3BP | 1 | 0 | 0 | 1 | 0 | 1 | 0 | 0 | 1 | 0 | 1 |
| | 1 | 1 | 0 | 1 | 0 | 0 | 1 | 0 | 1 | 0 | 1 |
| H3BP > T ≥ H4BP | 1 | 0 | 0 | 1 | 0 | 0 | 1 | 0 | 1 | 0 | 1 |
| | 1 | 1 | 0 | 1 | 1 | 0 | 1 | 0 | 1 | 0 | 1 |
| T < H4BP | 1 | 1 | 0 | 1 | 1 | 0 | 1 | 0 | 1 | 0 | 1 |
| | 1 | 1 | 0 | 1 | 1 | 0 | 1 | 0 | 1 | 0 | 1 |

LHBP - Low Heat Balance Point
HHBP - High Heat Balance Point
H1BP - Aux. Ht. 1 Balance Point
H2BP - Aux. Ht. 2 Balance Point
H3BP - Aux. Ht. 3 Balance Point
H4BP - Aux. Ht. 4 Balance Point

Note: Refer to Fig. 13

Table 19

Relay State Matrix for Cooling Mode

| Outdoor Ambient | Thermostat | | Low Comp. | High Comp. | Low Fan | Hi Fan | Low Blower | High Blower |
|---|---|---|---|---|---|---|---|---|
| | C1 | C1 + ΔTime | | | | | | |
| Below | 1 | 0 | 1 | 0 | 1 | 0 | 0 | 1 |
| LCSP | 1 | 1 | 0 | 1 | 0 | 1 | 0 | 1 |
| LCSP ≤ T ≤ | 1 | 0 | 1 | 0 | 0 | 1 | 0 | 1 |
| HCSP | 1 | 1 | 0 | 1 | 0 | 1 | 0 | 1 |
| T > HCSP | 1 | 0 | 0 | 1 | 0 | 1 | 0 | 1 |
| | 1 | 1 | 0 | 1 | 0 | 1 | 0 | 1 |

LCSP = LCBP - ΔT1 = Low Cool Balance Point - ΔT1

HCSP = HCBP - ΔT2 = High Cool Balance Point - ΔT2

$\Delta T_1$, $\Delta T_2$ = Temperature Offsets

Table 20

Heating Operating Sequence

1. Trickle Heat Off (2 second delay)
2. Outdoor Fan On (30 second delay)
3. Indoor Coil Solenoid Valve Set for Full Coil, Compressor Capacity Selected (2 second delay)
4. Full Voltage on Expansion Valve (20 second delay)
5. Compressor On (3 second delay)
6. Compressor Current Check (10 second delay)
7. Indoor Blower On, Expansion Valve Voltage Modulated (10 second delay)
8. Resistance Heat On

in series with the resistance heat elements are used to cause them to come on sequentially to minimize the surge on the power line.

During operation Number 6 of Table 20 an analog voltage proportional to the compressor current is monitored. If the voltage exceeds preset maximum and minimum values the compressor is shut off. After a 15 second wait the startup procedure is repeated starting with Step 5 of Table 20. If five attempts to start the compressor are unsuccessful a fault condition is assumed.

When the thermostat is satisfied, the compressor, outdoor fan, full coil solenoid, expansion valve and resistance heat (if required) are deenergized. The indoor blower runs until a preset minimum temperature is reached on the indoor coil. The anticycling timer prevents the unit from initiating a start sequence for three minutes.

When the unit reaches a capacity change point while running, the compressor is shut down. The starting sequence is repeated starting with Step 3 in Table 20.

The starting sequence in cooling is shown in Table 21. The compressor current check sequence is the same as in the heating mode.

Table 21

Cooling Operating Sequence

1. Outdoor Fan On (30 second delay)
2. Full Coil Solenoid On (if high-capacity mode) (2 second delay)
3. Full Voltage on Expansion Valve (20 second delay)
4. Compressor On (3 second delay)
5. Compressor Current Check (10 second delay)
6. Indoor Blower On, Expansion Valve Voltage Modulated

When the thermostat is satisfied the compressor, outdoor fan, full coil solenoid (if energized), reversing valve and expansion valve are deenergized. The indoor blower runs until the indoor coil temperature rises to a preset value. The anticycling timer prevents the unit from initiating a start sequence for three minutes. The capacity change sequence is the same as in the heating mode.

In the heating mode, defrost is initiated by two signals. The first is the temperature difference between the refrigerant entering the outdoor coil and the ambient air temperature. If the temperature difference exceeds a preset value (typically 20°F) at an ambient temperature below 40°F a defrost is initiated. If the preset temperature difference is exceeded at an ambient temperature above 40°F or within 10 minutes of a defrost termination then the system switches to the faulted mode (emergency heat) and shuts down. The second defrost initiation signal is the accumulated continuous running time below 40°F without a defrost. When the accumulated running time without a defrost cycle exceeds 256 minutes a defrost is initiated and the accumulator reset to zero. The accumulated time is also reset to zero when the compressor cycles off and ambient temperature is greater than 40°F.

Table 22

Defrost Operating Sequence

1. Reversing Valve Energized
   Outdoor Fan Off
   Full Voltage On Expansion Valve
   Resistance Heat On Full
   (wait for termination signal)

2. Outdoor Fan Reversed in Rotation Direction
   (45 second delay)

3. Outdoor Fan Off (45 second delay)

4. Outdoor Fan On Forward
   Reversing Valve Deenergized
   Resistance Heat as Required
   Expansion Valve Voltage Modulated

Table 23

Fault Codes

F1 - High Compressor Discharge Temperature
F2 - Outdoor Coil Condensing in Heating Mode
F3 - Outdoor Coil Evaporating in Cooling Mode
F4 - Defrost Signal above 40 F Ambient
F5 - Defrost Signal within 10 Minutes of Termination
F6 - High Outdoor Coil Temperature
F7 - High Crankcase Temperature
F8 - Fan Motor Thermal Cutout Open
F9 - Blower Motor Thermal Cutout Open
F10 - Low Suction Pressure Cutout
F11 - High Discharge Pressure Cutout
F12 - Compressor Motor Thermal Cutout Open
F13 - Low Compressor Running Current
F14 - High Compressor Running Current
F15 - Locked Rotor - Maximum Current
F16 - No Compressor Motor Current
F17 - Low Charge

The sequence of events during a defrost is shown in Table 22. Two methods of termination are used. When the refrigerant temperature leaving the outdoor coil reaches 50°F or the elapsed time since defrost initiation reaches 10 minutes the defrost is terminated.

The temperature sensors, compressor current sensor and internal clock are used to detect a total of 17 faults, shown in Table 23. When any of these faults occur all relays are deenergized instantly and the fault code is indicated on the microprocessor LED display. The system in faulted mode enables emergency resistance heat.

## 5. INDOOR UNIT PACKAGE

The adopted indoor package design is modular in three units. The first module contains the heat exchanger coil, compressor, and associated refrigerant plumbing. The second module contains the air mover and most of the electrical control elements. The third module contains the supplementary electrical resistance heaters, main fuses and single point electrical connections. An artist's sketch of this indoor package in the preferred module arrangement is shown in Figure 45, while an assembly drawing is shown in Figure 46 with some critical dimensions. Figures 7, 8, and 10 provide photographic views of the indoor unit.

The first module (See Figs. 8, 38, 39), the refrigeration machine module, contains the dual-capacity compressor, oil cooler, suction line accumulator, suction line filter/dryer, discharge line muffler, four-way reversing valve, bidirectional expansion device, heat exchanger coil, and coil partitioning solenoid valve in a sheet metal housing 22.5 inches wide by 36.0 inches deep by 28 inches high. Units less than 3.5 tons in capacity could have the depth dimension reduced to 28 inches.

In the interest of minimizing both heat loss and radiated sound, the compressor and the closely coupled suction line accumulator are each enveloped by a 1 inch thick laminated blanket composed of foam rubber and lead foil. The compressor is mounted via four vibration isolators to two lateral support beams. Each of these beams is mounted at both ends through vibration isolators to a subframe. The accumulator is mounted through a single vibration isolator directly to the subframe. A pair of longitudinal slide rails forms the interface between subframe and module base. This arrangement is very effective in blocking the transmission of vibration from the compressor to the module structure and the transmission of compressor noise to the connecting house duct system.

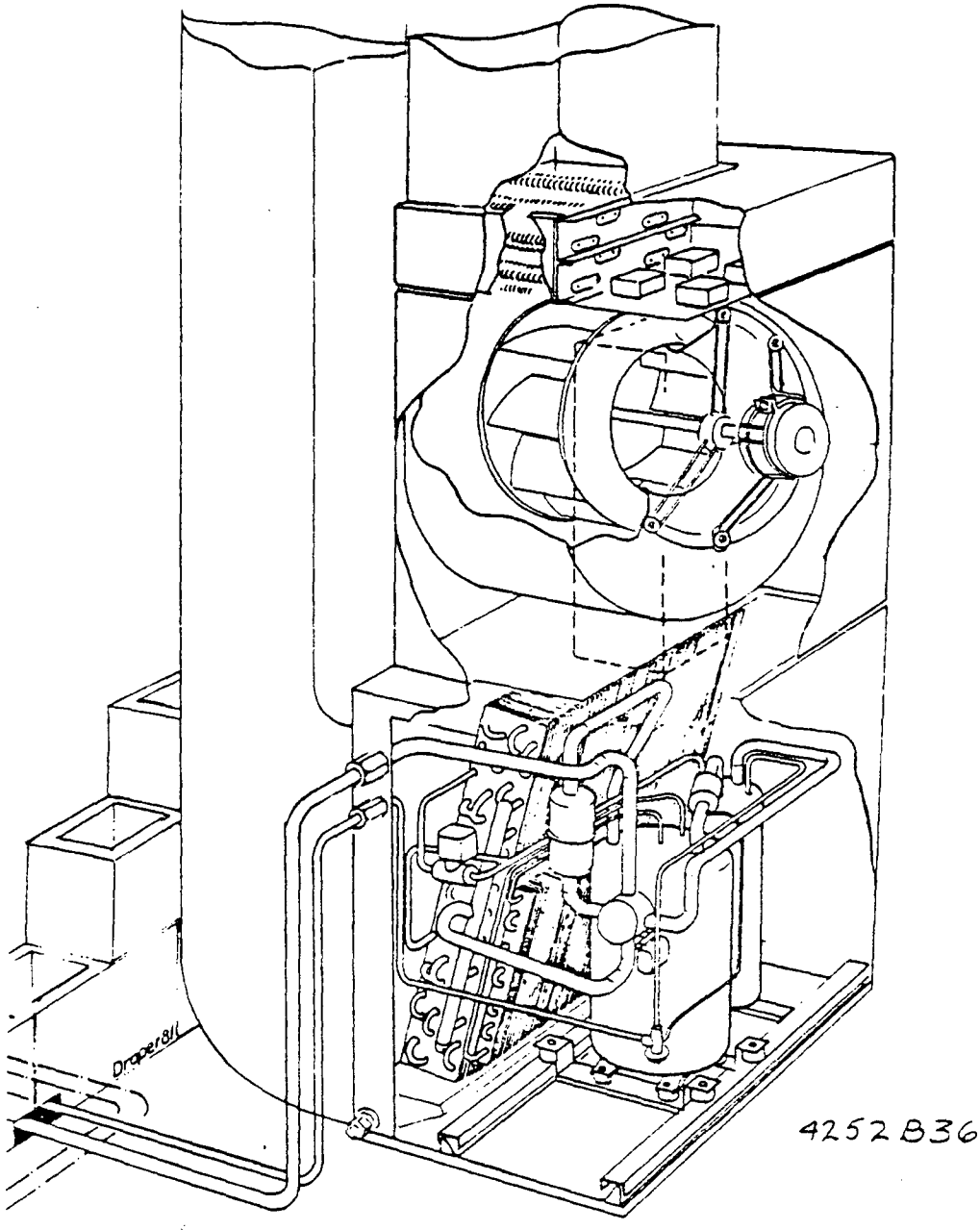


Fig. 45 - Sketch of indoor package assembly

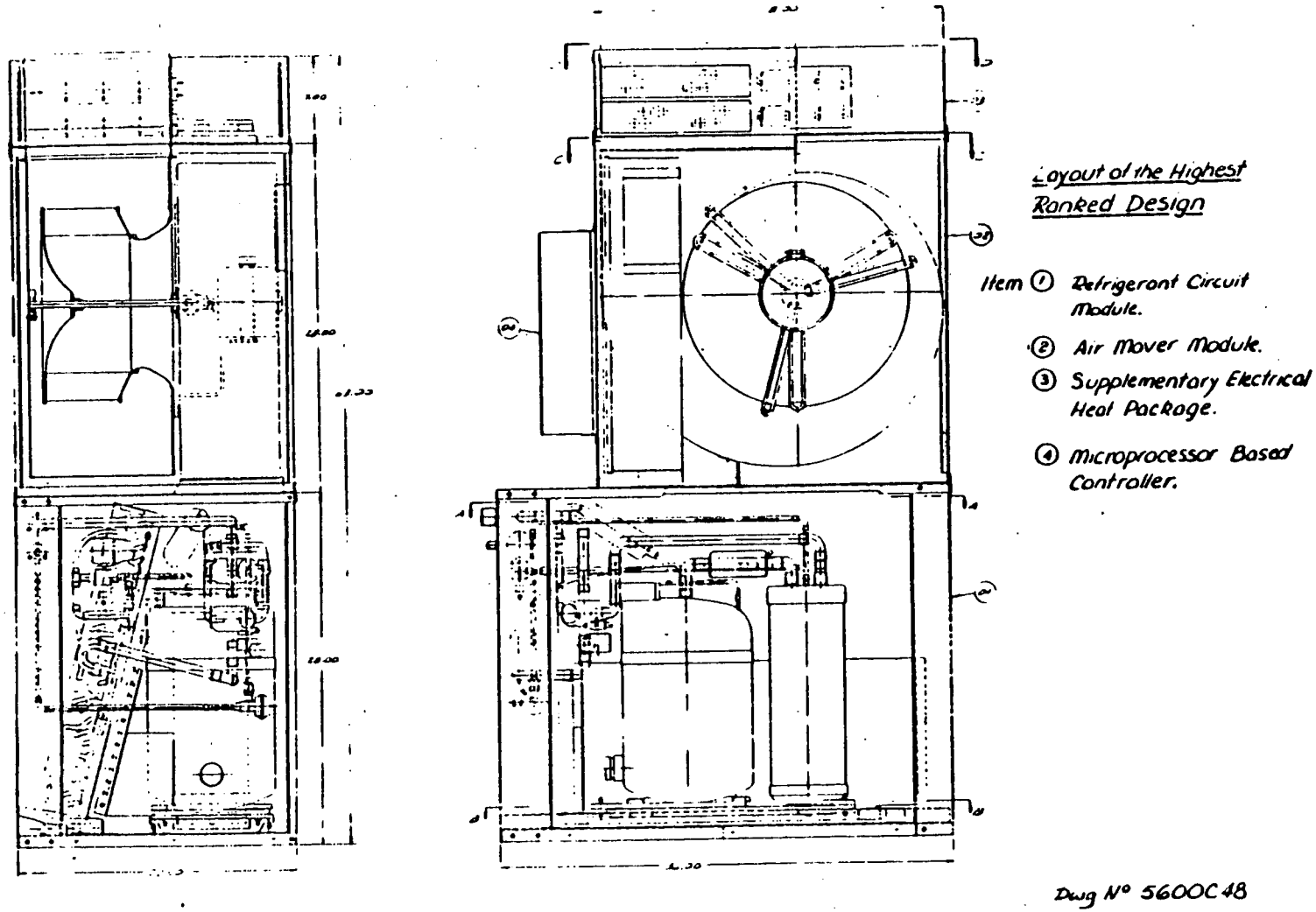


Fig. 46 - Selected indoor package design assembly

Compressor oil is cooled in a plate fin, single circuit, single-row, serpentine heat exchanger coil which is placed adjacent to the main heat exchanger. Lines connecting this oil cooler to the compressor penetrate the top of the compressor can.

In the event that the compressor must be removed, the end access panel is removed, electrical terminals disconnected, the refrigerant charge is removed, and four easily accessible refrigerant lines cut. Two clamps are then removed so that the subframe and its burden can be slid out of the module. Carried on the subframe are the compressor with its external oil cooler and muffler, the suction line accumulator, the suction line filter drier and the reversing and expansion valves. Carried on the module base or main frame are the heat exchanger coil and its partitioning valve. Following reinstallation, the refrigerant lines are reconnected by brazing using the standard sleeving technique.

Simply removing the end cover plate gives clear access to the reversing valve, the coil partitioning valve and the electric expansion valve in the event that these items would require service. The coil return bends are also exposed by removing this plate.

The heat exchange coil is a single four-row slab tilted at 15 degrees to the vertical. A solenoid activated partitioning valve blocks flow to one third of the tubes in the low capacity cooling mode in the interest of better dehumidification. Orientation of the coil is such that the tubes are horizontal and the plane of the fins is vertical. The bottom edge of the coil runs close to and parallel to the bottom 36 inch long edge of the module. A condensate tray is placed just below the bottom edge. The 15 degree tilt angle causes the top edge of the coil to run about midway along the top face of the module. Nearly equal top face areas exist on each side of the coil. This feature is vital to the provision of a wide variety of alternative airflow paths through the module. In turn this permits air to be ingested through any of four of the module faces. See Figure 46.

Refrigerant line connections are via 7/8 inch and 1/2 inch Aeroquip fittings located at the top coil side of the access end of the

refrigerant circuit module. The interconnect tubing between indoor and outdoor units is specified to be 1-1/8 inch and 1/2 inch diameter. The fact that this package arrangement has only one refrigerant connection per line is a distinct advantage over other concepts which house the compressor indoors but require twice as many line connections.

A further advantage of this package design over other concepts stems from the placement of the compressor in the air circulation path within the refrigeration machine module. In this system, during the heating mode, heat dissipated from the compressor and associated equipment is absorbed directly by the air to provide useful heating. In the cooling mode, with the preferred airflow path, compressor heat dissipation provides a reheat effect which necessitates colder coil surface temperatures and thereby enhances dehumidification performance at the expense of reduced total capacity.

The second module, the air mover and controls module, measures 22.5 inches in width, 28 inches in height, and 28 inches in depth and contains the high-efficiency air mover subassembly. The air mover subassembly consists of a 16.25 inch diameter blower wheel with backward-curved blading mounted in a volute scroll with the blower wheel carried on an integral bearing-supported shaft. This shaft is connected to the direct-drive high-efficiency motor by a flexible coupling. The motor is mounted to the scroll through a wire form belly band spider. The motor and blower use permanently lubricated ball bearings.

In order to promote quiet operation stationary sheet metal parts of the blower assembly are clad with 1/2 inch thickness of high density glass fiber. Glass fiber is also bonded to the inside sheet metal walls of the air mover module and the refrigeration machine module.

Support of the blower subassembly within the module is from two tongue and channel slides at the top of the module. The tongues are an integral part of the scroll sheet metal while the channels in which they run are an integral part of the module. After the blower subassembly is slid into the module, a single stiffening bracket is bolted between the two units. This entire arrangement greatly facilitates any service

which the blower motor or bearings might require. Electrical control components including autotransformer, capacitors, fuses, contactors and relays are contained within a 7.5 inch wide by 25 inch long by 6 inch deep steel box with a hinged door. This box is mounted vertically on two plates within the air mover module alongside the blower subassembly and, like the blower subassembly, is accessed via the removable end plate of the module. Connection between the control components and both the microprocessor controller and the thermostat is through two multiconnector Molex plugs which are mounted in the side of the box. Power to the control components enters from the supplementary heat module via a grommetted pass-through at the top of the box. Power to the two-speed reversible outdoor unit fan motor is carried in a seven wire cable, two wires of which are dedicated to the thermal cut out. A six wire cable connects the power control box to the two-speed blower motor and again two wires are reserved for the thermal cut out. Eight wires, six power and two thermal cut out, connect the control box to the compressor motor. All of these cables plus 24 VDC circuit pairs to the coil partitioning valve, electric expansion valve and the four supplementary heat relays pass through grommets in the walls of the box.

The microprocessor-based controller is enclosed in a separate box which can be mounted in a number of locations on the air mover module. Since this unit couples to the control component box by means of an umbilical cable it is an independent module and could be mounted on the wall of the structure.

The third module, the supplementary heat package, is produced as a right-hand assembly, but is easily field modified to be a left-hand assembly. It is aligned so that the heating elements are over the air mover discharge.

Four 5kW stages of heat are available by virtue of four bare wire heater assemblies. These are located in a duct section which is in effect a continuation of the blower discharge plenum. The heaters are time sequenced by thermal relays which are located within the module. The 240 VAC single phase service to the entire heat pump enters through this

module where it is distributed via separately fused circuits to the heaters and to the control box in the air mover module. Fuses protecting the entire heat pump, the four heating elements and the control box are located in the supplementary heat module.

This location for the single-point wiring connection has the advantage that all heavy gauge wire is localized in this module. Field wiring consists of interconnecting the refrigeration machine module, which is furnished with a wiring harness, to terminals in the control box of the air mover and controls module.

To accommodate upflow airflow paths other than that preferred, the air mover subassembly is removed, the housing rotated 180° about a horizontal axis through the access end, and the air mover subassembly rotated 180° about a vertical axis and reinstalled in the module housing. This module is then restacked above the refrigeration machine module. In order to horizontally align the modules, the air mover module is dropped alongside the refrigeration machine module, rotated 90° about a vertical axis and then 90° about a horizontal axis.

Figure 47 illustrates the various airflow alternatives available for both vertical stacking and horizontal alignment of the modules. Alternative 1, using vertical stacking, ingests air through the side of the module adjacent to the heat exchange coil. After passing through the heat exchange coil the air passes over the compressor and associated components before being drawn upwards into the air mover module. The air is then discharged vertically through the supplementary heat module. Simply rotating the refrigerant circuit module relative to the air handling module through 180 degrees about the vertical axis makes airflow path alternatives 2, 3, and 4 possible. These alternatives have slightly higher impedance to airflow and do not offer the reheat characteristic in the cooling mode. Setting the air mover module alongside the refrigerant circuit module and rotating it through 180 degrees about both the vertical and horizontal axes leads to airflow paths 5 and 6. Both of these have the reheat advantage but 5 is preferred because it offers the least

impedance to airflow. Rotating the refrigerant circuit module through 180 degrees about the vertical makes flow paths 7 and 8 possible.

Table 24 contains a breakdown of the estimated factory cost for the indoor heat pump modules.

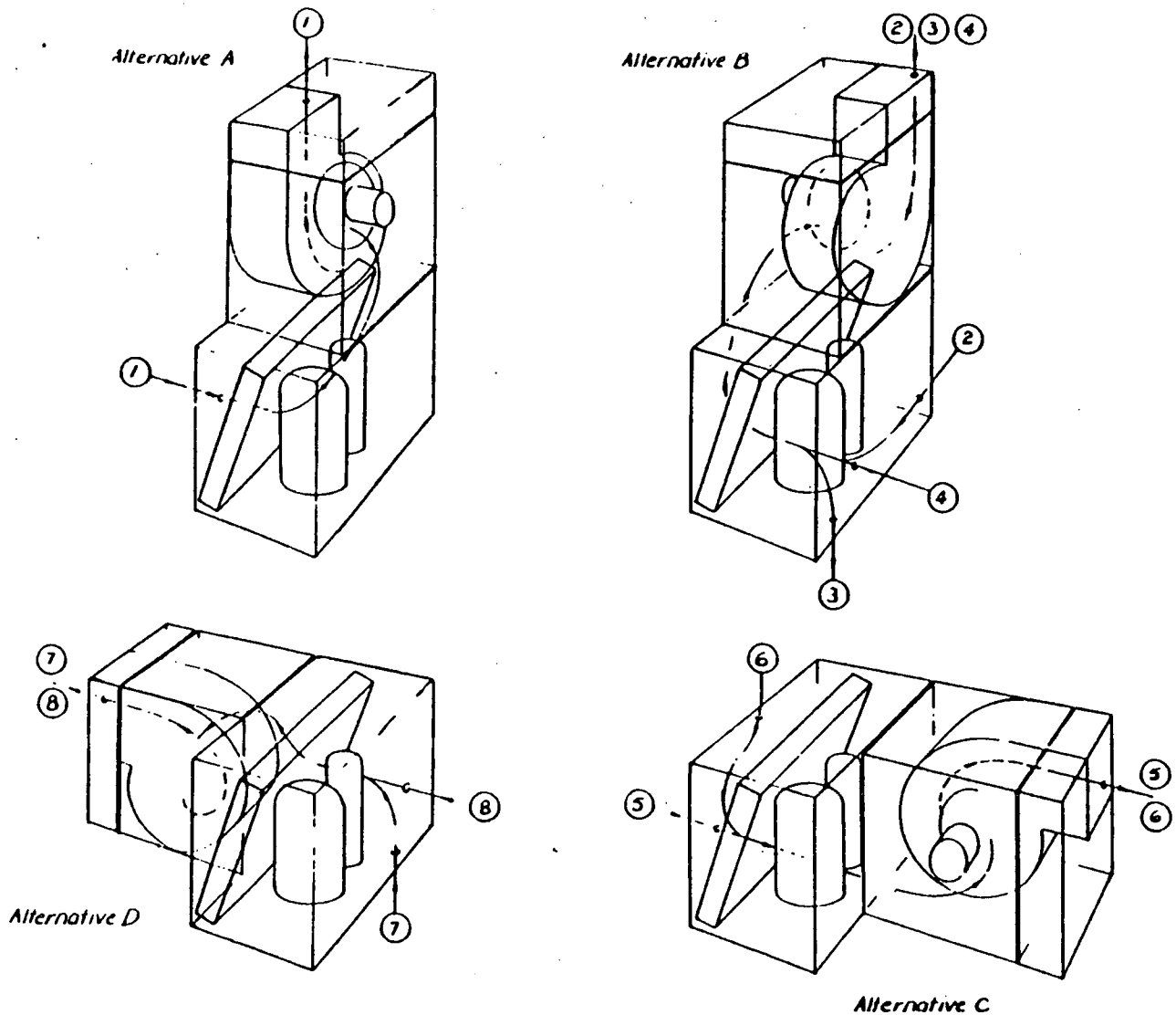


Fig. 47 - Airflow path and module arrangement options

Table 24 - Indoor Unit Cost Breakdown
(Estimated costs in 1981 dollars)

| | | | |
|---|---|---|---|
| 1. | Resistance Heat Module | | $ 80.07 |
| 2. | Air Handler Module | | |
| | Blower/scroll/motor subassembly | 55.00 | |
| | Package wrapper | 21.18 | |
| | Control box and internals | 128.46 | |
| | Total Air Handler Module | | 204.64 |
| 3. | Refrigeration Machine Module | | |
| | Oil-cooled dual-stroke compressor | 182.82 | |
| | Oil cooler heat exchanger | 5.15 | |
| | Refrigerant-to-air heat exchanger | 75.99 | |
| | Muffler, reversing valve, accumulator solenoid valve, check valves, distributor, filter dryer, high and low pressure cut out, high temperature cut out | 101.88 | |
| | Plumbing, fittings, header | 17.34 | |
| | Noise and thermal insulation | 20.50 | |
| | Slide out subframe | 13.33 | |
| | Base, wrapper, cover, access panels | 22.54 | |
| | Internal brackets and supports | 11.24 | |
| | Assembly | 20.00 | |
| | Total Refrigeration Machine Module | | 470.79 |
| 4. | Microprocessor Control System | | 90.00 |
| 5. | 25 feet Interconnect Tubing, Fittings, Insulation, Thermostat, Wire | | 92.51 |
| | Total Indoor System Factory Cost | | 938.01 |

## 6. OUTDOOR UNIT PACKAGE

The adopted outdoor unit package is shown in Figure 3. A cut-away view is provided in Figure 48 and an assembly drawing in Figure 49. The heat exchanger coil is formed from four slabs, each tilted at 22 degrees to the vertical and arranged to form a "W". Mechanical details of the slab sections are listed in Table 16. Air is drawn into the two center slabs of the "W" through the gap formed between the base of the unit and the ground on all four sides. The height of this gap is controlled by the support legs which are adjustable to give a minimum of seven inches and a maximum of 24 inches ground clearance. Additional air to the outside slabs of the "W" is drawn through screened or louvered panels which make up the lower halves of the unit side panels. Notice that the coil slabs are well protected from fin damage in shipment and during service.

The facility to raise the unit up to two feet off the ground without the use of a separate support frame is judged to be a valuable and unique feature. Great benefit is accrued in locations where heavy snowfalls are experienced. This feature is achieved by providing four long legs which are free to slide in channels formed by the bent sheet metal of the unit end plates. Locking is by a screw through the end plate. Additional benefits of this feature are that the unit can easily accommodate very uneven terrain, and the legs can be retracted completely for compactness when shipping.

From the coil the air is drawn upward through the fan package to discharge vertically. The fan subassembly is basically a rounded entrance, circular duct flared at its exit, into which a high-efficiency propeller fan, fan motor and motor cover are inserted and supported. The air exhaust end is covered with a wire form grille.

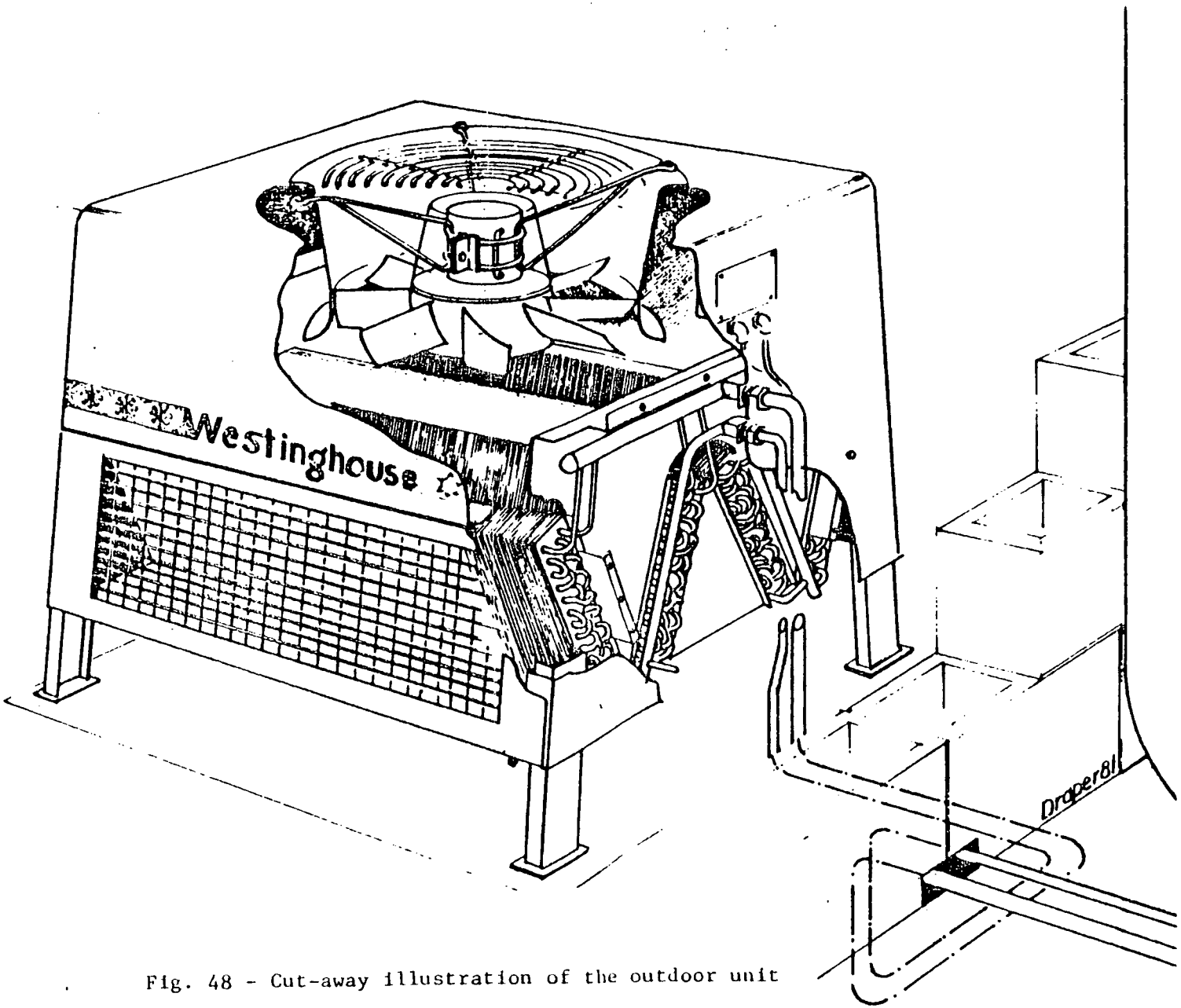


Fig. 48 - Cut-away illustration of the outdoor unit

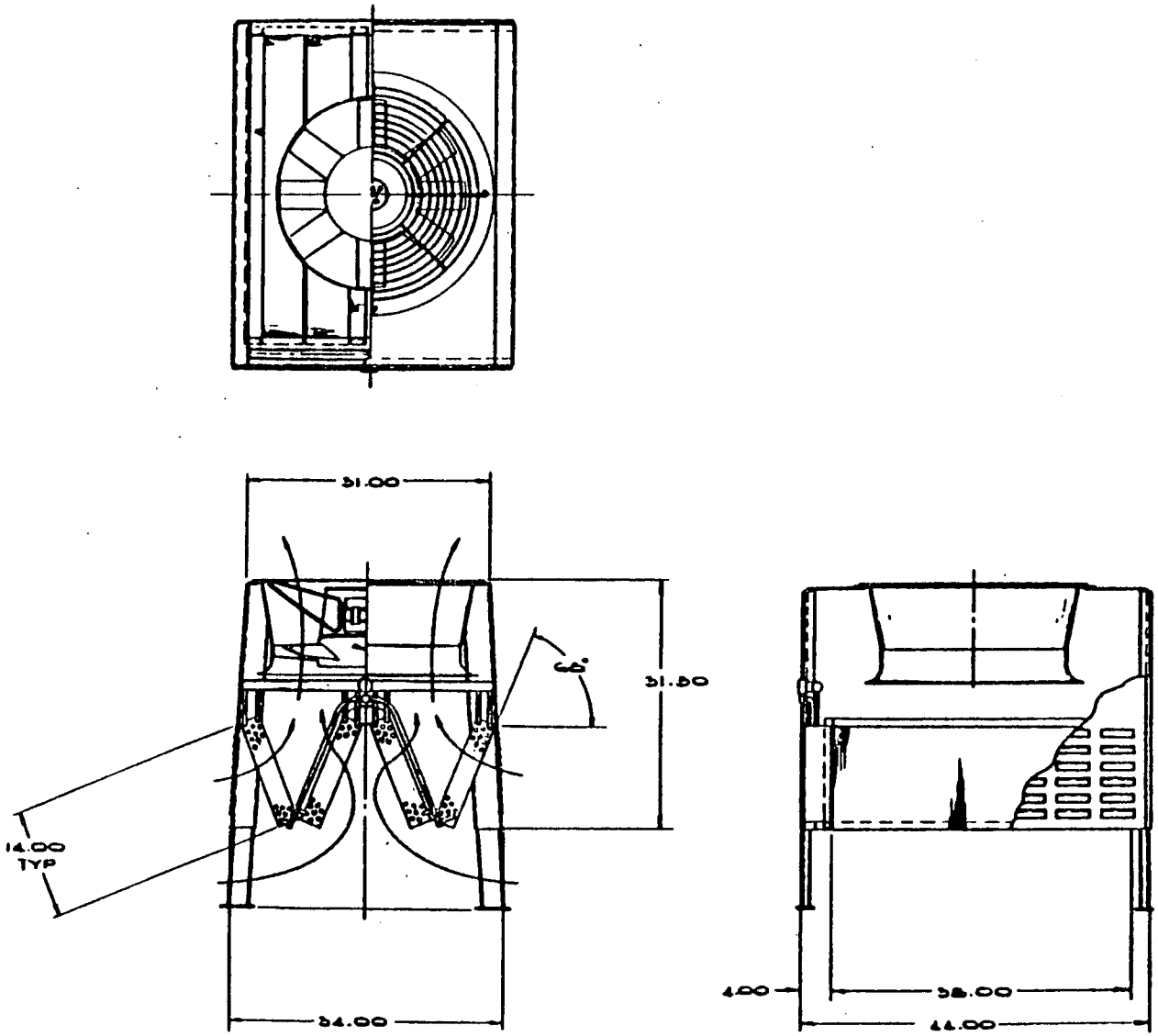


Fig. 49 - Outdoor unit assembly drawing

Mounting is achieved by dropping the fan subassembly, which has an externally protruding flange at its discharge plane, into a suitable hole in the top of the outdoor unit housing.

The sheet-metal structure consists of two trapezoidal-shaped end plates and an inverted "U" shaped wrapper, all of galvanized steel, and two grille panels which are electroplated for corrosion resistance. The four channel-shaped galvanized legs have flat plate steel feet and fit into long sockets which are formed as an integral part of the end plates.

During manufacture, the "W" shaped coil is prepared as a leak-tested subassembly, and subsequently attached to the housing end plates with sheet metal screws. The legs are prestowed in their sockets. The wrapper is then snapped into place and attached with screws to the end plates. The two grille panels are then attached. The prechecked air mover subassembly is then dropped into place and secured and terminals wired. Final inspection is the last operation before insertion into the shipping carton.

All services, refrigerant lines and electrical service are accessed at one end plate.

The overall unit dimensions with legs extended 7-1/2 inches is 39 inches high, 34 inches wide at the base, and 44 inches long.

Table 25 presents a cost breakdown of the outdoor unit.

Table 25

Outdoor Unit Cost Breakdown
(Estimated costs in 1981 dollars)

| | |
|---|---|
| Air Mover Subassembly (propeller, motor, shroud, motor cover, mounting bracket, grille) | $ 69.77 |
| Heat Exchanger | 140.00 |
| Plumbing Headers and Connections | 13.54 |
| Top Cover, End Cover and Legs | 43.45 |
| Baffles, Seals, Electrical Connector | 20.93 |
| Box, Screws | |
| Assembly and Test | 8.75 |
| Total Outdoor Unit Factory Cost | $296.44 |

## 7. COMPARISON WITH OPTIMIZED CONFIGURATION

The analytical system optimization study was performed in parallel with the advanced component development effort and was terminated because of project resource constraints before final component performance was available and before details of the package design were settled. Most notably, the superior performance of the final dual-stroke compressor relative to an earlier variant and the system performance impact of the oil cooler and reversing valve were absent from the optimization effort. In addition, manufacturing and field performance considerations forced hardware choices different from those modeled analytically. Some deviation must therefore be expected between design parameters for the preprototype system and those recommended by the optimization study as configuration RDHPOV. A comparison of design parameters is given in Table 26. The rationale for deviations is given in the following paragraphs.

### Compressor

At the time the optimization study was being executed, compressor development had not been completed, and as a result, characteristics for the Mod II compressor were not available. The optimization was performed using Mod I compressor characteristics (see Reference 9), without consideration of any system impact due to the oil cooler.

### Refrigerant Circuit

Heat pump heating performance was favored over cooling performance. Westinghouse experience with the Hi-Re-Li circuit made condenser subcooling control via the Hi-Re-Li scheme the perferred method for heating. It was adopted in the optimization analysis for both heating and cooling. The use of a bidirectional electric expansion valve made possible a more simple circuit that eliminated the complex check valve arrangement used in the Hi-Re-Li system and with superheat control in the cooling mode

Table 26 - Comparison of Parameters - Preprototype vs RDPOV

| RDHPOV | Parameter | Preprototype |
|---|---|---|
| | Compressor | |
| Mod I | W CD048 + Dual Stroke | Mod II |
| 6%/22.3% | Clearance Volume Hi/Lo | 3.2%/19.2% |
| 9.90/8.41 | EER Hi/Lo @ 30°F Evap, 110°F Cond. | 10.90/9.66 |
| | Refrigerant Circuit | |
| Subcool Control | Heating | Subcool Control |
| Subcool Control | Cooling | Superheat Control |
| | Indoor Air Mover | |
| ✓ | Centrifugal, SWSI, backward curved | ✓ |
| 65% | Static Efficiency | 66% |
| 1250 scfm | Flow | 1405 scfm |
| 0.87 inches $H_2O$ | ΔP | 1.09 inches $H_2O$ |
| ✓ | Motor - 2 speed controlled slip | ✓ |
| 65% | High Speed Efficiency | 70% est. |
| 43% | Low Speed Efficiency | 46% est. |
| | Outdoor Air Mover | |
| ✓ | Multi-van Axial - 8 blades | ✓ |
| 52% | Static Efficiency | 50% est. |
| 2526 scfm | Flow | 3070 scfm |
| 0.098 inches $H_2O$ | ΔP | 0.09 (dry) |
| ✓ | Motor - 2 speed controlled slip | ✓ |
| 65% | Efficiency at Full Speed | 65% est. |
| | Indoor Heat Exchanger | |
| ✓ | Plate Fin on Tube | ✓ |
| 4 | Rows | 4 |
| 5.19 sq. ft. | Face Area | 5.51 sq. ft |
| 0.035 in Al wall | Tubing - 0.375 D | 0.017 in Cu wall |
| ✓ | Tube Pitch - Equilateral 1.0 x 0.866 in. | ✓ |
| 0.0055 inch | Fins - Aluminum | 0.0045 inch |
| 16 | Fins/inch | 13 |
| 2 x 0.052 inch | Patterns/Pitch | 2 x 0.046 inch |
| 67% | Partition | 67% |
| | Outdoor Heat Exchanger | |
| ✓ | Plate Fin on Tube | ✓ |
| 3 | Rows | 3 |
| 14.26 sq. ft. | Face Area | 14.78 sq. ft. |
| 0.035 in Al wall | Tubing - 0.375 D | 0.017 in Cu wall |
| ✓ | Tube Pitch - Equilateral 1.0 x 0.866 in. | ✓ |
| 0.0055 inch | Fins - Aluminum | 0.0045 inch |
| 13 | Fins/inch | 13 |
| 2 x 0.052 inch | Patterns/Pitch | 2 x 0.046 inch |
| Not accounted for | Reversing Valve | Present |

allowed system charge control using standard techniques. This circuit was adopted after the optimization study was terminated.

Indoor Air Mover

The final hardware specification for indoor design airflow at 1400 cfm was made prior to the selection of configuration RDHPOV. At the time, when the blower specification had to be frozen, we were considering the relative merits of three speed indoor airflow and various partitioning ratios for the indoor coil. The specification of 1400 cfm covered the extreme case among alternatives being considered. Note that the operating point pressure rise corresponds to the design resistance for system RDHPOV - i.e., 0.87 inches $H_2O \times (1405/1250)^2 = 1.099$. The indoor air mover motor as supplied was both more efficient than the minimum specification (i.e., 65 percent) and more powerful. Note that under industry standard conditions, the shaft output exceeds the rated output by up to 50 percent. Thus the preprototype 1/3 hp motor would carry a nameplate indicating lower capacity.

Outdoor Air Mover

The specification for airflow rate had to be frozen before the optimization study was complete and corresponds to that anticipated for a conventional 3.5 ton unit. The pressure drop specification is commensurate with a conventional unit carrying a frost load. The overall impact of reducing the flow requirement to meet the optimized specification would be small. That is, cost would be reduced very little while air moving power might be reduced from 150 watts to about 90 watts.

Indoor Heat Exchanger

The fin density and pattern depth was reduced to improve condensate drainage based on engineering judgment and past experience. The resulting reduction in heat exchanger capacity was compensated for by increasing the face area with foreknowledge that the blower would have higher airflow capability. At contract inception 0.0055 inch fin stock was in standard use and specified for the optimization effort. Later adoption of 0.0045 inch fin stock material was made to reduce cost.

Outdoor Heat Exchanger

The deviation between recommended and installed surface area is a minor one (3.6 percent) covered by the particular configuration adopted for the coil. As for the indoor coil, fin thickness was reduced to save cost. The thicker stock was specified at the beginning of the optimization effort because it represented the then standard practice.

## 8. REFERENCES


1. Request for Proposal P-2129-86, ".... Research, Development and Demonstration of an Advanced Electric Heat Pump," Oak Ridge National Laboratory, February 28, 1979.

2. Kirschbaum, H. S., Veyo, S. E., "An Investigation of Methods to Improve Heat Pump Performance and Reliability in a Northern Climate," EPRI EM-319, Project 544-1, January, 1977.

3. Kastovich, J. C., Lawrence, R. R., Hoffman, R. R. and Pavlak, C., "Advanced Electric Heat Pump Market and Business Analysis, Final Report," ORNL/Sub/79-24712/1, Oak Ridge National Laboratory, April 1982.

4. Veyo, S. E., "Advanced Electric Heat Pump Component Development and Evaluation - Interim Report," ORNL/Sub/79-24712/2, Oak Ridge National Laboratory, September 1982.

5. Veyo, S. E., "An Optimized Two-Capacity Advanced Electric Heat Pump," ASHRAE Journal, November 1982, pp. 42-48.

6. 10CFR430, "Energy Conservation Program for Consumer Products; Test Procedures for Central Heat Pumps, Including Heat Pumps," Federal Register, V. 44, No. 249, December 27, 1979.

7. Wright, T., Lackey, R. S. and Veyo, S. E., "A High-Efficiency Heat Pump Fan," ASHRAE Transactions, Vol. 89, Part 2, 1983, (Symposium Paper DC 83-13, No. 2).

8. Ariewitz, D., Lackey, R. S. and Veyo, S. E., "A High-Efficiency Indoor Air Mover," ASHRAE Transactions, Vol. 89, Part 2, 1983, (Symposium Paper DC 83-13, No. 3).

9. Young, R. R., Veyo, S. E. and Kastovich, J. C., "A High-Efficiency Dual-Stroke Compressor for Heat Pumps," (Symposium Paper AT 84-19, No. 1) to be published in ASHRAE Transactions.

10. ARI Standard 270-75, "Sound Rating of Outdoor Unitary Equipment," 1975.

11. Office of Science and Technology, Executive Office of the President, Patterns of Energy Consumption in the United States, Washington, D.C., U.S. Government Printing Office, January 1972.

## 9. ACKNOWLEDGEMENT

This report, prepared by the authors, documents in one volume the effort and contribution of the following individuals.

J. C. Kastovich, Administrative Program Manager and Compressor Development Leader

S. E. Veyo, Technical Project Manager and Team Leader - Technology Improvement

R. R. Young, Dual-Stroke Compressor

W. A. English, Geared Compressor

R. W. Wolfe, Compressor Computer Analysis

T. J. Fagan, System Performance Analysis and Testing

K. H. Lee, Seasonal Performance Analysis

B. F. Habron, DOE Regulations

R. A. Lucheta, System Optimization

M. C. Chuang, Heat Exchanger Analysis

N. M. Farukhi, Heat Exchanger Analysis

T. Wright, Fan Development

D. Ariewitz, Blower Development

H. S. Kirschbaum, Motor Analysis

P. W. Kolody, Motor Analysis

R. Draper, Package Design, Heat Exchanger Analysis, Test Facilities

R. S. Lackey, Package Design, Prototype Design

J. A. Richard, Component Reliability

R. E. Fromson, Manufacturing Analysis

R. M. Hastings, Manufacturing Analysis

A. Meyerhoff, Manufacturing Analysis

F. J. Sisk, Consultant

P. T. Thayer, Consultant

R. G. Colclaser, Microprocessor Control System

R. A. Johnson, Controls

P. Malloy, Typing and Editing

The authors acknowledge the help and encouragement given by personnel of the Oak Ridge National Laboratory in the administration of this research project. In particular we recognize G. Privon, Program Manager.

## NOMENCLATURE FOR TABLE 8

| | |
|---|---|
| $\begin{pmatrix} BIN \\ J \end{pmatrix}$ | temperature bin index |
| $\begin{pmatrix} BIN \\ HRS \end{pmatrix}$ | fractional hours of occurrence of temperature bin for heating season |
| T(J) | bin center temperature (deg F) |
| QDOT1 | heat pump capacity - low capacity mode (Btu/h) |
| QDOT2 | heat pump capacity - high capacity mode (Btu/h) |
| EDOT1 | heat pump power input - low capacity mode (W) |
| EDOT2 | heat pump power input - high capacity mode (W) |
| BLH | building load (Btu/h) |
| CASE | 1, unit cycles on/off in low capacity |
| | 2, unit cycles low/high capacity |
| | 3, unit cycles on/off in high capacity |
| | 4, unit operates continuously in high capacity |
| DELTA | 1, ambient BIN temperature T(J) is such that unit is permitted to operate in heating mode |
| | 0, ambient BIN temperature T(J) is less than low temperature cut off temperature, and unit is not permitted to operate |
| | 0.5, ambient BIN temperature T(J) is greater than low temperature cut off value but less than value for which unit is permitted to turn on, once having been off |
| BLH/N | building load (BLH) in temperature bin times fractional hours of occurrence |
| E/N | heat pump electrical energy consumed per hours of operation in temperature bin times fractional hours of occurrence |
| RH/N | resistance heat electrical energy consumed per hours of operation in temperature bin times fractional hours of occurrence |
| HEAT INPUT | heat input to dwelling (Btu)/temperature bin |
| E.PUMP | electrical consumption of heat pump (Wh)/temperature bin |
| E.REST | electrical consumption of resistance heat (Wh)/temperature bin |
| E.CHE | electrical consumption of crankcase heater (Wh)/temperature bin |
| E.CTL | electrical consumption of control system (Wh)/temperature bin |
| E.SUM | total electrical consumption (Wh)/temperature bin |
| COP | coefficient of performance/temperature bin |

## NOMENCLATURE FOR TABLE 9

| | |
|---|---|
| $\begin{pmatrix} BIN \\ J \end{pmatrix}$ | temperature bin index |
| $\begin{pmatrix} BIN \\ HRS \end{pmatrix}$ | fractional hours of occurrence of temperature bin for cooling season |
| T(J) | bin center temperature |
| BLC | building cooling load |
| QSS1 | heat pump cooling capacity - low capacity mode |
| QSS2 | heat pump cooling capacity - high capacity mode |
| ESS1 | heat pump power input - low capacity cooling |
| ESS2 | heat pump power input - high capacity cooling |
| X1 | BLC/QSS1 |
| X2 | BLC/QSS2 |
| Q/N | $BLC * \begin{pmatrix} BIN \\ HRS \end{pmatrix}$ |
| E/N | electrical energy consumed per hour of operation in temperature bin times fractional hours of occurrence |

## APPENDIX A

## PROTOTYPE NUMBER ONE - SYSTEM INSTRUMENTATION

Instrumentation locations in the refrigerant circuit are shown schematically in Figure A1. Refrigerant temperatures, TR1, TR2, TR3, TR4, TR8 and TR9 and the oil inlet and outlet temperatures TO1 and TO2 are measured with ungrounded sheathed dual junction copper-constantan thermocouples inserted directly into the fluid stream through compression fittings. Dual junction thermocouples were used to permit recording temperatures on both a Fluke Model 2240B and a high speed Computer Products RTP data acquisition system. Since the Fluke data logger sends out pulses to detect open thermocouples, it cannot be used in parallel with other recording instruments on channels programmed to read thermocouples. On channels that read voltages, no pulses are sent and parallel readings can be performed. Less critical refrigerant temperatures, such as TR9A and the compressor crankcase temperature TC1 are measured with copper-constantan thermocouples glued to the surface and lagged with insulation. The compressor suction pressure is measured with a Rosemount pressure transmitter (PTR1) with a range of 0-1034 kPa (0-150 psig). The compressor discharge pressure is monitored with a Rosemount pressure transmitter (PTR2) with a 0-3447 kPa (0-500 psig) range. The refrigerant pressures in the indoor and outdoor coils are measured with Kulite pressure transducers (PTR3 and PTR9) with a 0-3447 kPa (0-500 psig) range and Sensotec differential pressure transducers (PTR4 and PTR8) with a -414 to +414 kPa (-60 to +60 psi) range. A more detailed description of all of the pressure instrumentation is given in Table A1.

Refrigerant flow is measured with two Micro-Motion Model B12A Coriolis type mass flow meters factory calibrated with a range 0-0.0605 kg/s (0-480 lb/hr). Two flow meters were selected to give good

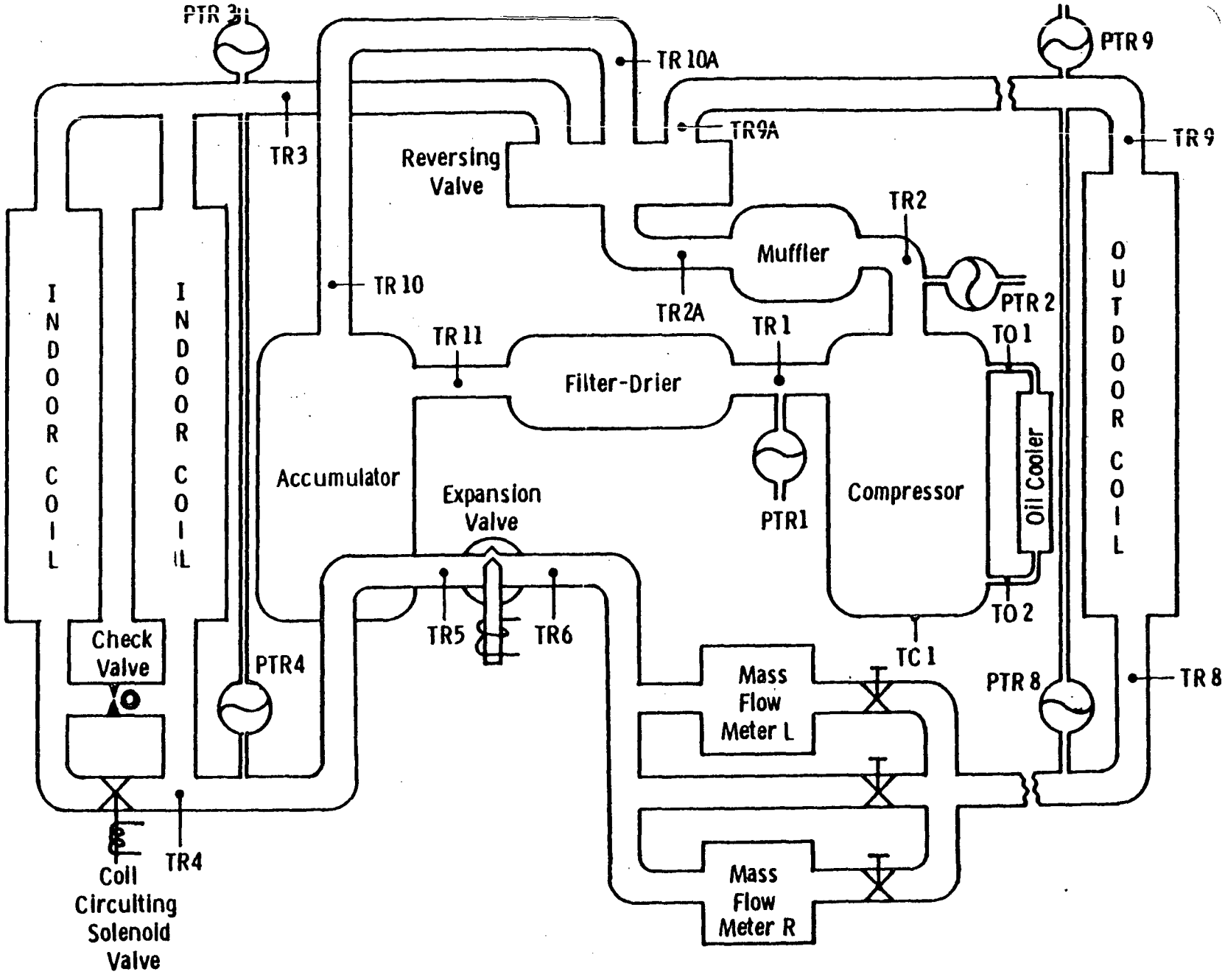


Fig. A1 - Refrigerant side instrumentation

Table A1 - PRESSURE INSTRUMENTATION

| Location | Manufacturer | Model Number | Serial Number | Input | Range | Output |
|---|---|---|---|---|---|---|
| PTA1 | Flotek | 100W12A2 | 11298-1-1 | 24VDC | 0-1 in $H_2O$ | 4-20 ma |
| PTA2 | Rosemount | 115-1DR2F12B2 | 252290 | 24VDC | -1 to +1 in $H_2O$ | 4-20 ma |
| PTA3 | Rosemount | 115-1DP3E12B1 | 252761 | 24VDC | 0 to 5 in $H_2O$ | 4-20 ma |
| PTA4 | Rosemount | 115-1APGE12B1 | 255026 | 24VDC | 0-17 psia | 4-20 ma |
| PTA5 | Rosemount | 115-1DR2F22 | 284405 | 24VDC | 0-2 in $H_2O$ | 4-20 ma |
| PTA6 | Rosemount | 115-1DR2F12B1 | 373572 | 24VDC | -1 to +1 in $H_2O$ | 4-20 ma |
| PTA7 | Rosemount | 115-1DP3E12B2 | 253061 | 24VDC | 0 to 5 in $H_2O$ | 4-20 ma |
| PTR1 | Rosemount | 115-1AP7E22D2 | 278669 | 24VDC | 0-150 psig | 4-20 ma |
| PTR2 | Rosemount | 115-1AP8E22D2 | 249837 | 24VDC | 0-500 psig | 4-20 ma |
| PTR3 | Kulite | ITP-1000-500 | 3679-5-261 | 10VDC | 0-500 psig | .19 mv/psi |
| PTR4 | Sensotec | A-5/41 | 50137 | 24VDC | -60 to +60 psig | .40 mv/psi |
| PTR8 | Sensotec | A-5/741 | 50644 | 24VDC | -60 to +60 psig | .40 mv/psi |
| PTR9 | Kulite | ITP-1000-500 | 3679-269 | 10VDC | 0-500 psig | .19 mv/psi |

Table A2 - REFRIGERANT FLOW INSTRUMENTATION

| | | | | | | |
|---|---|---|---|---|---|---|
| L | Micro-Motion Inc. | B12A | 1685 | 110VAC | 0-480 lb/hr | 1-5 VDC |
| R | Micro-Motion Inc. | B12A | 1684 | 110VAC | 0-480 lb/hr | 1-5 VDC |

Table A3 - **POWER INSTRUMENTATION**

| Function | Manufacturer | Model Number | Serial Number | Input | Range | Output |
|---|---|---|---|---|---|---|
| Total Heat Pump Power | F.W. Bell Co. | PR-2301SX | 101542 | 110VAC | 0-20 KW | 0-2 VDC |
| Current Transformer for Total Power | Sangamo | B65A | 7545966 | -- | 200:5 A | -- |
| Control Power | Rochester Inst. Systems | PCE-15 | 79533-1 | 110VAC | 0-200 W | 4-20 ma |
| Indoor Fan Power | Rochester Inst. Systems | PCE-15 | 79533-3 | 110VAC | 0-1000 W | 4-20 ma |
| Outdoor Fan Power | Rochester Inst. Systems | PCE-15 | 79533-2 | 110VAC | 0-400 W | 4-20 ma |
| Code Tester Heater Power | Ohio Semitronics | PC5-32-2E | 5389 | 110VAC | 0-40 kW | 4-20 ma |
| Reheater Power | Ohio Semitronics | PC5-19E | 5388 | 110VAC | 0-1500 W | 4-20 ma |

resolution over a wide range of flows. The flow meters can be used in parallel or either of the meters can be valved out. The flow meters are switched electrically to read flows in either direction. Both flow meters can be bypassed if desired. The meters are described in more detail in Table A2.

Indoor and outdoor air mover speeds are monitored by Electro Sensors Inc. Model DSC-10E digital tachometers. An aluminum disc containing 16 small permanent magnets is attached to the rotating part. A fixed magnetic sensor sends pulse signals to a counting circuit. Fan speeds are displayed on LED digital panel meters and 0-10 vdc analog signals are sent to the data acquisition system.

The voltage available in the laboratory is nominally 208 volts 60 Hz 1$\phi$ and is variable. To allow testing at 230 volts and minimize the effect of voltage swings, an autotransformer has been installed, which can provide up to 280 volts. During test runs the voltage is monitored and manually adjusted. The supply voltage is also recorded by the data acquisition system. The Fluke data acquisition system also records the voltage supplied to the expansion valve, the supply voltage to the Kulite pressure transducers (PTR3 and PTR9) and the 20 mV and 2V internal references voltages built into the Fluke data acquisition system. Electronic watt transducers are used to monitor power consumption with readings recorded by the data acquisition system. The power inputs of both the indoor and outdoor units are measured by F. W. Bell Model PR-2301SX electronic watt transducers. These units are used with Sangamo Type B65A 200:5A current transformers to give an output of 0.1 volts dc per kW. The outdoor unit fan power is measured using a Rochester Instrument Systems (RIS) Model PCE-15 watt transducer with a range of 0-400 watts applied to each winding. The indoor fan power is monitored using a RIS Model PCE-15 watt transducer with a 0-1000 watt range applied to each winding. The power consumed by the control system is measured with an RIS Model PCE-15 watt transducer with a 0-200 watt range. All of the watt transducers are described in detail in Table A3.

## APPENDIX B

## TEST FACILITY DESCRIPTION

The heat pump test facility, located at the Westinghouse Research and Development Center, provides accurately controlled temperature and humidity conditions for evaluating the performance of air to air heat pumps over the entire practical range of operating conditions. In addition to steady state performance measurements, the DOE heating and cooling cyclic performance tests and frost accumulation test[1] can be performed.

The outdoor test room can provide ambient temperatures from -32°C to 49°C (-25°F to 120°F) and a wide range of relative humidities. The indoor test room, can provide ambient temperatures from -1°C to 49°C (30°F to 120°F) with dew point temperatures ranging from -1°C (30°F) to saturation.

Each room is provided with a completely independent closed loop space conditioning system. A two-speed blower draws air from each room through washable filters near the floor at one end. The air passes along (not through) a finned tube direct expansion air to refrigerant heat exchanger used for moisture removal. The heat exchanger surface temperatures are controlled by evaporator pressure regulator valves. The air then passes through a second direct expansion air to refrigerant heat exchanger used for heat extraction. Each heat extraction coil has three independent refrigerant circuits controlled by solenoid valves to aid in capacity modulation. Next, moisture is added (if required) by direct injection of low pressure steam provided by electric package boiler. Heat addition is provided by bare nichrome wire heater banks with SCR power modulation. The conditioned air is returned to the rooms through perforated ceilings and through ducts

on both sides of the rooms to minimize stratification. The heat removal, heat addition, moisture removal and steam injection are modulated by a Texas Instrument Model PM550 digital PID control system. The wet and dry bulb temperatures are indicated by Analog Devices temperature sensors. In the indoor room the wet bulb temperature is controlled directly. Since the outdoor room must be able to operate with dew point below freezing, the control system monitors humidity using a Hygrometrix Inc. Model 8501-A relative humidity sensing system. The Hygrometrix Inc. "Xeritron" relative humidity probe is mounted on the inlet air sampling rake. This probe can sense relative humidities from 0 to 100% over a temperature range of -40°C to 125°C (-40°F to 257°F) with an acccuracy of +4% full scale. This is sufficiently accurate for the control system. As shown in Figure B1, air is drawn through a sampling rake constructed from PVC tubing by a small blower and passes over a dry bulb temperature sensor (D104) followed by an electric reheater, a second dry bulb sensor (D105) and a wet bulb sensor (W102). At dew point temperatures below 0°C (32°F) the heater is manually controlled to maintain a wet bulb temperature above 0°C (32°F) and the data reduction program calculates the specific humidity from the wet bulb temperature and the dry bulb temperature after reheat and the relative humidity from the specific humidity and the dry bulb temperature before reheat to provide a check of the Hygrometrix system. The control system setpoint may thus be offset from the measurement standard for humidity. The power input to the reheaters is monitored by a watt transducer. Figure B2 shows the inlet air sampler for the indoor room where D203 and W203 are the dry and wet bulb control sensors. The outdoor room refrigeration system has a nominal capacity of 35 kW (10 tons) operating on refrigerant 502. The indoor room refrigeration system operates on R22 with a nominal capacity of 26 kW (7.5 tons).

The primary means of determining system capacity is air side calorimetry, which requires accurate measurement of air flow, temperature and humidity. Both rooms are provided with "code testers" to facilitate these measurements.

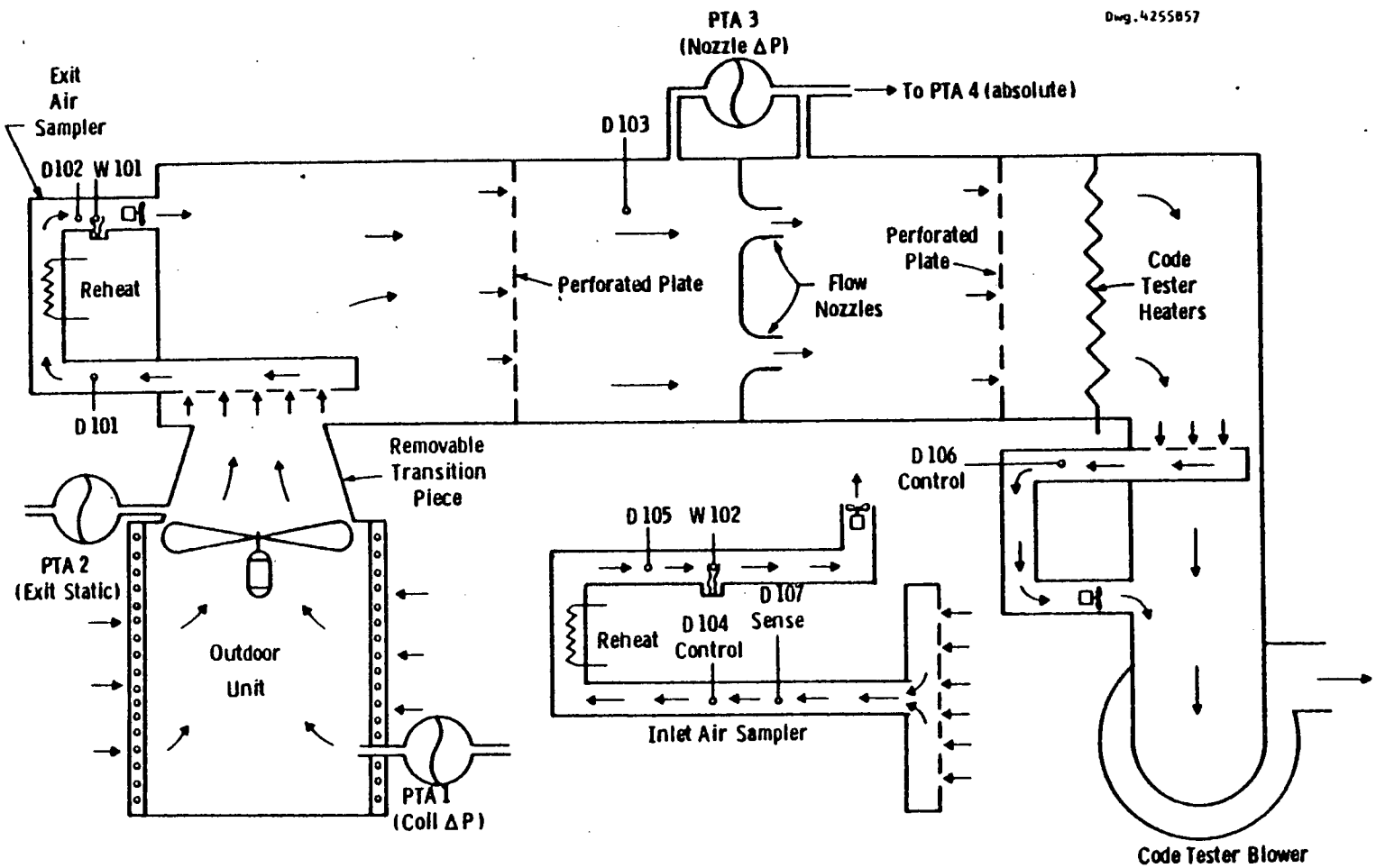


Fig. B1 - Outdoor room code tester and inlet air sampler

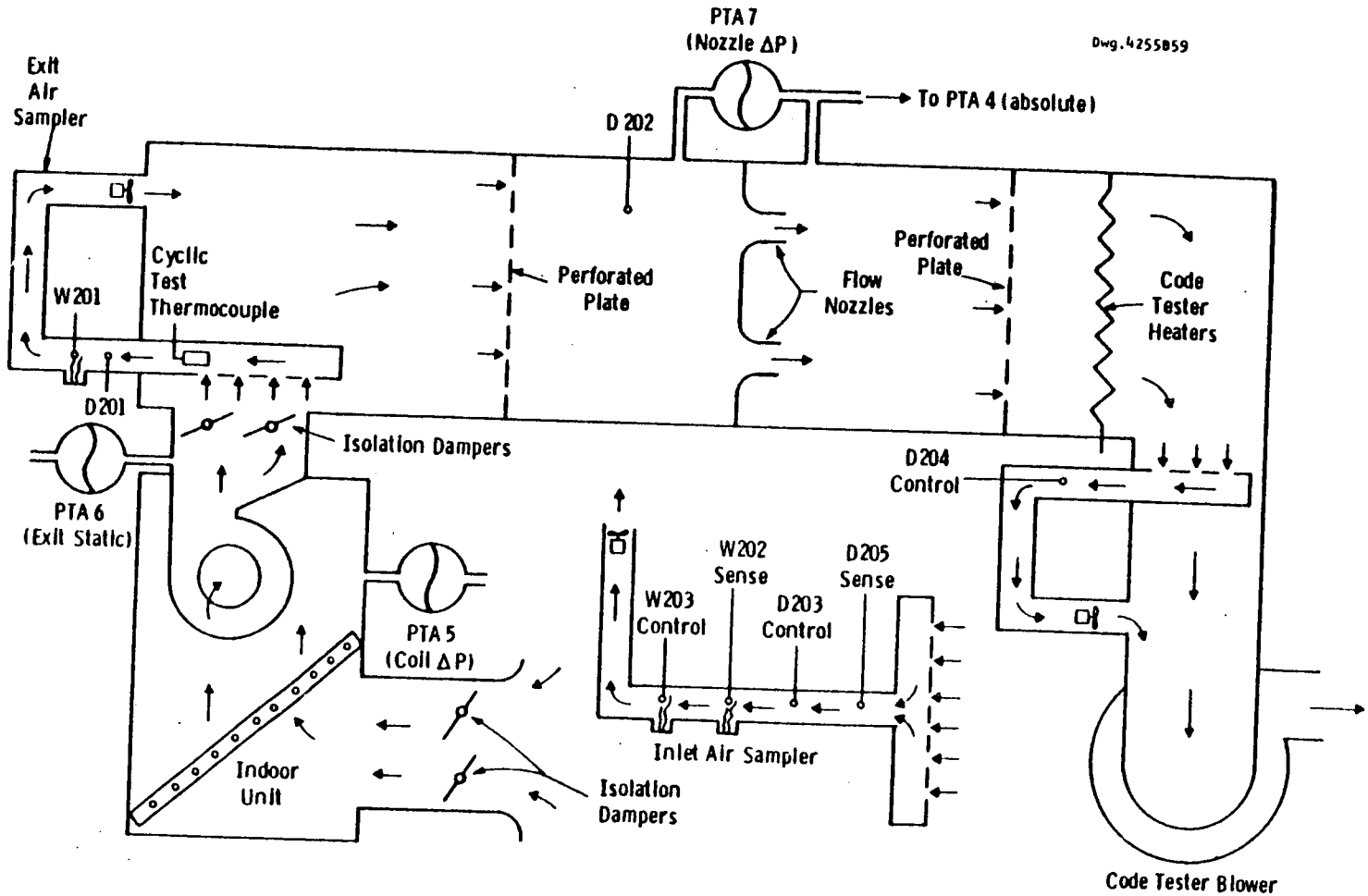


Fig. B2 - Indoor room code tester and inlet air sampler

The arrangement of components in the outdoor room code tester is shown in Figure B1. Air discharged from the test unit enters a duct constructed of aluminum skinned rigid urethane foam. Four pressure taps located at the code tester inlet are connected to a Rosemount pressure transducer (PTA2) with a -249 to +249 Pa (-1 to +1 in of $H_2O$) range. The 4-20 mA signal from the transmitter is used by the Texas Instruments control system to maintain a pre-set static pressure at the discharge of the test item by varying the speed of the code tester blower via a variable frequency drive. For this test series the static pressure was set to zero (atmospheric pressure) to simulate a free discharge.

Air is drawn through a sampling rake constructed of .05 m (2 inch) PVC tubing by a small blower and passes over an Analog Devices dry bulb temperature sensor (D101), an electric reheater, a second dry bulb sensor (D102), a wet bulb sensor (W101) and is returned to the code tester. At dew point temperatures below 0°C (32°F) the reheater is manually controlled to obtain a wet bulb temperature above freezing. The power input is monitored by an Ohio Semitronics Model PC5-19E watt transducer with a 0-1500 W range. The air passes through a perforated plate and enters the flow metering section, comprised of four .152 m (6 inch) spun aluminum flow nozzles in parallel. The L/D = 0.6 nozzles and pressure tap locations conform to ASHRAE Standard 51-75 (AMCA standard 210-74).[2] The nozzle pressure drop is measured by a Rosemount differential pressure transmitter (PTA3) with a range of 0-1245 Pa (0-5 inches of $H_2O$). The air temperature entering the nozzles is monitored with an Analog Devices temperature sensor (D103). At low air flows one or more nozzles are plugged to maintain the throat velocity range specified in ASHRAE Standard 37-78.[3] The air then passes through a second perforated screen and a bank of bare nichrome wire heaters. Following the heaters, the air temperature is measured by extracting air through a sampling rake, passing it over a Analog Devices temperature sensor (D106) and returning it to the inlet of the code tester blower.

When the outdoor coil serves as an evaporator the air temperature signal is used by the Texas Instruments control system to modulate the power input to the code tester heaters via an SCR power supply. By setting the air temperature downstream from the heaters equal to the room temperature and measuring the power input to the heaters with an Ohio Semitronics Model PC5-32-2E watt transducer, a check of the outdoor unit heat removal is obtained. The air then passes through the code tester blower and is returned to the room.

The indoor room code tester, shown schematically in Figure B2, is similar to the outdoor room unit. Since the air flows are lower, .102 m (4 inch) nozzles are used. Since dew point temperatures below 0°C (32°F) are not required, electric reheaters are not provided.

The discharge static pressure for the indoor unit is set to simulate the duct resistance of an actual space conditioning system. On high fan speed an exit static pressure of 87.2 Pa (.35 in $H_2O$) is used. On low fan speed the discharge static pressure is reduced in proportion to the square of the air flow ratio between low fan speed and high fan speed. A Rosemount pressure transmitter (PTA6) with a -249 to +249 Pa (-1 to 1 in $H_2O$) range was installed to measure indoor unit exit static pressure and control the indoor code tester blower speed through the Texas Instruments control system.

In order to perform the DOE cyclic heating and cooling tests, pneumatically actuated dampers are provided at the inlet and discharge of the indoor test unit. Since the Analog Devices temperature sensors have a time constant longer than the 2.5 sec specified in the DOE test procedure[1] for cyclic testing, a calibrated shielded copper-constantan thermocouple was added to the sampling rake. For cyclic and defrost tests the transition piece between the test unit and code tester in the outdoor room is removed to ensure proper transient air flow conditions.

Shielded copper-constantan thermocouples are also attached to the inlet air sampling rake in both rooms and in the air stream on the discharge side of the outdoor air to refrigerant heat exchanger.

Since precise psychrometry is required to obtain an accurate energy balance when the heat pump operates as an air conditioner, a second set of Analog Devices temperature senors has been added to the indoor room inlet air sampler (D205 and W202).

The absolute pressure is determined with a Rosemount pressure transmitter (PTA4) with a 0-117 kPa (0-17 psia) range. Through a solenoid valve manifold this pressure transmitter can be manually switched to read the absolute pressure in the building, outdoor room, indoor room, outdoor room code tester nozzle discharge plenum or indoor room code tester nozzle discharge plenum. Since the indoor unit air flow is the most critical measurements, the pressure in the indoor room code tester nozzle discharge plenum is monitored during the test runs.

A Digital Equipment Corporation (DEC) MINC-11/03 minicomputer is the core of the data acquisition/reduction system. The MINC is equipped with a DEC RX02 dual floppy disc drive, a DEC VT105 CRT terminal, a Texas Instruments 825 RO dot matrix printer, a Digital Pathways TCU-150 clock module with 1/16 sec resolution and a software package which includes RT-11, FORTRAN IV (ANSI-66 Standard) and an ensemble of IEEE interface and scientific subroutines.

The MINC can control and interrogate a Fluke Model 2240B data logger over the IEEE bus, Computer Products RTP high speed data acquisition system over the LSI bus, and, the Texas Instruments PM550 control system and a Hewlett-Packard 9825B programmable calculator via RS232 ports.

The Fluke 2240B data logger can read a mixture of up to 180 channels of thermocouple, millivolt or volt data at a rate of up to 13 channels per second. Thermocouple signals are converted internally to °F or °C. All readings are shown on a 5 digit LED display and can be recorded on an internal printer. The time, date and test number are displayed at the beginning of each scan.

The Computer Products RTP high speed data acquisition system consists of a RTP4780/30 wide range analog input controller with

RTP7504/31 uniform temperature reference plate with an RTD to measure the plate temperature. Up to 62 channels of voltage data can be read at a maximum rate of 200 channels per second. The MINC interface is an RTP 7410/65 I/O bus converter.

The MINC can read the 8 control parameters on the Texas Instruments PM550 control system via an RS232 port and can change the set points, gains and reset values.

A Hewlett-Packard 9825B programmable calculator can be used to emulate the heat pump microprocessor control system and energize 12 relay closures. It is used to send data initiated commands to the MINC over an RS232 port while data acquisition is in progress. Most of the steady state testing was performed in accordance with ASHRAE standard 37-78,[3] which requires a total of 7 data scans at 10 minute intervals. The DOE regulations require 4 scans at 10 minute intervals. Several tests were performed with 7 scans and the results and standard deviations compared to those obtained for the first 4 data scans of the same test. Since the differences were minimal the 4 scan procedure was adopted for tests not required for rating to reduce the time and cost of completing the test matrix.

For the cyclic tests a different data logging procedure is used to meet the DOE requirements[1] that critical temperatures be monitored "continuously", which DOE defines as every 5 seconds. This method scans the channels on the Fluke data logger once and then scans the output from the RTP data system continuously until the operator intervenes. The time from the clock module is recorded at the start of each scan. A complete scan of 71 channels in the RTP is recorded on a floppy disc every 4 seconds.

During defrost data is acquired continuously with 5 scans of the RTP data system for each scan of the Fluke data logger.

The MINC supervises the operation of both data acquisition systems and controls the transfer of the data to standard 8 inch floppy

discs. The discs are backed up with copies periodically to prevent data loss.

Test data recovered from 8 inch floppy discs is reduced on the MINC using a software library written in FORTRAN.

The steady state test data is reduced in accordance with ASHRAE standard 33-78[3] using the air enthalpy method, volatile refrigerant method and calibrated compressor method to provide redundant checks on the energy balance. Westinghouse proprietary subroutines for thermodynamic and transport properties and psychrometrics are utilized. The raw data is analyzed to determine the standard deviation, 95% confidence level and 98% confidence level.

The cyclic degradation and frost accumulation test data is reduced in accordance with DOE test procedures.[1]

## REFERENCES - APPENDIX B


B1. Department of Energy, Energy Conservation Program for Consumer Products; Test Procedures for Central Air Conditioners Including Heat Pumps, Federal Register, Vol. 44, No. 249, December 27, 1979.

B2. American Society of Heating, Refrigerating and Air Conditioning Engineers Standard 51-TS, Air Moving and Conditioning Association, Standard 210-74, Laboratory Methods of Testing Fans for Rating, 1975.

B3. American Society of Heating, Refrigerating and Air Conditioning Engineers, Standard 37-78 Methods of Testing for Rating Unitary Air Conditioners and Heat Pump Equipment, 1978.

# APPENDIX C

## SEASONAL PERFORMANCE TABLES

Note: Steady state heat pump performance data used to generate the following summary results are the same as those used for Table 1. These data were assembled prior to final error analysis and differ from the values presented in Table 2 by being 2% optimistic for low capacity heating performance at 62°F outdoor ambient. The effect upon seasonal performance estimates is not significant. See the Nomenclature and References 3 and 13 for definitions of terms and clarification.

WESTINGHOUSE DUAL STROKE

ESTIMATE OF HEAT PUMP SEASONAL PERFORMANCE BY WESTINGHOUSE/DOE PROCEDURE

*** INPUT DATA ***

HOUSE LEVEL= 2 HP SCALE FACTOR= 1.00

UNIT WITH: TWO-SPEED COMPRESSOR, TWO COMPRESSORS, OR CYLINDER UNLOADING

COOLING DATA:

| | | | | | | | |
|---|---|---|---|---|---|---|---|
| QSS(95F) | ,K=1 | 22551. | BTU/H | QSS(82F) | ,K=1 | 24991. | BTU/H |
| ESS(95F) | ,K=1 | 2630. | WATTS | ESS(82F) | ,K=1 | 2192. | WATTS |
| EERA | ,K=1 | 8.575 | | EERB | ,K=1 | 11.401 | |
| QSS(95F) | ,K=2 | 41446. | BTU/H | QSS(82F) | ,K=2 | 42734. | BTU/H |
| ESS(95F) | ,K=2 | 4571. | WATTS | ESS(82F) | ,K=2 | 3817. | WATTS |
| EERA | ,K=2 | 9.067 | | EERB | ,K=2 | 11.196 | |

HEATING DATA:

| | | | |
|---|---|---|---|
| QSS(47F) | ,K=1 | 28693. | BTU/H |
| ESS(47F) | ,K=1 | 2195. | WATTS |
| COPSS(47F) | ,K=1 | 3.830 | |
| QSS(17F) | ,K=1 | 10922. | BTU/H |
| ESS(17F) | ,K=1 | 1553. | WATTS |
| COPSS(17F) | ,K=1 | 2.061 | |
| QDEF(35F) | ,K=1 | 20689. | BTU/H |
| EDEF(35F) | ,K=1 | 1930. | WATTS |
| QSS(62F) | ,K=1 | 38225. | BTU/H |
| ESS(62F) | ,K=1 | 2575. | WATTS |
| COPSS(62F) | ,K=1 | 4.349 | |
| QSS(47F) | ,K=2 | 46829. | BTU/H |
| ESS(47F) | ,K=2 | 3948. | WATTS |
| COPSS(47F) | ,K=2 | 3.475 | |
| QSS(17F) | ,K=2 | 29392. | BTU/H |
| ESS(17F) | ,K=2 | 3181. | WATTS |
| COPSS(17F) | ,K=2 | 2.707 | |
| QDEF(35F) | ,K=2 | 38336. | BTU/H |
| EDEF(35F) | ,K=2 | 3649. | WATTS |

REGION: 2

UNIT COST OF ELECTRICITY: 0.0497 $/KWH

| | | |
|---|---|---|
| ELECTRIC POWER INPUT TO CRANKCASE HEATER, | W | 75.00 |
| ELECTRIC POWER INPUT TO CONTROL EQUIPMENT DURING THE COOLING SEASON, | W | 50.00 |
| ELECTRIC POWER INPUT TO CONTROL EQUIPMENT DURING THE HEATING SEASON, | W | 50.00 |

REGION 2 CONTINUED

COOLING SEASON SUMMARY:

| | | |
|---|---|---|
| COOLING CAPACITY AT 95 DEG. F: | 41446. | BTU/H |
| DEGRADATION COEFFICIENT, CD, K=1: | 0.100 | |
| DEGRADATION COEFFICIENT, CD, K=2: | 0.100 | |
| | (INPUT) | |

HEATING SEASON SUMMARY:

| | | |
|---|---|---|
| HEATING CAPACITY AT 47 DEG. F: | 46829. | BTU/H |
| DEGRADATION COEFFICIENT, CD, K=1: | 0.100 | |
| DEGRADATION COEFFICIENT, CD, K=2: | 0.100 | |
| | (INPUT) | |

REGIONAL DESIGN HEATING REQUIREMENT, DHR

| | | |
|---|---|---|
| MINIMUM: | 30506. | BTU/H |
| MAXIMUM: | 30506. | BTU/H |

| TBAL(DEG F) | QBAL(BTU/HR) | SLOPE(BTU/HR F) | CSLOPE | TNEUTH | TNEUTC |
|---|---|---|---|---|---|
| 19.242 | 30505.8 | -666.7 | 1.4 | 65.0 | 65.0 |

| TBAHI(DEG F) | BSCALE | QINTC(BTU/HR) | QINTH(BTU/HR) |
|---|---|---|---|
| 34.430 | 1.0000 | 0.0 | 0.0 |

*** ANNUAL COST COMPUTATION ***

TINSTA IS THE TOTAL INSTALLED COST IN $= 4037.47

IPRIME IS THE REAL INTEREST RATE= 0.03 YEAR IS THE NUMBER OF YEARS IN AMORTIZATION= 15.00

OWNER IS THE OWNERSHIP COST IN $= 338.21 MAINTA IS THE MAINTENANCE COST IN $= 100.94

ANNUAL IS THE ANNUAL COST IN $= 439.14

M IS THE MAXIMUM BIN NUMBER= 10

BLH(M,1) IS THE BUILDING LOAD AT THE M-TH BIN IN BTU/H= 32000.2

QQ IS THE HEAT PUMP CAPACITY AT THE M-TH BIN IN BTU/H= 29392.0

HDEF IS THE HEATING DEFICIENCY AT THE M-TH BIN IN KW= 0.8

XNUMB IS THE NUMBER OF 5KW HEATER REQUIRED= 0.2

REGION 2 CONTINUED

*** COMPUTATIONAL RESULTS FOR HEATING SEASON ***

| BIN J | T(J) DEG.F | BIN HRS | QDOT1 BTU/H | QDOT2 BTU/H | EDOT1 W | EDOT2 W | BLH BTU/H | CASE | DELTA | BLH/N BTU/H | E/N | RH/N W | BLH W | CASE | DELTA BTU/H | BLH/N | E/N | RH/N BTU/H | W |
|---|---|---|---|---|---|---|---|---|---|---|---|---|---|---|---|---|---|---|---|
| 1 | 62. | 0.259 | 38225. | 55548. | 2575.0 | 4331.5 | 2000. | 1 | 1.0 | 518.0 | 38.5 | 0.0 | 2000. | 1 | 1.0 | 518.0 | 38.5 | 0.0 | |
| 2 | 57. | 0.221 | 35048. | 52641. | 2448.3 | 4203.7 | 5333. | 1 | 1.0 | 1178.7 | 90.0 | 0.0 | 5333. | 1 | 1.0 | 1178.7 | 90.0 | 0.0 | |
| 3 | 52. | 0.144 | 31870. | 49735. | 2321.7 | 4075.8 | 8667. | 1 | 1.0 | 1248.0 | 98.1 | 0.0 | 8667. | 1 | 1.0 | 1248.0 | 98.1 | 0.0 | |
| 4 | 47. | 0.172 | 28693. | 46829. | 2195.0 | 3948.0 | 12000. | 1 | 1.0 | 2064.0 | 167.6 | 0.0 | 12000. | 1 | 1.0 | 2064.0 | 167.6 | 0.0 | |
| 5 | 42. | 0.136 | 25516. | 41914. | 2068.3 | 3831.0 | 15333. | 1 | 1.0 | 2085.3 | 176.1 | 0.0 | 15333. | 1 | 1.0 | 2085.3 | 176.1 | 0.0 | |
| 6 | 37. | 0.052 | 21774. | 39330. | 1971.9 | 3701.0 | 18667. | 1 | 1.0 | 970.7 | 89.2 | 0.0 | 18667. | 1 | 1.0 | 970.7 | 89.2 | 0.0 | |
| 7 | 32. | 0.011 | 0. | 36845. | 0.0 | 3571.0 | 22000. | 3 | 1.0 | 242.0 | 24.4 | 0.0 | 22000. | 3 | 1.0 | 242.0 | 24.4 | 0.0 | |
| 8 | 27. | 0.003 | 0. | 34361. | 0.0 | 3441.0 | 25333. | 3 | 1.0 | 76.0 | 7.8 | 0.0 | 25333. | 3 | 1.0 | 76.0 | 7.8 | 0.0 | |
| 9 | 22. | 0.001 | 0. | 31876. | 0.0 | 3311.0 | 28667. | 3 | 1.0 | 28.7 | 3.0 | 0.0 | 28667. | 3 | 1.0 | 28.7 | 3.0 | 0.0 | |
| | | | | | | | | | | 8411.4 | 694.7 | 0.0 | | | | 8411.4 | 694.7 | 0.0 | TOTAL |

| J | HEAT INPUT | E. PUMP | E. REST | E. CHE | E. CTL | E. SUM | COP |
|---|---|---|---|---|---|---|---|
| 1 | 1943545.87 | 144632.05 | 0.00 | 69069.23 | 48588.40 | 262289.69 | 2.17 |
| 2 | 4422379.00 | 337553.91 | 0.00 | 52725.76 | 41459.60 | 431739.25 | 3.00 |
| 3 | 4682519.50 | 367893.75 | 0.00 | 29502.29 | 27014.40 | 424410.44 | 3.23 |
| 4 | 7744166.50 | 629019.81 | 0.00 | 28158.49 | 32267.20 | 689445.50 | 3.29 |
| 5 | 7824210.00 | 660602.69 | 0.00 | 15272.15 | 25513.60 | 701388.44 | 3.27 |
| 6 | 3641959.50 | 334592.09 | 0.00 | 2088.35 | 9755.20 | 346435.63 | 3.08 |
| 7 | 907988.50 | 91695.29 | 0.00 | 1247.16 | 2063.60 | 95006.05 | 2.80 |
| 8 | 285153.41 | 29326.53 | 0.00 | 221.79 | 562.80 | 30111.12 | 2.77 |
| 9 | 107557.87 | 11285.64 | 0.00 | 28.33 | 187.60 | 11501.57 | 2.74 |

HSPF 10.55 SEASONAL LOAD 31559480.0

ELECTRICITY INPUT TO HEAT PUMP 2606601.5 ELECTRICITY INPUT TO RESISTANCE HEATER 0.0

ELECTRICITY INPUT TO CRANKCASE HEATER 198313.6 ELECTRICITY INPUT TO CONTROL EQUIPMENTS 187600.0

TOTAL ELECTRICITY INPUT 2992515.0

SEASONAL HEATING HOURS 3752.0 HEAT DELIVERED BY HEAT PUMP 31559482.0

HEAT DELIVERED BY RESISTANCE HEATER 0.0 HEAT DEFICIENCY -2.0

RUNNING HOURS HIGH CAPACITY 37.6 LOW CAPACITY 1129.1

REGION 2 CONTINUED

*** COMPUTATIONAL RESULTS FOR COOLING SEASON ***

| BIN J | T(J) DEG.F | BIN HRS | BLC BTU/H | QSS1 BTU/H | QSS2 BTU/H | ESS1 W | ESS2 W | CASE | X1 | X2 | Q/N BTU/H | E/N W | |
|---|---|---|---|---|---|---|---|---|---|---|---|---|---|
| 1 | 67. | 0.146 | 1867. | 27806. | 44220. | 1686.6 | 2947.0 | 1 | 0.067 | 0.000 | 272.5 | 18.2 | |
| 2 | 72. | 0.127 | 6533. | 26868. | 43725. | 1855.1 | 3237.0 | 1 | 0.243 | 0.000 | 829.7 | 62.0 | |
| 3 | 77. | 0.130 | 11200. | 25929. | 43229. | 2023.5 | 3527.0 | 1 | 0.432 | 0.000 | 1456.0 | 120.5 | |
| 4 | 82. | 0.189 | 15867. | 24991. | 42734. | 2192.0 | 3817.0 | 1 | 0.635 | 0.000 | 2998.8 | 273.0 | |
| 5 | 87. | 0.121 | 20533. | 24053. | 42239. | 2360.5 | 4107.0 | 1 | 0.854 | 0.000 | 2484.5 | 247.4 | |
| 6 | 92. | 0.105 | 25200. | 23114. | 41743. | 2528.9 | 4397.0 | 3 | 0.000 | 0.604 | 2646.0 | 290.2 | |
| 7 | 97. | 0.080 | 29867. | 22176. | 41248. | 2697.4 | 4687.0 | 3 | 0.000 | 0.724 | 2389.3 | 279.2 | |
| 8 | 102. | 0.068 | 34534. | 21237. | 40752. | 2865.8 | 4977.0 | 3 | 0.000 | 0.847 | 2348.3 | 291.2 | |
| 9 | 107. | 0.034 | 39200. | 20299. | 40257. | 3034.3 | 5267.0 | 3 | 0.000 | 0.974 | 1332.8 | 174.8 | |
| | | | | | | | | | | | 16758.1 | 1756.6 | TOTAL |

| J | BLDG LOAD | HP CAP | E. PUMP | E. CHE | E. CTL | E. SUM | COP |
|---|---|---|---|---|---|---|---|
| 1 | 1364853.62 | 1364853.62 | 91303.55 | 51156.28 | 36558.40 | 179018.25 | 2.23 |
| 2 | 4155325.25 | 4155325.25 | 310393.12 | 36101.89 | 31800.80 | 378295.84 | 3.22 |
| 3 | 7291684.00 | 7291684.00 | 603315.69 | 27737.07 | 32552.00 | 663604.75 | 3.22 |
| 4 | 15018064.00 | 15018064.00 | 1367173.87 | 25917.98 | 47325.60 | 1440417.50 | 3.05 |
| 5 | 12442605.00 | 12442605.00 | 1239219.75 | 6649.39 | 30298.40 | 1276167.50 | 2.86 |
| 6 | 13251233.00 | 13251234.00 | 1453411.12 | 15629.53 | 26292.00 | 1495332.62 | 2.60 |
| 7 | 11965841.00 | 11965841.00 | 1398261.00 | 8290.79 | 20032.00 | 1426583.75 | 2.46 |
| 8 | 11760178.00 | 11760178.00 | 1458499.50 | 3897.61 | 17027.20 | 1479424.37 | 2.33 |
| 9 | 6674696.50 | 6674696.50 | 875576.75 | 335.27 | 8513.60 | 884425.62 | 2.21 |

SEER 9.10 COOLING DELIVERED 83924488.0 ELECTRICITY INPUT TO HEAT PUMP 8797154.0

ELECTRICITY INPUT TO CRANKCASE HEATER 175715.8 ELECTRICITY INPUT TO CONTROL EQUIPMENT 250400.0

TOTAL ELECTRICITY INPUT 9223270.0 SEASONAL LOAD 83924488.0

COOLING DEFICIENCY 0.0 COOLING COST 458.4 SEASONAL COOLING HOURS 5008.0

RUNNING HOURS HIGH CAPACITY 1088.2 LOW CAPACITY 1668.3

REGION 2 CONTINUED

*** SUMMARY OF THE CALCULATION ***

HEAT PUMP OFF-TIME= 4837.79 ELECTRICITY INPUT DURING OFF-TIME= 241889.36

HEATING COST= 148.73 COOLING COST= 458.40

FIXED CHARGE= 439.14 SUM OF HEATING AND COOLING COSTS= 607.12

ENERGY COST OF CRANKCASE HEATER AND CONTROL EQUIPMENTS DURING OFF-TIME= 12.02

TOTAL COST= 1058.29

HEAT DELIVERED= 31559480.00 COOLING DELIVERED= 83924488.00

TOTAL BTU DELIVERED= 115483968.00 COST PER MBTU DELIVERED= 9.16

ESTIMATE OF HEAT PUMP SEASONAL PERFORMANCE BY WESTINGHOUSE/DOE PROCEDURE

*** INPUT DATA ***

HOUSE LEVEL= 2 HP SCALE FACTOR= 1.00

UNIT WITH: TWO-SPEED COMPRESSOR, TWO COMPRESSORS, OR CYLINDER UNLOADING

COOLING DATA:

| | | | | | | | |
|---|---|---|---|---|---|---|---|
| QSS(95F) | ,K=1 | 22551. | BTU/H | QSS(82F) | ,K=1 | 24991. | BTU/H |
| ESS(95F) | ,K=1 | 2630. | WATTS | ESS(82F) | ,K=1 | 2192. | WATTS |
| EERA | ,K=1 | 9.575 | | EERB | ,K=1 | 11.401 | |
| QSS(95F) | ,K=2 | 41446. | BTU/H | QSS(82F) | ,K=2 | 42734. | BTU/H |
| ESS(95F) | ,K=2 | 4571. | WATTS | ESS(82F) | ,K=2 | 3817. | WATTS |
| EERA | ,K=2 | 9.067 | | EERB | ,K=2 | 11.196 | |

HEATING DATA:

| | | | |
|---|---|---|---|
| QSS(47F) | ,K=1 | 28693. | BTU/H |
| ESS(47F) | ,K=1 | 2195. | WATTS |
| COPSS(47F) | ,K=1 | 3.830 | |
| QSS(17F) | ,K=1 | 10922. | BTU/H |
| ESS(17F) | ,K=1 | 1553. | WATTS |
| COPSS(17F) | ,K=1 | 2.061 | |
| QDEF(35F) | ,K=1 | 20689. | BTU/H |
| EDEF(35F) | ,K=1 | 1930. | WATTS |
| QSS(62F) | ,K=1 | 38225. | BTU/H |
| ESS(62F) | ,K=1 | 2575. | WATTS |
| COPSS(62F) | ,K=1 | 4.349 | |
| QSS(47F) | ,K=2 | 46829. | BTU/H |
| ESS(47F) | ,K=2 | 3948. | WATTS |
| COPSS(47F) | ,K=2 | 3.475 | |
| QSS(17F) | ,K=2 | 29392. | BTU/H |
| ESS(17F) | ,K=2 | 3181. | WATTS |
| COPSS(17F) | ,K=2 | 2.707 | |
| QDEF(35F) | ,K=2 | 38336. | BTU/H |
| EDEF(35F) | ,K=2 | 3649. | WATTS |

REGION: 3

UNIT COST OF ELECTRICITY: 0.0497 $/KWH

| | | |
|---|---|---|
| ELECTRIC POWER INPUT TO CRANKCASE HEATER, | W | 75.00 |
| ELECTRIC POWER INPUT TO CONTROL EQUIPMENT DURING THE COOLING SEASON, | W | 50.00 |
| ELECTRIC POWER INPUT TO CONTROL EQUIPMENT DURING THE HEATING SEASON, | W | 50.00 |

REGION 3 CONTINUED

COOLING SEASON SUMMARY:

| | | |
|---|---|---|
| COOLING CAPACITY AT 95 DEG. F: | 41446. | BTU/H |
| DEGRADATION COEFFICIENT, CD, K=1: | 0.100 | |
| DEGRADATION COEFFICIENT, CD, K=2: | 0.100 | |
| | (INPUT) | |

HEATING SEASON SUMMARY:

| | | |
|---|---|---|
| HEATING CAPACITY AT 47 DEG. F: | 46829. | BTU/H |
| DEGRADATION COEFFICIENT, CD, K=1: | 0.100 | |
| DEGRADATION COEFFICIENT, CD, K=2: | 0.100 | |
| | (INPUT) | |

REGIONAL DESIGN HEATING REQUIREMENT, DHR

| | | |
|---|---|---|
| MINIMUM: | 30506. | BTU/H |
| MAXIMUM: | 30506. | BTU/H |

| TBAL(DEG F) | QBAL(BTU/HR) | SLOPE(BTU/HR F) | CSLOPE | TNEUTH | TNEUTC |
|---|---|---|---|---|---|
| 19.242 | 30505.8 | -666.7 | 1.4 | 65.0 | 65.0 |

| TBAHI(DEG F) | BSCALE | QINTC(BTU/HR) | QINTH(BTU/HR) |
|---|---|---|---|
| 34.430 | 1.0000 | 0.0 | 0.0 |

*** ANNUAL COST COMPUTATION ***

TINSTA IS THE TOTAL INSTALLED COST IN $= 4037.47

IPRIME IS THE REAL INTEREST RATE= 0.03 YEAR IS THE NUMBER OF YEARS IN AMORTIZATION= 15.00

OWNER IS THE OWNERSHIP COST IN $= 338.21 MAINTA IS THE MAINTENANCE COST IN $= 100.94

ANNUAL IS THE ANNUAL COST IN $= 439.14

M IS THE MAXIMUM BIN NUMBER= 13

BLH(M,1) IS THE BUILDING LOAD AT THE M-TH BIN IN BTU/H= 42000.2

QO IS THE HEAT PUMP CAPACITY AT THE M-TH BIN IN BTU/H= 20673.5

HDEF IS THE HEATING DEFICIENCY AT THE M-TH BIN IN KW= 6.2

XNUMB IS THE NUMBER OF 5KW HEATER REQUIRED= 1.2

REGION 3 CONTINUED

*** COMPUTATIONAL RESULTS FOR HEATING SEASON ***

| BIN J | T(J) DEG.F | BIN HRS | QDOT1 BTU/H | QDOT2 BTU/H | EDOT1 W | EDOT2 W | BLH BTU/H | CASE | DELTA | BLH/N | E/N BTU/H | RH/N W | BLH W | CASE | DELTA BTU/H | BLH/N | E/N | RH/N BTU/H | W |
|---|---|---|---|---|---|---|---|---|---|---|---|---|---|---|---|---|---|---|---|
| 1 | 62. | 0.139 | 38225. | 55548. | 2575.0 | 4331.5 | 2000. | 1 | 1.0 | 278.0 | 20.7 | 0.0 | 2000. | 1 | 1.0 | 278.0 | 20.7 | 0.0 | |
| 2 | 57. | 0.126 | 35048. | 52641. | 2448.3 | 4203.7 | 5333. | 1 | 1.0 | 672.0 | 51.3 | 0.0 | 5333. | 1 | 1.0 | 672.0 | 51.3 | 0.0 | |
| 3 | 52. | 0.106 | 31870. | 49735. | 2321.7 | 4075.8 | 8667. | 1 | 1.0 | 918.7 | 72.2 | 0.0 | 8667. | 1 | 1.0 | 918.7 | 72.2 | 0.0 | |
| 4 | 47. | 0.142 | 28693. | 46829. | 2195.0 | 3948.0 | 12000. | 1 | 1.0 | 1704.0 | 138.4 | 0.0 | 12000. | 1 | 1.0 | 1704.0 | 138.4 | 0.0 | |
| 5 | 42. | 0.148 | 25516. | 41914. | 2068.3 | 3831.0 | 15333. | 1 | 1.0 | 2269.3 | 191.6 | 0.0 | 15333. | 1 | 1.0 | 2269.3 | 191.6 | 0.0 | |
| 6 | 37. | 0.119 | 21774. | 39330. | 1971.9 | 3701.0 | 18667. | 1 | 1.0 | 2221.3 | 204.1 | 0.0 | 18667. | 1 | 1.0 | 2221.3 | 204.1 | 0.0 | |
| 7 | 32. | 0.097 | 0. | 36845. | 0.0 | 3571.0 | 22000. | 3 | 1.0 | 2134.0 | 215.5 | 0.0 | 22000. | 3 | 1.0 | 2134.0 | 215.5 | 0.0 | |
| 8 | 27. | 0.054 | 0. | 34361. | 0.0 | 3441.0 | 25333. | 3 | 1.0 | 1368.0 | 140.7 | 0.0 | 25333. | 3 | 1.0 | 1368.0 | 140.7 | 0.0 | |
| 9 | 22. | 0.030 | 0. | 31876. | 0.0 | 3311.0 | 28667. | 3 | 1.0 | 860.0 | 90.2 | 0.0 | 28667. | 3 | 1.0 | 860.0 | 90.2 | 0.0 | |
| 10 | 17. | 0.012 | 0. | 29392. | 0.0 | 3181.0 | 32000. | 4 | 1.0 | 384.0 | 38.2 | 9.2 | 32000. | 4 | 1.0 | 384.0 | 38.2 | 9.2 | |
| 11 | 12. | 0.007 | 0. | 26486. | 0.0 | 3053.2 | 35334. | 4 | 1.0 | 247.3 | 21.4 | 18.1 | 35334. | 4 | 1.0 | 247.3 | 21.4 | 18.1 | |
| 12 | 7. | 0.005 | 0. | 23580. | 0.0 | 2925.3 | 38667. | 4 | 1.0 | 193.3 | 14.6 | 22.1 | 38667. | 4 | 1.0 | 193.3 | 14.6 | 22.1 | |
| 13 | 2. | 0.006 | 0. | 20674. | 0.0 | 2797.5 | 42000. | 4 | 1.0 | 252.0 | 16.8 | 37.5 | 42000. | 4 | 1.0 | 252.0 | 16.8 | 37.5 | |
| 14 | -3. | 0.006 | 0. | 17767. | 0.0 | 2669.7 | 45334. | 4 | 1.0 | 272.0 | 16.0 | 48.5 | 45334. | 4 | 1.0 | 272.0 | 16.0 | 48.5 | |
| 15 | -8. | 0.001 | 0. | 14861. | 0.0 | 2541.8 | 48667. | 4 | 1.0 | 48.7 | 2.5 | 9.9 | 48667. | 4 | 1.0 | 48.7 | 2.5 | 9.9 | |
| | | | | | | | | | | 13822.7 | 1234.2 | 145.3 | | | | 13822.7 | 1234.2 | 145.3 | TOTAL |

| J | HEAT INPUT | E. PUMP | E. REST | E. CHE | E. CTL | E. SUM | COP |
|---|---|---|---|---|---|---|---|
| 1 | 1383056.87 | 102922.38 | 0.00 | 49150.72 | 34576.25 | 186649.36 | 2.17 |
| 2 | 3343216.75 | 255182.95 | 0.00 | 39859.46 | 31342.50 | 326384.91 | 3.00 |
| 3 | 4570389.50 | 359084.00 | 0.00 | 28795.82 | 26367.50 | 414247.31 | 3.23 |
| 4 | 8477443.00 | 688580.06 | 0.00 | 30824.75 | 35322.50 | 754727.31 | 3.29 |
| 5 | 11299989.00 | 953220.50 | 0.00 | 22037.04 | 36815.00 | 1012072.56 | 3.27 |
| 6 | 11051189.00 | 1015288.69 | 0.00 | 6336.90 | 29601.25 | 1051226.87 | 3.08 |
| 7 | 10616703.00 | 1072152.00 | 0.00 | 14582.50 | 24128.75 | 1110863.25 | 2.90 |
| 8 | 6805834.00 | 699944.12 | 0.00 | 5293.59 | 13432.50 | 718670.19 | 2.77 |
| 9 | 4278521.00 | 448929.03 | 0.00 | 1127.11 | 7462.50 | 457518.63 | 2.74 |
| 10 | 1910409.50 | 189905.70 | 45621.79 | 0.00 | 2985.00 | 238512.48 | 2.35 |
| 11 | 1230489.50 | 106326.53 | 90278.42 | 0.00 | 1741.25 | 198346.20 | 1.82 |
| 12 | 961838.06 | 72767.66 | 109960.13 | 0.00 | 1243.75 | 183971.55 | 1.53 |
| 13 | 1253706.25 | 83505.38 | 186522.77 | 0.00 | 1492.50 | 271520.66 | 1.35 |
| 14 | 1353206.62 | 79689.55 | 241093.41 | 0.00 | 1492.50 | 322275.47 | 1.23 |
| 15 | 242117.99 | 12645.62 | 49277.34 | 0.00 | 248.75 | 62171.71 | 1.14 |

HSPF 9.41 SEASONAL LOAD 68768112.0

ELECTRICITY INPUT TO HEAT PUMP 6140144.0 ELECTRICITY INPUT TO RESISTANCE HEATER 722753.9

ELECTRICITY INPUT TO CRANKCASE HEATER 198007.9 ELECTRICITY INPUT TO CONTROL EQUIPMENTS 248750.0

TOTAL ELECTRICITY INPUT 7309656.0

SEASONAL HEATING HOURS 4975.0 HEAT DELIVERED BY HEAT PUMP 66301352.0

HEAT DELIVERED BY RESISTANCE HEATER 2466759.0 HEAT DEFICIENCY 2466760.0

RUNNING HOURS HIGH CAPACITY 323.3 LOW CAPACITY 1598.3

REGION 3 CONTINUED

*** COMPUTATIONAL RESULTS FOR COOLING SEASON ***

| BIN J | T(J) DEG.F | BIN HRS | BLC BTU/H | QSS1 BTU/H | QSS2 BTU/H | ESS1 W | ESS2 W | CASE | X1 | X2 | Q/N BTU/H | E/N W | |
|---|---|---|---|---|---|---|---|---|---|---|---|---|---|
| 1 | 67. | 0.236 | 1867. | 27806. | 44220. | 1686.6 | 2947.0 | 1 | 0.067 | 0.000 | 440.5 | 29.5 | |
| 2 | 72. | 0.232 | 6533. | 26868. | 43725. | 1855.1 | 3237.0 | 1 | 0.243 | 0.000 | 1515.7 | 113.2 | |
| 3 | 77. | 0.188 | 11200. | 25929. | 43229. | 2023.5 | 3527.0 | 1 | 0.432 | 0.000 | 2105.6 | 174.2 | |
| 4 | 82. | 0.183 | 15867. | 24991. | 42734. | 2192.0 | 3817.0 | 1 | 0.635 | 0.000 | 2903.6 | 264.3 | |
| 5 | 87. | 0.116 | 20533. | 24053. | 42239. | 2360.5 | 4107.0 | 1 | 0.854 | 0.000 | 2381.9 | 237.2 | |
| 6 | 92. | 0.040 | 25200. | 23114. | 41743. | 2528.9 | 4397.0 | 3 | 0.000 | 0.604 | 1008.0 | 110.6 | |
| 7 | 97. | 0.006 | 29867. | 22176. | 41248. | 2697.4 | 4687.0 | 3 | 0.000 | 0.724 | 179.2 | 20.9 | |
| | | | | | | | | | | | 10534.6 | 950.0 | TOTAL |

| J | BLDG LOAD | HP CAP | E. PUMP | E. CHE | E. CTL | E. SUM | COP |
|---|---|---|---|---|---|---|---|
| 1 | 1667427.00 | 1667427.00 | 111544.57 | 62497.08 | 44663.00 | 218704.66 | 2.23 |
| 2 | 5737079.00 | 5737079.00 | 428546.47 | 49844.32 | 43906.00 | 522296.78 | 3.22 |
| 3 | 7969735.00 | 7969735.00 | 659417.88 | 30316.33 | 35579.00 | 725313.19 | 3.22 |
| 4 | 10990180.00 | 10990180.00 | 1000494.31 | 18966.71 | 34632.75 | 1054093.75 | 3.05 |
| 5 | 9015410.00 | 9015410.00 | 897888.75 | 4817.88 | 21953.00 | 924659.62 | 2.86 |
| 6 | 3815299.00 | 3815299.25 | 418466.53 | 4500.06 | 7570.00 | 430536.59 | 2.60 |
| 7 | 678275.31 | 678275.31 | 79259.46 | 469.96 | 1135.50 | 80864.92 | 2.46 |

SEER 10.08 COOLING DELIVERED 39873408.0 ELECTRICITY INPUT TO HEAT PUMP 3595618.0

ELECTRICITY INPUT TO CRANKCASE HEATER 171412.4 ELECTRICITY INPUT TO CONTROL EQUIPMENT 189250.0

TOTAL ELECTRICITY INPUT 3956280.2 SEASONAL LOAD 39873408.0

COOLING DEFICIENCY 0.0 COOLING COST 196.6 SEASONAL COOLING HOURS 3785.0

RUNNING HOURS HIGH CAPACITY 112.1 LOW CAPACITY 1459.8

REGION 3 CONTINUED

*** SUMMARY OF THE CALCULATION ***

HEAT PUMP OFF-TIME= 4776.45 ELECTRICITY INPUT DURING OFF-TIME= 238822.69

HEATING COST= 363.29 COOLING COST= 196.63

FIXED CHARGE= 439.14 SUM OF HEATING AND COOLING COSTS= 559.92

ENERGY COST OF CRANKCASE HEATER AND CONTROL EQUIPMENTS DURING OFF-TIME= 11.87

TOTAL COST= 1010.93

HEAT DELIVERED= 68768112.00 COOLING DELIVERED= 39873408.00

TOTAL BTU DELIVERED= 108641520.00 COST PER MBTU DELIVERED= 9.31

ESTIMATE OF HEAT PUMP SEASONAL PERFORMANCE BY WESTINGHOUSE/DOE PROCEDURE

*** INPUT DATA ***

HOUSE LEVEL= 2 HP SCALE FACTOR= 1.00

UNIT WITH: TWO-SPEED COMPRESSOR, TWO COMPRESSORS, OR CYLINDER UNLOADING

COOLING DATA:

| | | | | | | | |
|---|---|---|---|---|---|---|---|
| QSS(95F) | ,K=1 | 22551. | BTU/H | QSS(82F) | ,K=1 | 24991. | BTU/H |
| ESS(95F) | ,K=1 | 2630. | WATTS | ESS(82F) | ,K=1 | 2192. | WATTS |
| EERA | ,K=1 | 8.575 | | EERB | ,K=1 | 11.401 | |
| QSS(95F) | ,K=2 | 41446. | BTU/H | QSS(82F) | ,K=2 | 42734. | BTU/H |
| ESS(95F) | ,K=2 | 4571. | WATTS | ESS(82F) | ,K=2 | 3817. | WATTS |
| EERA | ,K=2 | 9.067 | | EERB | ,K=2 | 11.196 | |

HEATING DATA:

| | | | |
|---|---|---|---|
| QSS(47F) | ,K=1 | 28693. | BTU/H |
| ESS(47F) | ,K=1 | 2195. | WATTS |
| COPSS(47F) | ,K=1 | 3.830 | |
| QSS(17F) | ,K=1 | 10922. | BTU/H |
| ESS(17F) | ,K=1 | 1553. | WATTS |
| COPSS(17F) | ,K=1 | 2.061 | |
| QDEF(35F) | ,K=1 | 20689. | BTU/H |
| EDEF(35F) | ,K=1 | 1930. | WATTS |
| QSS(62F) | ,K=1 | 33225. | BTU/H |
| ESS(62F) | ,K=1 | 2575. | WATTS |
| COPSS(62F) | ,K=1 | 4.349 | |
| QSS(47F) | ,K=2 | 46829. | BTU/H |
| ESS(47F) | ,K=2 | 3948. | WATTS |
| COPSS(47F) | ,K=2 | 3.475 | |
| QSS(17F) | ,K=2 | 29392. | BTU/H |
| ESS(17F) | ,K=2 | 3181. | WATTS |
| COPSS(17F) | ,K=2 | 2.707 | |
| QDEF(35F) | ,K=2 | 38336. | BTU/H |
| EDEF(35F) | ,K=2 | 3649. | WATTS |

REGION: 4

UNIT COST OF ELECTRICITY: 0.0497 $/KWH

| | |
|---|---|
| ELECTRIC POWER INPUT TO CRANKCASE HEATER, W | 75.00 |
| ELECTRIC POWER INPUT TO CONTROL EQUIPMENT DURING THE COOLING SEASON, W | 50.00 |
| ELECTRIC POWER INPUT TO CONTROL EQUIPMENT DURING THE HEATING SEASON, W | 50.00 |

REGION 4 CONTINUED

COOLING SEASON SUMMARY:

| | | |
|---|---|---|
| COOLING CAPACITY AT 95 DEG. F: | 41446. | BTU/H |
| DEGRADATION COEFFICIENT, CD, K=1: | 0.100 | |
| DEGRADATION COEFFICIENT, CD, K=2: | 0.100 | |
| | (INPUT) | |

HEATING SEASON SUMMARY:

| | | |
|---|---|---|
| HEATING CAPACITY AT 47 DEG. F: | 46829. | BTU/H |
| DEGRADATION COEFFICIENT, CD, K=1: | 0.100 | |
| DEGRADATION COEFFICIENT, CD, K=2: | 0.100 | |
| | (INPUT) | |

REGIONAL DESIGN HEATING REQUIREMENT, DHR

| | | |
|---|---|---|
| MINIMUM: | 30506. | BTU/H |
| MAXIMUM: | 30506. | BTU/H |

| TBAL(DEG F) | QBAL(BTU/HR) | SLOPE(BTU/HR F) | CSLOPE | TNEUTH | TNEUTC |
|---|---|---|---|---|---|
| 19.242 | 30505.8 | -666.7 | 1.4 | 65.0 | 65.0 |

| TBAHI(DEG F) | BSCALE | QINTC(BTU/HR) | QINTH(BTU/HR) |
|---|---|---|---|
| 34.430 | 1.0000 | 0.0 | 0.0 |

*** ANNUAL COST COMPUTATION ***

TINSTA IS THE TOTAL INSTALLED COST IN $= 4037.47

IPRIME IS THE REAL INTEREST RATE= 0.03 YEAR IS THE NUMBER OF YEARS IN AMORTIZATION= 15.00

OWNER IS THE OWNERSHIP COST IN $= 338.21 MAINTA IS THE MAINTENANCE COST IN $= 100.94

ANNUAL IS THE ANNUAL COST IN $= 439.14

M IS THE MAXIMUM BIN NUMBER= 15

BLH(M,1) IS THE BUILDING LOAD AT THE M-TH BIN IN BTU/H= 48666.9

QO IS THE HEAT PUMP CAPACITY AT THE M-TH BIN IN BTU/H= 14861.2

HDEF IS THE HEATING DEFICIENCY AT THE M-TH BIN IN KW= 9.9

XNUMB IS THE NUMBER OF 5KW HEATER REQUIRED= 2.0

REGION 4 CONTINUED

*** COMPUTATIONAL RESULTS FOR HEATING SEASON ***

| BIN J | T(J) DEG.F | BIN HRS | QDOT1 BTU/H | QDOT2 BTU/H | EDOT1 W | EDOT2 W | BLH BTU/H | CASE | DELTA | BLH/N BTU/H | E/N | RH/N W | BLH W | CASE | DELTA BTU/H | BLH/N | E/N | BTU/H |
|---|---|---|---|---|---|---|---|---|---|---|---|---|---|---|---|---|---|---|
| 1 | 62. | 0.145 | 38225. | 55548. | 2575.0 | 4331.5 | 2000. | 1 | 1.0 | 290.0 | 21.6 | 0.0 | 2000. | 1 | 1.0 | 290.0 | 21.6 | 0.0 |
| 2 | 57. | 0.106 | 35048. | 52641. | 2448.3 | 4203.7 | 5333. | 1 | 1.0 | 565.3 | 43.2 | 0.0 | 5333. | 1 | 1.0 | 565.3 | 43.2 | 0.0 |
| 3 | 52. | 0.057 | 31870. | 49735. | 2321.7 | 4075.8 | 8667. | 1 | 1.0 | 494.0 | 38.8 | 0.0 | 8667. | 1 | 1.0 | 494.0 | 38.8 | 0.0 |
| 4 | 47. | 0.085 | 28693. | 46829. | 2195.0 | 3948.0 | 12000. | 1 | 1.0 | 1020.0 | 82.9 | 0.0 | 12000. | 1 | 1.0 | 1020.0 | 82.9 | 0.0 |
| 5 | 42. | 0.094 | 25516. | 41814. | 2068.3 | 3831.0 | 15333. | 1 | 1.0 | 1441.3 | 121.7 | 0.0 | 15333. | 1 | 1.0 | 1441.3 | 121.7 | 0.0 |
| 6 | 37. | 0.117 | 21774. | 39330. | 1971.9 | 3701.0 | 18667. | 1 | 1.0 | 2184.0 | 200.6 | 0.0 | 18667. | 1 | 1.0 | 2184.0 | 200.6 | 0.0 |
| 7 | 32. | 0.175 | 0. | 36845. | 0.0 | 3571.0 | 22000. | 3 | 1.0 | 3850.0 | 388.8 | 0.0 | 22000. | 3 | 1.0 | 3850.0 | 388.8 | 0.0 |
| 8 | 27. | 0.059 | 0. | 34361. | 0.0 | 3441.0 | 25333. | 3 | 1.0 | 1494.7 | 153.7 | 0.0 | 25333. | 3 | 1.0 | 1494.7 | 153.7 | 0.0 |
| 9 | 22. | 0.055 | 0. | 31876. | 0.0 | 3311.0 | 28667. | 3 | 1.0 | 1576.7 | 165.4 | 0.0 | 28667. | 3 | 1.0 | 1576.7 | 165.4 | 0.0 |
| 10 | 17. | 0.052 | 0. | 29392. | 0.0 | 3181.0 | 32000. | 4 | 1.0 | 1664.0 | 165.4 | 39.7 | 32000. | 4 | 1.0 | 1664.0 | 165.4 | 39.7 |
| 11 | 12. | 0.028 | 0. | 26486. | 0.0 | 3053.2 | 35334. | 4 | 1.0 | 989.3 | 85.5 | 72.6 | 35334. | 4 | 1.0 | 989.3 | 85.5 | 72.6 |
| 12 | 7. | 0.017 | 0. | 23580. | 0.0 | 2925.3 | 38667. | 4 | 1.0 | 657.3 | 49.7 | 75.1 | 38667. | 4 | 1.0 | 657.3 | 49.7 | 75.1 |
| 13 | 2. | 0.008 | 0. | 20674. | 0.0 | 2797.5 | 42000. | 4 | 1.0 | 336.0 | 22.4 | 50.0 | 42000. | 4 | 1.0 | 336.0 | 22.4 | 50.0 |
| 14 | -3. | 0.002 | 0. | 17767. | 0.0 | 2669.7 | 45334. | 4 | 1.0 | 90.7 | 5.3 | 16.2 | 45334. | 4 | 1.0 | 90.7 | 5.3 | 16.2 |
| 15 | -8. | 0.001 | 0. | 14861. | 0.0 | 2541.8 | 48667. | 4 | 1.0 | 48.7 | 2.5 | 9.9 | 48667. | 4 | 1.0 | 48.7 | 2.5 | 9.9 |
| | | | | | | | | | | 16702.1 | 1547.6 | 263.5 | | | | 16702.1 | 1547.6 | 263.5 T |

| J | HEAT INPUT | E. PUMP | E. REST | E. CHE | E. CTL | E. SUM | COP |
|---|---|---|---|---|---|---|---|
| 1 | 1906179.37 | 141851.38 | 0.00 | 67741.32 | 47654.25 | 257246.95 | 2.17 |
| 2 | 3715954.25 | 283633.50 | 0.00 | 44303.42 | 34836.90 | 362773.81 | 3.00 |
| 3 | 3247078.25 | 255114.77 | 0.00 | 20458.27 | 18733.05 | 294306.09 | 3.23 |
| 4 | 6704493.50 | 544572.31 | 0.00 | 24378.15 | 27935.25 | 596885.69 | 3.29 |
| 5 | 9473931.00 | 799889.62 | 0.00 | 18492.25 | 30893.10 | 849275.00 | 3.27 |
| 6 | 14355504.00 | 1318860.75 | 0.00 | 8231.64 | 38452.05 | 1365544.37 | 3.08 |
| 7 | 25306176.00 | 2555601.75 | 0.00 | 34759.12 | 57513.75 | 2647874.50 | 2.80 |
| 8 | 9824493.00 | 1010397.37 | 0.00 | 7641.50 | 19390.35 | 1037429.25 | 2.77 |
| 9 | 10363481.00 | 1087400.88 | 0.00 | 2730.09 | 18075.75 | 1108206.75 | 2.74 |
| 10 | 10937527.00 | 1087253.12 | 261195.03 | 0.00 | 17089.90 | 1365537.87 | 2.35 |
| 11 | 6502920.50 | 561917.00 | 477105.56 | 0.00 | 9202.20 | 1048224.75 | 1.82 |
| 12 | 4320674.00 | 326879.69 | 493951.97 | 0.00 | 5587.05 | 826418.75 | 1.53 |
| 13 | 2208539.00 | 147103.75 | 328580.03 | 0.00 | 2629.20 | 478312.97 | 1.35 |
| 14 | 595955.00 | 35095.44 | 106178.02 | 0.00 | 657.30 | 141930.75 | 1.23 |
| 15 | 319887.63 | 16707.47 | 65105.53 | 0.00 | 328.65 | 82141.65 | 1.14 |

HSPF 8.91 SEASONAL LOAD 109782800.0

ELECTRICITY INPUT TO HEAT PUMP 10172279.0 ELECTRICITY INPUT TO RESISTANCE HEATER 1732116.1

ELECTRICITY INPUT TO CRANKCASE HEATER 228735.8 ELECTRICITY INPUT TO CONTROL EQUIPMENTS 328650.0

TOTAL ELECTRICITY INPUT 12461781.0

SEASONAL HEATING HOURS 6573.0 HEAT DELIVERED BY HEAT PUMP 103871088.0

HEAT DELIVERED BY RESISTANCE HEATER 5911712.5 HEAT DEFICIENCY 5911712.0

RUNNING HOURS HIGH CAPACITY 2047.6 LOW CAPACITY 1584.5

REGION 4 CONTINUED

*** COMPUTATIONAL RESULTS FOR COOLING SEASON ***

| BIN J | T(J) DEG.F | BIN HRS | BLC BTU/H | QSS1 BTU/H | QSS2 BTU/H | ESS1 W | ESS2 W | CASE | X1 | X2 | Q/N BTU/H | E/N W | |
|---|---|---|---|---|---|---|---|---|---|---|---|---|---|
| 1 | 67. | 0.370 | 1867. | 27806. | 44220. | 1686.6 | 2947.0 | 1 | 0.067 | 0.000 | 690.7 | 46.2 | |
| 2 | 72. | 0.250 | 6533. | 26868. | 43725. | 1855.1 | 3237.0 | 1 | 0.243 | 0.000 | 1633.3 | 122.0 | |
| 3 | 77. | 0.202 | 11200. | 25929. | 43229. | 2023.5 | 3527.0 | 1 | 0.432 | 0.000 | 2262.4 | 187.2 | |
| 4 | 82. | 0.143 | 15867. | 24991. | 42734. | 2192.0 | 3817.0 | 1 | 0.635 | 0.000 | 2268.9 | 206.6 | |
| 5 | 87. | 0.036 | 20533. | 24053. | 42239. | 2360.5 | 4107.0 | 1 | 0.854 | 0.000 | 739.2 | 73.6 | |
| | | | | | | | | | | | 7594.6 | 635.6 | TOTAL |

| J | BLDG LOAD | HP CAP | E. PUMP | E. CHE | E. CTL | E. SUM | COP |
|---|---|---|---|---|---|---|---|
| 1 | 1510495.50 | 1510495.50 | 101046.45 | 56615.11 | 40459.50 | 198121.06 | 2.23 |
| 2 | 3572117.75 | 3572117.75 | 266828.88 | 31034.92 | 27337.50 | 325201.31 | 3.22 |
| 3 | 4947893.50 | 4947893.50 | 409389.94 | 18821.45 | 22088.70 | 450300.09 | 3.22 |
| 4 | 4962182.00 | 4962182.00 | 451733.69 | 8563.67 | 15637.05 | 475934.41 | 3.05 |
| 5 | 1616638.37 | 1616638.37 | 161008.92 | 863.94 | 3936.60 | 165809.45 | 2.86 |

SEER 10.28 COOLING DELIVERED 16609327.0 ELECTRICITY INPUT TO HEAT PUMP 1390008.0

ELECTRICITY INPUT TO CRANKCASE HEATER 115899.1 ELECTRICITY INPUT TO CONTROL EQUIPMENT 109350.0

TOTAL ELECTRICITY INPUT 1615257.1 SEASONAL LOAD 16609327.0

COOLING DEFICIENCY 0.0 COOLING COST 80.3 SEASONAL COOLING HOURS 2187.0

RUNNING HOURS HIGH CAPACITY 0.0 LOW CAPACITY 680.4

REGION 4 CONTINUED

*** SUMMARY OF THE CALCULATION ***

HEAT PUMP OFF-TIME= 4447.57 ELECTRICITY INPUT DURING OFF-TIME= 222373.59

HEATING COST= 619.35 COOLING COST= 80.28

FIXED CHARGE= 439.14 SUM OF HEATING AND COOLING COSTS= 699.63

ENERGY COST OF CRANKCASE HEATER AND CONTROL EQUIPMENTS DURING OFF-TIME= 11.05

TOTAL COST= 1149.82

HEAT DELIVERED= 109782800.00 COOLING DELIVERED= 16609327.00

TOTAL BTU DELIVERED= 126392128.00 COST PER MBTU DELIVERED= 9.10

ESTIMATE OF HEAT PUMP SEASONAL PERFORMANCE BY WESTINGHOUSE/DOE PROCEDURE

*** INPUT DATA ***

HOUSE LEVEL= 2 HP SCALE FACTOR= 1.00

UNIT WITH: TWO-SPEED COMPRESSOR, TWO COMPRESSORS, OR CYLINDER UNLOADING

COOLING DATA:

| | | | | | | | |
|---|---|---|---|---|---|---|---|
| QSS(95F) | ,K=1 | 22551. | BTU/H | QSS(82F) | ,K=1 | 24991. | BTU/H |
| ESS(95F) | ,K=1 | 2630. | WATTS | ESS(82F) | ,K=1 | 2192. | WATTS |
| EERA | ,K=1 | 8.575 | | EERB | ,K=1 | 11.401 | |
| QSS(95F) | ,K=2 | 41446. | BTU/H | QSS(82F) | ,K=2 | 42734. | BTU/H |
| ESS(95F) | ,K=2 | 4571. | WATTS | ESS(82F) | ,K=2 | 3817. | WATTS |
| EERA | ,K=2 | 9.067 | | EERB | ,K=2 | 11.196 | |

HEATING DATA:

| | | | |
|---|---|---|---|
| QSS(47F) | ,K=1 | 28693. | BTU/H |
| ESS(47F) | ,K=1 | 2195. | WATTS |
| COPSS(47F) | ,K=1 | 3.830 | |
| QSS(17F) | ,K=1 | 10922. | BTU/H |
| ESS(17F) | ,K=1 | 1553. | WATTS |
| COPSS(17F) | ,K=1 | 2.061 | |
| QDEF(35F) | ,K=1 | 20689. | BTU/H |
| EDEF(35F) | ,K=1 | 1930. | WATTS |
| QSS(62F) | ,K=1 | 38225. | BTU/H |
| ESS(62F) | ,K=1 | 2575. | WATTS |
| COPSS(62F) | ,K=1 | 4.349 | |
| QSS(47F) | ,K=2 | 46929. | BTU/H |
| ESS(47F) | ,K=2 | 3948. | WATTS |
| COPSS(47F) | ,K=2 | 3.475 | |
| QSS(17F) | ,K=2 | 29392. | BTU/H |
| ESS(17F) | ,K=2 | 3181. | WATTS |
| COPSS(17F) | ,K=2 | 2.707 | |
| QDEF(35F) | ,K=2 | 38336. | BTU/H |
| EDEF(35F) | ,K=2 | 3649. | WATTS |

REGION: 5

UNIT COST OF ELECTRICITY: 0.0497 $/KWH

| | | |
|---|---|---|
| ELECTRIC POWER INPUT TO CRANKCASE HEATER, | W | 75.00 |
| ELECTRIC POWER INPUT TO CONTROL EQUIPMENT DURING THE COOLING SEASON, | W | 50.00 |
| ELECTRIC POWER INPUT TO CONTROL EQUIPMENT DURING THE HEATING SEASON, | W | 50.00 |

REGION 5 CONTINUED

COOLING SEASON SUMMARY:

| | | |
|---|---|---|
| COOLING CAPACITY AT 95 DEG. F: | 41446. | BTU/H |
| DEGRADATION COEFFICIENT, CD, K=1: | 0.100 | |
| DEGRADATION COEFFICIENT, CD, K=2: | 0.100 | |
| | (INPUT) | |

HEATING SEASON SUMMARY:

| | | |
|---|---|---|
| HEATING CAPACITY AT 47 DEG. F: | 46829. | BTU/H |
| DEGRADATION COEFFICIENT, CD, K=1: | 0.100 | |
| DEGRADATION COEFFICIENT, CD, K=2: | 0.100 | |
| | (INPUT) | |

REGIONAL DESIGN HEATING REQUIREMENT, DHR

| | | |
|---|---|---|
| MINIMUM: | 30506. | BTU/H |
| MAXIMUM: | 30506. | BTU/H |

| TBAL(DEG F) | QBAL(BTU/HR) | SLOPE(BTU/HR F) | CSLOPE | TNEUTH | TNEUTC |
|---|---|---|---|---|---|
| 19.242 | 30505.8 | -666.7 | 1.4 | 65.0 | 65.0 |

| TBAHI(DEG F) | BSCALE | QINTC(BTU/HR) | QINTH(BTU/HR) |
|---|---|---|---|
| 34.430 | 1.0000 | 0.0 | 0.0 |

*** ANNUAL COST COMPUTATION ***

TINSTA IS THE TOTAL INSTALLED COST IN $= 4138.05

IPRIME IS THE REAL INTEREST RATE= 0.03 YEAR IS THE NUMBER OF YEARS IN AMORTIZATION= 15.00

OWNER IS THE OWNERSHIP COST IN $= 346.63 MAINTA IS THE MAINTENANCE COST IN $= 103.45

ANNUAL IS THE ANNUAL COST IN $= 450.08

M IS THE MAXIMUM BIN NUMBER= 13

BLH(M,1) IS THE BUILDING LOAD AT THE M-TH BIN IN BTU/H= 58667.0

QO IS THE HEAT PUMP CAPACITY AT THE M-TH BIN IN BTU/H= 6142.7

HDEF IS THE HEATING DEFICIENCY AT THE M-TH BIN IN KW= 15.4

XNUMB IS THE NUMBER OF 5KW HEATER REQUIRED= 3.1

REGION 5 CONTINUED

*** COMPUTATIONAL RESULTS FOR HEATING SEASON ***

| BIN J | T(J) DEG.F | BIN HRS | QDOT1 BTU/H | QDOT2 BTU/H | EDOT1 W | EDOT2 W | BLH BTU/H | CASE | DELTA | BLH/N | E/N BTU/H | RH/N W | BLH W | CASE | DELTA BTU/H | BLH/N | E/N BTU/H | RH/N BTU/H | W |
|---|---|---|---|---|---|---|---|---|---|---|---|---|---|---|---|---|---|---|---|
| 1 | 62. | 0.119 | 38225. | 55549. | 2575.0 | 4331.5 | 2000. | 1 | 1.0 | 238.0 | 17.7 | 0.0 | 2000. | 1 | 1.0 | 238.0 | 17.7 | 0.0 | |
| 2 | 57. | 0.094 | 35048. | 52641. | 2448.3 | 4203.7 | 5333. | 1 | 1.0 | 501.3 | 39.3 | 0.0 | 5333. | 1 | 1.0 | 501.3 | 38.3 | 0.0 | |
| 3 | 52. | 0.051 | 31970. | 49735. | 2321.7 | 4075.8 | 8667. | 1 | 1.0 | 442.0 | 34.7 | 0.0 | 8667. | 1 | 1.0 | 442.0 | 34.7 | 0.0 | |
| 4 | 47. | 0.053 | 28693. | 46829. | 2195.0 | 3948.0 | 12000. | 1 | 1.0 | 696.0 | 56.5 | 0.0 | 12000. | 1 | 1.0 | 696.0 | 56.5 | 0.0 | |
| 5 | 42. | 0.073 | 25516. | 41814. | 2068.3 | 3831.0 | 15333. | 1 | 1.0 | 1119.3 | 94.5 | 0.0 | 15333. | 1 | 1.0 | 1119.3 | 94.5 | 0.0 | |
| 6 | 37. | 0.138 | 21774. | 39330. | 1971.9 | 3701.0 | 18667. | 1 | 1.0 | 2576.0 | 236.7 | 0.0 | 18667. | 1 | 1.0 | 2576.0 | 236.7 | 0.0 | |
| 7 | 32. | 0.119 | 0. | 36845. | 0.0 | 3571.0 | 22000. | 3 | 1.0 | 2618.0 | 264.4 | 0.0 | 22000. | 3 | 1.0 | 2618.0 | 264.4 | 0.0 | |
| 8 | 27. | 0.075 | 0. | 34361. | 0.0 | 3441.0 | 25333. | 3 | 1.0 | 1900.0 | 195.4 | 0.0 | 25333. | 3 | 1.0 | 1900.0 | 195.4 | 0.0 | |
| 9 | 22. | 0.084 | 0. | 31876. | 0.0 | 3311.0 | 28667. | 3 | 1.0 | 2408.0 | 252.7 | 0.0 | 28667. | 3 | 1.0 | 2408.0 | 252.7 | 0.0 | |
| 10 | 17. | 0.065 | 0. | 29392. | 0.0 | 3181.0 | 32000. | 4 | 1.0 | 2080.0 | 206.8 | 49.7 | 32000. | 4 | 1.0 | 2080.0 | 206.8 | 49.7 | |
| 11 | 12. | 0.040 | 0. | 26486. | 0.0 | 3053.2 | 35334. | 4 | 1.0 | 1413.3 | 122.1 | 103.7 | 35334. | 4 | 1.0 | 1413.3 | 122.1 | 103.7 | |
| 12 | 7. | 0.031 | 0. | 23580. | 0.0 | 2925.3 | 38667. | 4 | 1.0 | 1198.7 | 90.7 | 137.0 | 38667. | 4 | 1.0 | 1198.7 | 90.7 | 137.0 | |
| 13 | 2. | 0.017 | 0. | 20674. | 0.0 | 2797.5 | 42000. | 4 | 1.0 | 714.0 | 47.6 | 106.2 | 42000. | 4 | 1.0 | 714.0 | 47.6 | 106.2 | |
| 14 | -3. | 0.019 | 0. | 17767. | 0.0 | 2669.7 | 45334. | 4 | 1.0 | 861.3 | 50.7 | 153.5 | 45334. | 4 | 1.0 | 861.3 | 50.7 | 153.5 | |
| 15 | -8. | 0.013 | 0. | 14861. | 0.0 | 2541.8 | 48667. | 4 | 1.0 | 632.7 | 33.0 | 128.8 | 48667. | 4 | 1.0 | 632.7 | 33.0 | 128.8 | |
| 16 | -13. | 0.004 | 0. | 11955. | 0.0 | 2414.0 | 52000. | 4 | 1.0 | 208.0 | 9.7 | 46.9 | 52000. | 4 | 1.0 | 208.0 | 9.7 | 46.9 | |
| 17 | -18. | 0.001 | 0. | 9049. | 0.0 | 2286.2 | 55334. | 4 | 1.0 | 55.3 | 2.3 | 13.6 | 55334. | 4 | 1.0 | 55.3 | 2.3 | 13.6 | |
| 18 | -23. | 0.001 | 0. | 6143. | 0.0 | 2158.3 | 58667. | 4 | 0.0 | 58.7 | 0.0 | 17.2 | 58667. | 4 | 0.0 | 58.7 | 0.0 | 17.2 | |
| | | | | | | | | | | 19720.8 | 1753.7 | 756.5 | | | | 19720.8 | 1753.7 | 756.5 | TOTAL |

| J | HEAT INPUT | E. PUMP | E. REST | E. CHE | E. CTL | E. SUM | COP |
|---|---|---|---|---|---|---|---|
| 1 | 1552005.75 | 115494.98 | 0.00 | 55154.79 | 38799.95 | 209449.72 | 2.17 |
| 2 | 3269210.75 | 249534.19 | 0.00 | 38977.12 | 30648.70 | 319160.00 | 3.00 |
| 3 | 2882296.25 | 226454.78 | 0.00 | 18159.96 | 16628.55 | 261243.28 | 3.23 |
| 4 | 4538638.50 | 368650.81 | 0.00 | 16502.90 | 18910.90 | 404064.63 | 3.29 |
| 5 | 7299209.00 | 616276.56 | 0.00 | 14247.39 | 23801.65 | 654325.56 | 3.27 |
| 6 | 16798178.00 | 1543272.97 | 0.00 | 9632.30 | 44994.90 | 1597900.00 | 3.08 |
| 7 | 17072064.00 | 1724061.25 | 0.00 | 23449.21 | 38799.95 | 1786310.50 | 2.90 |
| 8 | 12389962.00 | 1274242.37 | 0.00 | 9636.93 | 24453.75 | 1308333.00 | 2.77 |
| 9 | 15702646.00 | 1647619.25 | 0.00 | 4136.61 | 27388.20 | 1679144.12 | 2.74 |
| 10 | 13563747.00 | 1348314.50 | 323910.88 | 0.00 | 21193.25 | 1693418.62 | 2.35 |
| 11 | 9216392.00 | 796388.00 | 676187.31 | 0.00 | 13042.00 | 1485617.37 | 1.82 |
| 12 | 7816544.00 | 591359.00 | 893610.06 | 0.00 | 10107.55 | 1495076.62 | 1.53 |
| 13 | 4656017.00 | 310122.47 | 692708.75 | 0.00 | 5542.85 | 1008374.12 | 1.35 |
| 14 | 5616732.50 | 330769.03 | 1000711.19 | 0.00 | 6194.95 | 1337675.25 | 1.23 |
| 15 | 4125640.25 | 215478.84 | 839676.06 | 0.00 | 4238.65 | 1059393.50 | 1.14 |
| 16 | 1356374.75 | 62966.78 | 306047.63 | 0.00 | 1304.20 | 370318.59 | 1.07 |
| 17 | 360630.47 | 14908.09 | 98433.35 | 0.00 | 326.05 | 103667.49 | 1.02 |
| 18 | 382567.22 | 0.00 | 112091.20 | 489.08 | 326.05 | 112906.32 | 0.99 |

HSPF 7.62 SEASONAL LOAD 128599112.0

ELECTRICITY INPUT TO HEAT PUMP 11435914.0 ELECTRICITY INPUT TO RESISTANCE HEATER 4933377.0

ELECTRICITY INPUT TO CRANKCASE HEATER 190386.3 ELECTRICITY INPUT TO CONTROL EQUIPMENTS 326050.0

TOTAL ELECTRICITY INPUT 16885728.0

SEASONAL HEATING HOURS 6521.0 HEAT DELIVERED BY HEAT PUMP 111761512.0

HEAT DELIVERED BY RESISTANCE HEATER 16837616.0 HEAT DEFICIENCY 16837600.0

RUNNING HOURS HIGH CAPACITY 2589.7 LOW CAPACITY 1492.9

REGION 5 CONTINUED

*** COMPUTATIONAL RESULTS FOR COOLING SEASON ***

| BIN J | T(J) DEG.F | BIN HRS | BLC BTU/H | QSS1 BTU/H | QSS2 BTU/H | ESS1 W | ESS2 W | CASE | X1 | X2 | Q/N BTU/H | E/N W |
|---|---|---|---|---|---|---|---|---|---|---|---|---|
| 1 | 67. | 0.268 | 1867. | 27806. | 44220. | 1686.6 | 2947.0 | 1 | 0.067 | 0.000 | 500.3 | 33.5 |
| 2 | 72. | 0.226 | 6533. | 26868. | 43725. | 1855.1 | 3237.0 | 1 | 0.243 | 0.000 | 1476.5 | 110.3 |
| 3 | 77. | 0.234 | 11200. | 25929. | 43229. | 2023.5 | 3527.0 | 1 | 0.432 | 0.000 | 2620.8 | 216.8 |
| 4 | 82. | 0.188 | 15867. | 24991. | 42734. | 2192.0 | 3817.0 | 1 | 0.635 | 0.000 | 2982.9 | 271.6 |
| 5 | 87. | 0.075 | 20533. | 24053. | 42239. | 2360.5 | 4107.0 | 1 | 0.854 | 0.000 | 1540.0 | 153.4 |
| 6 | 92. | 0.008 | 25200. | 23114. | 41743. | 2528.9 | 4397.0 | 3 | 0.000 | 0.604 | 201.6 | 22.1 |
| | | | | | | | | | | | 9322.2 | 807.6 TOTAL |

| J | BLDG LOAD | HP CAP | E. PUMP | E. CHE | E. CTL | E. SUM | COP |
|---|---|---|---|---|---|---|---|
| 1 | 1120102.62 | 1120102.62 | 74930.64 | 41982.73 | 30002.60 | 146915.98 | 2.23 |
| 2 | 3305974.50 | 3305974.50 | 246948.61 | 28722.64 | 25300.70 | 300971.94 | 3.22 |
| 3 | 5868000.50 | 5868000.50 | 485519.78 | 22321.48 | 26196.30 | 534037.56 | 3.22 |
| 4 | 6678820.50 | 6678820.50 | 608008.44 | 11526.22 | 21046.60 | 640581.31 | 3.05 |
| 5 | 3448077.25 | 3448077.25 | 343410.88 | 1842.67 | 8396.25 | 353649.73 | 2.96 |
| 6 | 451384.66 | 451384.69 | 49508.41 | 532.40 | 895.60 | 50936.41 | 2.60 |

SEER 10.30 COOLING DELIVERED 20872360.0 ELECTRICITY INPUT TO HEAT PUMP 1908326.8

ELECTRICITY INPUT TO CRANKCASE HEATER 106928.1 ELECTRICITY INPUT TO CONTROL EQUIPMENT 111950.0

TOTAL ELECTRICITY INPUT 2027204.9 SEASONAL LOAD 20872360.0

COOLING DEFICIENCY 0.0 COOLING COST 100.8 SEASONAL COOLING HOURS 2239.0

RUNNING HOURS HIGH CAPACITY 11.3 LOW CAPACITY 840.3

REGION 5 CONTINUED

*** SUMMARY OF THE CALCULATION ***

HEAT PUMP OFF-TIME= 3825.82 ELECTRICITY INPUT DURING OFF-TIME= 191291.14

HEATING COST= 839.22 COOLING COST= 100.75

FIXED CHARGE= 450.08 SUM OF HEATING AND COOLING COSTS= 939.97

ENERGY COST OF CRANKCASE HEATER AND CONTROL EQUIPMENTS DURING OFF-TIME= 9.51

TOTAL COST= 1399.56

HEAT DELIVERED= 128599112.00 COOLING DELIVERED= 20872360.00

TOTAL BTU DELIVERED= 149471472.00 COST PER MBTU DELIVERED= 9.36

## APPENDIX D
## REVERSING VALVE STUDY

Based on a component failure mode and effects analysis study, the heat pump reversing valve was identified as a critical component. Standard production valves of approximately 4 ton capacity were obtained from each of three major manufacturers for qualification testing.

The test stand shown in Figure D1 was designed and fabricated using a closed loop refrigeration system to exercise all three reversing valves simultaneously under identical conditions. Refrigerant pressure drop and temperature rise through the valve suction path were measured directly on the cycle test rig for both energized and deenergized valve states for a high to low side pressure difference across the valve of 150 psi and 225 psi.

A separate test station, shown schematically in Figure D2, was assembled to measure high pressure side to low pressure side leakage through the reversing valves by feeding regulated high pressure nitrogen through the valve at room temperature during designated breaks in the 100,000 cycle durability test. This was done for both energized and deenergized valve states.

At zero cycle time, before being installed in the life cycle test stand, each valve was tested for leakage. The results are shown on the zero cycle time curve in Figure D3. The relatively high leakage through a new valve $A_1$ especially at the higher operating point of 225 psig, was of a major concern. The vendor was contacted and informed of the test results and the concern regarding the high leakage rate of their valve. Vendor A confirmed the leakage loss measurements, and indicated that this curve was typical of leakage loss across their valves. They expressed no concern since the leakage at 150 psig, the point at which they test their valves, was well below the 2 percent leakage rate normally used as an acceptable guideline.

At 13,000 cycles the valves were again tested. As can be seen in Figure D4, the curves show valves $B_1$ and $C_1$ having very little change and if anything a slight improvement due to the wear-in affect. Valve $A_1$, however, shows a considerable increase in leakage rate even in the low pressure range. At 150 psig the leakage was now well above the 2 percent acceptable figure.

At the 33,000 cycle point the valves were again tested. Valves $B_1$ and $C_1$ again showed very little change. Leakage through valve $A_1$, however, had increased to the extent that above 50 psig it was beyond the recording range of our flowmeter (500 cu in/min). The leakage rate at 33,000 cycles is shown on Figure D5.

Vendor A was contacted again and informed of the excessive leakage through the valve after 33,000 cycles. They requested that we send the subject valve, along with our test data showing the leakage deterioration, to their Engineering Department for analysis. Vendor A analyzed the test valve and verified that there were indeed large leakage paths at each end of the valve. At this point, they informed us that they had recently made some modifications to the internal parts of their reversing valve in order to decrease leakage through the valve and requested that we replace valve A with the modified design which they would supply. However, in order to not delay the test program, a backup valve $A_2$ was substituted. Valve $A_2$ at zero cycle time, shows the leakage rate just slightly better than that of the original valve $A_1$ at zero cycles. Valve $A_2$ failed in the same fashion as $A_1$ after 34,000 cycles. Valves $B_1$ and $C_1$ were still performing satisfactorily after 67,000 cycles. Valve $A_2$ was replaced by $D_1$ from a fourth vendor.

Leakage characteristics at the completion of this test program, 100,000 cycles, are shown in Figure D6. Vendor B was selected for the advanced heat pump.

The suction path refrigerant pressure drop and temperature rise through the three sample valves is given at 13,000 cycles in Table D1 for a 150 psi high-to-low side pressure differential and in Table D2 for a

225 psi differential. Through 67,000 cycles of operation there is no definitive change in this measure of reversing valve performance for valves B and C. The heat leak and pressure drop characteristics of valve B are less and therefore superior.

Table D1 - Reversing Valve Suction Path Pressure Drop and Temperature Rise
(R22 at 150 psi across valve at 13,000 cycles)

| | Solenoid State | Compressor Disc. Port | | Evaporator Port | | Suction Port | | Cond. Port | Mass Flow | Valve Loss | |
|---|---|---|---|---|---|---|---|---|---|---|---|
| | | P(psia) | T(°F) | P(psia) | T(°F) | P(psia) | T(°F) | T(°F) | (lbm/m) | ΔP(psi) | ΔT(°F) |
| A | Off | 240 | 231 | 92.0 | 72 | 90 | 75 | 221 | 17.5 | 2.0 | 3.0 |
| | On | 240 | 241 | 91.6 | 76 | 90 | 79 | 230 | | 1.6 | 3.0 |
| | Off | 225 | 232 | 76.5 | 47 | 75 | 51 | 220 | 14.0 | 1.5 | 4.0 |
| | On | 225 | 236 | 76.3 | 49 | 75 | 54 | 225 | | 1.3 | 5.0 |
| | Off | 215 | 227 | 66.2 | 34 | 65 | 40 | 216 | 12.0 | 1.6 | 6.0 |
| | On | 215 | 225 | 66.1 | 35 | 65 | 40 | 214 | | 1.1 | 5.0 |
| | Off | 208 | 230 | 59.2 | 31 | 58 | 36 | 218 | 10.2 | 1.2 | 6.0 |
| | On | 208 | 228 | 58.9 | 30 | 58 | 36 | 216 | | 0.9 | 6.0 |
| | Off | 198 | 236 | 48.8 | 22 | 48 | 29 | 222 | 8.0 | 0.8 | 7.0 |
| | On | 198 | 239 | 48.6 | 20 | 48 | 28 | 224 | | 0.6 | 8.0 |
| B | Off | 240 | 231 | 91.7 | 57 | 90 | 60 | 223 | 17.5 | 1.7 | 3.0 |
| | On | 240 | 229 | 91.8 | 58 | 90 | 60 | 219 | | 1.8 | 2.0 |
| | Off | 225 | 228 | 76.0 | 45 | 75 | 50 | 219 | 14.0 | 1.0 | 5.0 |
| | On | 225 | 227 | 76.3 | 47 | 75 | 50 | 217 | | 1.3 | 3.0 |
| | Off | 215 | 228 | 65.9 | 35 | 65 | 40 | 219 | 12.0 | 0.9 | 5.0 |
| | On | 215 | 227 | 66.2 | 36 | 65 | 40 | 216 | | 1.2 | 4.0 |
| | Off | 208 | 229 | 58.9 | 30 | 58 | 36 | 219 | 10.2 | 0.9 | 6.0 |
| | On | 208 | 228 | 59.0 | 29 | 58 | 35 | 217 | | 1.0 | 6.0 |
| | Off | 198 | 234 | 48.6 | 18 | 48 | 25 | 222 | 8.0 | 0.6 | 7.0 |
| | On | 198 | 237 | 48.7 | 18 | 48 | 26 | 223 | | 0.7 | 8.0 |
| C | Off | 240 | 254 | 92.6 | 79 | 90 | 83 | 240 | 17.5 | 2.6 | 4.0 |
| | On | 240 | 259 | 92.8 | 78 | 90 | 82 | 253 | | 2.8 | 4.0 |
| | Off | 225 | 238 | 77.0 | 57 | 75 | 62 | 225 | 14.0 | 2.0 | 5.0 |
| | On | 225 | 240 | 77.3 | 59 | 75 | 63 | 232 | | 2.3 | 4.0 |
| | Off | 215 | 240 | 66.7 | 47 | 65 | 53 | 224 | 12.0 | 1.7 | 6.0 |
| | On | 215 | 240 | 66.8 | 48 | 65 | 53 | 232 | | 1.8 | 5.0 |
| | Off | 208 | 242 | 59.5 | 36 | 58 | 44 | 226 | 10.2 | 1.5 | 8.0 |
| | On | 208 | 241 | 59.6 | 37 | 58 | 43 | 232 | | 1.6 | 6.0 |
| | Off | 198 | 248 | 49.1 | 27 | 48 | 37 | 231 | 8.0 | 1.1 | 10.0 |
| | On | 198 | 246 | 49.2 | 29 | 48 | 37 | 235 | | 1.2 | 8.0 |

Table D2 - Reversing Valve Suction Path Pressure Drop and Temperature Rise
(R22 at 225 psi across valve at 13,000 cycles)

| | Solenoid State | Compressor Disc. Port | | Evaporator Port | | Suction Port | | Cond. Port | Mass Flow | Valve Loss | |
|---|---|---|---|---|---|---|---|---|---|---|---|
| | | P(psia) | T(°F) | P(psia) | T(°F) | P(psia) | T(°F) | T(°F) | (lbm/m) | ΔP(psi) | ΔT(°F) |
| A | Off | 315 | 252 | 91.8 | 55 | 90 | 60 | 240 | 15.8 | 1.8 | 5 |
| | On | 315 | 260 | 91.4 | 59 | 90 | 63 | 248 | | 1.4 | 4 |
| | Off | 300 | 260 | 76.3 | 45 | 75 | 50 | 247 | 12.5 | 1.3 | 5 |
| | On | 300 | 258 | 76.1 | 44 | 75 | 50 | 244 | | 1.1 | 6 |
| | Off | 290 | 260 | 66.0 | 33 | 65 | 40 | 246 | 10.5 | 1.0 | 7 |
| | On | 290 | 262 | 65.8 | 33 | 65 | 40 | 247 | | 0.8 | 7 |
| | Off | 283 | 267 | 58.9 | 25 | 58 | 35 | 252 | 9.3 | 0.9 | 10 |
| | On | 283 | 266 | 58.7 | 25 | 58 | 35 | 250 | | 0.7 | 10 |
| | Off | 273 | 276 | 48.6 | 14 | 48 | 27 | 257 | 7.0 | 0.6 | 13 |
| | On | 273 | 281 | 48.5 | 14 | 48 | 27 | 261 | | 0.5 | 13 |
| B | Off | 315 | 231 | 91.3 | 76 | 90 | 80 | 262 | 15.8 | 1.3 | 4 |
| | On | 315 | 229 | 91.6 | 73 | 90 | 77 | 256 | | 1.6 | 4 |
| | Off | 300 | 228 | 75.9 | 46 | 75 | 52 | 251 | 12.5 | 0.9 | 6 |
| | On | 300 | 227 | 76.1 | 46 | 75 | 52 | 251 | | 1.1 | 6 |
| | Off | 290 | 228 | 65.7 | 35 | 65 | 41 | 252 | 10.5 | 0.7 | 6 |
| | On | 290 | 227 | 65.9 | 35 | 65 | 42 | 251 | | 0.9 | 7 |
| | Off | 283 | 229 | 58.7 | 27 | 58 | 35 | 257 | 9.3 | 0.7 | 8 |
| | On | 283 | 228 | 58.8 | 28 | 58 | 36 | 256 | | 0.8 | 8 |
| | Off | 273 | 234 | 48.5 | 14 | 48 | 25 | 259 | 7.0 | 0.5 | 11 |
| | On | 273 | 237 | 48.6 | 14 | 48 | 25 | 252 | | 0.6 | 11 |
| C | Off | 315 | 277 | 92.2 | 76 | 90 | 81 | 262 | 15.8 | 2.2 | 5 |
| | On | 315 | 280 | 92.2 | 78 | 90 | 83 | 272 | | 2.2 | 5 |
| | Off | 300 | 274 | 76.6 | 55 | 75 | 61 | 254 | 12.5 | 1.6 | 6 |
| | On | 300 | 273 | 76.6 | 56 | 75 | 62 | 264 | | 1.6 | 6 |
| | Off | 290 | 273 | 66.3 | 44 | 65 | 52 | 256 | 10.5 | 1.3 | 8 |
| | On | 290 | 276 | 66.4 | 47 | 65 | 54 | 265 | | 1.4 | 7 |
| | Off | 283 | 278 | 59.1 | 32 | 58 | 42 | 258 | 9.3 | 1.1 | 10 |
| | On | 283 | 278 | 59.2 | 33 | 58 | 42 | 266 | | 1.2 | 9 |
| | Off | 273 | 287 | 48.8 | 23 | 48 | 36 | 264 | 7.0 | 0.8 | 13 |
| | On | 273 | 292 | 48.8 | 25 | 48 | 37 | 276 | | 0.8 | 12 |

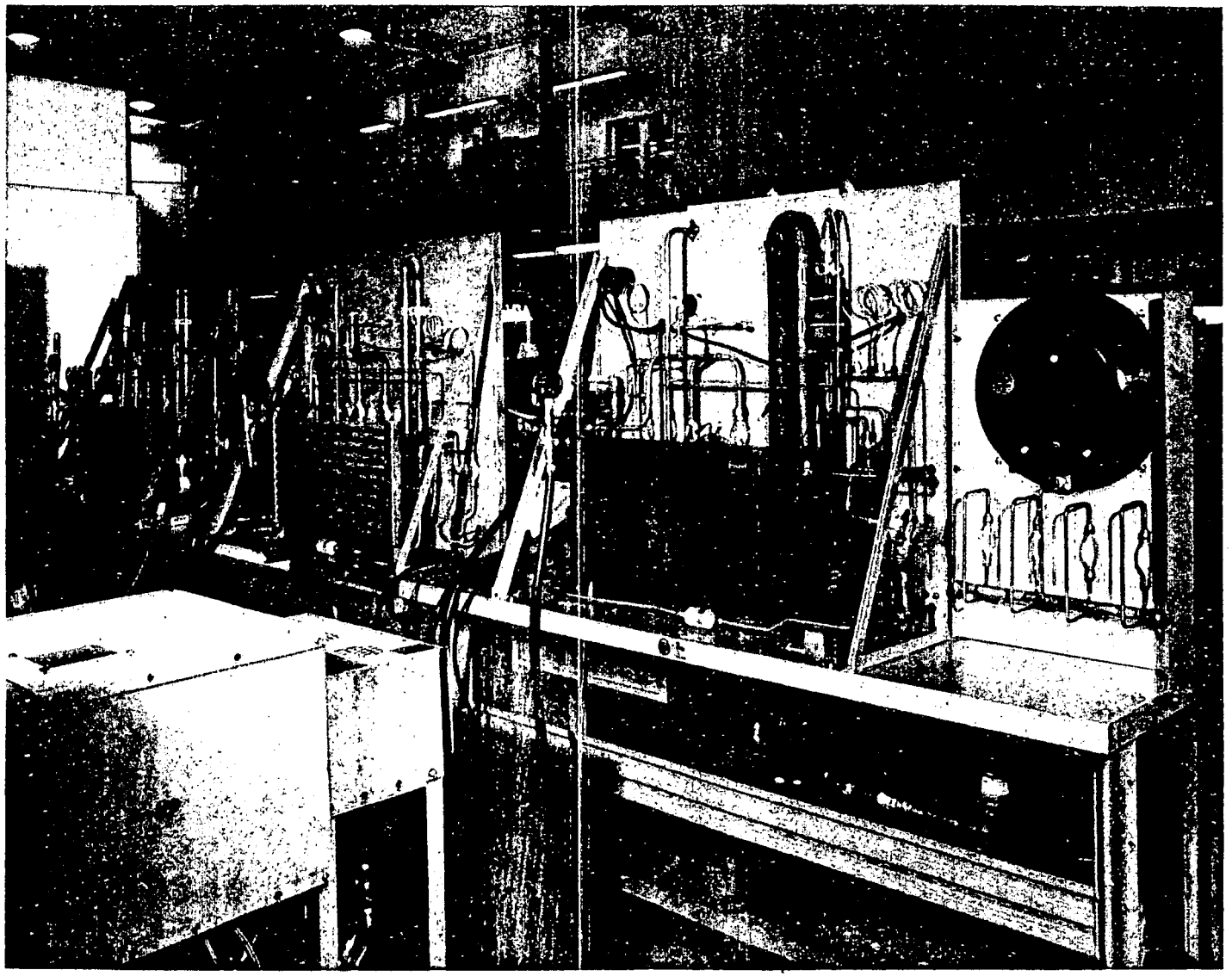

Fig. D1 - Reversing valve test stand

REVERSING VALVE
LEAKAGE TEST

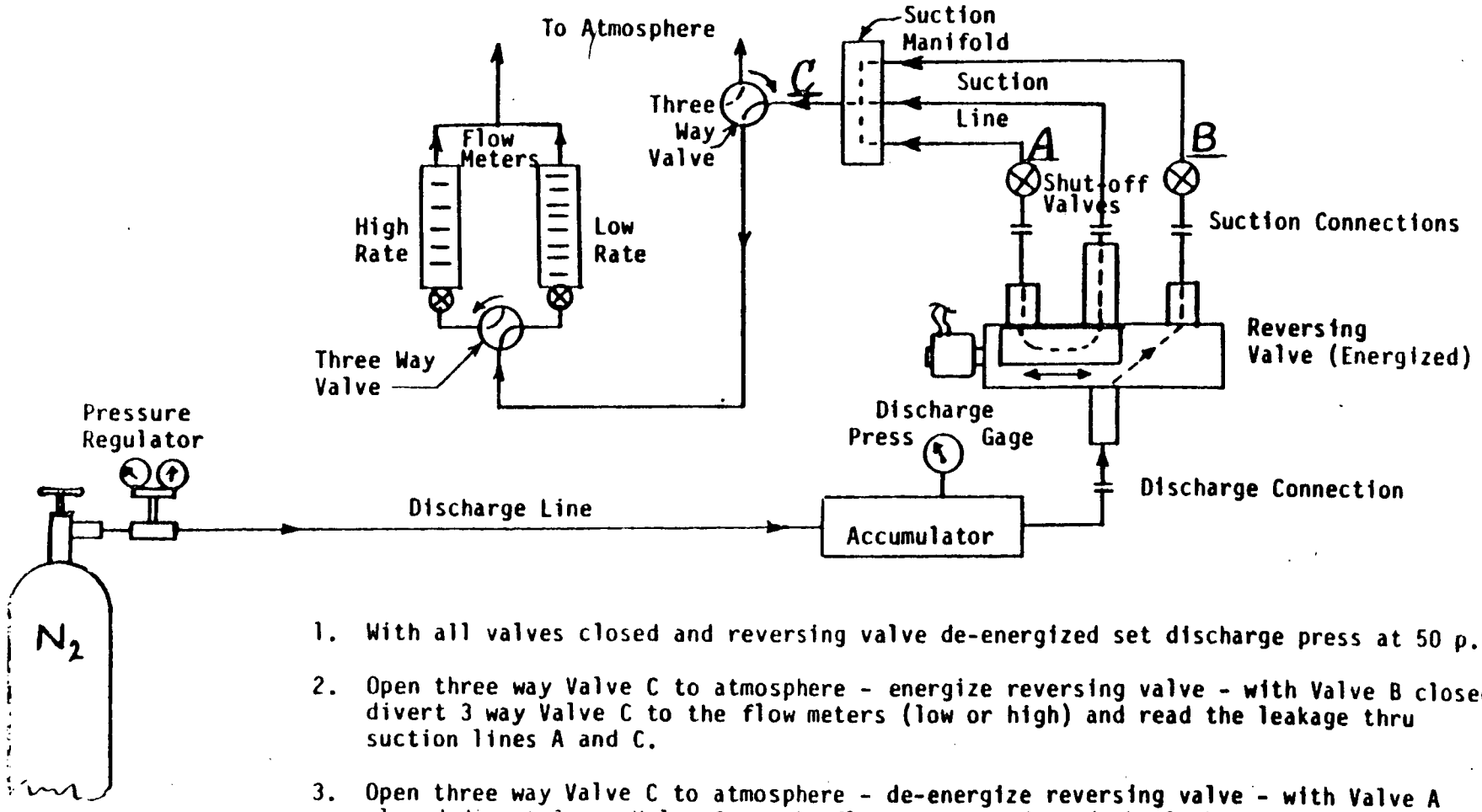


1. With all valves closed and reversing valve de-energized set discharge press at 50 p.s.i.g.

2. Open three way Valve C to atmosphere - energize reversing valve - with Valve B closed, divert 3 way Valve C to the flow meters (low or high) and read the leakage thru suction lines A and C.

3. Open three way Valve C to atmosphere - de-energize reversing valve - with Valve A closed divert 3 way Valve C to the flow meters and read the leakage thru suction lines B and C.

4. With the discharge pressure set at 100, 150, 200, 250 and 300 p.s.i.g. repeat steps 2 and 3. Record the valve leakage in both the energized and de-energized positions. Take the average of at least five readings at each pressure.

NOTE

Three way Valve C must be open to atmosphere for proper switching of the reversing valve.

Fig. D2 - Reversing valve leakage test

9/1[illegible]
J. A. Ric[illegible]

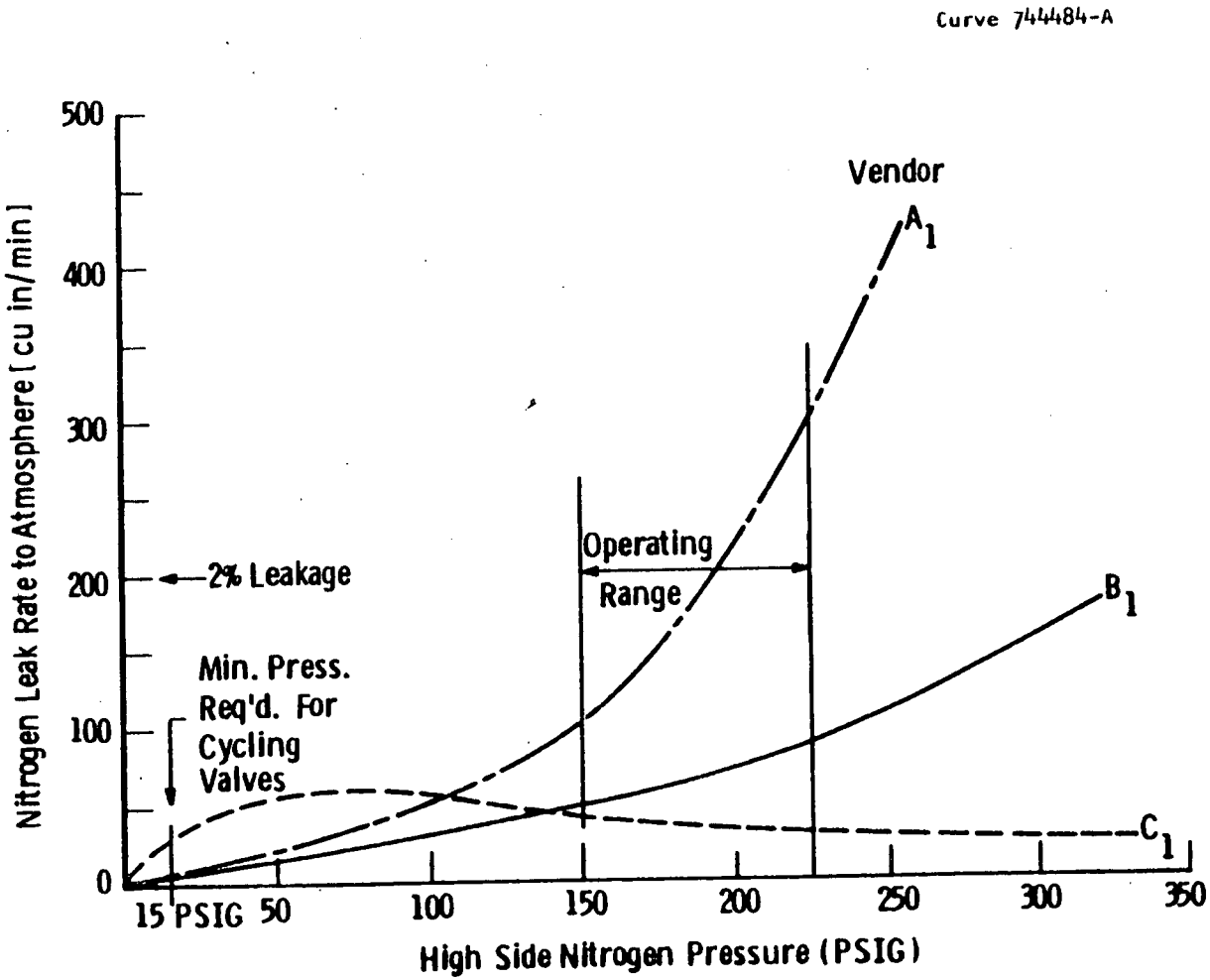


Fig. D3 - Reversing valve leakage vs pressure at zero cycles

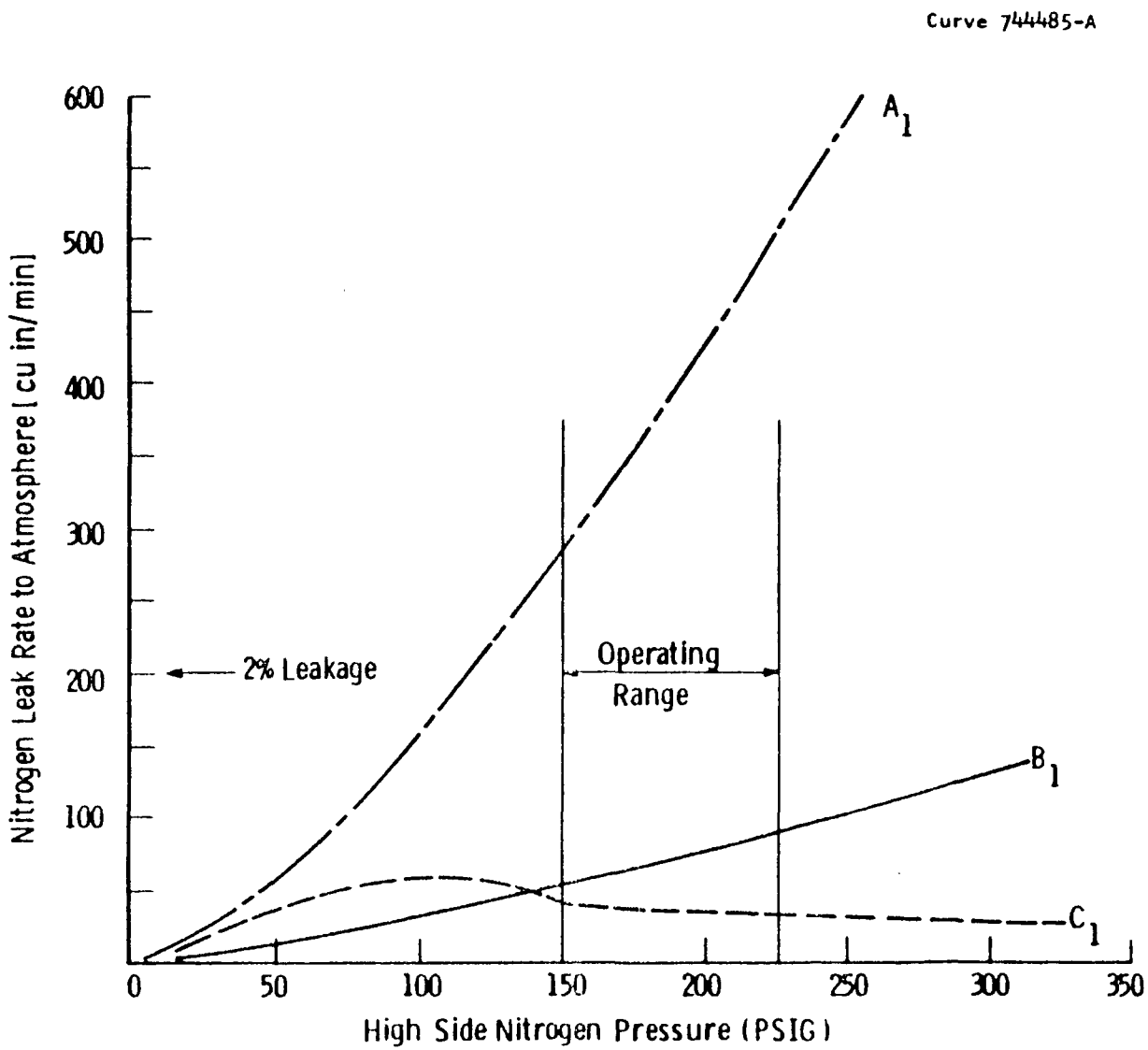


Fig. D4 - Reversing valve leakage for pressure at 13,000 cycles

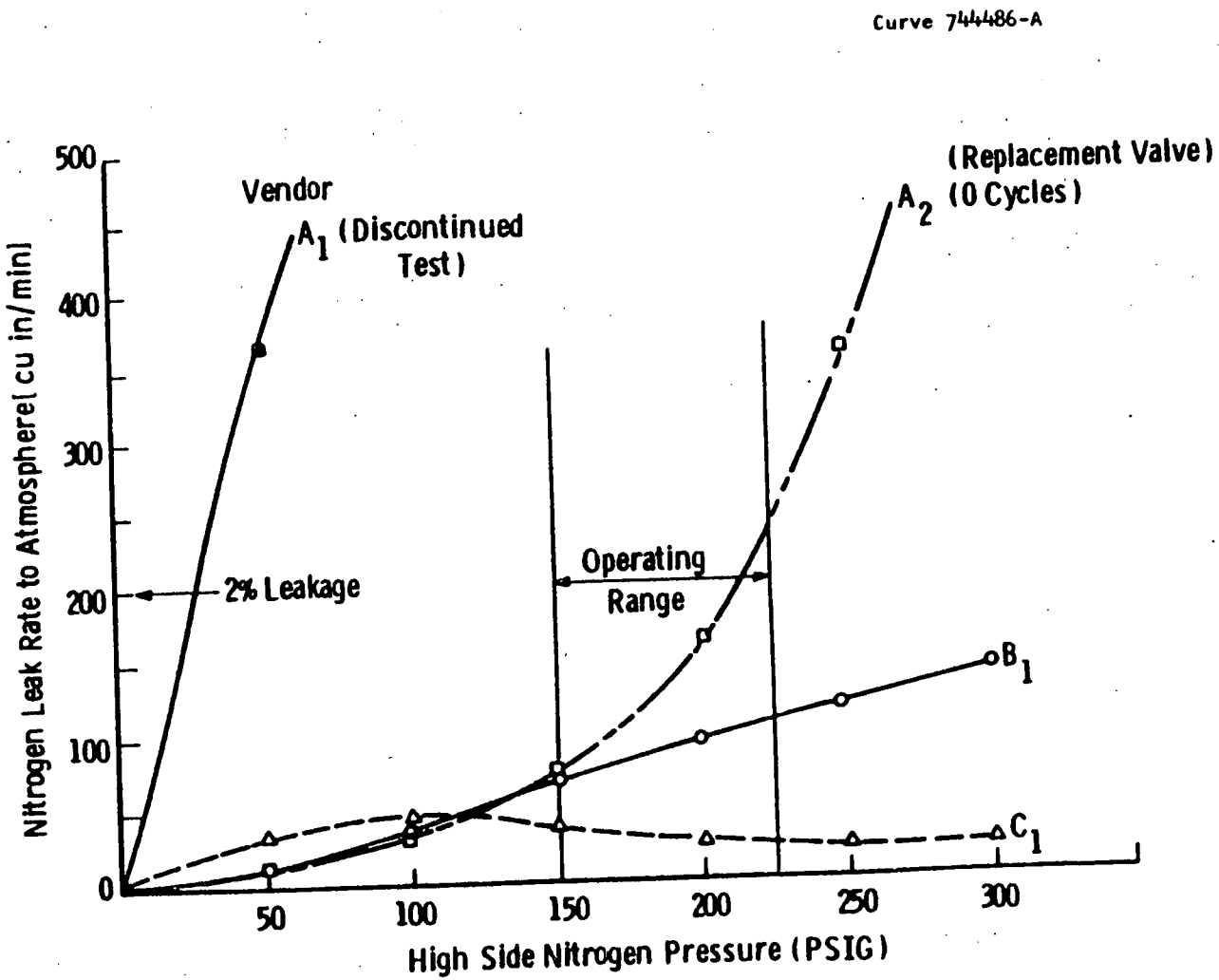


Fig. D5 - Reversing valve leakage vs pressure at 33,000 cycles

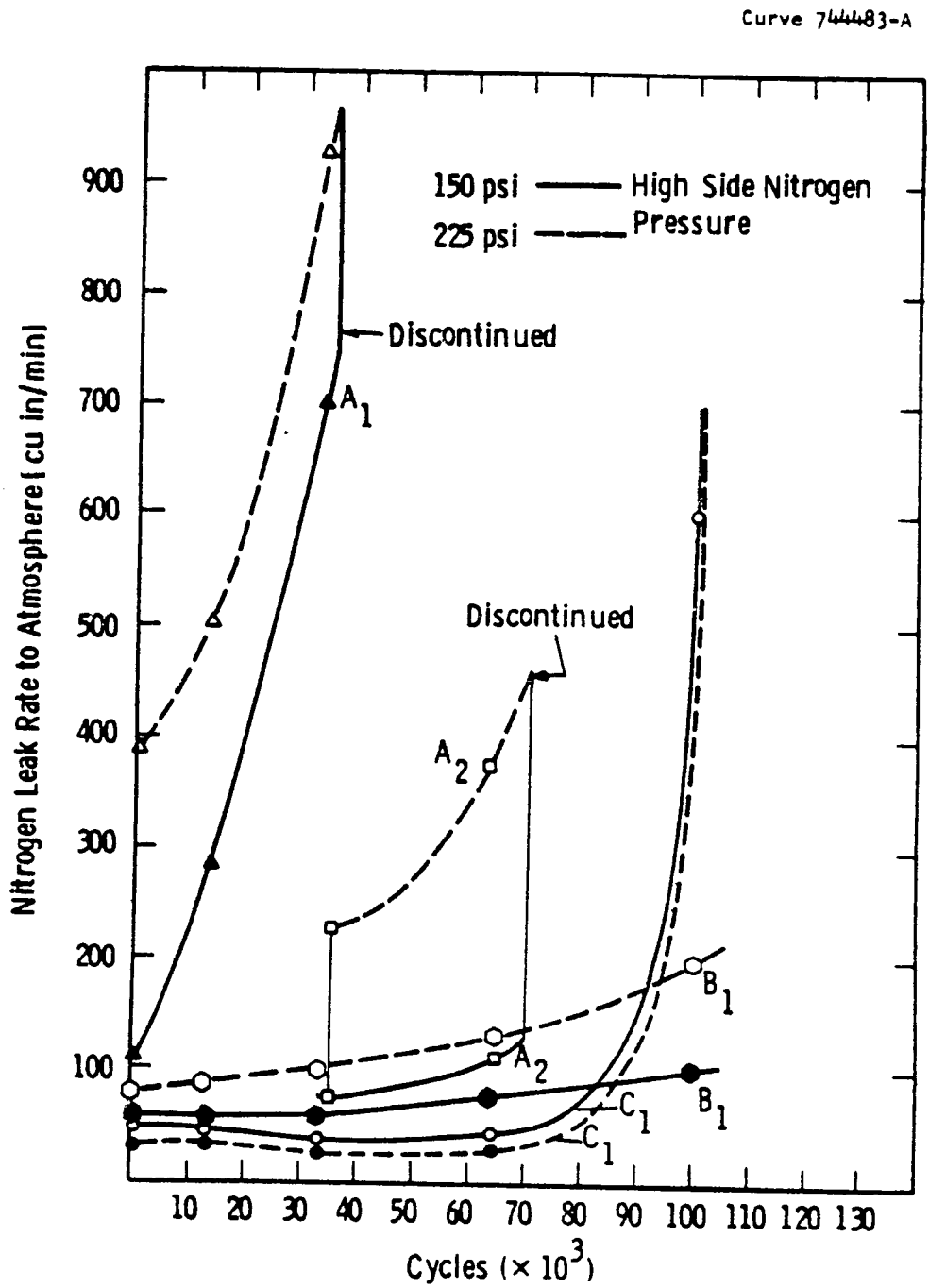


Fig. D6 - Reversing valve leakage vs cycle time

LIST OF TABLES


| | | Page |
|---|---|---|
| Table 1 - | Comparison of Seasonal Performance (1600 sq. ft Level 2 House) | 6 |
| Table 2 - | Preprototype Number One Measured Heating Performance | 28 |
| Table 3 - | Preprototype Number One Measured Cooling Performance | 29 |
| Table 4 - | Measured Cyclic Degradation Coefficients - Preprototype Number One) | 31 |
| Table 5 - | Measured Cyclic Degradation Coefficient as a Function of Cycle Number | 32 |
| Table 6 - | Preprototype Number Two Measured Heating Performance | 34 |
| Table 7 - | Preprototype Number Two Measured Cooling Performance | 36 |
| Table 8 - | Seasonal Heating Performance in Minneapolis | 38 |
| Table 9 - | Seasonal Cooling Performance in Minneapolis | 39 |
| Table 10 - | Preprototype Dual-Stroke Compressor Performance - High Capacity | 50 |
| Table 11 - | Preprototype Dual-Stroke Compressor Performance - Low Capacity | 51 |
| Table 12 - | Analysis of Incremental Costs for the Dual-Stroke Compressor | 56 |
| Table 13 - | Fan Noise at 860 rpm | 67 |
| Table 14 - | Details of Oil Cooler | 85 |
| Table 15 - | Details of Indoor Refrigerant-to-Air Heat Exchanger | 88 |
| Table 16 - | Details of Outdoor Refrigerant-to-Air Heat Exchanger | 93 |
| Table 17 - | Prototype No. 2 Plumbing | 101 |
| Table 18 - | Relay State Matrix for Heating Mode | 107 |
| Table 19 - | Relay State Matrix for Cooling Mode | 108 |
| Table 20 - | Heating Operating Sequence | 109 |
| Table 21 - | Cooling Operating Sequence | 110 |
| Table 22 - | Defrost Operating Sequence | 111 |
| Table 23 - | Fault Codes | 111 |
| Table 24 - | Indoor Unit Cost Breakdown | 122 |
| Table 25 - | Outdoor Unit Cost Breakdown | 127 |
| Table 26 - | Comparison of Parameters - Preprototype vs RDHPOV | 129 |